DESIGN
REALIZATION
AND
FIELD TESTING
OF A
VERTICAL - AXIS WIND TURBINE

Thesis

by

Erdal Yazgaç

Submitted to the Faculty of the Engineering School

in Partial Fulfillment of

the Requirements for the Degree of

Master of Science

in

Mechanical Engineering

Boğaziçi University

1981

ABSTRACT

The purpose of this invertiqation is to set up an experimental system for the field testing of the performance characteristics and practical serviceability of a vertical axis wind turbine.

Based on previous research work, a Savonius Wind turbine prototype was manufactured in the ideal dimensions. With the caupling of the necessary apparatus, it was tested on the roof of the engineering building of the campus under natural conditions.

According to the experimental results,

1/ The efficiency of the prototype is much higher than the models tested in a wind tunnel. It varies between 34-53%, and does not fall below 34% of the power in the wind in relatively lower and higher speeds.

2/ The efficiency reaches its peak value of 53% as the outer rim of the turbine reaches a velocity equal to that of the wind. At high wind speeds, the rotational velocity of the rotor rim is about twice the wind speed.

3/ In a region of similar wind regime as the testing region, a $1m^2$ area turbine when reinforced with the necessary flywheel system and control circuitry, is found powerful enough to charge a car battery continuously.

4/ For two regions of annual averages 10-15 mph, any size prototype turbine of the same diameter as that tested is found to have a generating capacity of about 95 $\frac{\text{kw-hr}}{\text{YEAR-m}^2}$ and 220 $\frac{\text{kw-hr}}{\text{YEAR-m}^2}$ for constant torque operation.

ÖZÜ

Bu araştırmanın gayesi, dikey eksenli bir rüzgar türbününün açık havada doğal şartlar altında, verim karakteristikleri ve pratik yararlılık açısından incelenmesini mümkün kılacak deney sistemini kurmaktır.

Savonius tipi bir rüzgar türbünü prototipi, ön çalışmalarla tespit edilen ideal ölçülerde imal edilmiştir. Gerekli ölçüm cihazlarının da kuplajı ile Mühendislik Binasının çatısında denenmiştir.

Söz konusu deneylerle varılan neticelere göre,

1/ Prototip türbünün verimi, rüzgar tünelinde modeller üzerindeki bulgulara kıyasla çok daha yüksek olup, %34-53 arasında değişmektedir. Düşük ve yüksek hızlarda elde edilen güç, rüzgardaki gücün % 34'ünün altına düşmemektedir.

2/ Verim, türbün kanadının en dış noktası rüzgara eşit bir sürate yaklaştığında, en yüksek değer olan % 53'e ulaşmaktadır. Yüksek rüzgar hızlarında, kanatların dış kenarının hızı, rüzgar süratinin yaklaşık iki mislisidir.

3/ Rüzgar rejimi deney sahasından pek farklılık göstermeyen bir yerde, $1 m^2$ lik bir türbün, gerekli volan sistemi ve kontrol devreleriyle takviye edildiğinde, bir oto aküsünü sürekli şarj edebilecek güçte görülmüştür.

4/ Yıllık rüzgar ortalaması saatte 10-15 mil olan iki bölge için, bu türbünün aynı çaptaki herhangi bir prototipi, sabit tark çalışma esasına göre 95 $\frac{\text{kw-saat}}{\text{sene-m}^2}$ - 220 $\frac{\text{kw-saat}}{\text{sene-m}^2}$ kapasitesinde bulunmuştur.

ACKNOWLEDGEMENTS

The author is extremely grateful to Dr. Emre Aksan for his valuable suggestions, appreciated guidiance and patient supervision throughout the course of this work.

The author is deeply indebted to the members of the machine shop, İsmail Üzümcü,Suphi Özmıhçı and Mustafa Ünal for their kind helps in the manufacturing of necessary components.

Special appreciation is expressed to Fehmi Günsoy and Cevat Gül ; members of the Electrical Engineering Department for their contributions in instrumentation.

Particular thanks are extended to Sedat Gözde and Subhi Toplu their kind interest in the work and valuable asistance in documentation and construction.

TABLE OF CONTENTS

LIST.OF FIGURES

LIST OF TABLES PAGE

MOMENCLATURE

A = Effective rotor area.
a = Axial interference factor.
C_p = Power coefficient ($=\eta_p$).
C'_p = Betz efficiency.
C_T = Torque coefficient
D = Rotor diameter.
F = Thrust force on blades
f = Flow concentration factor.
g = Gravitational acceleration constant.
H = Height of rotor.
I = Current.
i = Transmission step-up ratio.
$\dot{m}$ = Mass flow rate.
n = Revolutions per minute of rotor.
P' = Power delivered by the wind turbine
P_G = Power density of the Wind turbine
Q = Volumetric flow rate.
R = Resistance.
Re_D = Reynolds' number ($=\rho\mu$).
r = Radius of rotor blades.
s = Venting distance between rotor blades.
T' = Torque delivered by the rotor
v = Wind Speed.
W_K = Work done.
W_o = Rotation rate under no-load.
w = Rotation rate under load.
X_o = Tip speed ratio under no-load.
X = Tip speed ratio under load. ($=\eta_v$)
x = Center to center distance of rotor.
Z = Height above a reference.

β = Flow deflecting factor.

γ = Averaging factor of torque ; weight density.

μ = Viscosity coefficient of air.

π_A = Aspect ratio.

π_B = Pressure coefficient.

π_P = Power ratio.

π_V = Tip speed ratio.

π_μ = Viscosity coefficient.

π = Torque coefficient.

ρ = Air density.

ν = Kinematic viscosity of air.

η = Yearly generating efficiency of the turbine under constant torque ; ratio of power coefficient to Betz efficiency.

PRAISED BE MY LORD GOD
ESPECIALLY FOR OUR BROTHER
THE WIND AND FOR AIR AND
CLOUD CALMS AND ALL
WEATHER BY WHICH THOU
UPHOLDEST IN LIFE ALL
CREATURES

(FRANCIS OF ASSISI)

CHAPTERS

I- INTRODUCTION

1.1/ Philosophy of This Work :

Nowhere is the problem of energy more critical than in populous developing countries which are poor in conventional fuel resources. The cost of imported fuel is draining their meager foreign exchange reserves, crippling their economies, and retarding real growth. Under such circumstances, the traditional trend of judging a power generating device on the basis of its ability to deliver power competitively with conventional generators may be misleading (7)

Large scale conventional power plant, such as hydro-power has an important part to play in development. It does not however provide a complete solution in a small time period. There is an important complementary role for the greater use of small scale rural based power plant. Such a plant can be used to assist development since it can be made locally using local resources on a relatively miniscule bu get enabling a rapid build up in total equipment to be made without a corresponding and unnacceptably large demand on central funds.

A typical characteristic of developing nations is that, a sizable percentage of the population live in small communities in a dispersed fastion, thus it has been recognised that, availability of small scale energy systems at the rural level can make a difference between gradual progress and perennial poverty.

This energy can be generated from our renewable energy potential with particular emphasis on systems that can be built with the intermediate technology and materials available.

In the short term, we require mechanisms to enable the rapid increase in enargy per capita, and in the long term, we should be working towards a way of life which makes use of energy efficiently and without the impairment of the environment, or of causing safety problems. Such a program should as far as possible be based on renewable energy resources.

1.2/ A Perspective Look Over Wind Power Utilization

Harnessing wind power thru windmills is not a new concept. It has been used for centuries in direct applications as,

- water pumping
- grain grinding
- fodder cutting, .. ect. (1)

However, especially with the development of internal combustion engines and availability of cheap fuel in the beginning of 20th century, the ideas related with the utilizati and development of power generating devices from wind were left aside without any serious attention due to the major inherent drawbacks such as,

1/ Comparatively large valume to power ratio, implying higher cost per unit power output.

2/ Uncertainty in the continuous availability of power.

On the other hand, by time, it was realized that fossil fuel the conventional source of energy, was depleting at a fast rate, which caused the continuous increase of prices. With the cost of imported fuels and the possibility of prolonged drought conditions, the entire energy problem has taken more critical dimensions. Utilization of energy is an essential component of development, however, limited fossil fuel reserves will be needed for more productiwe purposes than

---

(1) A detailed engineering study about utilization of wind power in civilization history can be found in ref.((3)).

for simply burning to generate electricity

It was as late as 1970's when scientists and engineers re-started to pay interest in developing equipment for utilization of non- conventioanal renewable energy sources like solar, tidal, geothermal, ocean thermal gradient as well as the wind.

1.3/ Elementary Remarks

The problem of finding the amount of recoverable wind energy and methods of evaluation is itemized as follows:

1.3.1/ The Pressure Storage System

In a sense, the wind is one of the nature's solar energy storage systems. The sun heats the earth's surface, causing the air to expand and build up a pressure gradient between one region and another. The pressure gradient is the storage system, and the wind, the conversion device for relieving the pressure.

The strength of surface winds at any location is governed by the magnitude of the pressure gradient just above the planetary boundary layer and the atmospheric stability in the boundary layer.

The pressure gradient, which is due to the differential absorbtion of solar radiation is reinforced near the coasts due to the thermal contrast between the land and the sea, giving rise to relatively stronger winds at coastal regions.

There is no present technology capable of controlling the pressure storage system to create the required steady and strong winds, neither a hope to make use of hurricanes or tornadoes which are estimated to develop more energy than a hydragen bomb explosion.

These man-made conversion devices, the windmills are constrained to operate in a narrow band at about 8 to 60 miles an hour, and are able to convert only 59.3% of the power in the wind passing this the cross-sectional area.(*)

1.3.2/ Wind Velocity as a Function of Height Above the Ground:

Unlike the case of solar energy, the surfaces normal to the wind are in vertical direction such that, speed and constancy increase with height above the ground. Thru dimensional a n a l y s i s, a general equation can be obtained for determining wind velocity at a specific height over some reference height above the ground. Namely,

$$v = v' \left(\frac{h}{h'}\right)^{\frac{1}{N}}$$

where,

h = height above ground.

h' = reference height above the ground $\ni$ $h' < h$

v' = wind speed measured at reference height h'

v = wind speed at desired height h.

and,

$\frac{1}{N}$ is the estimated power law increase.

The quantity substituted for N depends upon terrain conditions. In open farm country and level or slightly rolling terrain, a factor 7 can be substituted for N In level and rolling country with numerous obstructions, such as in suburban areas, the factor is 5. An estimate of 3 is appropriate for city outskirts and near suburbs as well as areas with large obstructions.

(*) Derivation of this factor (called Betz Limit) is given in § 2.2

The above equation is generally used as h' = 30 feet above the ground. Taking h' as such, giving arbitrary values to v', we obtain different velocity profiles. Tables given below are related to the two curves submitted in order to illustrate the corresponding velocity profiles.

a/ let v' = 10 ft/sec at h=h'=30 feet.=> v = 10 ft/sec assigning arbitrary values to h, below table is formed:

h	v	v-v'
40	10.4	0.4
50	10.7	0.7
60	11.0	1.0
70	11.3	1.3
80	11.5	1.5
90	11.7	1.7
100	11.8	1.8
110	12.0	2.0
120	12.2	2.2
130	12.3	2.3
140	12.5	2.5
150	12.6	2.6

TABLE 1.3.1 Wind Velocity Variation with Heigh Above the Ground for a Reference Value of 10 ft/sec.

b/Let v' = 20 ft/sec at h=h'=30 feet => v = 20 ft/sec: assigning arbitrary values to h, below table is constructed:

h		
40	20.8	0.8
50	21.5	1.5
60	22.1	2.1
70	22.6	2.6
80	23.0	3.0
90	23.4	3.4
100	23.8	3.8
110	24.1	4.1
120	24.4	4.4
130	24.7	4.7
140	24.9	4.9
150	25.2	5.2

TABLE 1.3.2. Wind Velocity Variation with
Above the Ground for a
Reference Value of 20 ft/sec

The velocity profile curves related to tables a/ and b/ above are submitted below.

From observation of the curves, we conclude that the changing behavior of wind speed with respect to a reference height above the ground is more violent as wind speed at the reference height increases. It is due to this fact that ultimate limit of wind energy per unit area is not measurable unlike the case of solar energy.

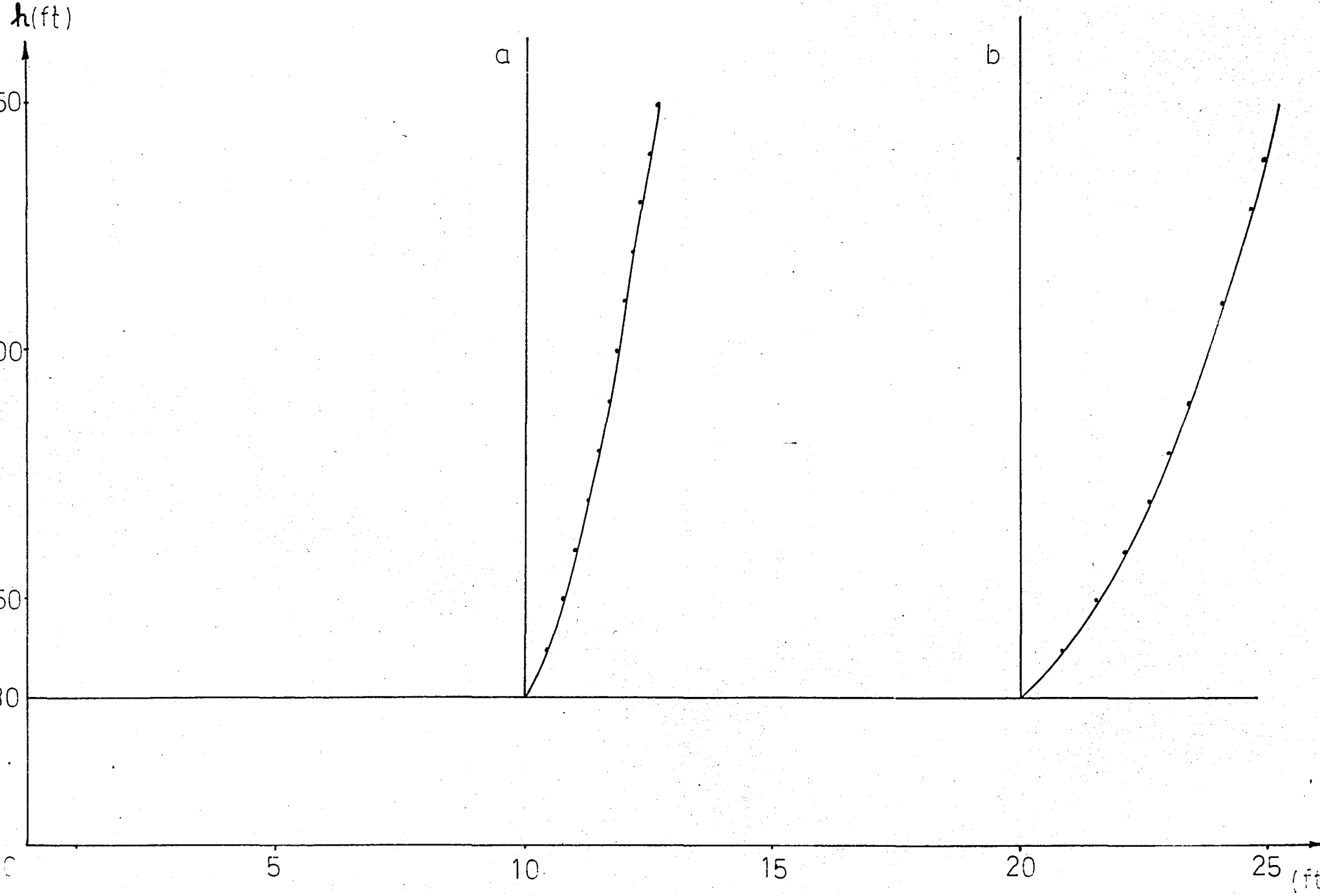

FIG.1.3.1. Wind Velocity Variation With Height Above the Ground for Reference Values of 10 ft/sec and 20 ft/sec Respectively

1.3.3/ Wind Velocity Modifying Items:

Influences of local tapography, and artifical obstructions modify the true wind speed a considerable amount.

Over certain preferred locations like mountain gaps, estuaries, creeks and gulfs, wind speeds attain unusually high values, while at the vicinity of an obstruction 2 or 3 mph fluctuations around the true speed can be recorded.

Therefore, published weather bureau data are not much reliable for statistical predictions, since they are placed either at locations representative of general area, or at stations chosen largely for temperature and solar measurements, or in general weather conditions.

1.3.4/ Nature of Wind:

Wind energy is randomly intermittent. There are periods of calm interspersed with periods of storms or gusts Therefore,

a/ Eleborate steps have to be taken to obtain predictable statistical averages of wind speed at a certain region to predict the annular energy capacity which is proportional to the cube of wind speed.(1)

b/ Intervals of calm must be considered in planning the energy storing block of the wind generating system, or means of augmentation of wind energy by other sources must be searched.

The above points about the nature of wind conclude to the result that, the question 'How much wind energy is there?' is somewhat naive. The only practical question to ask is,

---

(1) *Statistical treatment of wind data is considered in § 2.1*

'How much wind energy can man harvest at one locality?' This question is answered by combining responses from two sources:

i/ Long term measurements of wind speeds at a chosen Locality.
ii/ A computation of the output potential of the wind machine.
These two facts have to be suitably balanced in a windmill design, to reach meaningful results.

1.3.5./ Power in the Wind:

Power in the wind is directly proportional to:
a/ cube of wind speed
b/ area normal to its direction.
Namely,
$P = K A v^3$ (*)
Where,
P = power in the wind thru normal area A.
K = Constant, involving the density of fluid (air for our case)
v = Wind speed.

Importance of long term wind survey of a site before installing a windmill cames from the cubic proportionality of power to wind speed. There is 4.6 times as much energy in the wind at 25 mph as at 15, and 2.7 times as much as at 18 mph. A difference of even 2 mph in average wind speed can make a significant difference in the total output for the year. Differences of 2 to 5 mph can easily occur within a Locality.

(*) *The derivation of this equation is made in the forecoming sections. (It has to be reduced by a factor of 0.593 to predict the maximum output of the ideal wind machine.)*

1.4/ Classification of Wind Machines:

Wind machines can be classified with respect to numerous criteria ((3)) Some of these are.

1.4.1/ Axis:

a/ horizontal axis.
b/ vertical axis.

1.4.2./ Speed of Rotation/Solidity Ratio:

a/ high solidity (Low speed of rotation; high starting torque delivery; moderate or Low efficiency.)
b/ Low solidity (high speed of rotation; Low starding torque delivery; higher efficiency.)

1.4.3./ Mounting of Blades: (for speed regulation)

a/ fixed pitch blade
b/ variable pitch blade.

1.4.4./Scale:

a/ Small scale (from 0 - 5 kw output)
b/ Medium scale (from 5-100 kw output)
c/ Large scale (over 100 kw output)

These items are analysed below:

1.4.1/ Axis : The most critical differentiation of windmills is in their type of axis around which the rotating structure is revolving either being horizontal or vertical .

The decision on the type of axis of a WGS (Wind power Generating System) is strategic in serviceability, practicality, as well as efficiency of the system.

Typically, the horizontal-axis wind machines are of the propeller type which have existed for centuries in various forms.(*)
An illustrative figure for this class of windmills is given below:

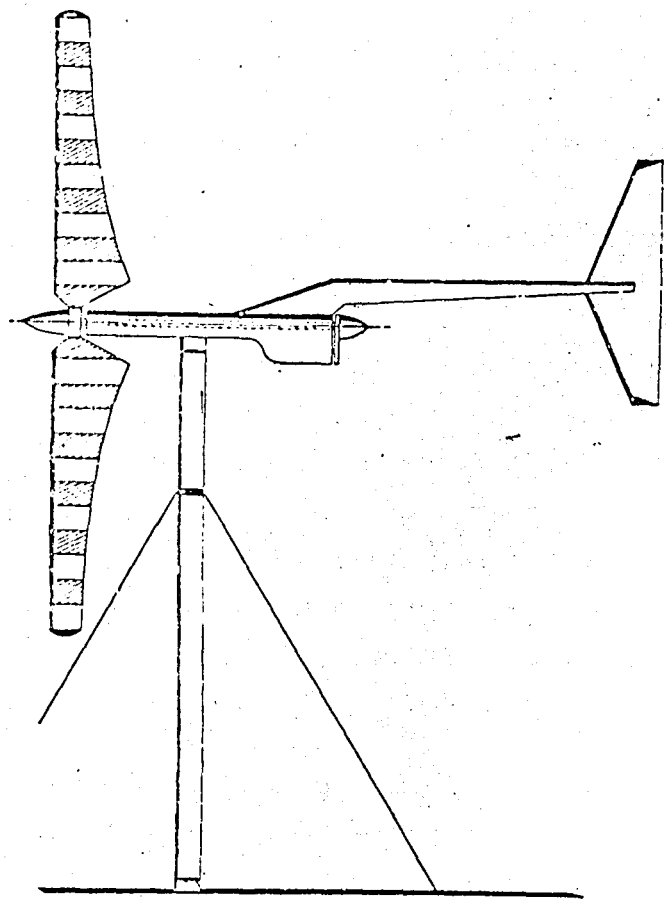

FIG. 1.4.1 PRINCETON SAILWING WIND GENERATOR

Source: T.E. Sweeney and W.B. Nixon, PB-231 341, December 1973

(*) *Detailed analysis about main engineering projects involving horizontal-axis wind machines can be found in references ((3)), ((11)), ((8)) and ((9)).*

A major drawback of the horizontal axis is that, plane of blade rotation must constantly change as the wind direction changes. (Usually accomplished in practice by affixing a "tail" or vertical stabilizer to the rear of the rotor, and allowing the rotational axis to pivot into the wind.) This introduces gyroscopic loods, and a design constraint that the response of the machine to changes in wind direction must be sufficiently rapid to track and capture the available kinetic energy.

Another problem is the power-take-off. If the aim is to generate electric energy, there are 2 alternatives:

a/ Connecting the generator directly to the propeller at the top of the tower,
b/ Locating it at ground level, with a suitable mechanism providing the necessary connection with the propeller.

The 1st choice needs a strong tower structure due to vibration problems induced by excessive load, high above the ground; and the 2nd choice necessitates a complex drive train. Both of the choices associated with coupling the generator to the rotor suffer from the inherent drawbacks mentioned above, having remedies which will increase complexity and cost, while the level of power generated will probably not compensate the expenses.(16)

The vertical-axis windmills (of which the cup anemometer is a typical example; see fig below) on the other hand, have some appealing inherent features, such as:

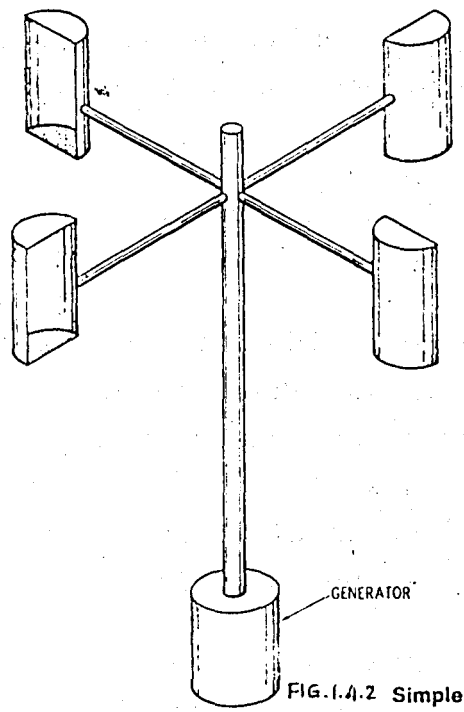

FIG.1.4.2 Simple vertical-axis rotators.

a/ No necessity of a special tower structure; such machines fixed by guy wires can serve as their own tower.

b/ Omnidirectional nature; ie response to wind pressure re gardless of wind direction, permitting the rotor to extract the energy of a given wind or gust instantaneously regardless of any rapid changes in direction.

c/ Power-take-off at ground level.

In general, there is a reduction in both complexity and maintenance by using such a structure.

The items below, inherent in horizontal axis designs are thus avoided:

a/ Excessive generator weight on the top of the supporting tower necessisating a stronger tower or a complex drive train.

b/ Efficiency drop (with respect to wind-tunnel test results) due to the fact that wind changes direction much

more rapidly than a horizontal-axis system can adjust itself. This feature becomes more apparent in larger systems of higher inertia.

c/ Yaw problems and yaw mechanisms related to this problem (51)

The horizontal-axis machines were improved over the years and recieved substantial attention perhaps largely due to the availability and advance of propeller theory. However, with the recent upsurge in wind energy, a number of projects were started to re-evaluate and develop the old ideas of the rather inventive period of the 1920's.

Two most out standing examples of vertical-axis windmills under current investigation are the Darrieus and Savonius (*) rotors. They are introduced in the figures below:

DARRIEUS ROTOR

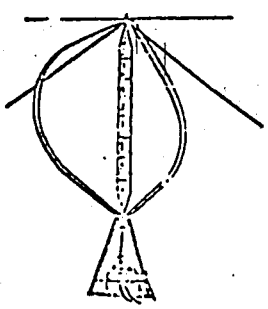

BACKGROUND

PATENTED IN 1931 (US AND FRANCE)

CURRENTLY UNDER STUDY AT NATIONAL AERONAUTICAL ESTABLISHMENT, OTTAWA, CANADA

CHARACTERISTICS

EFFICIENCY ~ 35%

TIP SPEED TO WIND SPEED ~ 6 TO 8

POTENTIALLY LOW CAPITAL COST

CURRENTLY NOT SELF STARTING

S-ROTOR

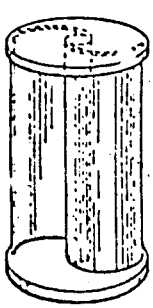

BACKGROUND

PATENTED IN 1929 (US AND FINLAND) BY S. J. SAVONIUS

CURRENTLY USED AS AN OCEAN CURRENT METER

OTHER APPLICATIONS SHOWN FEASIBLE

CHARACTERISTICS

TIP SPEED TO WIND SPEED ~ .8 TO 1.8

EFFICIENCY ~ 31%

SELF STARTING

VERTICAL AXIS ROTORS OPERATE INDEPENDENTLY OF WIND DIRECTION AND THUS HAVE A POTENTIAL FOR HIGH EFFICIENCY IN CHANGING WINDS

FIG. 14.3 VERTICAL AXIS WIND ROTORS

Source: W. Vance, PB-231 341, December 1973

(*) *Savonius rotors are explained in detail in chapter 3.*

The Darrieus turbine was invented by G.J.M. Darrieus of France; patend applications were filed in France and in the United States in 1925 and 1926 respectively. It appears that the Darrieus turbine concept lay dormant until the mid 1960's, when it was independently re-invented by the National Aeronautical Establishment of the National Research Counal of Canada (NAE/NRC). Extensive wind tunnel test programs have been undertaken since then by numerous research laboratories such as, NRC, Canada (Catenary blades) (32), Sandia, USA (Circular arc with straight ends) (36,40) WVU, USA (Vertical straight blades) (33); BHEL, India (Vertical blades with inclined ends) (34,35,38) ect.[1]

The S shaped rotor was developed and patented by S.J. Savonius in 1929. It has not attracted much research attention due to the inherent high inertia and low speed characteristics,[2] which makes it infeasible for electric power generation.

---

(1) *Theoretical as well as experimental analysis of Darrieus turbines can also be found in references (1), (3), (8), (9), (10), (11) and (19).*

(2) *Various investigations on S rotors may be found in references. (24), (23), (21).*

1.4.2./ Speed of Rotation / Solidity Ratio:

Windmills are often classed as low(1) or high speed (2) models. A low speed system is a very heavy affair but it develops a high torque at start. It does make more efficient use of light wind in the conversion between wind energy and mechanical energy. Such an installation can be adapted for operation as a water pump, and can be used in other devices that require a conversion between wind and some sort of mechanical activity.

The reverse is valid in the case of a high speed or high-rpm windmill. Despite the lower efficiencey (especially in a low wind), it is more suitable to the conversion of wind energy to electrical energy.

---

(1) *Tip speed ratio*(3) *not being more than 2.*

(2) *Tip speed ratio being more than 2 at the normal region of operation.*

(3) *Tip speed ratio is the rotational tip velocity of the mill* to wind velocity

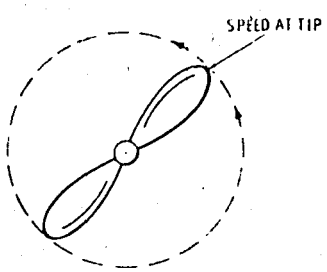

It is thus given by,

$$X=\frac{wD}{2v^{\infty}}$$

FIG. 1.4.4. Tip Speed

In fact, it is the ratio of the speed of motion of the very tip of table blade to wind speed. A typical figure might be 4. Using this figure as an example, the tipspeed of a particular blade when made active by a 12 mph wind would be 48(=12x4)mph.

Less weight is involved, and it presents a structure less subject to damage from strong gusty winds. Its high speed of rotation is more adaptable to low ratio gearing of electrical generators, and in some installations, can provide direct drive of the generator axle (20).

For horizontal-axis wind machines, speed of rotation is directly related to the number of blades. A 2 or 3 bladed rotor is a high speed (low torque, low solidity[1]) device, while a windmill having many blades is usually a low speed (high torque, high solidity) system.

Among the vertical-axis wind rotators. The Savonius and Darrieus designs are examples of low speed (high solidity) and high speed (low solidity) extremes.

For a given rotor radius, a high-speed windmill has a much higher tip speed than a lower-speed one(20). The derivation of this and other dimensionless parameters is submitted in §2.7.

(1) The speed of rotation of a windmill is strongly dependent on the area of the blades compared to the projected area exposed to the wind. This leads to the definition of the solidity ratio in the ultimate.

$$\sigma \triangleq \frac{A'}{A},$$

σ = Solidity ratio.

A = Area projected against the wind.

A' = total area of blades.

1.4.3./ Mounting of Blades

Mechanisms are designed so that the rotor blades adjust themselves automotically as a precaution to the wind velocity exceeding a predetermined level, thus,

a/ undesired stresses at the blades due to overspeeding are avoided.

b/ The safety of the coupled mechanism or device (such as a generator) is guarenteed.

Such wind machines are referred to as variable pitch blade machines. These systems are commonly used in horizontal-axis wind machines simply by using appropriate torsion springs at the hub which bring the blades to feathering position in case of wind gusts. Below is such a mechanism for a 4 bladed Savonius rotor.

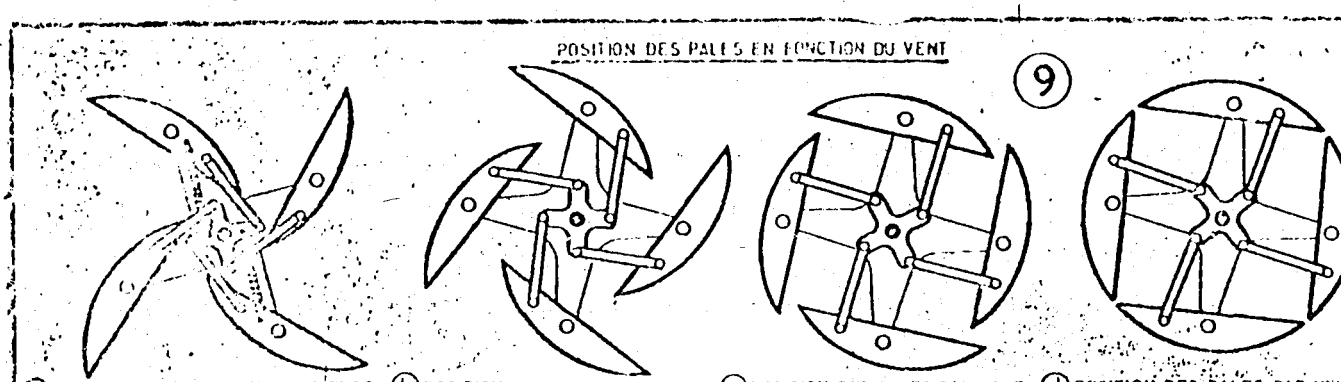

FIG. 1.4.5. Blade Positions for a Variable Pitch Blade 4-cup savonius rotor.

1.4.4./ Scale :

Naturally, the scale of power follows immediately upon demand analysis. However, there are some limitations to match demands over a certain level, mainly because the low energy density (energy per unit area) of wind, and the theoretical restriction that only 59.3% of the energy in the wind can be utilized. Due to these two facts, it is necessary to use relatively large area installations for capturing of moderate levels of power.(1) In horizontal-axis windmills, this can be achieved by increasing the blade diameter. Since power, is directly proportional to cross-sectional area, therefore the square of blade diameter. (recall, $P = KAv^3$; $\Rightarrow$ $P = K'D^2v^3$) Hovewer, the engineering problems induced in the establishment of large horizantal-axis units generally increase the cost of generation to un-economic levels.

The largest and most outstanding WGS ever built was the Smith-Putnam machine installed in 1940's with $2220m^2$ swept area by 2 blades, generating 1-25 MW at 15.3m/sec wind velocity.(2) It ended up in failure like most large-scale installations of its time.

The vertical-axis windmill technology is not at a competing level yet in generating large - scalepower (over 100 KW.) Small (1-5 kw) and medium (5-100 kw) scale applications have been carried out with considerable success in numerous realizations(1).

---

(1) *Quantitative details can be found in § 2.3*

(2) *Seereference ((8)) written by P.C. Putnam. Detailed information and analysis about medium/large Scale power production with horizontal-axis turbines can be found in references. ((2)),(16),(6),(34),(39),(41).*

2/ GENERAL THEORETICAL CONSIDERATIONS

2-1/ Power in the Wind:

Computation of the power in the wind derives in the ultimate from the fundamental, physical equation for kinetic energy per unit mass:

$$\frac{KE}{m} = \frac{1}{2} v^2 . \qquad 2.1.1.$$

Recalling the equation of mass discharge ,

$$m = \rho A v \qquad 2.1.2.$$

The power (energy/time) expression is,

$$Pw = \frac{1}{2} Av^3 \text{ from side by side product of 2.1.1 and 2.1.2.} \qquad 2.1.3.$$

It is naturally not possible to harvest all be energy in the wind. The maximum amount depends on the power coefficient C'_p

$\therefore \quad 0 < C'_p < 1$

Thus, 2.1.3. can be written as,

$$P' = C'_p \frac{1}{2} \rho A v^3 \qquad 2.1.4.$$

or,

$$P' = C'_p Pw.$$

where,

P'= power output of wind machine

Pw power in the wind, ($=\frac{1}{2}\ \rho A v^3$)

2.1.4. can be derived also from the energy equation of fluid mechanics as given by 2.5.3.

With the determination of Cp', an expression can be obtained to predict the fraction of the total amount which can be recovered.

2.2/ Amount of Power Recoverable From the Wind, Determination of Cp' (The Windmill Law):

A.Betz, of the Institute of Gottingen, in his studies of the windmill publishedin 1927, applied the simple momentum theory, established by W.J.M. Rankine and W.E. Froude for the ship 'S propeller, to the windmill. He treated the air as an ideal fluid and assumed an idealized rotor called an actuator disc. He neglected the angular momentum of the air stream in the wake i.e. his theory is strictly a linear momentum theory. The result of that investigation shows that the ideal rotor (called an ideal windmill) can extract 16/27 (59.3%) of the power from the wind. This theory is still used today by many known wind power researchers.

The figure below shows the velocity and pressure distributions existing when an ideal rotor (actuator disc) extracts energy from an air stream. (2)

Some modifications have been done due to the different objectives of a windmill and a propeller. As far as the flow picture is concerned, the windmill is the reverse of the propeller. In the windmill, the slipstream widens as it passes the machine, and the pressure P_2 (referring to the below figure) is greater than the pressure P_3.

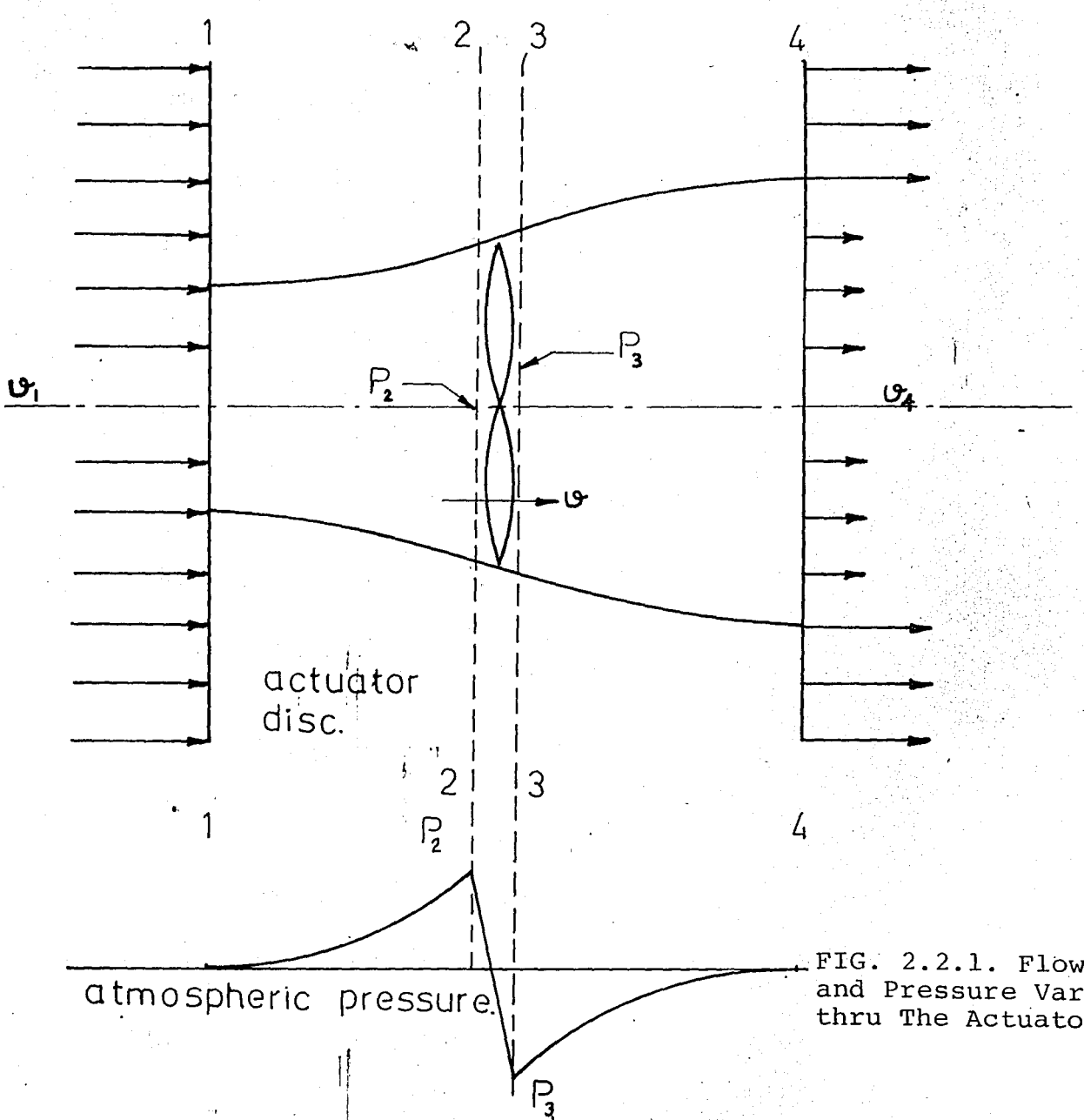

FIG. 2.2.1. Flow Picture and Pressure Variation thru The Actuator Disc.

The velocity thru the windmill as thru the propeller may be shown to be the numerical average of inlet and exit velocities Namely,

$v = (v_1 + v_4)/2$. This fact is used in the derivation of an efficiency expression. A step -by- step procedure developed from te extension of the outlines in references ((3)) and

([6]) is given below:

The force exerted on the windmill by the flow is,

$$F = (p_2 - P_3)A \qquad 2.2.1$$

A being the area of the windmill,
or,

$$F = v_1 \rho_1 v_1 A_1 - v_4 \rho_4 v_4 A_4 \qquad 2.2.2.$$

Assuming incompressible flow, ie,

$$\rho_1 = \rho_4 = \rho_1 \qquad 2.2.3.$$

also recalling the valumetric flow rote,

$$Q_1 = Q_4 = Q = v_1 A_1 = v_4 A_4 = vA \qquad 2.2.4.$$

2.2.3 and 2.2.4 $\longrightarrow$ 2.2.2,

$$\Rightarrow F = v_1 \rho Q - v_a \rho Q$$

$$\Rightarrow F = \rho Q (v_1 - v_4) \qquad 2.2.5.$$

Equating 2.2.1 and 2.2.5,

$$(P_2 - P_3)A = \rho Q (v_1 - v_4) \qquad 2.2.6.$$

The energy principle between 1 2 reads

$$(W_k) + \text{losses} + \frac{P_2}{\gamma} + Z_2 + \frac{v^2}{2g} = \frac{P_1}{\gamma} Z_1 + \frac{v_1^2}{2g}$$

Neglecting the work, losses and the potential difference terms,

$$\frac{P_2}{\gamma} + \frac{v_2^2}{2g} = \frac{P_1}{\gamma} + \frac{v_1^2}{2g} \qquad 2.2.7.$$

Application of the principle of energy between 3 and 4,

$$\frac{P_4}{\gamma} + \frac{v_4^2}{2g} = \frac{P_3}{\gamma} + \frac{v_3^2}{2g} \qquad 2.2.8.$$

Adding 2.2.7 and 2.2.8 side by side, we have,

$$\frac{P_2}{\gamma} + \frac{P_4}{\gamma} + \frac{v_2^2}{2g} + \frac{v_4^2}{2g} = \frac{P_1}{\gamma} + \frac{P_3}{\gamma} + \frac{v_1^2}{2g} + \frac{v_3^2}{2g} \qquad 2.2.9.$$

We also have,

$$v_2 = v_3 \qquad 2.2.10.$$

and

$$P_1 = P_4 \qquad 2.2.11.$$

2.2.10 and 2.2.11 $\longrightarrow$ 2.2.9,

$$\Rightarrow \frac{P_2-P_3}{\gamma} = \frac{v_1^2 - v_4^2}{2g}$$

$$\Rightarrow P_2-P_3 = \frac{\gamma}{2g} (V_1^2-v_4^2)$$

$$\Rightarrow P_2-P_3 = \frac{\rho}{2} (v_1^2 - v_4^2) \qquad 2.2.12.$$

2.2.12. $\longrightarrow$ 2.2.6,

$$\frac{\rho}{2} (v_1^2-v_4^2)A = \rho Q(v_1-v_4)$$

using 2.2.4,

$$\frac{1}{2} (v_1^2-v_4^2) A = vA(v_1-v_4)$$

$$\Rightarrow \frac{1}{2}(v_1-v_4)(v_1+v_4)A = vA(v_1-v_4)$$

Thus,

$$v = \frac{v_1 v_4}{2} \qquad 2.2.13.$$

2.2.12. ——————>2.2.1,

$$F = \frac{\rho}{2}(v_1^2-v_4^2)A$$

Power output of the windmill is,

$$P' = Fv = \frac{\rho}{2}(v_1^2-v_4^2)Av.$$

using 2.2.4,

$$P' = \frac{Q}{2}(v_1^2-v_4^2) \qquad 2.2.14.$$

We have assumed a frictionless machine, such that the power delivered to the windmill must be exactly that extracted from the air, which in turn is represented by the decrease of the kinetic energy of the slipstream between sections 1 and 4.

On the other hand, the theoretical available power in a streamtube of cross-sectional area A and wind velocity v_1 was derived to be

$$P' = \frac{1}{2}\rho A v_1^3 \qquad (2.1.3.)\ 2.2.15.$$

It is customary to define windmill efficiencies by the ratio of this power output (=P') to the total power available (=Pw)

$$Cp' = \frac{P'}{Pw} = \frac{\frac{Q}{2}(v_1^2 - v_4^2)}{\frac{1}{2}\rho A v_1^3} \qquad 2.2.16$$

From 2.2.4,

$Q = vA$

using 2.2.13,

$$Q = \left(\frac{v_1 + v_4}{2}\right) A \qquad 2.2.17.$$

2.2.17 ——> 2.2.16,

$$\Rightarrow Cp' = \frac{\left\{\left(\frac{v_1 + v_4}{2}\right) A\right\} \frac{\rho}{2}(v_1^2 - v_4^2)}{\frac{1}{2}\rho A v_1^3}$$

$$\Rightarrow Cp' = \frac{(v_1 + v_4)(v_1^2 - v_4^2)}{2v_1^3}$$

$$= \frac{v_1\left(1+\frac{v_4}{v_1}\right) v_1^2 \left(1-\frac{v_4^2}{v_1^2}\right)}{2v_1^3}$$

$$= \frac{v_1^3\left(1+\frac{v_4}{v_1}\right)^2 \left(1-\frac{v_4}{v_1}\right)}{2v_1^3}$$

$$= \frac{1}{2}\left(1+\frac{v_4}{v_1}\right)^2 \left(1-\frac{v_4}{v_1}\right) \qquad 2.2.18.$$

Let $\frac{v_4}{v_1} = x$

$$\Rightarrow Cp' = \frac{1}{2}(1 + x)^2(1-x)$$

$$\frac{1}{2}(1 + x - x^2 - x^3)$$

The maximum theoretical efficiency is found by differentiating Cp' with respect to $x \left(= \frac{v_4}{v_1}\right)$ and setting the result equal to zero.

$$\Rightarrow \frac{dCp'}{dx} = 0 = \frac{1}{2} - x - \frac{3}{2} x^2$$

$$\Rightarrow 3x^2 = 2x - 1 = 0$$

$$\Rightarrow x_1, x_2 = \frac{-2 \pm \sqrt{4-(4)(3)(-1)}}{(2)(3)}$$

$$x_1 = \frac{-2\ 4}{6} = \frac{1}{3}\ ;\ x_2 = \frac{-2-4}{6} = -1$$

$\frac{v_4}{v_1} = \frac{1}{3}$ is the value that maximizes Cp'

2.2.19 ———>2.2.18,

$(Cp')_{max} = \frac{16}{27}$ (corresponding to 59.3 percent)

Thus 2.1.4. becomes,

$$P'_{max} = \frac{16}{27} \cdot \frac{1}{2} A v^3 \qquad 2.2.20$$

However, this thereotical efficiency is never realized in practice due to friction and all kinds of other losses. Thus it is necessary to modify 2.2.20 with an another efficiency η, which probably changes with the Reynolds' number for a particular wind turbine.

$$P' = \eta \frac{16}{27} \cdot \frac{1}{2} \rho A v^3 \qquad 2.2.21.$$

or,

$$P' = \eta Cp' Pw$$

where,

$$Cp \triangleq \eta Cp'$$

2.3./ Power Density of Wind and Wind Machines:

Derivation of equations 2.1.3, 2.2.20 and 2.2.21 enables us to visualize the magnitude op power that can be extracted from a certain area. Defining the power density as the ratio of power to area of rotor, 2.1.3, 2.2.20 and 2.2.21 can be written as,

$$\frac{Pw}{A} = \frac{1}{2} \rho V_\infty^3 \qquad 2.3.1.$$

$$\frac{P'_{max}}{A} = Cp' \frac{1}{2} \rho v_\infty^3 \qquad 2.3.2.$$

$$\frac{P'}{A} = \eta Cp' \frac{1}{2} \rho v_\infty^3 \qquad 2.3.3$$

Thus, we can plot the power density us wind velocity of the

three equations above on the same axes for comparison.

We recall that $Cp' = \frac{16}{27}$ and assume the density of air is $\rho = 1.23 \frac{kgf}{m^3}$. (sea level value) and $\eta = 0.40 \forall Re_D$.

Expressing the velocity and power in various units, equations 2.3.1, 2.3.3 which are given in numerous forms in different references may be tabulated as below:

	2.3.1	2.3.2	2.3.3		
unit of power density	$1/2\rho Av_\infty^3$	$Cp'\frac{1}{2}\rho Av_\infty^2$	$\eta Cp'\frac{1}{2}\rho Av_\infty^3$	unit of wind velocity	
$\frac{kw}{m^2}$	$6.2x10^{-4}v_\infty^3$	$3.67x10^{-4}v_\infty^3$	$1.47x10^{-4}v_\infty^3$	$\frac{m}{sec}$	(i)
	$1.33xy0^{-5}v_\infty^3$	$7.88x10^{-6}v_\infty^3$	$3.15x10^{-6}v_\infty^3$	$\frac{km}{hr}$	(ii)
	$5.5x10^{-5}v_\infty^3$	$3.25x10^{-5}v_\infty^3$	$1.30x10^{-5}v_\infty^3$	$\frac{mi}{hr}$	(iii)
$\frac{kw}{ft^2}$	$5.1x10^{-6}v_\infty^3$	$3.02x10^{-6}v_\infty^3$	$1.21x10^{-6}v_\infty^3$	$\frac{mi}{hr}$	(iv)
$\frac{hp}{m^2}$	$8.2x10^{-4}v_\infty^3$	$4.86x10^{-4}v_\infty^3$	$1.94x10^{-4}v_\infty^3$	$\frac{m}{sec}$	(v)
	$4.76x10^{-5}v_\infty^3$	$1.04x10^{-5}v_\infty^3$	$4.17x10^{-6}v_\infty^3$	$\frac{km}{hr}$	(vi)
	$7.33x10^{-5}v_\infty^3$	$4.34x10^{-5}v_\infty^3$	$1.74x10^{-5}v_\infty^3$	$\frac{mi}{hr}$	(vii)
$\frac{hp}{ft^2}$	$6.81x10^{-6}v_\infty^3$	$4.03x10^{-6}v_\infty^3$	$1.61x10^{-6}v_\infty^3$	$\frac{mi}{hr}$	(viii)

TABLE 2.3.1. Power Density Equations in Various Units of Power and Velocity.

Plots of pertinent relations (iii) and (vii) will help to visualize directly the electrical and mechanical power obtainable from wind at various velocities. Related tables and their graphs are as follows:

	2.3.1	2.3.2	2.3.3.
v (mph)	$5.5\text{x}10^{-5}v_\infty^3$	$3.25\text{x}10^{-5}v_\infty^3$	$1.30\text{x}10^{-5}v_\infty^3$
5	$6.88\text{x}10^{-3}$	$4.06\text{x}10^{-3}$	$1.63\text{x}10^{-3}$
7	$1.89\text{x}10^{-2}$	$1.11\text{x}10^{-2}$	$4.46\text{x}10^{-3}$
9	$4\text{x}10^{-2}$	$2.37\text{x}10^{-2}$	$9.48\text{x}10^{-3}$
11	$7.32\text{x}10^{-2}$	$4.33\text{x}10^{-2}$	$1.73\text{x}10^{-2}$
13	$1.21\text{x}10^{-1}$	$7.14\text{x}10^{-2}$	$2.86\text{x}10^{-2}$
15	$1.80\text{x}10^{-1}$	$1.1\text{x}10^{-1}$	$4.39\text{x}1\text{x}^{-2}$
17	$2.7\text{x}10^{-1}$	$1.6\text{x}10^{-1}$	$6.39\text{x}10^{-2}$
19	$3.77\text{x}10^{-1}$	$2.23\text{x}10^{-1}$	$8.92\text{x}10^{-2}$
21	$5.1\text{x}10^{-1}$	$3\text{x}10^{-1}$	$1.2\text{x}10^{-1}$
23	$6.69\text{x}10^{-1}$	$3.95\text{x}10^{-1}$	$1.58\text{x}10^{-1}$
25	$8.59\text{x}10^{-1}$	$5.07\text{x}10^{-1}$	$2.03\text{x}10^{-1}$
27	1.08	$6.39\text{x}10^{-1}$	$2.55\text{x}10^{-1}$
29	1.34	$7.93\text{x}10^{-1}$	$3.17\text{x}10^{-1}$
31	1.63	$9.68\text{x}10^{-1}$	$3.87\text{x}10^{-1}$
33	1.97	1.17	$4.67\text{x}10^{-1}$

iii

TABLE 2.3.2. Power Density Values (in $\frac{kw}{m^2}$) for various wind speeds.

v (mph)	$7.33\times10^{-5}v_\infty^3$	$4.34\times10^{-5}v_\infty^3$	$1.74\times10^{-5}v_\infty^3$
5	9.16×10^{-3}	5.43×10^{-3}	2.18×10^{-3}
7	2.51×10^{-2}	1.49×10^{-2}	5.97×10^{-3}
9	5.34×10^{-2}	3.16×10^{-2}	1.27×10^{-2}
11	9.76×10^{-2}	5.78×10^{-2}	2.32×10^{-2}
13	1.61×10^{-1}	9.53×10^{-2}	3.82×10^{-2}
15	2.47×10^{-1}	1.46×10^{-1}	5.87×10^{-2}
17	3.6×10^{-1}	2.13×10^{-1}	8.55×10^{-2}
19	5.03×10^{-1}	2.98×10^{-1}	1.19×10^{-1}
21	6.79×10^{-1}	4.02×10^{-1}	1.61×10^{-1}
23	8.92×10^{-1}	5.28×10^{-1}	2.12×10^{-1}
25	1.15	6.78×10^{-1}	2.72×10^{-1}
27	1.44	8.54×10^{-1}	3.42×10^{-1}
29	1.79	1.06	4.24×10^{-1}
31	2.18	1.29	5.18×10^{-1}
33	2.63	1.55	6.25×10^{-1}

TABLE 2.3.3. Power Density Values (in $\frac{hp}{m^2}$) For Varius Wind Speed.

ity
)

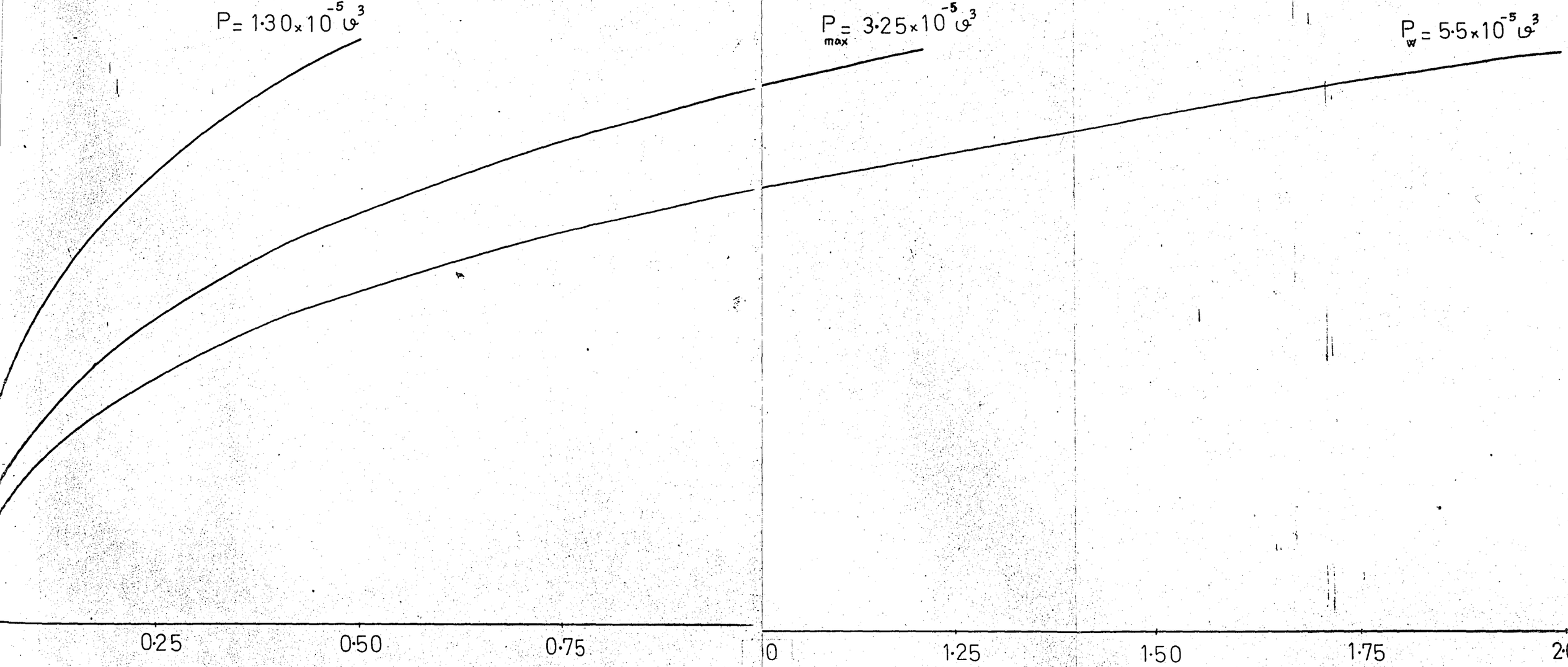

2.3.1. Wind Velocity vs Power Density Plots.

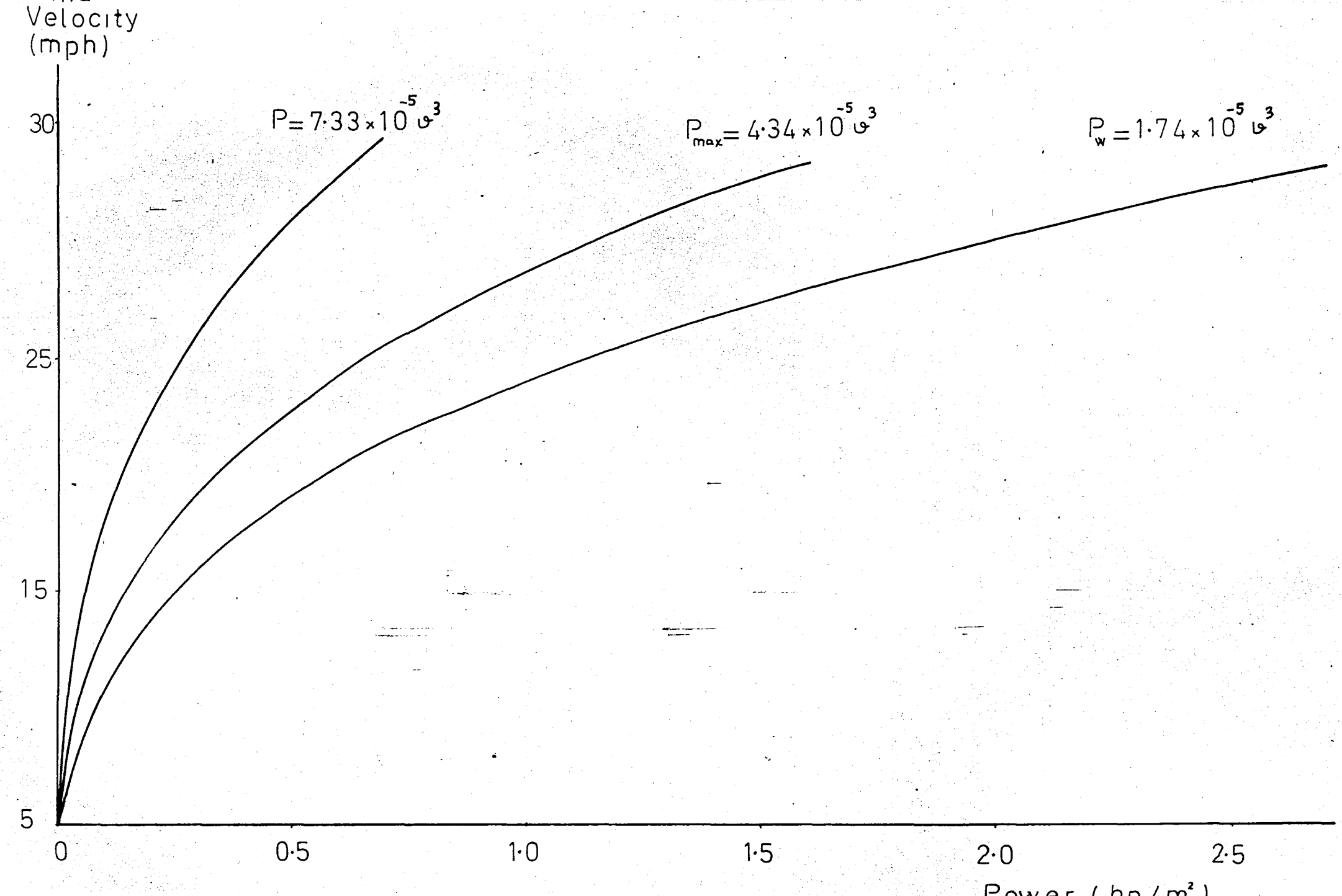
Velocity
(mph)
30
25
15
5
$P = 7{\cdot}33 \times 10^{-5} \omega^3$
$P_{max} = 4{\cdot}34 \times 10^{-5} \omega^3$
$P_w = 1{\cdot}74 \times 10^{-5} \omega^3$
0
0·5
1·0
1·5
2·0
2·5
Power (hp/m²)

From these graphs, one can immediately visualize the power density of wind, of the ideal wind machine, and of some windmill that produces 40% of the power of the ideal windmachine $\forall$ Re_D.

The arguments of this section were based on two simple facts:

1/ The power contained in a freely moving wind stream can be computed by taking the product of volumetric flow rate, and kinetic energy per unit volume, namely,

$$P = (Av)\left(\frac{\rho v^2}{2}\right)$$

$$= \frac{1}{2}\rho A v^3$$

2/ The ideal windmill can convert only about 59% at the above power into shaft work.

The results as presented in the form of graphs above indicate that, the energy in the wind is quite small; thus, far to bring forth another era of cheap energy.

Efforts of some wind power investigators claiming there is more power in the wind than due to that of kinetic energy (implying a violation of the above facts) are briefly mentioned in §2.5.

2.4. Wind Power Evaluation

Evaluation of wind power at a particular site(*) can be made by an analysis using long term weather bureau statistics so as to construct the information in a matrix,

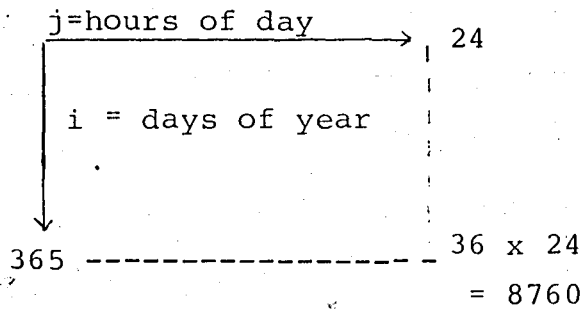

Which can be used to plot the velocity versus time characteristic of that region, denoting the number of hours per year at which the wind velocity is equal to or greater than the abscissa value ((1)).

(*) *A more involved approach than presented here can be found in ref. (37).*

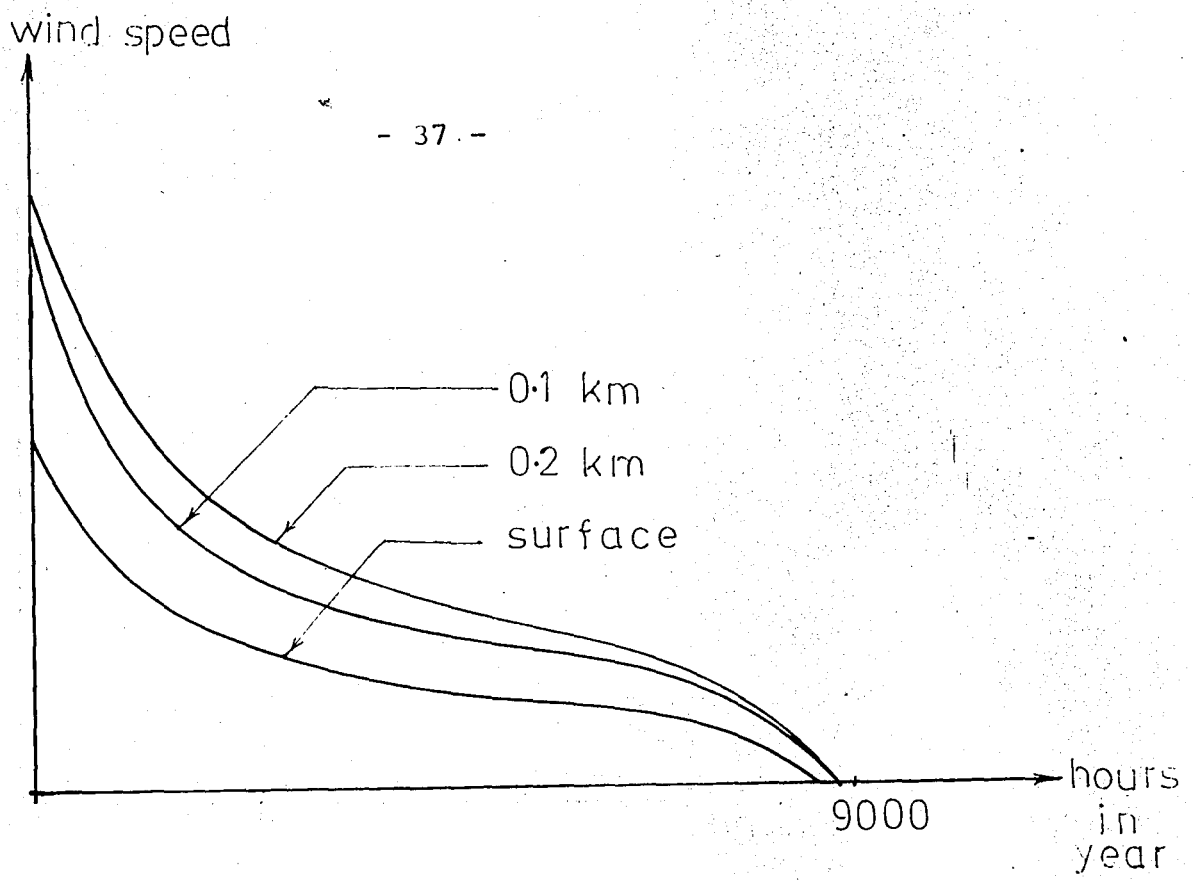

FIG. 2.4.1. Velocity Duration curves (for jodhpur) (14)

This is called the wind velocity duration curve of the porticular region of consideration.

It is interesting to note that, wind speed corresponding to 50% of time (ie, 4380 hours) is approximately equal to the annual average of the region.

Using eq. 2.3.2, this curve may be converted to power duration curve, denoting the number of hours per year at which wind power is equal to or greater than the abscissa value.

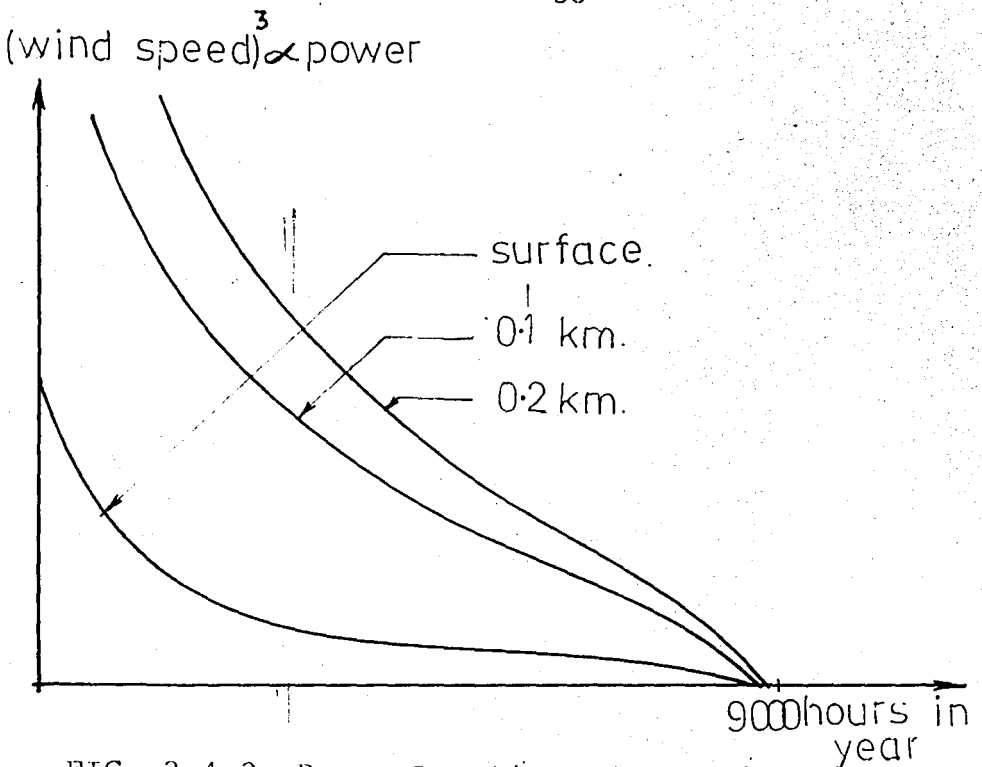

FIG. 2.4.2. Power Duration curves (for jodhpur) (14).

Velocity and power duration curves have typical shapes for all wind regimes.

Aerc generators always operate between a starting speed v_s and a rated speed v_R ; the ratio vR/v_s being a measure of efficiency of collection of a wind turbine (4)

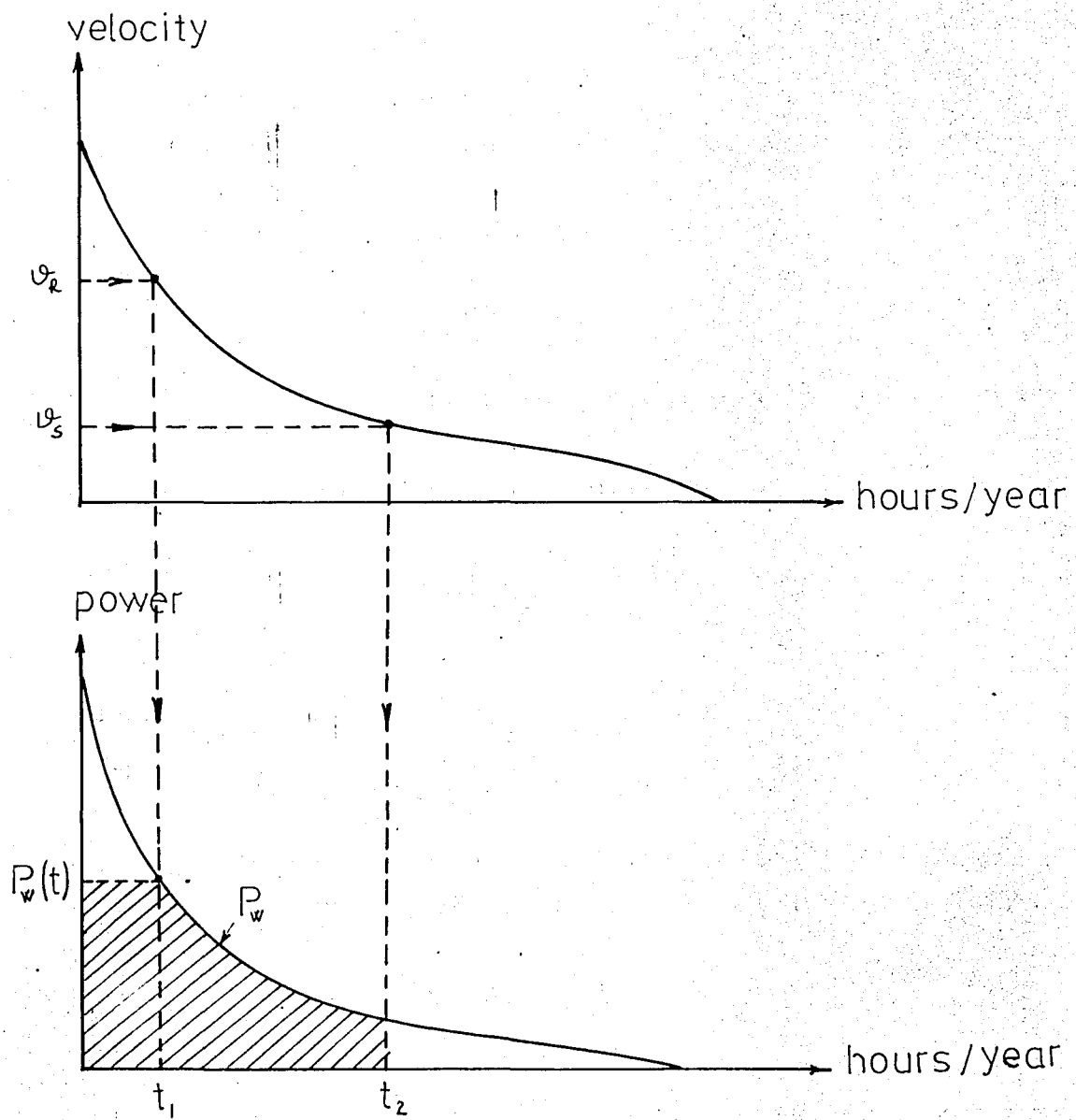

FIG. 2.4.3. Illustration of Cut in/Rated velocity/ Power.

The energy available from wind may be calculated by integrating the area below wind power duration curve. That is ,

$$W_K = Pw(t_1)t_1 + \int_{t_1}^{t_2} Pw\, dt \qquad 2.4.1$$

Where,

W_K = Annual wind energy
P_w = Wind power function.
t = time
$t_1; t_2$ = duraction of period of interest.

Recalling eq. 2.1.3. namely,

$P_w = \frac{1}{2} \frac{\rho_w}{gl} A v^3$, inserting in eq. 2.4.1., the wind energy density based on area can be defined as,

$$\left(\frac{Wk}{A} \right) = \frac{P_w(t_1)t_1}{A} + \frac{\rho_w}{2gl} \int_{t_1}^{t_2} v^3\, dt \qquad 2.4.2.$$

where,

$\left(\frac{W_R}{A} \right)$ Wind energy density based on area.

gl = local gravitational acceleration ($\cong$ 9.8 m/sec^2).
ρ_w = weight density of air at sea level ($\cong$ 1.23 kgf/m^3)-

2.5. Vortex Augmentor Concept

Solar thermal energy diffuseness necessisates large area collectors unless use is made of optical lenses which can focus the rays of the sun into a smaller area. In the case of wind energy conversion, there is a similar problem of a dilute energy supply which is revealed thru the power density plots of §2.4. Devising a "lens for the wind"

which could focus the energy of the wind into a smaller area is an achievement of importance.

There are some instances in nature in which the wind is concencrated to an awesome extent: one is the tornado. Necessary focusing effect of tornado - like vorticial concencration of natural wind was realized by suitably designed aerodynamic surfaces (17, 18).

These surfaces are configured in such a way as to direct the aeradynamic vortices to an appropriately designed rotor system for the purpose of transforming the energy of the wind to shaft work. Such a system constitutes the vortex augmentor concept (29).

The augmentor amplifies the wind speed in the vortex locality, so that, the swirling flow tends to concenrate the low kinetic energy density wind from a large area into a high kinetic energy density flow in a small vortex area.

Some wind power investigators claim that it is possible to make use of the "pressure energy" of wind by concencrating the flow. This claim is based on the energy equation of fluid mechanics, which is derived thru mathematical manupulations on the first law of thermodynamics. The derivation can be found in texts ((4,5)). The energy equation reads,

$$\frac{dQ}{dt} - \frac{dWs}{dt} \quad \frac{\partial}{\partial t} \int_{c.s} e \rho \, dv \quad \int_{c.s} (e \quad p/\rho) \; \underset{\sim}{v}.d\underset{\sim}{A}$$

where,

$$e = u + \frac{1}{2} v^2 + gz$$

and,

$\frac{dWs}{dt}$ is the time rate of work for all work except <u>flow work</u>.

Flow work is the work done at the boundary of the system by normal and tangential stresses. Work done at the boundary of the system due to normal stresses (hydrostatic pressure) is referred to as the flow work. This can be derived to be equal to,

$$\left(\frac{dW}{dt}\right)_{\text{flow work}} = \int_{c.s.} (p/\rho)\ \underset{\sim}{v}.d\underset{\sim}{A} \qquad 2.5.2$$

The energy equation states that, the time rate of heat added to the system minus the work done by the system (other than flow work) is equal to the time rate of change of stored energy in the control volume plus the net rate of efflux of stored energy and flow work out of the control volume.

Thus, the shaft power output of a flow system is given by,

$$P' = Cp \oiint (p/\rho + v^2/2)\rho \underset{\sim}{v}.d\underset{\sim}{A}. \qquad 2.5.3.$$

where,

Cp is the system efficiency.

The integration is carried out over a control surface enclosing the entire system, with flow passing into and out of the system.

Notice that, taking $p/\rho = 0$ reduces 2.5.3. to the familiar equation 2.2.21.

The claim stated before aims to concencrate the incoming flow sa as to accelerate it within the system continuously, and let it slow down only after it exits from the system. Thus, in contrast to conventional wind turbines that use only the wind kinetic energy $\frac{v^2}{2}$ it would be possible to use the wind pressure energy p/ρ which in magnitude is 3000 times larger than the wind kinetic energy for a wind of 15 mph, and more than 750 times larger for 30 mph winds (5). In this way, it was planned to be freed from the classical 0.593 restriction of the conventional wind turbines where incoming wind is continuously slowed. Some figures about proposed designs are given below:

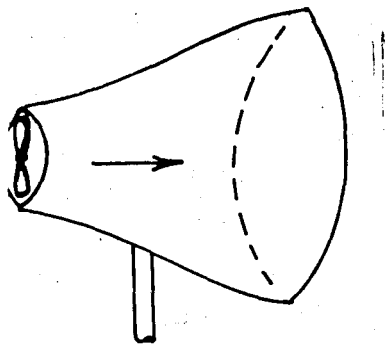

DIFFUSER

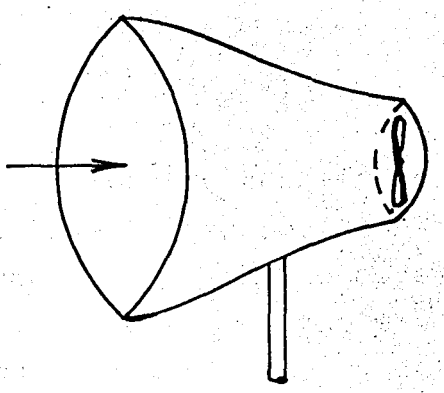

CONCENCRATOR

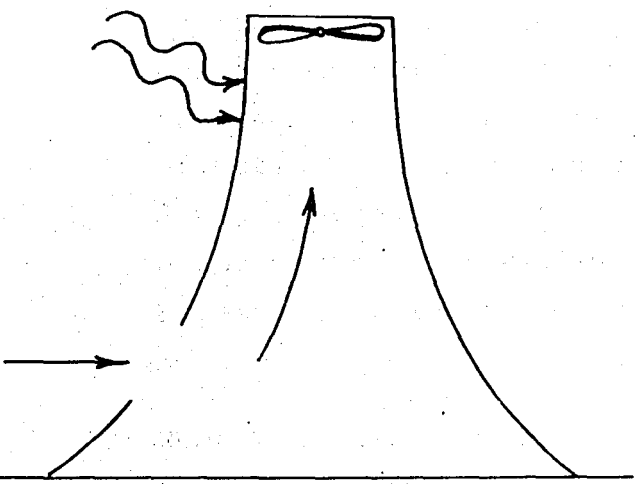

SUNLIGHT

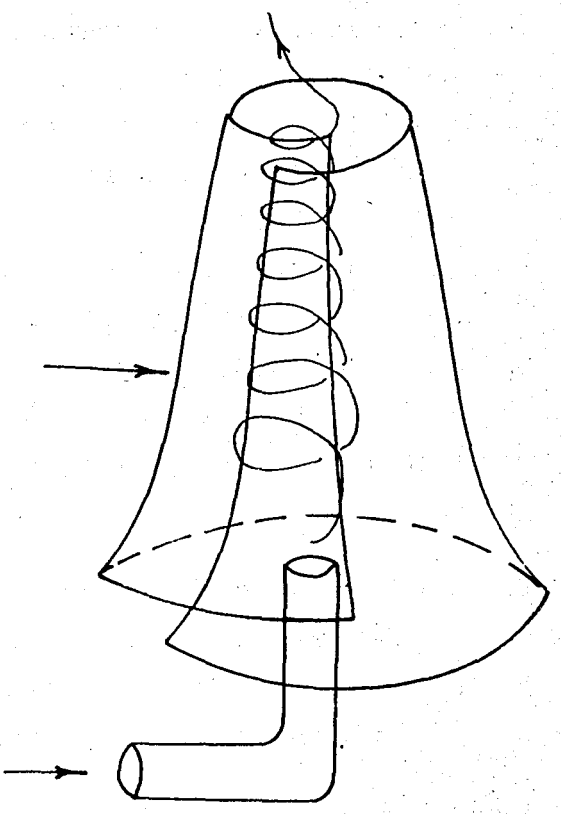

CONFINED VORTEX

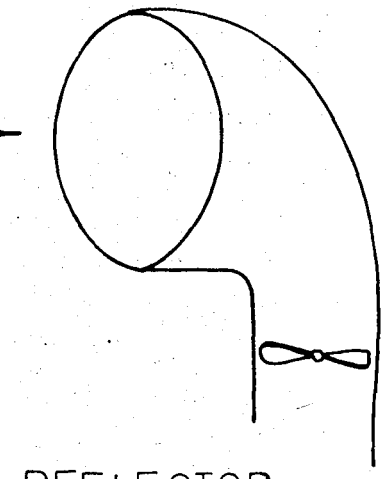

DEFLECTOR

FIG. 2.5.1. Proposed Systems to Concencrate Wind Energy I

Among the most outstanding attempts in this field, Sforza and co-workers (29) for example have placed rotational axis of a propeller type windmill coaxially with the core of a vortex, generated by a delta wing of incidence to the wind, so that the turbine ingets the angular kinetic energy of the upstream vortex. Yen (5) and others have devised an alternate mode of vortex augmentation in which a confined vortex is generated in a tower, and the low pressure core is used as a pump for a propeller - type turbine flow to discharge into. Both approaches have yielded enhanced power coefficients (compared to Betz limit) based on the propeller disk area. In contrast to vortex augmentation, is the concept of diffuser augmented shrouded propeller type wind turbine,(28) which has a potential energy concencrating factor of 3 to 4 at the turbine. It suffers of course from the usual gyroscopic loods of horizontal axis machines, and in common with all other devices based on augmentation by stationary structure, a potenti problem with cost effectiveness. However, studies by Oman and Foreman (30) indicate diffuser - augmented wind turbines may be produced cost effectively.

Recent studies by Loth (27) and Wiley (26) indicate that, when the projected area of the generating structure is used as a reference, all vortex wind mechines have an efficiency below that of a propeller with the conventional Betz limit.

Thus it can be concluded that, the only merit of augmented systems is to concencrate the dilute engry of wind into a small area to produce usable power at wind speed much lower than those required to operate conventional wind power systems. Ceteris Paribus, the area below the power vs. time plot of the place at which the system is installed will

increase by the shifting of the cut-in-power border to the right.

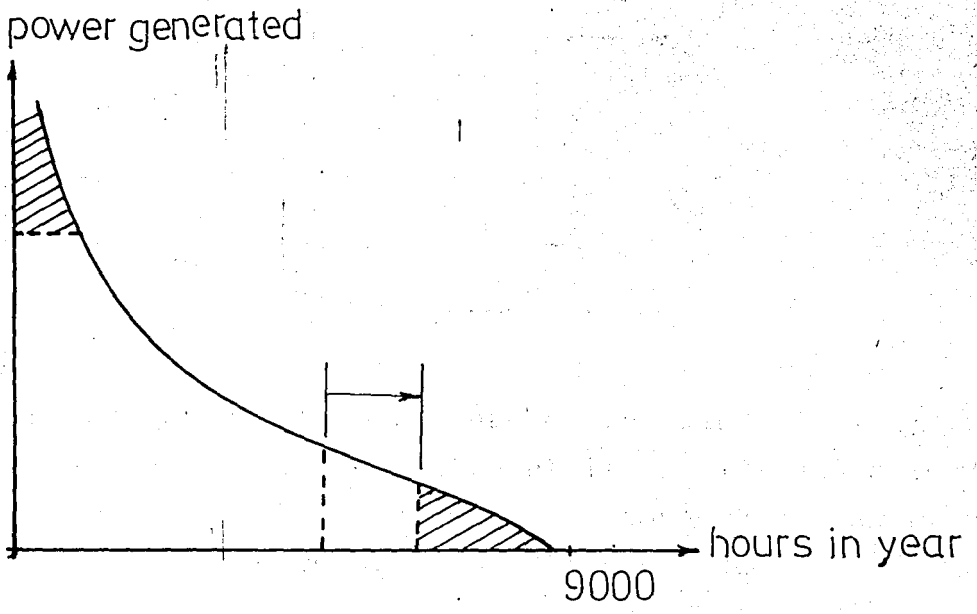

FIG. 2.5.2. Reduction in Power Loss Dere to cut-in

This may open up new possibilities of harnessing the wind in those regions where winds are always blowing, but at generally low speeds.

2.6. Extension of the Windmill Law, the Power Envelope.

The relation between input wind velocity, power and angular velocity is derived using the outline of ref.(2) so as to see the ideal (*) windmill performance characteristics, which, being the upper bound (envelope) may serve as a basis of comparison with data gathered from various wind turbine models or prototypes.

Consider the familiar actuator disk extracting energy from an air stream:

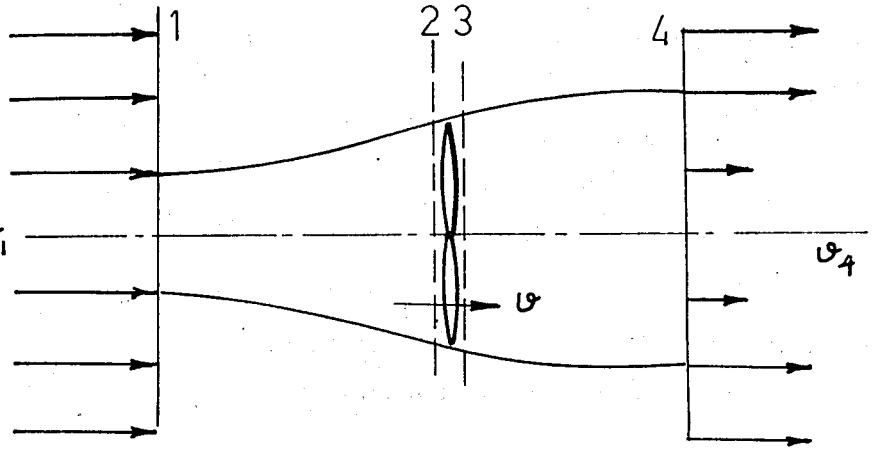

FIG. 2.6.1 Flow Thru the Actuator Disc.

In the derivation procedure of the windmill law, the energy equation was written between (1) and (2) and also (3) and (4), plus the utilization of Newton's 2 nd law provided 3 equations, the solution of which yielded,

$$v = \frac{v_1 + v_4}{2} \qquad 2.6.1$$

Now, let,

$$v = v_1(1-a) \qquad 2.6.2$$

This constitutes a definition of the axial interference factor "a" introduced by Glauert ((10))

The elementary thrust on the annular area of the actuator disk is,

$$dF = 2\rho \cdot (v_1 - v)\, v \cdot 2\pi r\, dr. \qquad 2.6.3.$$

Putting 2.6.2 into 2.6.3,

(*) Air is treated as on ideal fluid, with no friction.

$$dF = 2\rho\{v_1 - v_1(1-a)\}\{v_1(1-a)\}\ 2\pi r dr,$$

$$dF = 4\pi r\rho v_1^2(1-a)a\ dr \qquad 2.6.4$$

where,

$r \triangleq$ local radius.
$\rho \triangleq$ air density. (ideal fluid assumed)
$v_1 \triangleq$ wind velocity for upstream.

If we reglect the rotation of fluid in the wake, the elementary power becomes,

$$dP = dF.v$$

$$\therefore dP = 4\pi r\rho v_1^3(1-a)^2\ a\ dr. \qquad 2.6.5$$

Assuming the axial interference factor, (which can be obtained from (1) and (2) as $a = (v_1 - v_4)/2v_1$) is independent of r, (4) can be integrated for total power. For this case,

$$P = 4\pi\rho v_1^3(1-a)^2 a \int_0^R r\ dr$$

$$\therefore P = 2\pi\rho v_1^3(1-a)^2\ a\ R^2 \qquad 2.6.6$$

where,

$R \triangleq$ outer radius of disk.

Optimization of 2.6.6. with respect to "a" gives,

$$\frac{\partial P}{\partial a} = 2\pi\rho v_1^3 R^2 \{(1-a)^2-2a(1-a)\} = 0$$

$$= 2\pi\rho v_1^3 R^2 (3a^2-4a\ 1) = 0$$

$$\Rightarrow (3a-1)(a-1) = 0$$

$$\Rightarrow a = \frac{1}{3}, \text{ or }, a\ \ 1.$$

$a = \frac{1}{3}$ ($\Rightarrow v_1/v_1 = 1/3$) is the required optimal value, since 2. $a = 1$ makes the theory irrelevant.

Using 2.6.7,

$$\Rightarrow P = 2\pi\rho v_1^3 (1-\frac{1}{3})^2 (\frac{1}{3})\ R^2$$

$$\Rightarrow P = \frac{8}{27} .\pi R^2.\rho v_1^3$$

$$\Rightarrow P = \frac{16}{27} \cdot \frac{1}{2} .\pi R^2.\rho v_1^3 (=P'_{max}) \qquad 2.6.8.$$

where,

$P_{wind} = \frac{1}{2} R^2. v_1^3$ in the circular aera of the actuator disk considered.

This is the theorem of Betz which says that on ideal machine can extract no more than $\frac{16}{27}$ (59.3%) of the power in the wind.

The elementary torque on an annular area is,

$$dT = \{\rho(v_1-v)(v)\ 2\pi r dr\}(r) \qquad 2.6.9.$$

Define the local angular velocity of the fluid w'as,

$$(v_1 - v) = w'r \qquad 2.6.10$$

Substitution of 2.6.10 in 2.6.9 yields,

$$dT = 2\pi r^3 \rho v w' dr. \qquad 2.6.11.$$

Now, Let,

$$W' = 2wa' \qquad 2.6.12$$

Where,

W being the rotor angular velocity.

Equation 2.6.12 constitutes the definition of the rototional interference factor "a'", introduced by Glauert ((17)).

Upon substitution of 2.6.12 and 2.6.2 in 2.6.11,

$$dT = 4\pi r^3 \rho v_1 w(1-a)a' \, dr. \qquad 2.6.13$$

Elementary shaft power is,

$$dP = (dT)(w). \qquad 2.6.14.$$

Substitution of 2.6.13. into 2.6.14 yields the elementary power from the rotor as,

$$dP = 4\pi r^3 \rho v_1 w^2 (1-a)a' \, dr \qquad 2.6.15.$$

The total power is,

$$P = 4\pi\rho v_1 w^2 \int_o^R (1-a)\, a'\, r^3 \, dr. \qquad 2.6.16$$

To check the nature of dependence of the interference factors on the radius, we entertain the principle of energy at the disk element, reading,

$$(Wk)_{2\to 3} + \text{losses} + \frac{P_3}{\rho} + gZ_3 + \frac{v_3^2}{2} = \frac{P_2}{\rho} + g\,Z_2 + \frac{v_2^2}{2}$$

Where,

Losses are reglected,

$v_2 = v_3 = v_1$

$Z_2 = Z_3$

Thus,

$$\frac{P_2 - P_3}{\rho} = (Wk)_{2\to 3} \qquad 2.6.17.$$

The pressure difference $P_2 - P_3$ can be subtituted by thrust force per unit area from equation 2.6.4, while the elementary rotor power can be used on the right hand side, if consistency of the units is provided as,

$$\dot{m}\left(\frac{P_2 - P_3}{\rho}\right) = (\dot{Wk})_{2\to 3} \qquad 2.6.18$$

Recalling,

$$\dot{m} = \rho v A \qquad (2.1.2)\ 2.6.19$$

Using 2.6.2, and the expression of annular area element,

$$\dot{m} = \rho v_1 (1-a)\, 2\pi r\, dr. \qquad 2.6.20$$

Substitution of 2.6.20, 2.6.4 and 2.6.15 into 2.6.18 yields,

$$\left\{\frac{\rho v_1 (1-a) 2\pi r dr}{\rho}\right\}\left\{\frac{4\pi r \rho v_1^2 (1-a) a' dr}{2\pi r dr}\right\} = 4\pi r^3 \rho v_1 w^2 (1-a) a' dr.$$

$$\Rightarrow v_1^2(1-a)a = r^2w^2a'$$

$$\Rightarrow x^2a' = (1-a)a, \qquad 2.6.21$$

Where,

$x \triangleq \frac{wr}{v_1}$, local tip speed ratio.

2.6.21 can be obtained by equating the elementary power expressions 2.6.5 and 2.6.15, namely,

$$4\pi r\rho v_1^3(1-a)^2a\,dr = 4\pi r^3\rho v_1w^2(1-a)a'\,dr.$$

$$\Rightarrow x^2a' = (1-a)a. \qquad 2.6.21.$$

From 2.6.21, it is understood that, the interference factors depend on the local tip speed ratio x. This necessisates a change of the integration variable of 2.6.16 from r to x. By definition,

$$x = \frac{wr}{v_1}$$

$$\Rightarrow r = \frac{v_1}{w}x \qquad 2.6.22$$

$$\Rightarrow dr = \frac{v_1}{w}dx \qquad 2.6.23$$

Substitution of 2.6.22 and 2.6.23 into 2.6.16,

$$\Rightarrow P = 4\pi\rho v_1w^2\int_0^X (1-a)a'\frac{v_1^3}{w^3}x^3\frac{v_1}{w}dx$$

$$\Rightarrow P = 4\pi\rho v_1^5w^{-2}\int_0^X (1-a)a'x^3\,dx. \quad (=P') \qquad 2.6.24$$

Where,

$X = \frac{WR}{v_1}$, tip speed ratio.

Dividing 2.6.24 by the power in the Wind.

$$\frac{P'}{P_{wind}} = \frac{4\pi\rho v_1^5 w^{-2} \int_0^X (1-a)a' x^3 \, dx}{\frac{1}{2}\cdot\pi R^2 \cdot \rho v_1^3}$$

$$\Rightarrow \frac{P'}{P_{wind}} = \frac{8}{X^2} \int_0^X (1-a)a' x^3 dx. \qquad 2.6.25.$$

Now, optimization can be achieved by solving 2.6.21, its derivative, and the derivative of the integrand of 2.6.25. When these results are substituted back into 2.6.25, and the integration performed the desired result is obtained as shown (2).

$$\frac{P'}{P_{wind}} = \frac{1}{540(c-9)} \{2c^4 - 57C^3 + 565C^2 - 2110C + 960 - \frac{1920}{C^2}\{C + (1-c)\ln(1-c)\}\} \quad 2.2.2$$

Where,

$$C = 3 + 6(X^2\ 1)^{\frac{1}{2}} \cos\left(\frac{\tan^{-1}X - 2\pi}{3}\right) \qquad 2.6.27.$$

$X \triangleq$ optimized tip speed ratio.

The function (26) is indeterminate at both X=0 , and X =∞. Use of L' Hôpitol's rule however enobles one to find that.

as, $X \to 0$, $c \to 0$, $\frac{P'}{P_{wind}} \longrightarrow 0$,

and,

$$\text{as, } X \to \infty \quad , C \to 1 \ , \quad \frac{P'}{P_{wind}} \to \frac{16}{27} = 0.593.$$

These results can be seen in the plot of 2.6.26. given below:

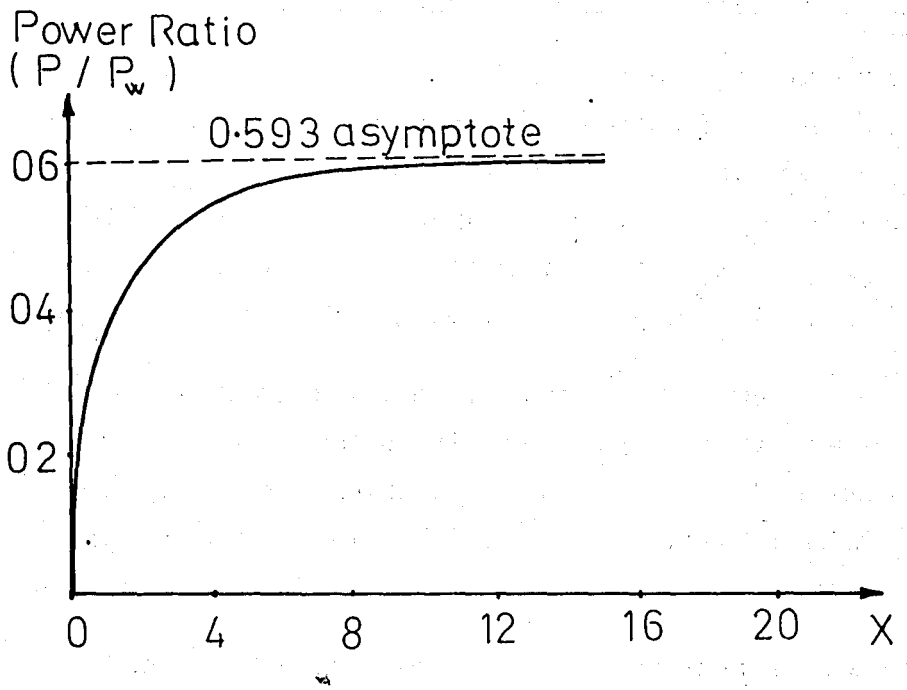

FIG. 2.6.2. Power Envelope of the Actuator Disc (WR/v_1)

This curve constitutes the extension of the windmill law. It can be interpreted as follows: 'The design output of an ideal windmill increases monotonically with its optimized tip speed ratio, beginning with zero and terminating at the asymptotic value of 16/27 of the power in the wind when the tip speed ratio approaches the limiting value of infinity.'

This illustrates the merit in using a high speed mill. It also shows the reason why low speed mills are innefficent albeit they possess other frequently desirable attributes.

It shows that when Betz neglected the Kinetic energy of rotation in the wake, he found just the asymptote, not the envelope of all performance curves.

2.7. Modelling of a Vertical Axis Wind Machine

The variables associated with the 'performance' are, power, diameter of rotor, length of rotor, area facing the flow, revolutions per unit time, flow velocity, density of fluid, viscosity, torque, and pressure drop on forward and backward sides of a blade element (with respect to the coming wind). Thus, we have garameters in total.

From the high number of quantities, we feel the necessity of using Buckingham Pi theorem to serve as a tool to organise the variables involved into the smallest number of significant dimensionless groupings, from which an equation can be evaluated.

A dimensional layout of the variables involved yields,

Power,

$$P = ML^2 T^{-3} \qquad 2.7.1$$

Diameter of rotor,

$$D = L. \qquad 2.7.2$$

Height of rotor,

$$H = L \qquad 2.7.3$$

area of rotor,

$$A = L^2 \ (=HD). \qquad 2.7.4$$

Revolutions per unit time,
$w = T^{-1}$. 2.7.5

Velocity of coming wind,
$v_\infty = LT^{-1}$. 2.7.6

Density of fluid,
$\rho = ML^{-3}$ 2.7.7

Viscosity of fluid,
$\mu = ML^{-1}T^{-1}$ 2.7.8

Torque,
$T = ML^2T^{-2}$ 2.7.9

Pressure drop,
$\Delta P = ML^{-1}T^{-2}$ 2.7.10

2.7.2. → 2.7.4.

$A = HD = D^2$ 2.7.11

$\Rightarrow \pi_A = \frac{H}{D}$

or, upon substitution of (3) → (4),

$A = HD = H^2$

$\rightarrow \pi_A = \frac{D}{H}$ 2.7.12

2.7.11 or 2.7.12. is called 'rotor aspect ratio' ; this is one of the dimensionless parameters that affects the performance of a wind turbine.

2.7.2. → 2.7.7.
$\rho = MD^{-3}$
$\Rightarrow M = \rho D^3$ 2.7.13
2.7.3 → 2.7.7
$\Rightarrow M = \rho H^3$ 2.7.14

2.7.3. —> 2.7.6

$$v_\infty = HT^{-1}$$

$$\Rightarrow T^{-1} = \frac{v_\infty}{H}$$

2.7.2. —> 2.7.6.

$$\Rightarrow T^{-1} = \frac{v_\infty}{D} \qquad 2.7.16.$$

2.7.5. —> 2.7.15.

$$\Rightarrow v_\infty = wH$$

(5) —> (16)

$$v_\infty = wD \qquad 2.7.18$$

We know that it is eg. 2.7.18. that fits physical situations not 2.7.17.

The true form of 2.7.18. is,

$$v_\infty = \frac{wD}{2} \quad (=wr) \qquad 2.7.19.$$

Thus,

$$\pi_{v_\infty} = \frac{wD}{2v_\infty} \quad (=\frac{wr}{v_\infty}) \qquad 2.7.20.$$

π_{v_∞} is defined as the 'tip speed ratio' ; it is the ratio of the tangential velocity of the outer diameter of the rotor to the wind velocity.

This dimensionless parameter is a measure of how 'fost the rotor is.

2.7.13, 2.7.4 and 2.7.16 —>2. 7. 1.

$$=>P = (\rho D^3)\ (A)\ \left(\frac{v_\infty}{D}\right)^3$$

$$=>P = \rho A\ v_\infty^3 \qquad 2.7.21$$

The power contained in a cross-sectionel area A normal to a fluid of density and flow velocity v_∞ was derived to be

$$P = \frac{1}{2}\ \rho A\ v_\infty^3 \ . \qquad 2.7.22$$

Thus.

$$\pi_p = \frac{P}{\frac{1}{2}\rho HDv^3} \qquad 2.7.23$$

π_p, which appears in literature as C_p is generally called the power coefficient. HDv^3 is power in the pluid, while P is the maximum power that a wind machine can extract.

2.7.13, 2.7.2 and 2.7.16 — 2.7.8

$$=> \mu = (\rho D^3)(D^{-1})(v_\infty D^{-1})$$

$$=> \mu = \rho v_\infty D$$

Thus, the dimensionless parameter associated with the viscosity variable is,

$\pi_\mu = \frac{\mu}{v_\infty D}$, or in well known form,

$$\pi_\mu = \frac{\rho v_\infty D}{\mu} = \frac{v_\infty D}{\nu} \qquad 2.7.24$$

Where,

$\nu \triangleq \frac{\mu}{\rho}$ is the kinematic viscosity.

π_μ generally appears in literature as, Re_D, which is the abbreviated form of the term 'Reynold's number'.

2.7.13, 2.7.14 and 2.9.16 $\rightarrow$ 2.7.9.

$$\Rightarrow T = (\rho D^3)\ (A)\ \left(\frac{V_\infty}{D}\right)^2$$

$$= \rho D A\ V_\infty^2$$

Thus, the associated dimensionless coefficient for the torque is,

$$\pi_T = \frac{T}{\rho H D^2 V_\infty^2} \qquad 2.7.25$$

2.7.13, 2.7.2 and 2.7.16 — 2.7.10.

$$\Rightarrow \Delta P = (\rho D^3)\ (A)\ \left(\frac{V_\infty^2}{D^2}\right)$$

$$= \rho V_\infty^2$$

Thus the term related to the pressure drop is,

$$\pi_{\Delta P} = \frac{\Delta P}{\rho V_\infty^2} \qquad 2.7.26.$$

Recalling that ΔP is the pressure difference at the front and back of a blade (with respect to the oncoming flow), and, multiplying the denominator by $\frac{1}{2}$ (according as terms can be multiplied by any constant, or raised to any power without affecting their dimensionless status), we have,

$$\pi_B = \frac{P_\infty - P_B}{\frac{1}{2}\rho V^2} \qquad 2.7.27.$$

Which is called the 'pressure coefficient'.

We thus have <u>six</u> dimensionless groupings corresponding to <u>nine</u> variables analysed in equations 2.7.1 to 2.7.10. We note that one of the three relations among 2.7.2, 2.7.3 and 2.7.4 is 'dummy'. Warranting the rule of thumb of dimensional analysis that the number of dimensionless π terms is the difference of the number of variables involved (=9) and the number of dimensions (=3).

The complete set of dimensionless gropings or parameters associated to a vertical-axis wind turbine are collected below:

1- $\pi_A = \frac{H}{D}$ ($\triangleq$ aspect ratio) 2.7.12

2- $\pi_{V\infty} = \frac{wD}{2w_\infty}$ ($\triangleq$ tip speed ratio) X 2.7.20

3- $\pi_p = \frac{P}{\frac{1}{2}\rho HDv_\infty^3}$ ($\triangleq$ power ratio) Cp 2.7.23

4- $\pi_\mu = \frac{\rho V\infty\ D}{\mu}$ ($\triangleq$ viscosity coefficient, or Reynolds' number) Re_D 2.7.24.

5- $\pi_T = \frac{T}{\rho HD^2 v_\infty^2}$ ($\triangleq$ Torque coefficient) C_T 2.7.25

6- $\pi_B = \frac{P_\infty - P_B}{\frac{1}{2}\rho v_\infty^2}$ $\triangleq$ Blade rear pressure coefficient relative to the free stream, or just pressure coefficient 2.7.27.

2.8. Theoretical Modelling for A Simplified Case.

Power equation is derived for a rotor of below or similar geometric configuration. The results are valid for the vertical-axis wind turbines of Lebost (22) and Baker (12,13). The Savonius rotor data was seen to have a correlation with the outcame of the theory according to the limited data available.

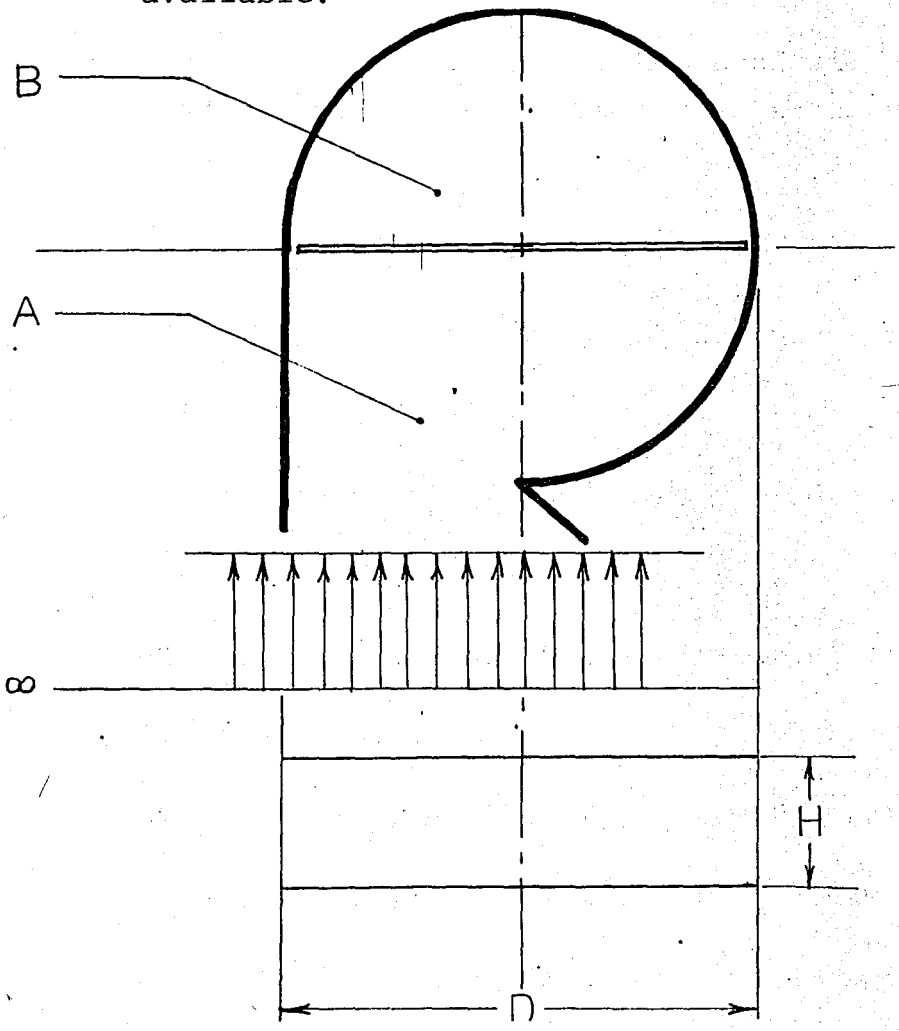

FIG. 2.8.1 Simple Shrouded Wind Rotor.

$$v_A = fv_\infty \quad \text{+ flow concentration factor } f > 1. \qquad 2.8.1$$

$$\frac{p_\infty}{\rho_\infty} + \frac{v_\infty^2}{2} = \frac{PA}{\rho A} + \frac{v_A^2}{2} \qquad 2.8.2$$

2.8.1 → 2.8.2.

$$P_A \triangleq P_\infty + \frac{1}{2}\rho v_\infty^2 (1-f^2) \qquad 2.8.3.$$

$\beta \triangleq$ flow deflecting factor F → βF ∀ v.

$$dF = \beta\rho v_A (v_A - wr)\, H\, dr + (P_A - P_B)\, H\, dr \qquad 2.8.4.$$

Where, the tems on the right hand side are associated with blade force from momentum exchange and net Pressure force an blade.

$$\underset{\sim}{dT} = d\underset{\sim}{F} \times \underset{\sim}{r}$$

$dT = \gamma\, r\, dF$ is averaging factor of torque. 2.8.5.

2.8.4 → 2.8.5.

$$dT = \gamma r\{\beta\rho v_A (v_A - wr)\, Hdr + (P_A - P_B)\, Hdr\} \qquad 2.8.6.$$

2.8.3. → 2.8.6.

$$dT = \gamma r\{\beta\rho\, v_A (v_A - wr)\, Hdr + [P_\infty + \frac{1}{2}\rho v_\infty^2 (1-f^2) - P_B] Hdr\} \qquad 2.8.7.$$

2.8.1 → 2.8.7.

$$dT = \gamma\{(P_\infty - P_B) + \frac{1}{2}\rho v_\infty^2 (1-f^2) + \beta\rho f v_\infty (fv - wr)\} Hr\, dr \qquad 2.8.8.$$

$$dT = \gamma\{(P_\infty - P_B) + \frac{1}{2}\rho v^2 (1-f^2) + \beta\rho f^2 v_\infty^2 - fv\, wr\} Hrdr$$

$$\Rightarrow dT = \{(P_\infty - P_B) + \frac{1}{2}\rho v^2 (1-f^2) + \beta\rho f^2 v_\infty^2\}\gamma Hrdr - \gamma\beta\rho f v_\infty Hr^2 dr \qquad 2.8.9.$$

$$\pi_B \triangleq \frac{P_\infty - P_B}{\frac{1}{2}\rho v_\infty^2} \qquad 2.8.10.$$

2.8.10 $\rightarrow$ 2.8.9.

$$dT = \gamma H\{\frac{1}{2}\pi_B \rho v_\infty^2 + \frac{1}{2}\rho v_\infty^2 (1-f^2) + \beta\rho f^2 v_\infty^2\} r dr - \gamma\beta\rho f v_\infty w H r^2 dr.$$

$$\Rightarrow dT = \frac{1}{2}\gamma H\rho v_\infty^2 \{\pi_B + 1 - f^2 + 2\beta f^2\} r\, dr - \gamma\beta\rho f v_\infty w H r^2 dr$$

$$\frac{1}{2}\gamma H\rho v_\infty^2 \{1 + f^2(2\beta-1) \pi_B\} r\, dr - \gamma\beta\rho f v_\infty w H r^2 dr \qquad 2.8.11$$

$$T = \int_0^{D/2} T$$

2.8.11. $\rightarrow$ 2.8.12.

$$T = \int^{D/2} \frac{1}{2}\gamma H\rho v_\infty^2 \{1 + f^2(2\beta-1) + \pi_B\} r\, dr - \int_0^{D/2} \gamma\beta\rho f v_\infty w H r^2 dr$$

$$= \frac{1}{2}\gamma H\rho v_\infty^2 \{1 + f^2(2\beta-1) + \pi_B\} \left(\frac{r^2}{2}\right)\Big|_0^{D/2} - \gamma\beta\rho f v_\infty w H \left(\frac{r^3}{3}\right)\Big|$$

$$= \frac{1}{16}\gamma H\rho v_\infty^2 \{1 + f^2(2\beta-1) + \pi_B\} D^2 - \frac{1}{24}\gamma\beta\rho f v_\infty w H D^3 \qquad 2.8.13.$$

$$\equiv C (X_o - X)$$

Where,

C is a constant,
Tip speed ratio under no load, $X_o \triangleq \frac{w_o D}{v_\infty}$, and,

tip speed ratio under load $X \triangleq \frac{wD}{v_\infty}$.

2.8.13. is re-arranged as,

$$T = \frac{1}{12}\gamma\beta\rho f\ v_\infty^2\ HD^2\{\frac{3}{4}\cdot\frac{\{1+f^2(2\beta-1)+\pi_B\}}{\beta f} - \frac{wD}{v_\infty}\} \qquad 2.8.14$$

$$\Rightarrow T = \frac{1}{12}\gamma\beta\rho\ f\ v_\infty^2\ HD^2(X_O-X) \qquad 2.8.15$$

$$= \frac{1}{12}\ \gamma\beta\rho f\ v_\infty^2\ HD^2(\frac{w_o-v}{2v_\infty})\ D \qquad 2.8.16$$

Where,

$$X_O = \frac{w_O D}{2v_\infty} = \frac{3}{4}\cdot\frac{\{1+f^2(2\beta-1)+\pi_B\}}{\beta f}$$

$$\Rightarrow w_O = \frac{3v_\infty}{2D}\cdot\frac{\{1+f^2(2\beta-1)+\pi_B\}}{\beta f}$$ is the angular velocity at no load.

Recall,

$$C_T = \frac{T}{\rho v_\infty^2\ HD^2} \Rightarrow \rho v_\infty^2\ HD^2 = (\frac{T}{C_T}) \qquad 2.8.17$$

2.8.17. → 2.8.15.

$$T = \frac{1}{12}\gamma\beta f(\frac{T}{C_T})\ (X_O-X)$$

$$\Rightarrow C_T = \frac{\gamma\beta f}{12}(X_O-X) \qquad 2.8.18$$

$= \frac{\gamma \beta f}{12} X_o (1-\frac{X}{X_o})$ where $\frac{X}{X_o} \triangleq$ normalized rotation rate.

$C_T = \frac{\gamma \beta f}{12} X_o \triangleq$ no rotation torque coefficient.

On the other hand,

$$Cp \triangleq \frac{P}{\frac{1}{2}\rho HD\ v_\infty^3} = \frac{wT}{\frac{1}{2}HD\ v^3} \qquad 2.8.19$$

Using 2.8.17. and 2.8.19.,

$$\frac{Cp}{C_T} = \frac{wT/\frac{1}{2}\rho HD\ v_\infty^3}{T/\rho HD^2 v_\infty^2}$$

$$= \frac{2wT}{T} \frac{\rho HD^2 v_\infty^2}{\rho HD\ v_\infty^3}$$

$$= \frac{2wD}{v_\infty}$$

$$= 4X$$

$$\Rightarrow Cp = 4XC_T \qquad 2.8.20$$

2.8.17 $\rightarrow$ 2.8.20.

$$Cp = 4X \frac{\gamma \beta f}{12} X_o (1-\frac{X}{X_o})$$

$$\Rightarrow Cp = 4X\, C_T^* \left(1-\frac{X}{X_o}\right) \qquad 2.8.21$$

$$C_T^* = f(X_o) \qquad X_o = g(Re) \quad \Rightarrow \quad C_T^* = f\{g\,(Re)\} \qquad 2.8.22$$

2.8.22. —> 2.8. 21.

$$C_p = 4X\, f\{g(Re)\} \left(1-\frac{X}{X_o}\right) \qquad 2.8.23$$

To maximize the power coefficient,

$$\frac{\partial Cp}{\partial X} = 4f\{g(Re)\}\left(1-\frac{X}{X_o}\right) + 4X\left(1-\frac{X}{X_o}\right)\frac{\partial f\{g(Re)\}}{\partial X} + 4Xf\{g(Re)\}\left(-\frac{1}{X_o}\right) = 0$$

The term $\frac{\partial f\{g(Re)\}}{\partial X} = 0$ since $f\{g(Re)\} = C_T^*$ is not X dependent.

$$\Rightarrow 4f\{g(Re)\}\, X_o - 8\, f\{g(Re)\}\, X = 0$$

$$\therefore \quad 4X_o - 8X = 0$$

$$\Rightarrow X = \frac{X_o}{2} \text{ so that Cp is at maximum.} \qquad 2.8.24$$

$$w = \frac{w_o}{2} \text{ at maximum power.} \qquad 2.8.25$$

2.8.24 → 2.8.23.

$$(Cp)_{max} = 4\ (\frac{X_o}{2})\ f\{g(Re)\}(1-\frac{X_o}{2X_o})$$

$$= X_o\ f\{g(Re)\} \qquad 2.8.26$$

$$Cp = \frac{P'}{\frac{1}{2}\rho HD\ v^3} = 4X\ f\{g(Re)\}\ (1-\frac{X}{X_o})$$

Where, P' is the power available,

$$P' = 2f\{g(Re)\}\rho HD\ v_\infty^3\ X\ (1-\frac{X}{X_o}) \qquad 2.8.27$$

$$= 2f\{g(Re)\}\rho HD\ v_\infty^3\ \frac{wD}{2v_\infty}\ (1-\frac{wD}{2v_\infty}\ \frac{2v_\infty}{w_oD}$$

$$= f\{g(Re)\}\rho HD^2v_\infty^2\ w\ (1-\frac{w}{w_o}) \qquad 2.8.28$$

$$= f\{g(Re)\}\rho HD^2v_\infty^2\ \frac{w}{w_o}\ (w_o-w)$$

Where, $w_o = \frac{2X_o\ V_\infty}{D}$ and $v_\infty = \frac{w_oD}{2X_o}$

$$P' = \frac{1}{4}\ f\{g(Re)\}\rho HD^4\ X_o^{-2}\ w\ w_o\ (w_o-w) \qquad 2.8.29$$

At maximum power, $w = \frac{w_o}{2}$

$$P' = \frac{1}{2}\ f\{g(Re)\}\ X_o^{-2}\rho HD^4\ w^3 \qquad 2.8.30$$

3. SAVONIUS ROTOR

3.1. General Information

This rotor was invented by S.J. Savonius in 1929; applications of which have included pumping water, driving an electrical generator, providing ventilation (attic and vehicular), and aqitating water to keep stock pands ice-free during the winter. It is also commonly used as a meter to measure the speed of ocean currents (21).

The construction of a Savonius rotor is essentially that of an S. shaped airfoil with a shaft down the center of the S. One can imagine the shape of a Savonius rotor by thinking of a cylindrical body cut lengthwise in half and turned around to create the letter S, such that there remains a venting system between the two halves ((1)).

An illustrative figure is provided below to visualize the configuration of blades and flow pattern.

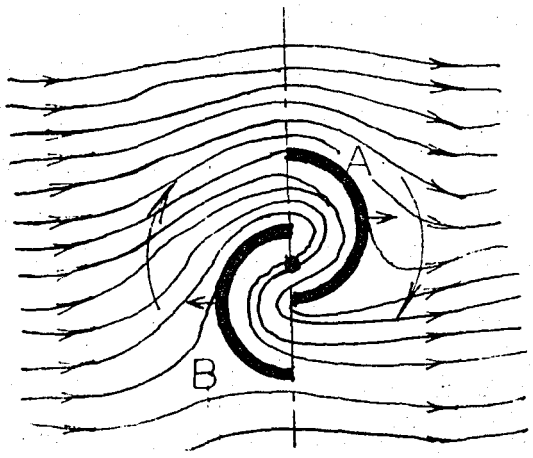

FIG. 3.1.1. Flow thru a Savonius Rotor.

Air striking one of the convace sides "A" of a two blade arrangement is pressed thru the center went of the rotor to the relatively convex side "B" This activity sets up the rotational pattern shown above. The resisting pressure at the back side of the concave blade is released by venting action and the rotor turns in the same sense (regardless of the incident flow direction) with a couple effect. Thus, no vane assembly is needed to orient the impeller into the wind. In general, there is a reduction in both complexity and maintenance by using such a structrure. Relatively high efficiency and steady output may be expected in a working field subject to gusting and changing wind directions, since no time loss encounters for reorientation by a vane to accomadate a change in wind direction.

There is every indication that the Savonius has a high starting torque. This means that in general application it will begin to rotate and generate energy at a low wind speed of rotation is slower, but more power can be made available. The slow speed does necessitate a higher gear ratio if the Savonius is to be used as a wind electric generator. However, the mechanical structure can be simplified because the generator can be mounted at the base by using a long vertical axis. There is much to be learned about the Savonius s-rotor. What is the most efficient and/or effective aspect ratio (ratio of height to diameter)? How do the shape, number of blades, and venting system affect operation? ((12))

The below figure, from ref ((13)) points out the development alternatives that should receive some attention from the

standpoint of both test and analysis.

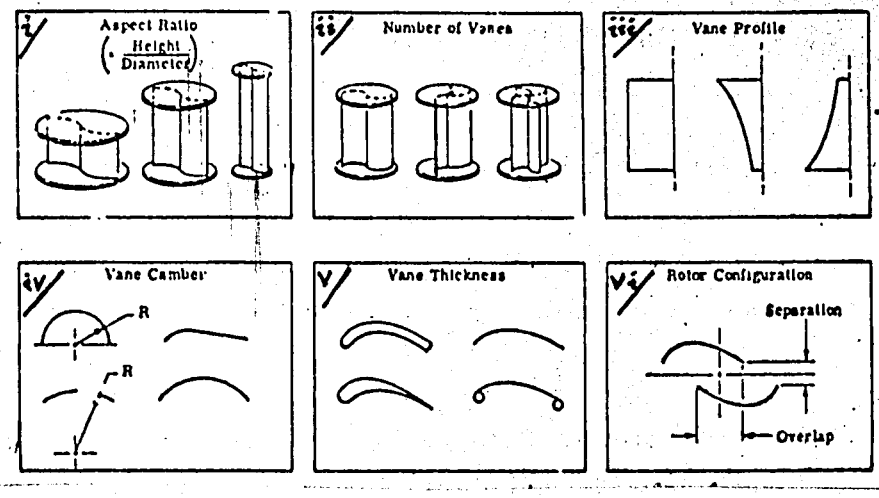

FIG.3.1.2. Development Alternatives of A Savonius Rotor.
Source: W.Vance, PB-231 341, December 1973

These points have provided the initiative for an attempt to predict the optimum design parameters and practical serviceabilit of a 1:1 prototype.

A resumé from previous investigations for Savonius rotor development is submitted below:

3.2. Aspect Ratio

The tests performed on two Savonius rotor models of the same diameter and gap ratio, but of different lengths(*). The models were tested against a blower. The rotation rates were measured under some known resistance load by means of an ascilloscope, and wind velocities were read from a mechanical anemometer. Despite the relatively poor experimental conditions, results were satisfactory to prove that the rotation rate of a Savonius rotor is independent of the aspect ratio. Related plot, given below indicates log X

(*) *During the accomplishment of the graduation project of the author, (May 1977).*

vs log Re_D data belonging to distinct aspect ratio models, fall on to the same straight line.

Thus, the conclusion of ref.(25) reading, 'The large number of design parameters along with the unknown influence of Reynolds' number and aspect ratio do not permit the exact determination of the optimum design parameters' looses its validity.

Experimental details, rough data and computational details are given in §APPENDIX A1 and A2.

On the other hand, the aspect ratio,(*) as reported by Vance, has significant effect on acceleration, output torque and inertia of the rotor. Preliminary test results have revealed the relations,

Torque output ~ $AR^{-\frac{1}{2}}$
Rotor inertia ~ AR^{-1}
Rotor acceleration ~ $AR^{\frac{1}{2}}$

Under constant Wind velocity (31).

(*) *Aspect ratio was taken by Vance as AR = H/D. Experiments were carried out for constant height and varying diameter models.*

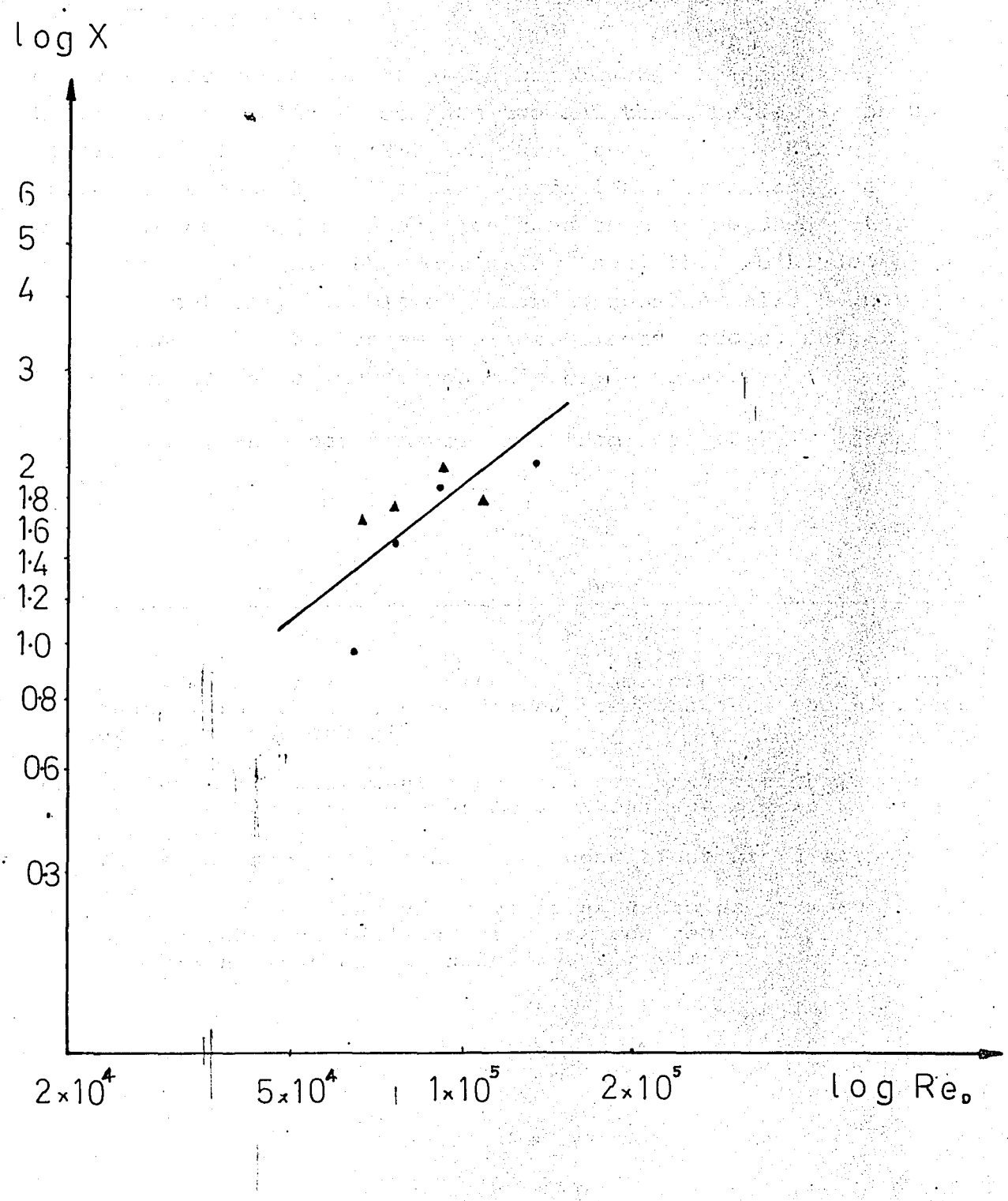

FIG. 3.2.1. Reynolds' Number Dependence of Tip Speed Ratio for Various Aspect Ratios.

3.3. Number of Vanes

Considerable research attention was devated by Sheldahl, Blackwell and Feltz to compare two and three bucket Savonius rotors. Their work[1] (21) indicates that, a two blade rotor has a much higher power coefficient, in accordance with sivasegaram (25) whose tests on several hundred rotor configurations gave the conclusion that, the two bladed, rotor is not only capable of reaching substantially higher performances[2] than three and more bladed rotors, but also more responsive to improvements in blade geometry.

The geometry and performance plot from ref. (21) is given below:

---

(1) Tests were carried out with 1m. diameter rotors in a wind tunnel; the data were corrected to compensate the blockage effect of the tunnel.

(2) In general, experimental performance predic tion is done by gathering data to plot Cp us X characteristic curve of the rotor.
Three methods under controlled conditions are distinguished as,
a/ Varying the load under constant Reynolds' number ,
b/ Varying Reynolds' number under constant load,
c/ Varying load and Reynolds' number simultaneously.

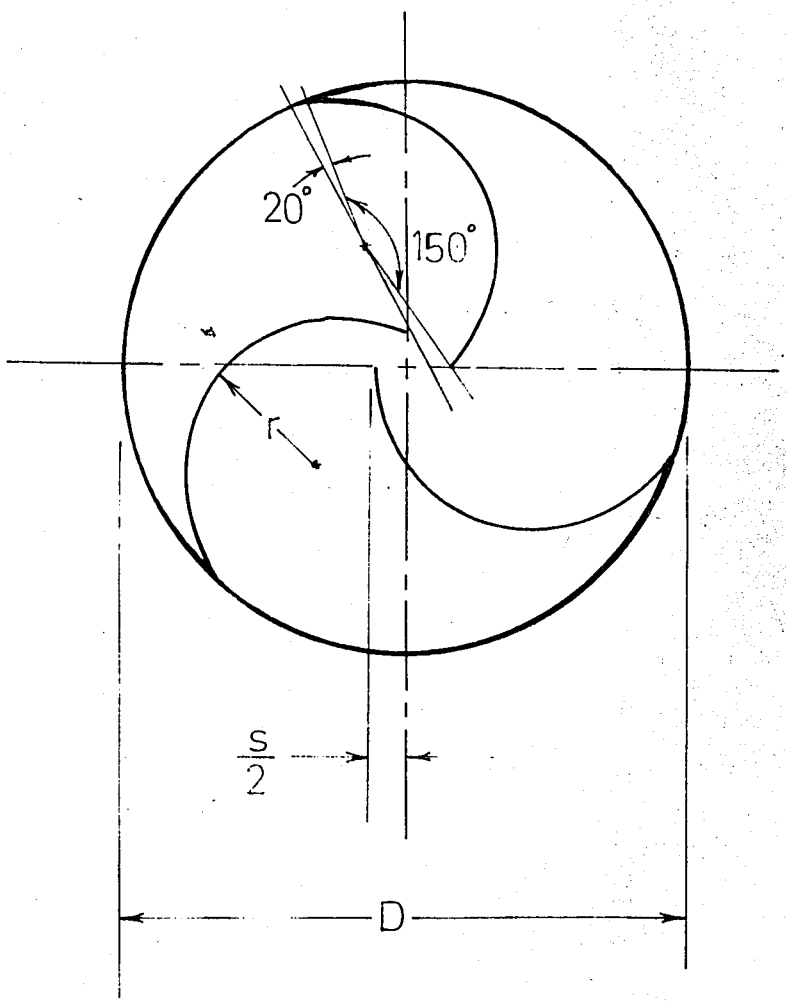

FIG:3.3.1. Schematic of the 3-bucket Savonius Rotor with 150° Buckets.

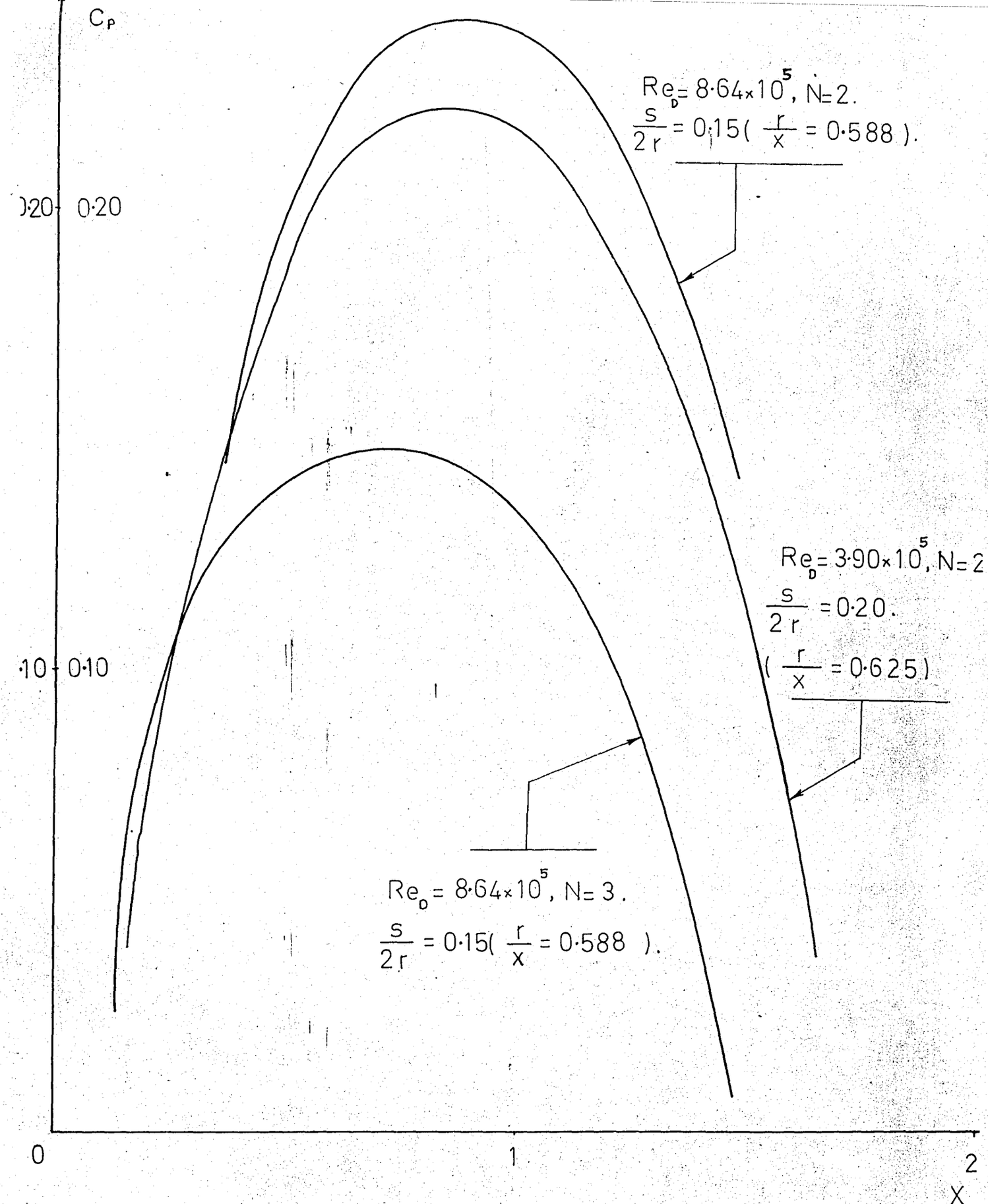

FIG. 3.3.2. Variation of Power Coefficient for 2 and 3 Bucket Rotors (from wind tunnel tests of 1 m. dia. models). [21]

The experimental work (*) by Braasch reveals the same fact that power coefficient of 3-bucket rotors are considerably less than those with 2 vanes (33).

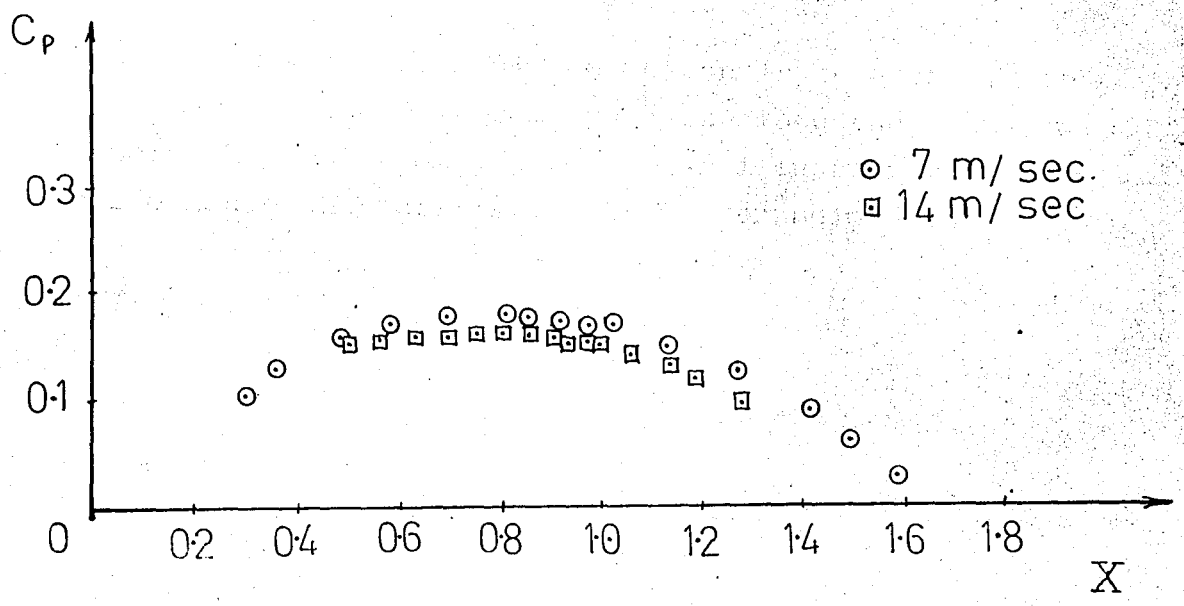

FIG. 3.3.3. Varistion of Power Coeflicient under Various Reynolds' Numbers for 3-Bucket Savonius Rotors.

(*) *The experiments were performed in a wind turnel with 0.5 m. Vane diameter; 1.5 m. high rotors. The test hardware employed an air motor drive system. The geometry of circular blades were exactly same as those used in ref. (21).*

3.4. Vane Geometry

Investigations are mostly devoted to the analysis of the effect of blade shape on performance.

Among these, the most outstanding are the works of Newman (*) (24), and Kenfield (23), who tested modified designs of the Savonius rotor proposed by Bach.

The geometry of the modified design is such that, the curvature of blades decrease in some pattern along the main diameter toward the center of the rotor. An illustrative figure and performance characteristics are given below:

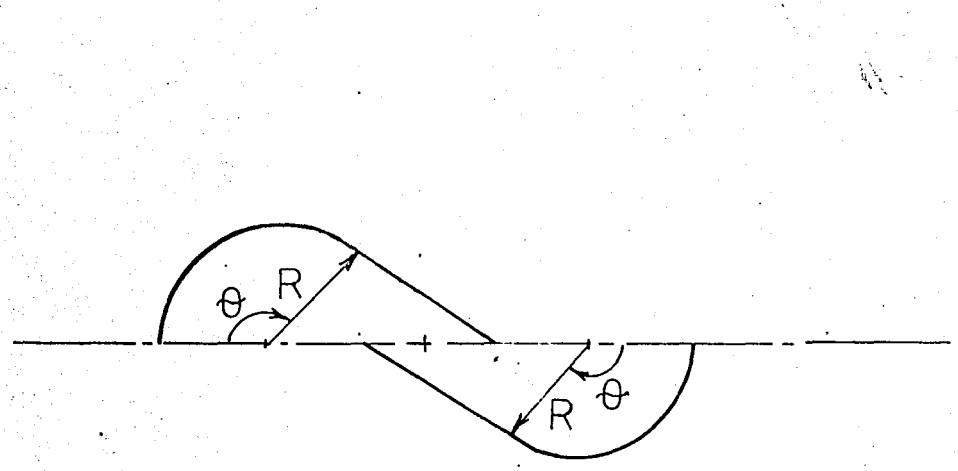

FIG.3.4.1. Modified savonius Rotor.

(*) *The tests by Newman were performed with 1' dia. Models in a wind tunnel. The torque, and hence the power output was measured with a viscous dynamometer. No attempt was made for correction of data against blockage effect.*

The work reported by Kentfield (*) (23) describes a preliminary experimental attempt to equip a modified Savonius wind turbine with aerodynamic devices to improve the rotor performance, particularly at low velocity ratios. An ordinary Savonius rotor of conventional design was used to compare the results.

The geometry of the conventional Savonius rotor, as well as as the modified versions, together with the results of comparative trials are given below:

(*) *The tests were carried out in a wind tunnel using models of D = 5" with the rotor height equal to the diameter. The free stream velocity was measured at the model section without the model present, using both a micromanometer and also a D.C. type hot wire probe anemometer. The power output of the wind turbine was recorded by means of a simple, specially constructed, hydraulic dynamometer. The rotor speed was established from the use of a colibrated stroboscope. No tunnel blackage correction was applied.*

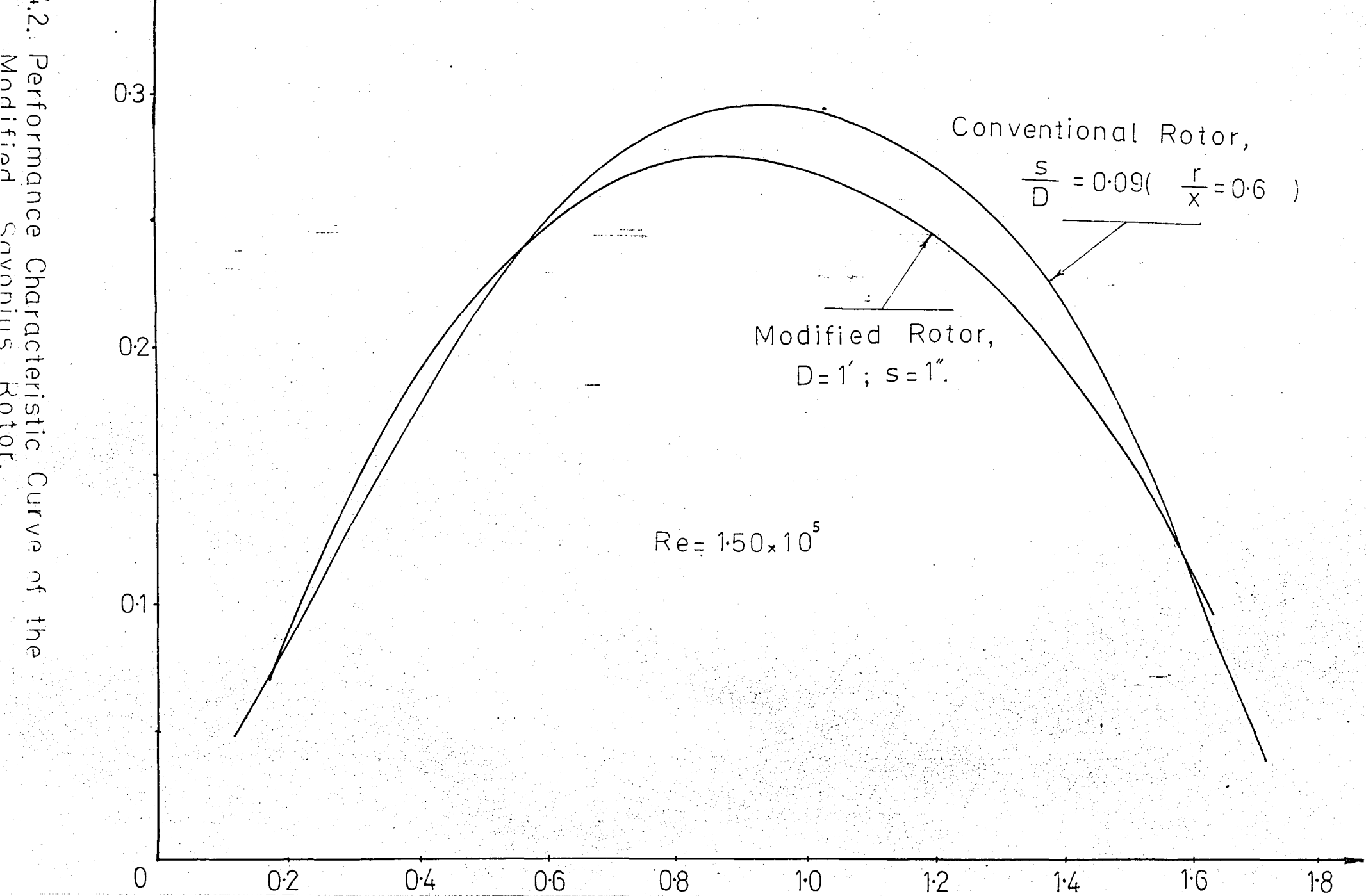

4.2. Performance Characteristic Curve of the Modified Savonius Rotor.

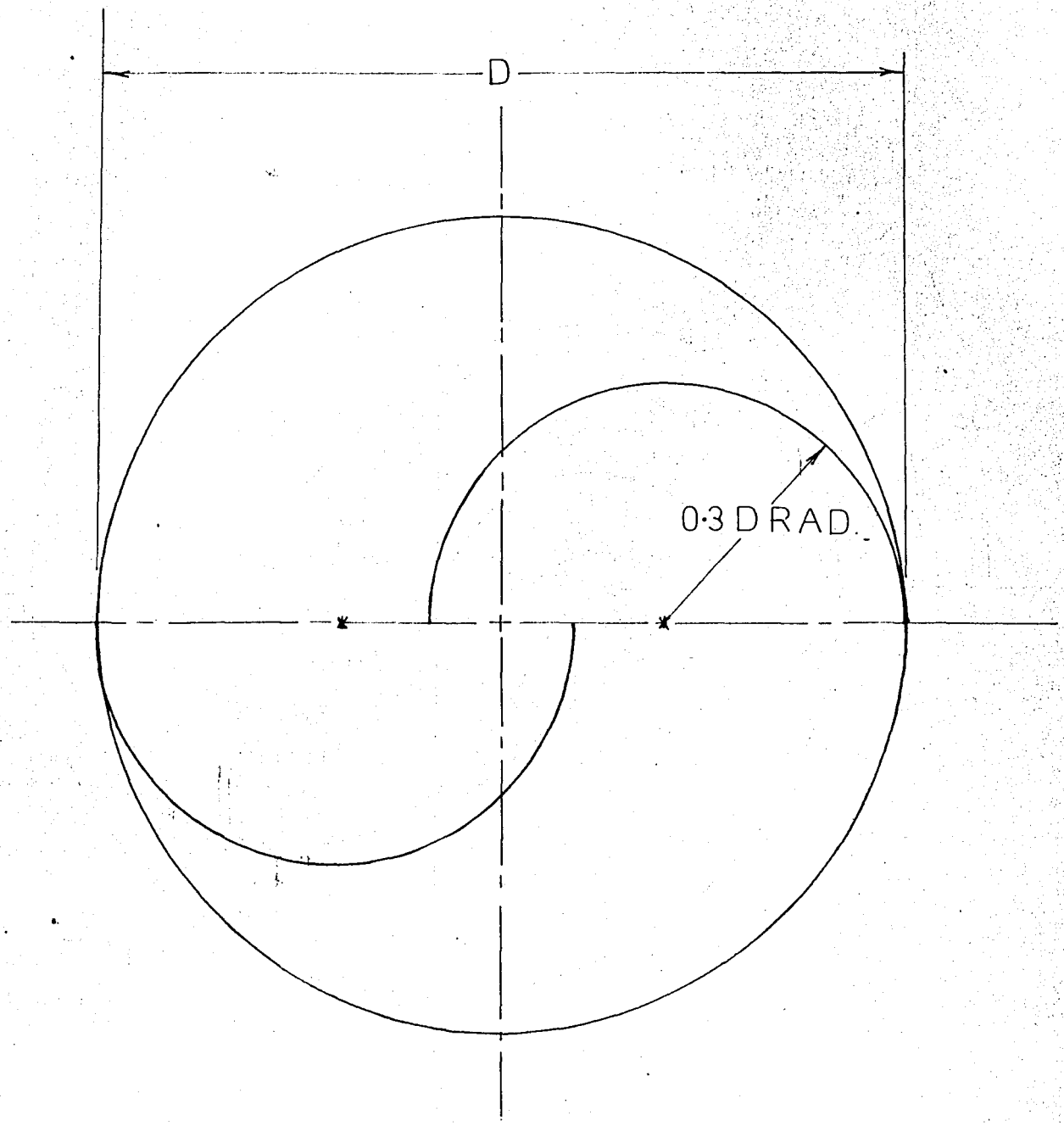

FIG. 3.4.3. Conventional Savonius Rotor, Overlap Ratio as Recommended by Savonius($\frac{r}{x} = 0.75$).

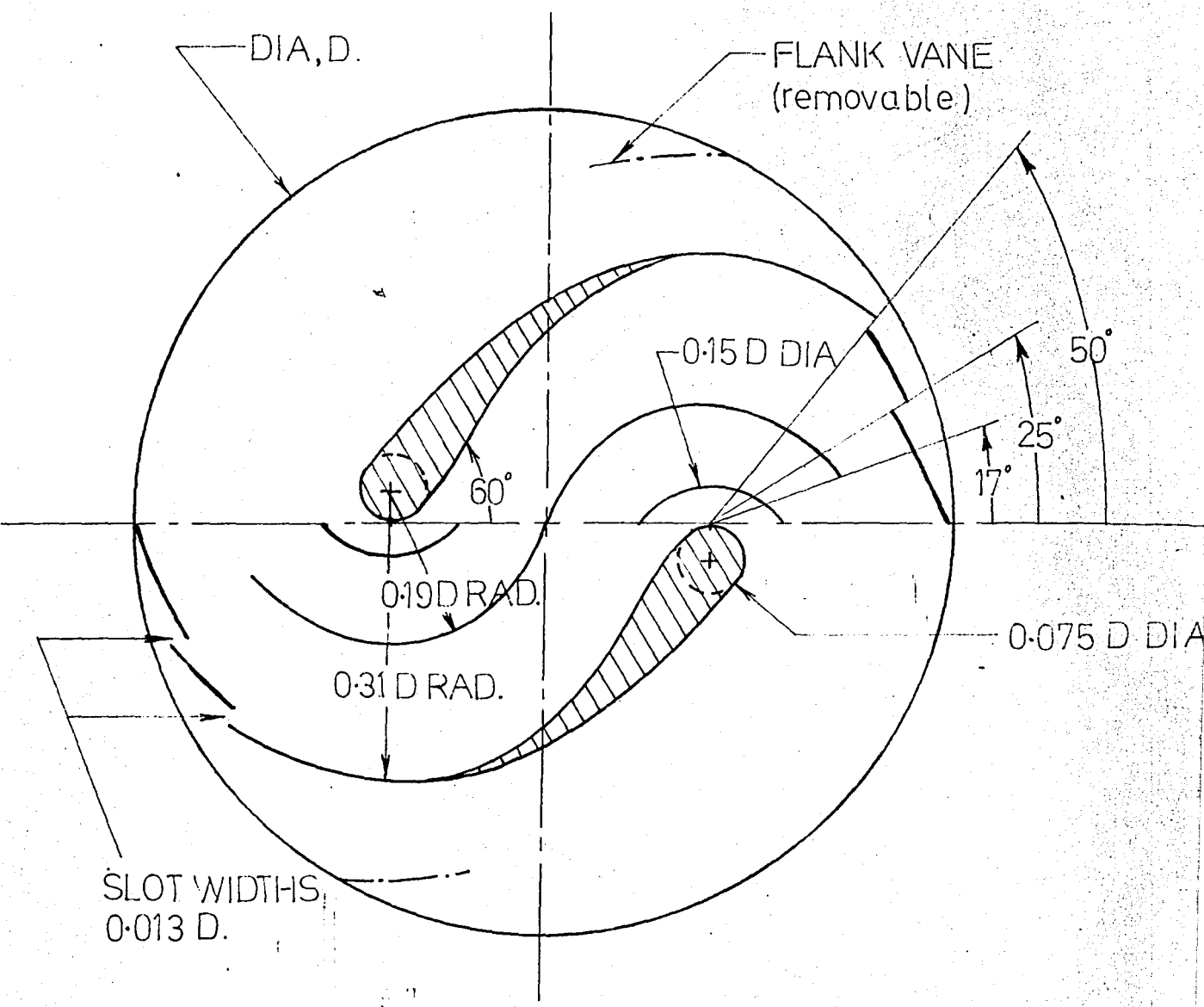

FIG. 3.4.4. Modified Savonius Rotor.(also showing flank vane locations).

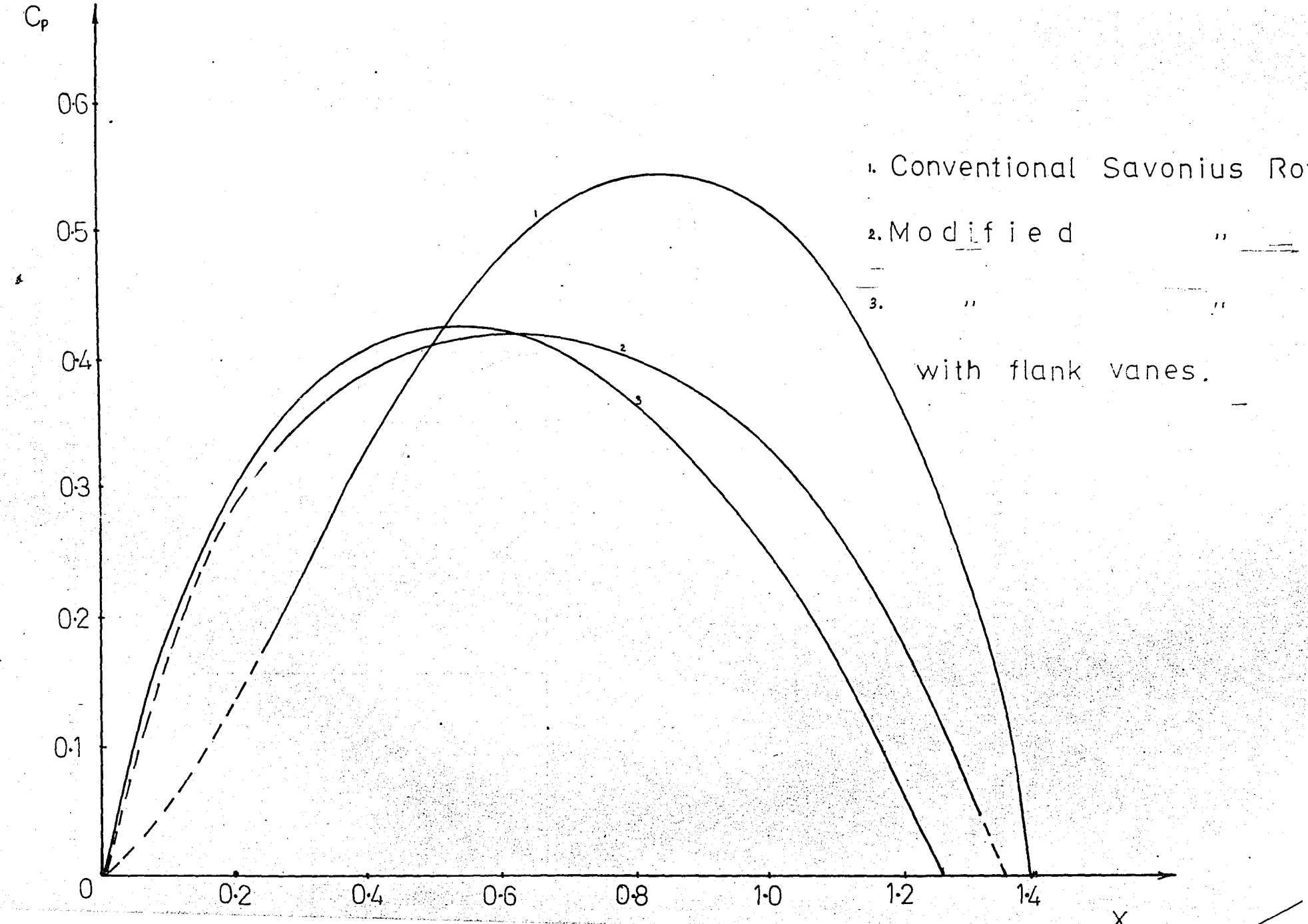

FIG. 3.4.5. Comparison of Conventional S-Rotor with Modified Versions.

3.5. Rotor Configuration

Optimum spacing between the circular blades is investigated by various researchers. An illustrative figure of the cross-section supplied with the necessary parameters is given below:

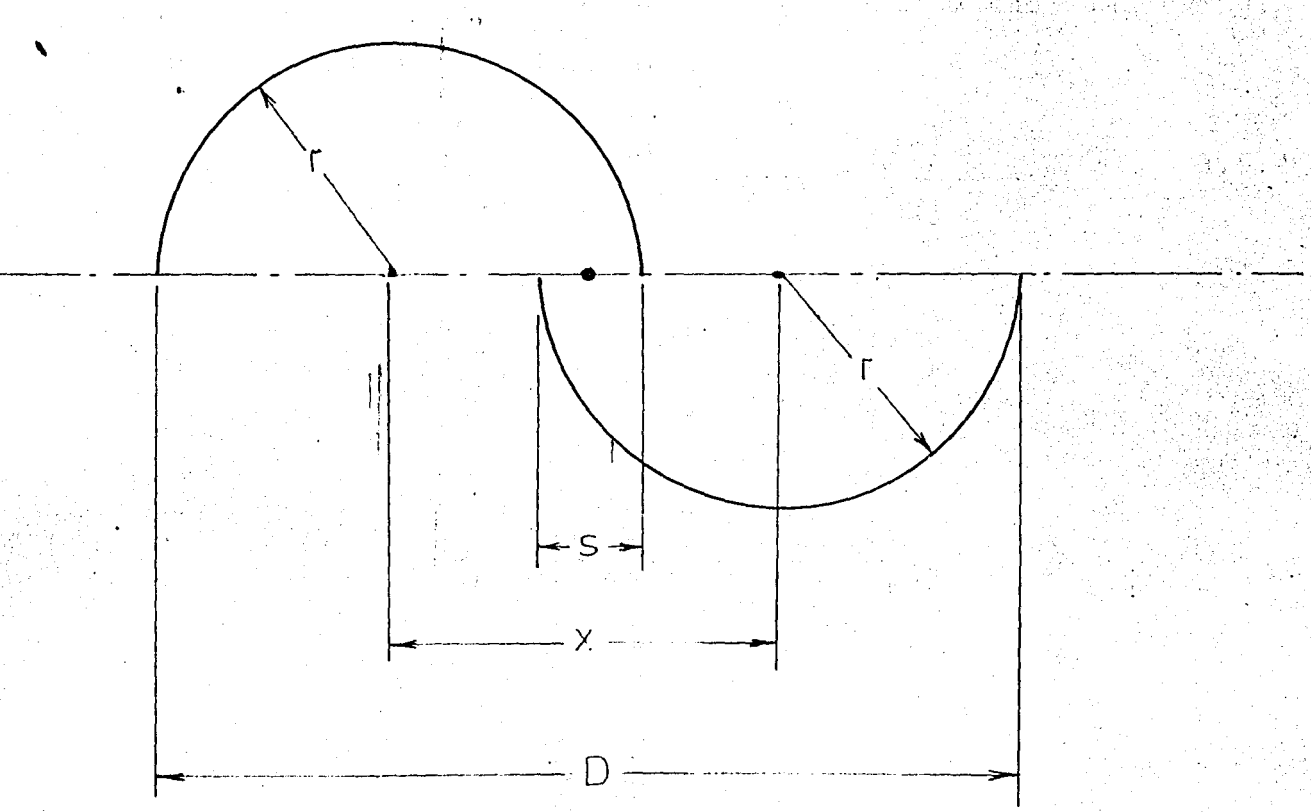

FIG. 3.5.1. Cross-Section of a Savonius Rotor with Necessary Parameters Illustrated.

Obviously, the relations between the parameters are,

$$D = x + 2r \qquad 3.5.1$$

$$x = 2r-s \qquad 3.5.2$$

$$D = 4r-s \qquad 3.5.3$$

The mojor factor to affect the output characteristics of a Savonius rotor is the amount of averlapping of the circular blades. Referring to the parameters in the figure, this can be given either as

$\frac{r}{x}$, or $\frac{s}{D}$ or $\frac{s}{2r}$, all of which representing the same thing.

The conversion relations are,

$$\frac{r}{x} = \frac{r}{2r-s} = \frac{\frac{D+s}{4}}{\frac{D+s}{2}-s} = \frac{(D+s)}{4} \cdot \frac{2}{(D-s)} = \frac{1+\frac{s}{D}}{2(1-\frac{s}{D})} \qquad 3.5.4$$

$$\frac{s}{D} = \frac{2r-x}{2r+x} = \frac{2(\frac{r}{x})-1}{2(\frac{r}{x})+1}$$

$$\frac{r}{x} = \frac{(D+s)}{4} \cdot \frac{2}{(D-s)} = \frac{(4r-s+s).2}{4.(4r-s-s)} = \frac{2(4r)}{4(4r-2s)} = \frac{r}{2r-s} .$$

$$= \frac{\frac{r}{2r}}{\frac{2r}{2r}-\frac{s}{2r}} = \frac{(\frac{1}{2})}{1-\frac{s}{2r}} = \frac{1}{2(1-\frac{s}{2r}} \qquad 3.5.6$$

$$\frac{s}{2r} = \frac{2r-x}{2r} = \frac{2(\frac{r}{x})-1}{2(\frac{r}{x})} \qquad 3.5.7$$

Savonius (1930) recommended a gap ratio $\frac{s}{D} = 0.2$ (corresponding to $\frac{r}{x} = 0.75$) ((3)). However, no details are available on the experimental procedure.

It was only in mid 70's that investigators started to work on the Savonius rotor.

Based an experimental work on wind tunnel models, Newman (*) (1978) suggests $\frac{s}{D} = \frac{1}{5}$ (corresponding to $\frac{r}{x} = 0.6$) (24).

Graphical results are submitted below:

(*) Experimental techniques were mentioned in §3.3.

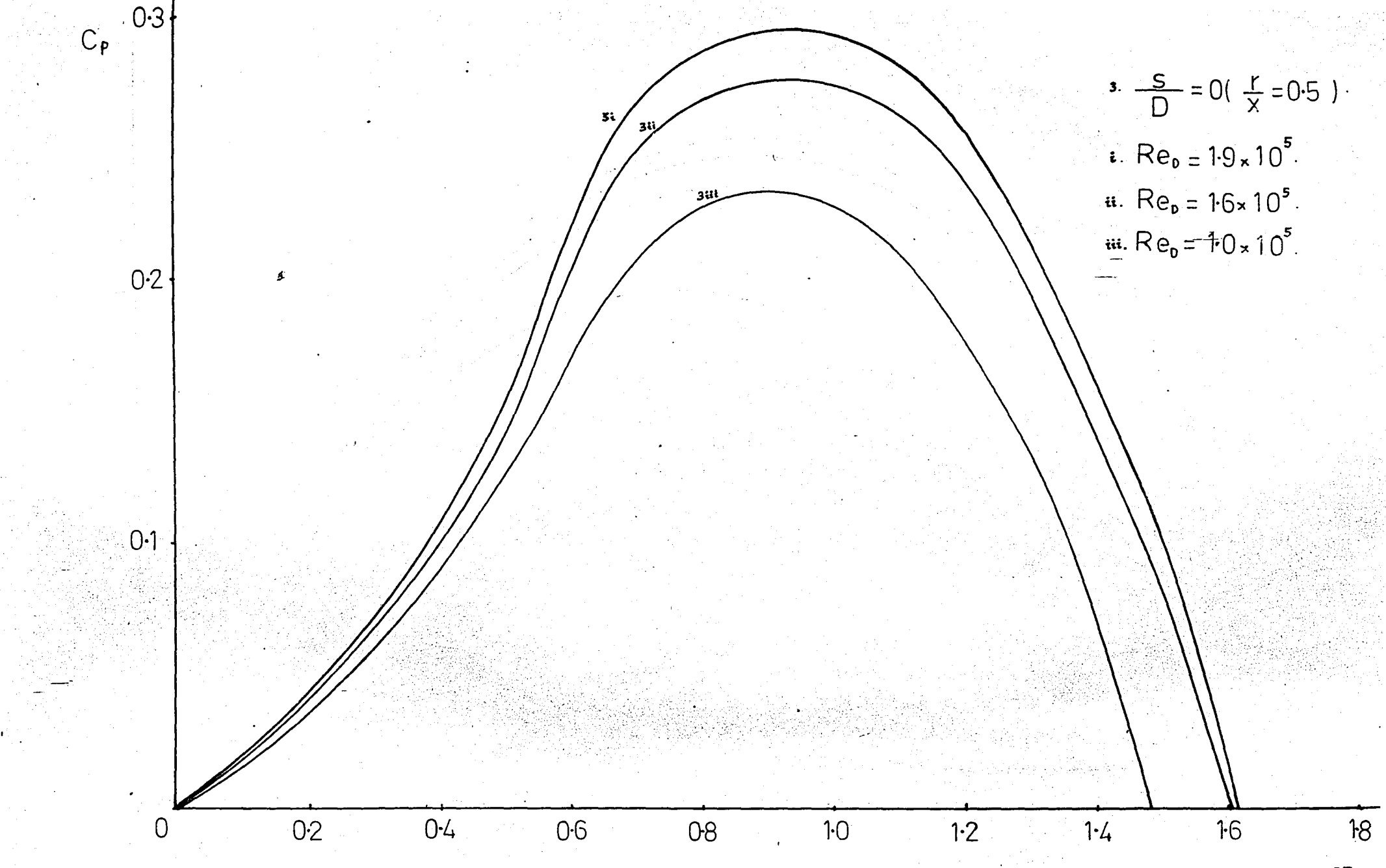

FIG 3.53. Effect of Reynolds' Number on Power Coefficient of Rotor 3.

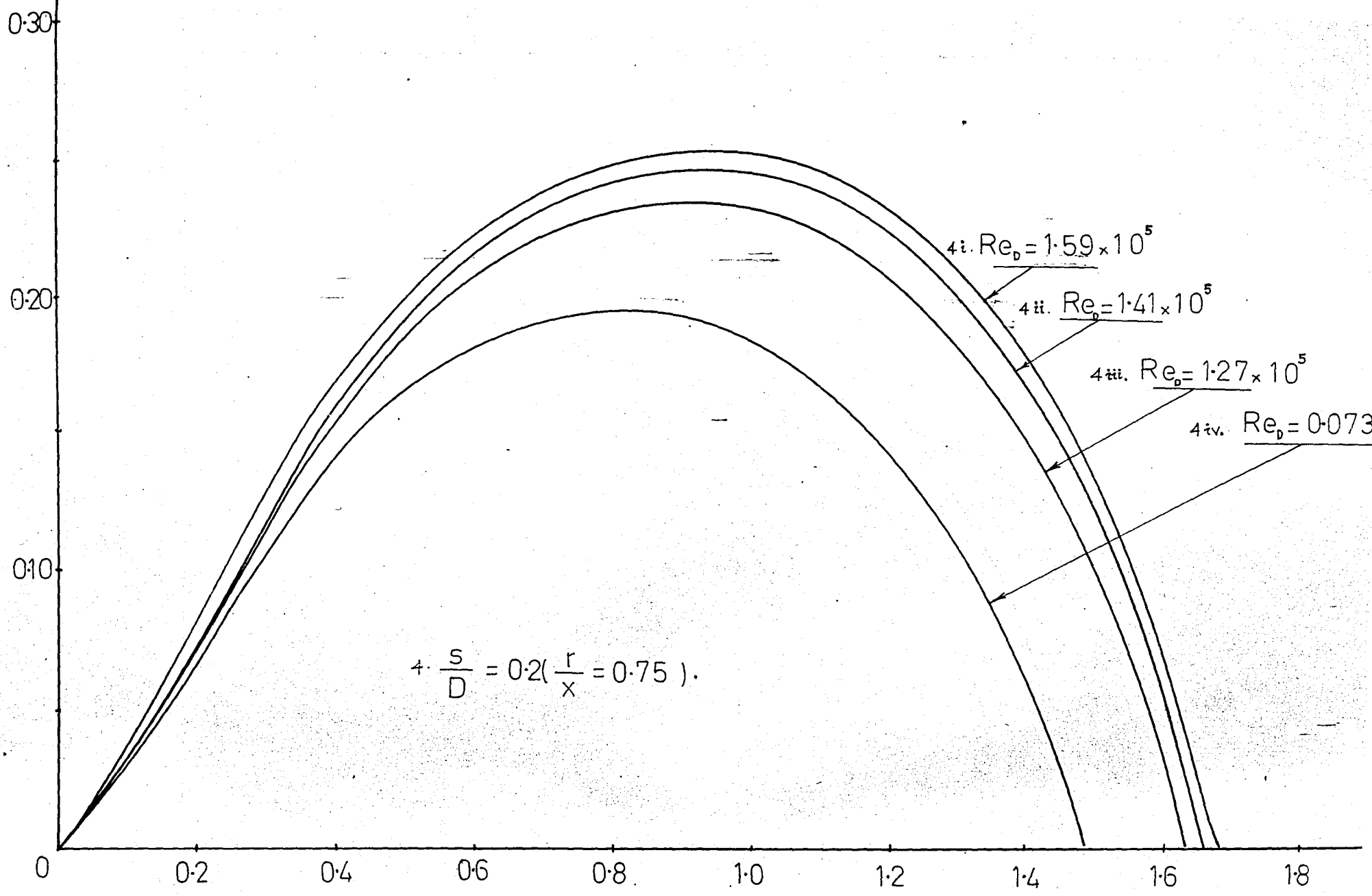

FIG. 3.5.4. Effect of Reynolds' Number on Power Coefficient for Rotor 4.[24].

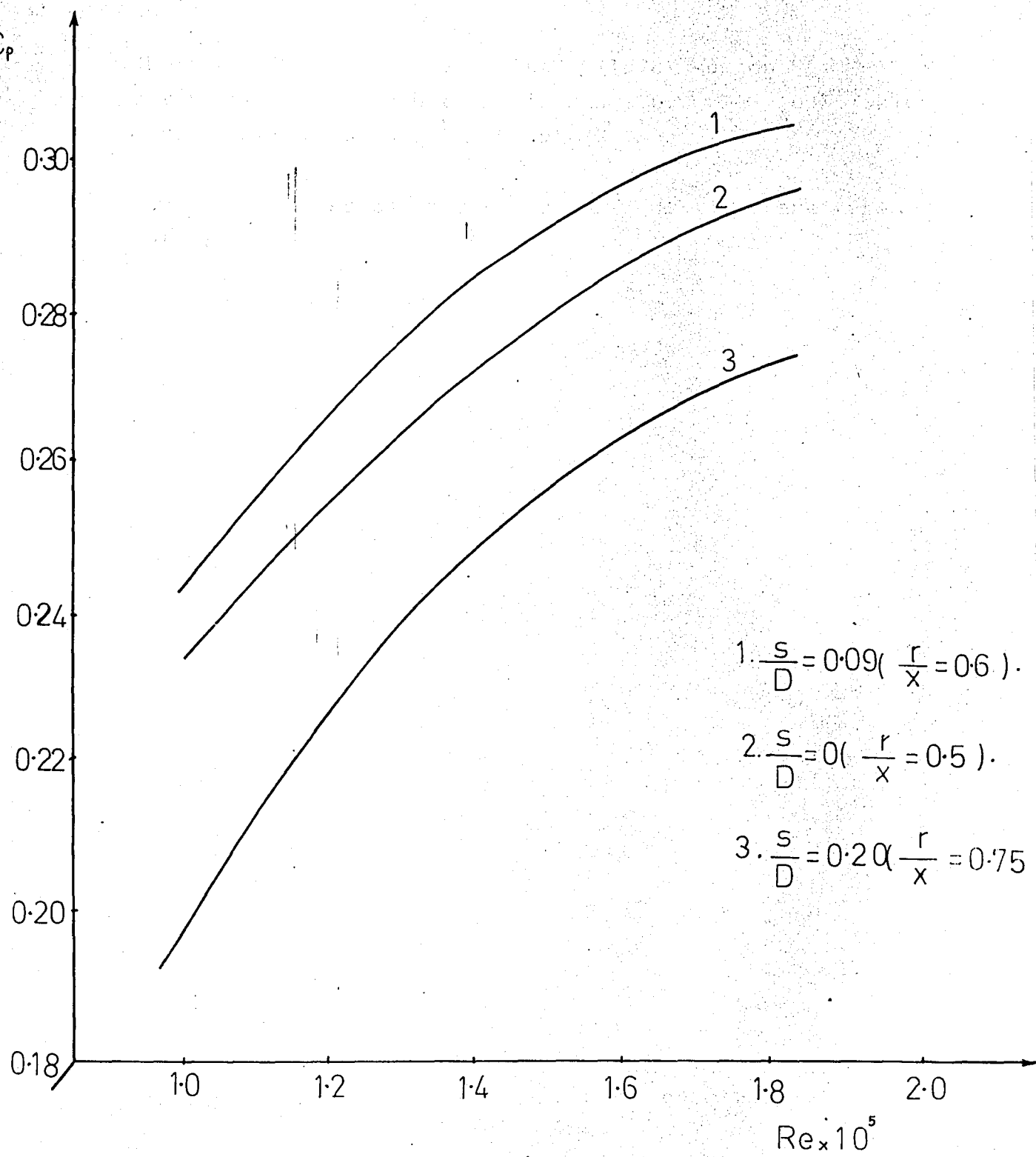

FIG. 3.5.5. Optimum Power Coefficient of Rotors at Various Reynolds' Numbers.

Sheldahl, Blackwell and Feltz(*) (1978) suggest a dimensional gap width to be in range $0.1 \leq \frac{s}{2r} \leq 0.15$ (which corresponds to $0.56 \leq \frac{r}{x} \leq 0.59$). (21).

Comparative results of various configurations are taken below:

(*) *Experimental techniques were mentioned in §3.2.*

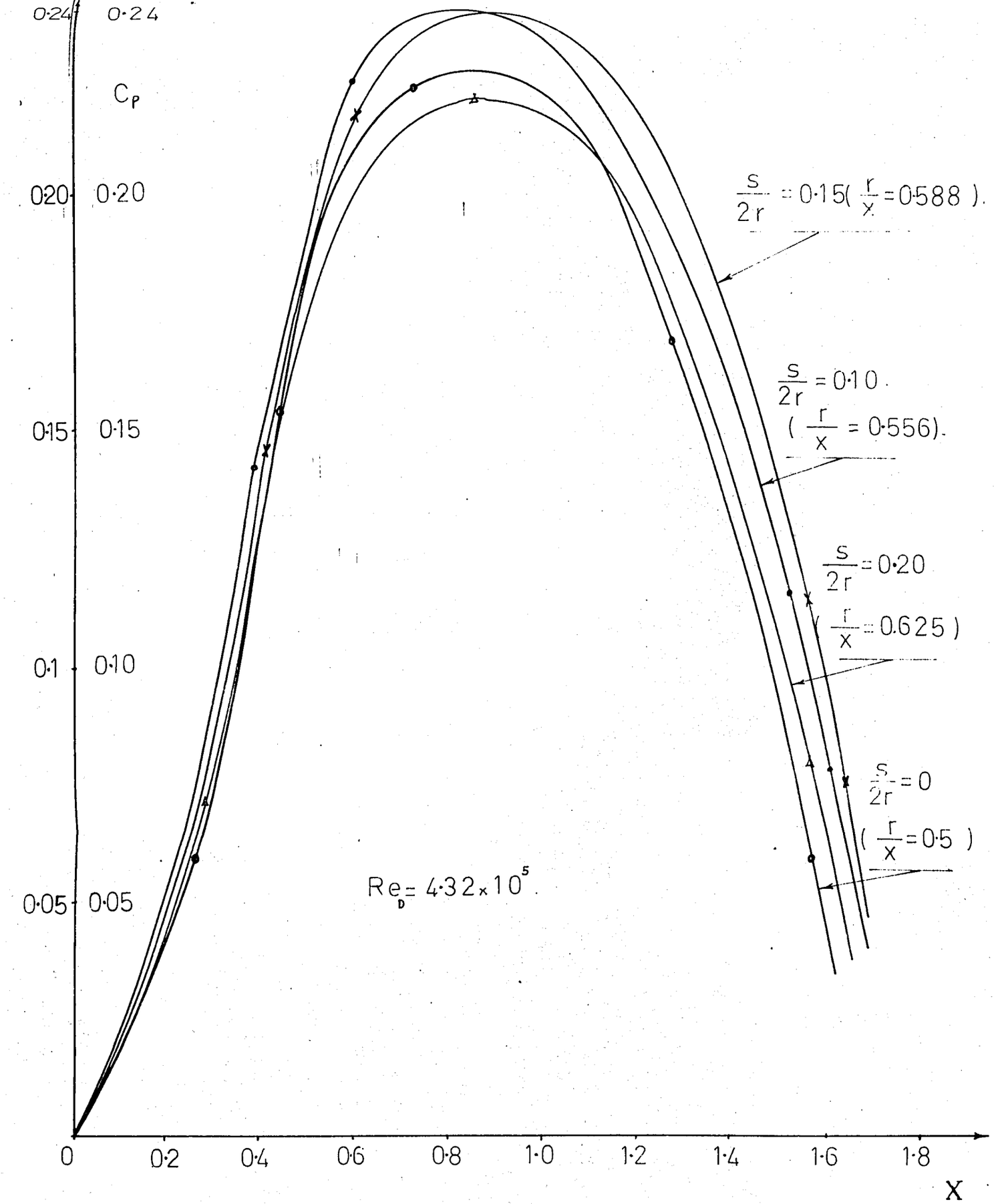

FIG. 3.5.6. Variation of Power Coefficient for Various Gap Width Ratios.(from wind tunnel tests of ≈ 1 m dia models)[21].

Independent of the above efforts, same problem was analysed in the graduation project of the author (1977). The results involving the relationship of two main dimensionless parameters of various configurations are submitted here, while the experimental details dogether with the rough data are given in APPENDIX A 1.

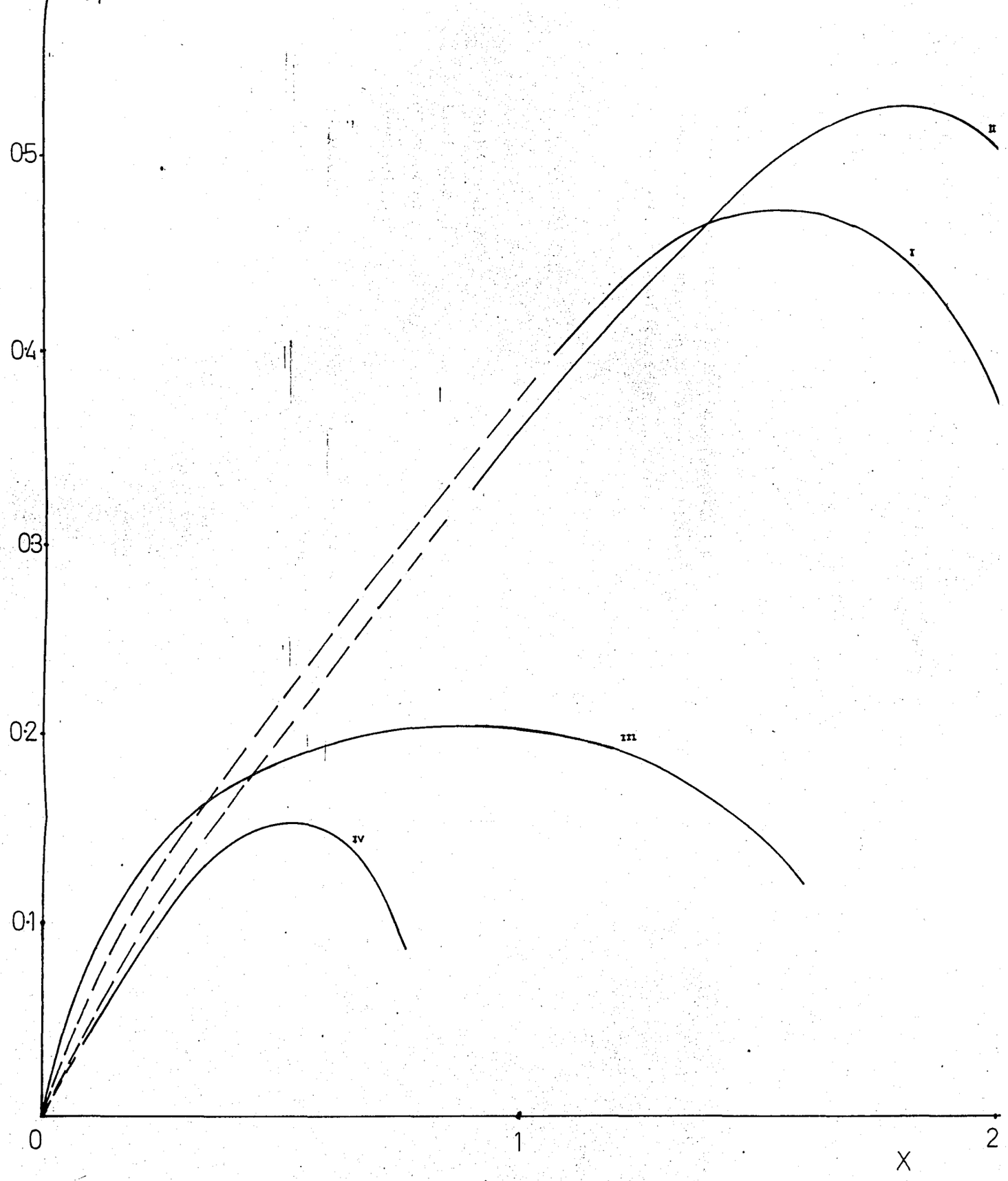

FIG. 3.5.7. Power coefficient vs Velocity Ratio to Determine the Best Gap Ratio $\frac{r}{x}$.

It is seen that, gap ratios of arrengements (III) and (IV) with $\frac{r}{x}$, 1 and 2 respectively show very poor performance characteristics when compared to models (I) and (II) (with $\frac{r}{x}$ 0.67 and 0.8 respectively).

Configuration (II) is more efficient at high velocity ratios, while no data were available for tip speed ratios, less than 1 ; moreover, gap ratios less than 0.67 (recommended range according to more recent work), were not tested at all. In this work, it was concluded that $\frac{r}{x} = 0.8$ is the most efficient ratio according to the available experiments.

This experimental investigation which was subject to numerous uncertainties (especially in the measurement of power output) proves to be insufficient when compared to recent efforts of various researchers mentioned above.

3.6. Conclusion Remarks About Existing Literature

After the resume of the existing work on Savonius wind Turbine development, now cames to one's mind the question that the what extent are the results obtained from experimentation of models can be trusted to make size and performance predictions over 1:1 ratio prototypes?

According to the existing work, a few words of caution should be added about comparing the reported performances of wind turbines.

Sivasegaram points out that, most of the published data are subject to substantial experimental uncertainty, and tend to overestimate the performance of models. Tests performed with the models placed inside the wind tunnel lead to an

overestimation of the performance, and there is no reliable correction procedure available (25).

In this respect, model tests in a wind tunnel can only represent the relative merits of the models under investigation. The power coefficients obtained from such tests cannot be generalized to 1:1 ratio prototypes.

Newman, indicates that the full-scale performance of Savonius rotors has not yet been determined with precision. All model tests to data, including present ones, give only an approximate indication of full-scale performance because,

a/ Corrections for wind-tunnel interference are too large be thrustworthy.
b/ The measurements indicate a significant scale effect, the power coefficient incerasing with Reynolds' number for the model scales sofar been tested (24).

In order to carry out the model experiments under realistic Reynolds' numbers, very high wind velocities 15-20 m/sec were used to compensate small rotor diameters, which resulted in unrealistic efficiency predictions.

It is reported by Vermeulen that, an attempt to establish the sensitivty of the models to a change of Reynolds' number by varying the flow velocity produced little effect. This may be due to the relatively high inherent turbulence level in the wind tunnel (23).

Thus, our survey of the existing literature revealed the conclusion that an effort claiming an advancement in the investigation of the Savonius rotor should entertain experimentation in field conditions with actual size prototypes.

Although such tests were known to be hampered by the lock of appropriate instrumentation and absence of adequately steady winds as well as construction, handling and maintenance difficulties, an impeller (of 1.236 m^2 effective area) was designed(1) and realized to be erected to the roof of the Engineering Building.

After some initial testing period in the operation zone, the rotor was coupled to the necessary instruments(2) to take data of associated parameters for the prediction of performance characteristics of the full scale Savonius rotor under real operation conditions. Related results are submitted in the next chapter.

---

(1) Necessary design details are provided in §APPENDIX A-3 and A-4.

(2) This point is explained in §APPENDIX A-5

4. MANIFESTATION OF EXPERIMENTAL RESULTS

This secton is composed of three ports:

1/ Torque and power delivered by the rotor are plotted against wind speed and rotation rate both. Namely

$$\left\{\begin{matrix} T \text{ vs } v \\ T \text{ vs } w \end{matrix}\right\} \quad \left\{\begin{matrix} P \text{ vs } v \\ P \text{ vs } w \end{matrix}\right\} \quad \text{, and } (v \text{ vs } w).$$

2/ The quantities are formed into dimensionless parameters (those derived in 2.7) and the relations between these parameters are given as

$$\left\{\begin{matrix} C_T \text{ vs } Re_D \\ C_T \text{ vs } X \end{matrix}\right\} \quad \left\{\begin{matrix} C_p \text{ vs } Re_D \\ C_p \text{ vs } X \end{matrix}\right\} \quad \text{, and } (Re_D \text{ vs } X), \text{ as caunterparts}$$

of the results of part 1. These are valid for all rotors of same diameter D, and gap ratio r/x independent of height(*).

Also, some data related with the no-load tip speed ratio at low velocities are used to check the correlation with the simple theory submitted in § 2.8.

3/ To test the practical serviceability, the rotor was connected to a car alternator to give electrical power at a cut in rpm of 1000 of the alternator. In this part, related current and voltage output of the system vs wind velocity is given.

A step - up transmission ratio of i = 3.94 was used to increase the rotation rate of the rotor, which was coupled to a dynamic torque transducer. Related data and experimental details are submitted in § A.8, A.5 and A.7 respectively.

The transmission ratio entertained in experimentation with the alternator was, 17.25. The transmission system is explained in § A.6.

(*) *This is proved in part 2 of this §.*

4.1. Evaluation of Results Associated With the Basic Variables

A combined equation of relating the output torque T', or power P' to wind velocity v and rotation rate w, (derived in part 2) can be stated as,

$$\frac{T'}{A} = -0.07\,\rho D^2\,wv + 0.27\rho Dv^2 \quad (=T) \qquad 4.2.4.i$$

Taking $\rho = 123\ \frac{kg}{m^3}$ and D 0.97m as constants, (i) reduces to

$$T\ \left(=\frac{T'}{A}\right) = -0.08\,wv + 0.32v^2 \qquad 1.4.4.ii$$

Similarly for power , $P_G = Tw$

$$\Rightarrow P_G\left(=\frac{P'}{A}\right) = -0.07\rho D^2\,w^2\,v + 0.27\,\rho Dwv^2 \qquad 4.2.5.i.$$

or, taking ρ and D constant,

$$P_G = -0.08\,w^2v + 0.32\,wv^2 \qquad 4.2.5.iii.$$

In part 2, it is proved that equations 4.2.4 i-ii and 4.2.5 i-ii above are valid not only for this particular rotor, but for all Savonius wind turbines of the same diameter (D = 0.97m) and gap ratio (r/x= 0.63) independent of rotor height.

Torque and power relations vs wind speed and rotation rate are given in the below figures.

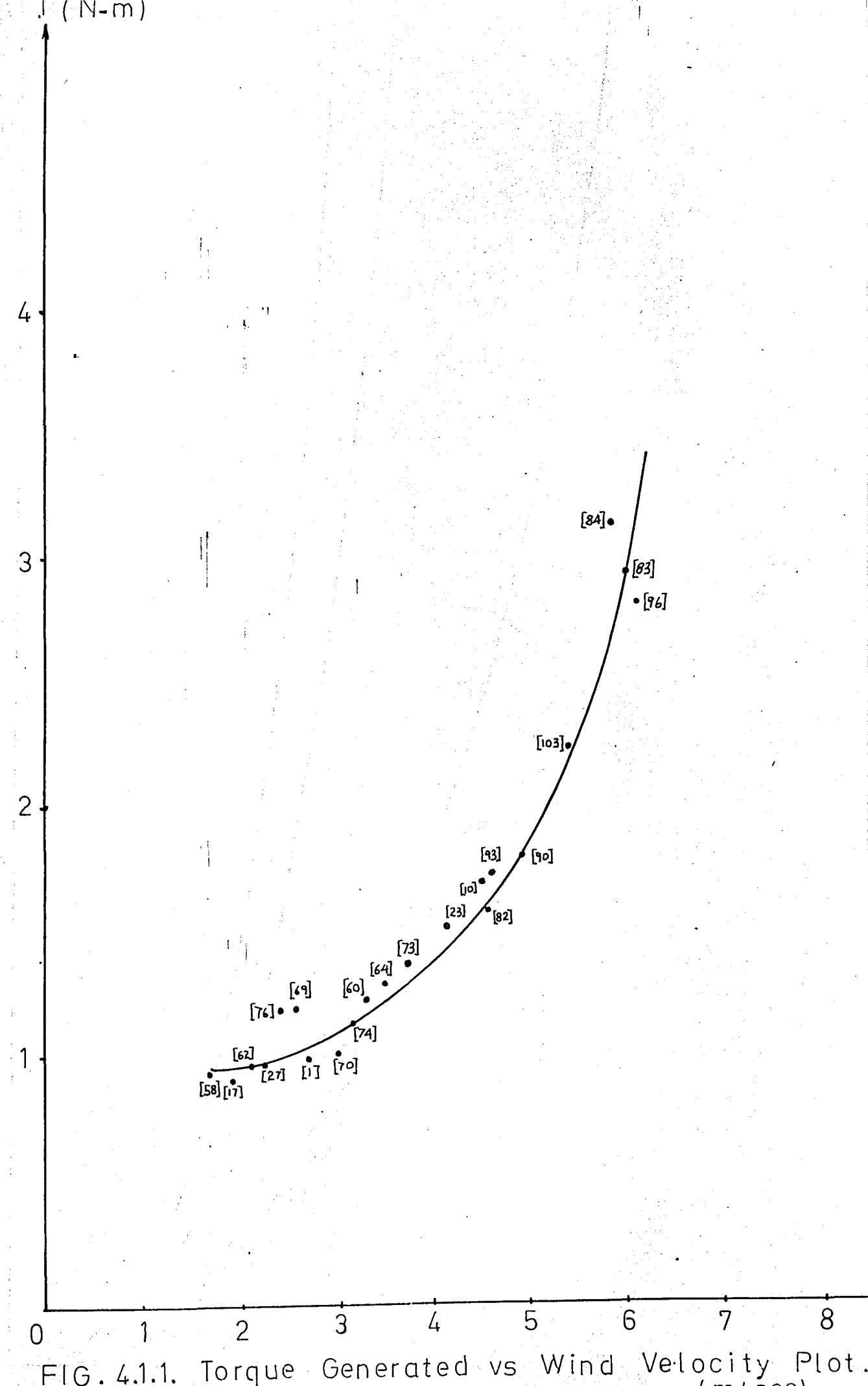

FIG. 4.1.1. Torque Generated vs Wind Velocity Plot.

(m/sec)

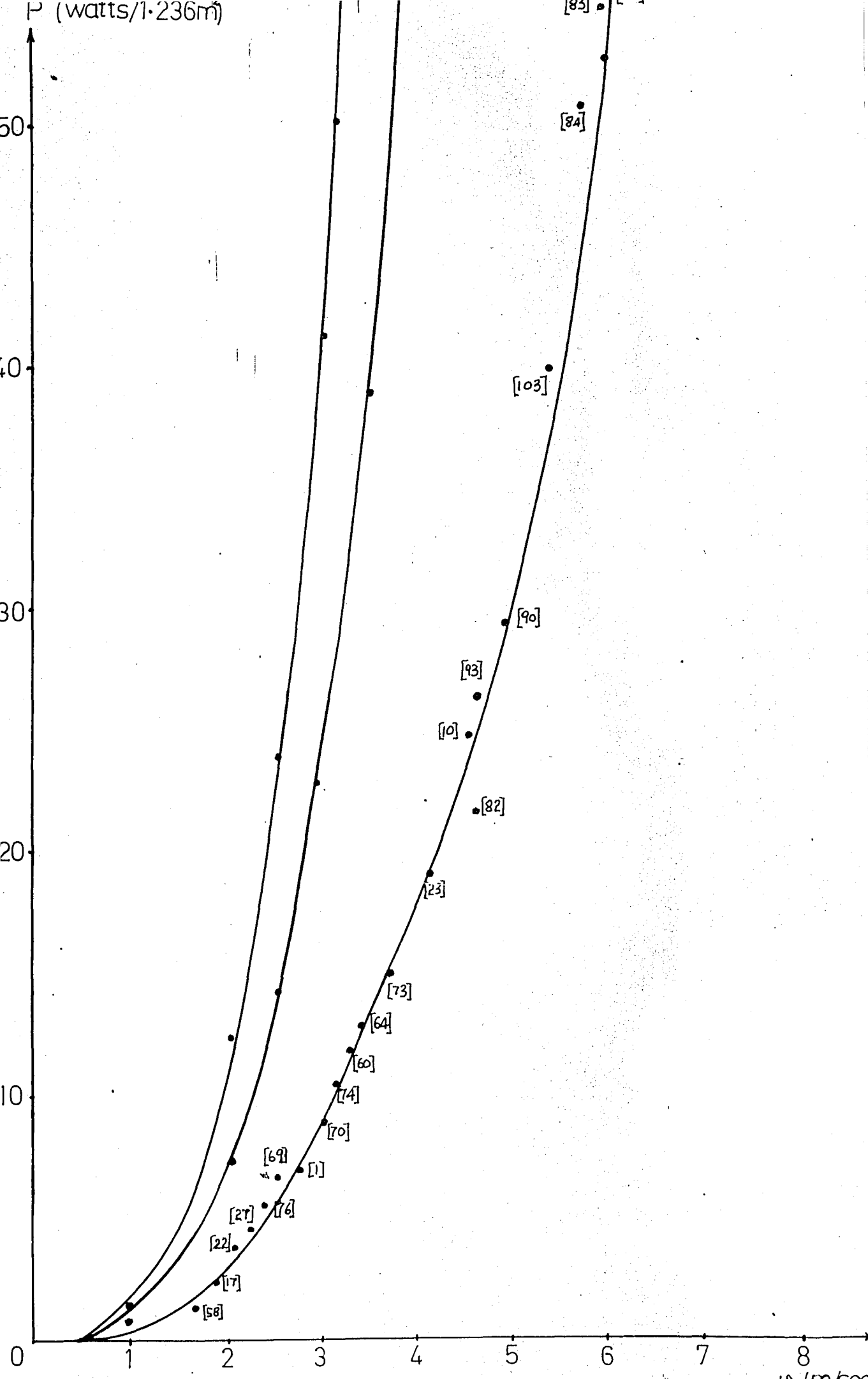

FIG.412 Power Generated vs Wind Velocity Plot.

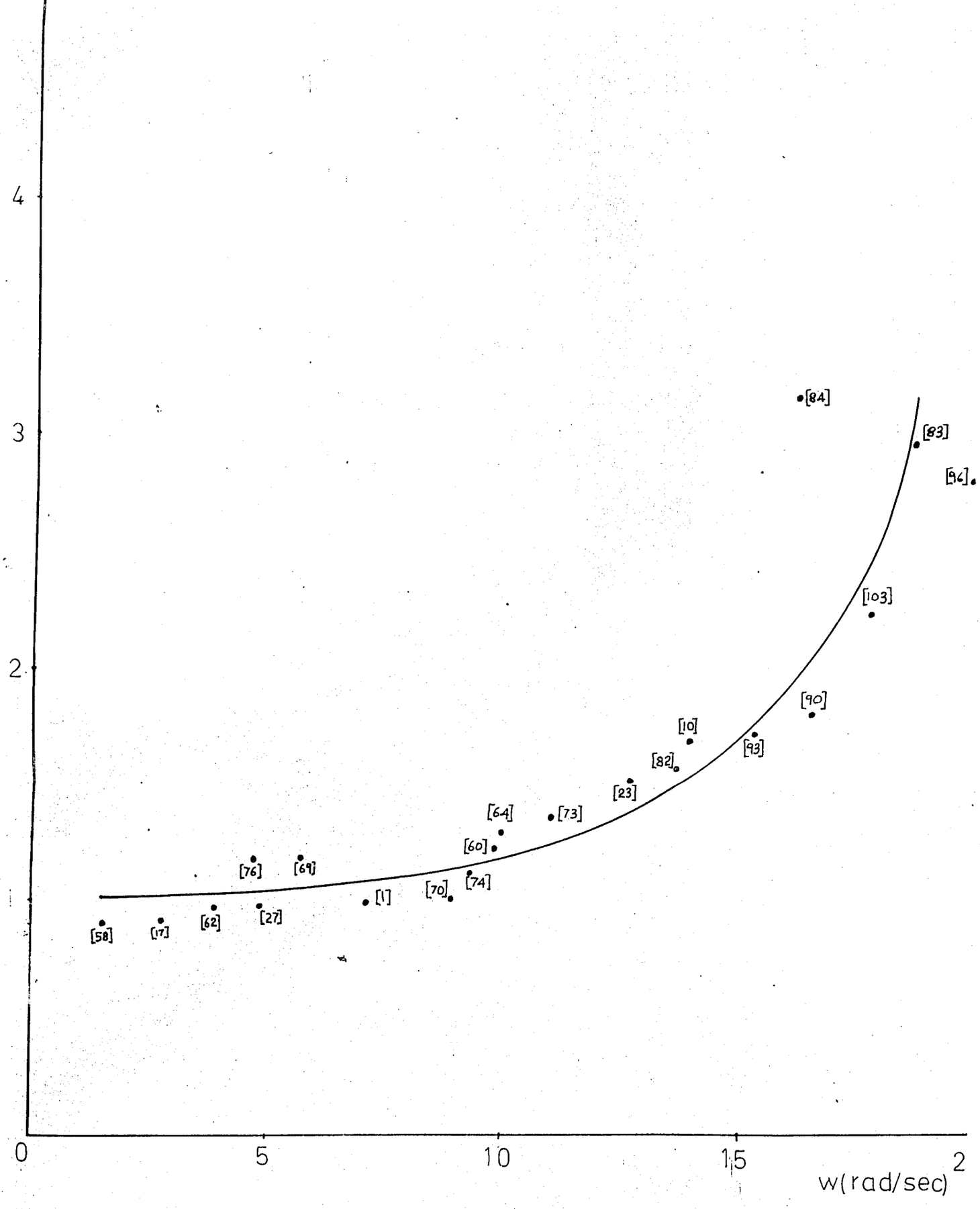

FIG. 4.1.3. Torque Generated vs Rotation Rate Plot.

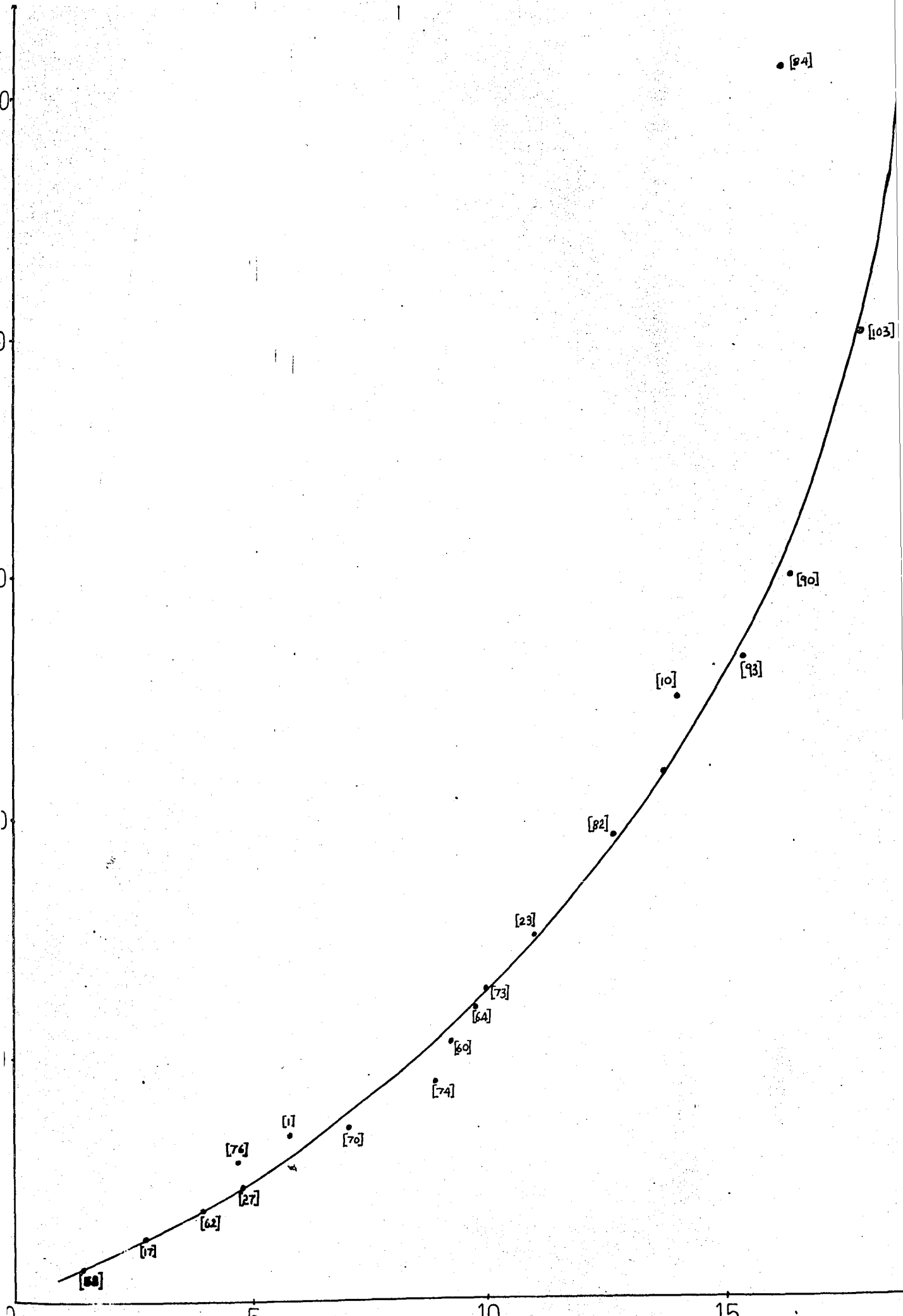

FIG.4.1.4. Power Generated vs Rotation Rate Plot.

w (rad/sec

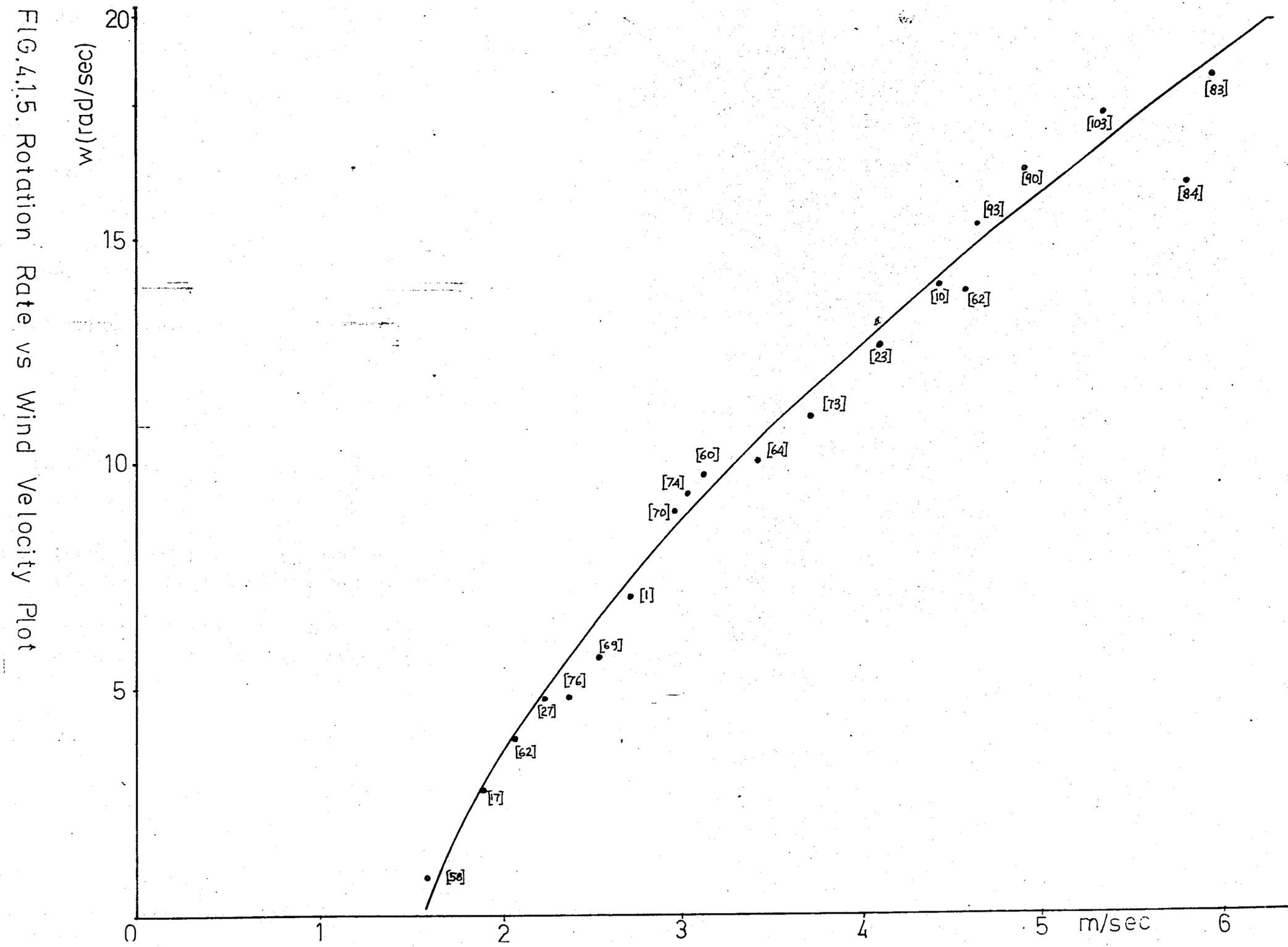

FIG.4.1.5. Rotation Rate vs Wind Velocity Plot

4.2. Evaluation of Results Associated with the Relations Between Pertinent Dimensionless Parameters

The main arguement related to the generality of functional relations between dimensionless parameters submitted in this part is based on:

X vs Re_D relationship being the same $\forall \frac{D}{H}$ a constant D (*)

i/ w vs v "

=> ii/ C_p vs X "

$= P_G\left(\frac{\text{Power Delivered}}{m^2}\right)$ vs v "

=>all functional relations between dimensionless parameters are valid for all aspect ratios of the same diameter.

The sensitivity of X-Re_D dependence, and thus all other relations to a change in the rotor diameter may be the subject of an another investigation.

C_p vs X curve is supposed to fit the relation,

$$C_p = - 0.54X^2 + 108\ X.$$

(*) *Tip speed ratio X being independent of Reynolds' number Re_D for constant diameter(=D) and gap ration($=\frac{r}{x}$), and variable aspect ratio ($=\frac{D}{H}$) Savonius rotors is given in Chapter 3. , and related §A.2.*

From the definitions of power and torque coefficients, and the power equation, $P = Tw$,

$$C_p = 4X\ C_T\ . \qquad 4.2.2.$$

Equating the right hand sides of 4.2.1 and 4.2.2 we obtain,

$$C_T = -0.14X + 0.27 \qquad 4.2.3.$$

as the C_T vs X equation, which when plotted shows good correlation with the experimental data verifying the validity of 4.2.1.

If the definition of X $(=\frac{wD}{2v})$ is introduced in 4.2.1 or 4.2.3, with the equation for power $(P = Tw)$, we obtain combined equations relating the output torque T or power P to wind velocity v and rotation rate w Namely,

$$T = -0.07\rho D^2\ wv + 0.27\ \rho D\ v^2, \qquad 4.2.4$$

and

$$P_G = -\ 0.07\ \rho D^2\ w^2 v + \ 0.27\ \rho D\ wv^2. \qquad 4.2.5$$

The plot of equation $\frac{C_P}{C_T}$ vs 4X gives a straight line thru the origin of slope 0.82. Ideally, the slope has to be 1.00. This may indicate a systematic error namely, either an Overestimation of the rotation rate, or an underestimation of wind velocity or both.

From C_p vs Re_D behavior of the system, one observes that, the power coefficient which is low at very low wind speeds rapidly increase to the peak value of 0.53 at Reynolds' numbers corresponding to wind speeds 2-2.60 m/sec ; then approach to the constant value of about 0.32 for higher values of Re_D. According to this behavior, the turbine is most effective in the low velocity range of about 2-2.60m/sec. however, the efficiency at higher Reynolds' numbers not falling beyond a certain limit gives chance higher design speeds[1]

This important feature of the system is proved by integration[2] of velocity duration curves of two regions (taken from E.W. Golding of ref(15)) with annual averages of 10 mph and 15 mph. The results (submitted in tabular form in A.8) are plotted as kw-hr/ YEAR-m^2 vs wind speed indicate that design speed of the Savonius turbine as well as the yearly output under constant torque mode of operation, strongly depends an the annual wind

---

(1) *The design speed may be defined as the speed at or above which the rotor is capable to give the constant desired torque at a maximum yearly work density.* *(measuredin* $\frac{kw\text{-}hr}{YEAR\text{-}m^2}$, *or,* $\frac{hp\text{-}hr}{YEAR\text{-}m^2}$ *).*

(2) *The integration technique is.*
i/ choose a wind speed
ii/ Compute the corresponding power density from $P_G \tilde{=} 0.47v^{2.4}$
iii/ Find total duration in one year of that speed from velocity duration curve.
iv/ Multiply the quantities found in ii/ and iii/ to obtain kw-hr/$_{YEAR\text{-}m^2}$. *The locus of successive trials indicate a single maximum capacity for a given wind regime corresponding to the design speed.*

duration characteristic of the particular place where it is planned to operate.

The capacity is found to be about 221 $\frac{kw-hr}{YEAR-m}$2 at a design speed of 16.16 mph at a region of 15 mph average, while respective values are about 95 $\frac{kw-hr}{YEAR-m}$2 corresponding to a design speed of 15.53 mph. at a region of 10 mph average.

It can be found that, approximately 15 m^2 area rotor must be used for continuous production of 1hp(736 w) thru half time of the year for constant torque mode of operation at 15 mph annual average.

Defining the yearly collection efficiency η as the ratio of the work density of the turbine to that of wind at a particular wind velocity, it is seen from the η vs velocity ratio plot for the two wind regimes that,

i/ The efficiency of collection decreases (although annual capacity increases) probably to a constant value of about 20% as speed reaches the design speed.

ii/ The efficiencies are identical for the two regimes under consideration; indicating the independency of work density ratio of the turbine from the wind speed characteristic of a region.

C_T vs Re_D dependence indicates that the torque coefficient is highest at low wind speeds which is an advantage of the Savonius rotor to overcome the statie friction of the device to which it is coupled. The coefficient of torque stabilizes at a value of about 0.05 at higher Reynolds' numbers.

From X vs Re_D plot, it is observed that the tip speed ratio

increases at a decreasing rate to the possible asymptote value of 2, as wind speed increases.

At low Reynolds' numbers where the power coefficient reaches its maximum value, the tip speed ratio X ($\simeq$ 1) was found to be approximately half the value of no-load tip speed ratio X_o. This result was predicted theoretically for a simplified case, explained in §2.8. Unfortunately data over a wide range of Re_D to check complete correlation of the case were unavailable. It was feared that, excessive centrifugal stresses would cause permanent harm in the rotor blades during no-load operation.

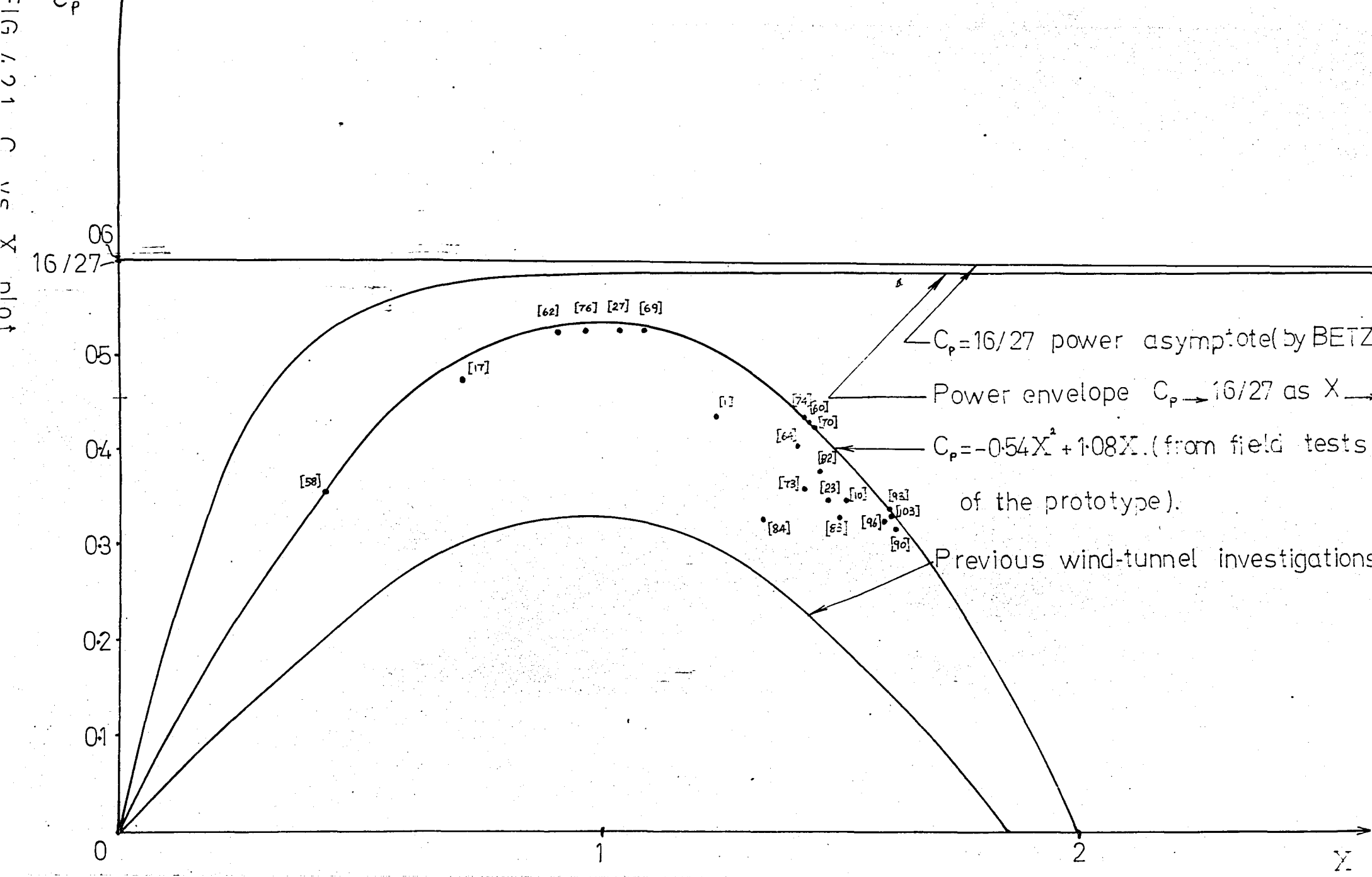
C_p
0·6
16/27
0·5
0·4
0·3
0·2
0·1
0
1
2
X
[62] [76] [27] [69]
[17]
[1]
[74] [60] [70]
[64]
[82]
[58]
[73] [23] [10] [93] [103]
[84] [83] [96] [90]
C_p = 16/27 power asymptote (by BETZ
Power envelope $C_p \rightarrow 16/27$ as X
$C_p = -0{\cdot}54X^2 + 1{\cdot}08X$. (from field tests
of the prototype).
Previous wind-tunnel investigations

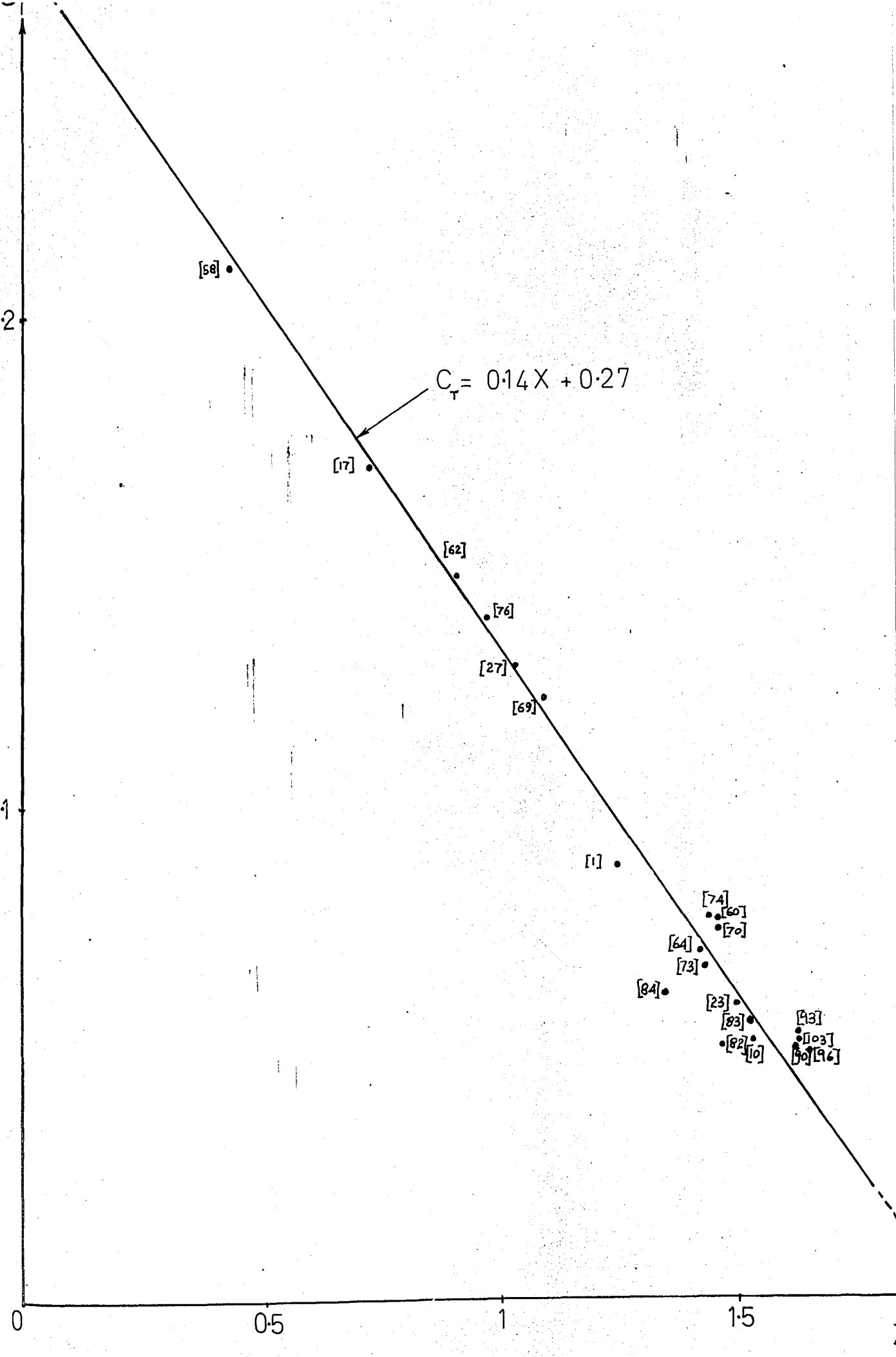

FIG.4.2.2. Torque Coefficient vs Tip Speed Plot.

FIG 4.2.3 (C_p/C_T) vs 4X Plot.

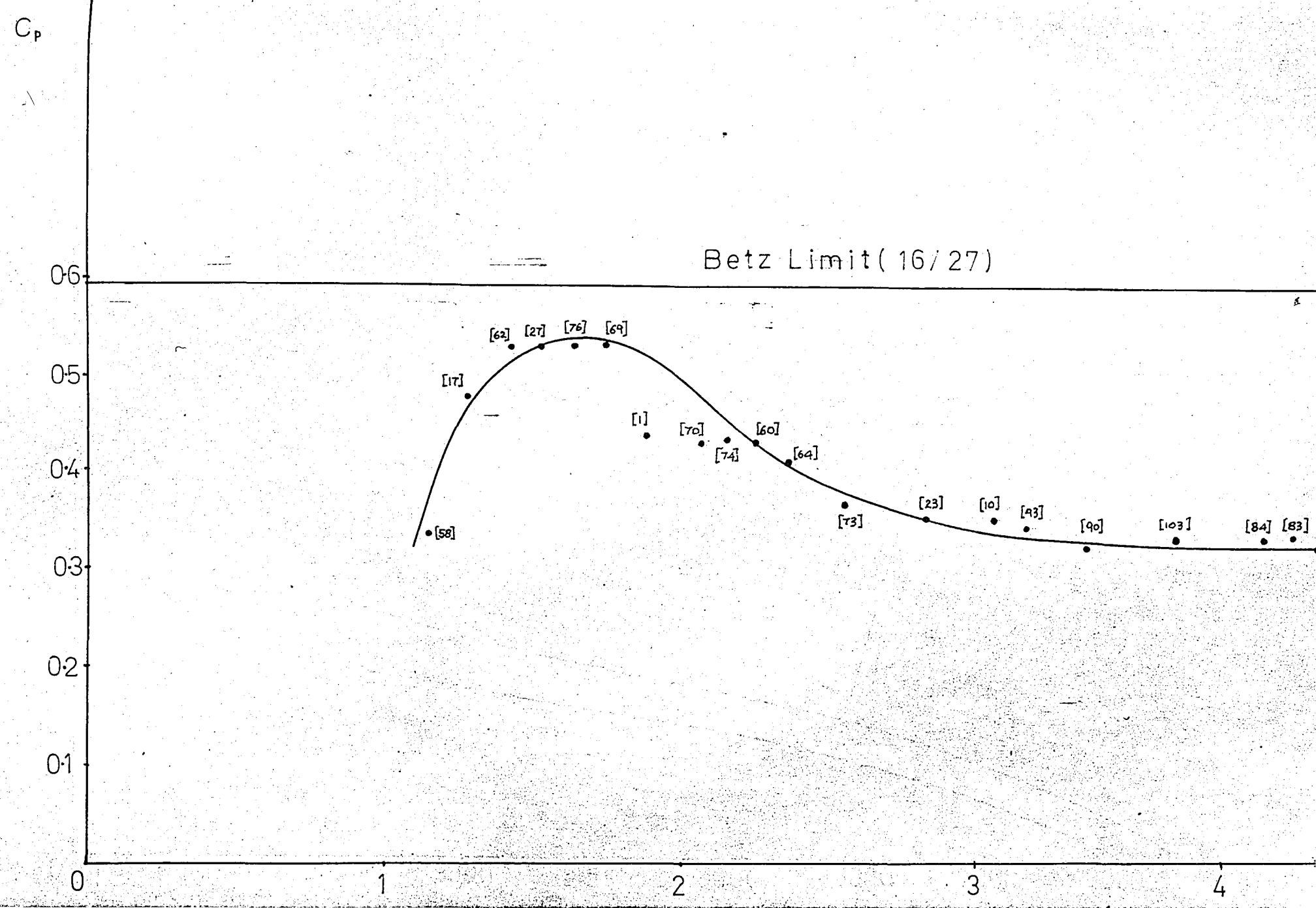

FIG. 4.2.4. Power Coefficient vs Reynolds Number Plot.

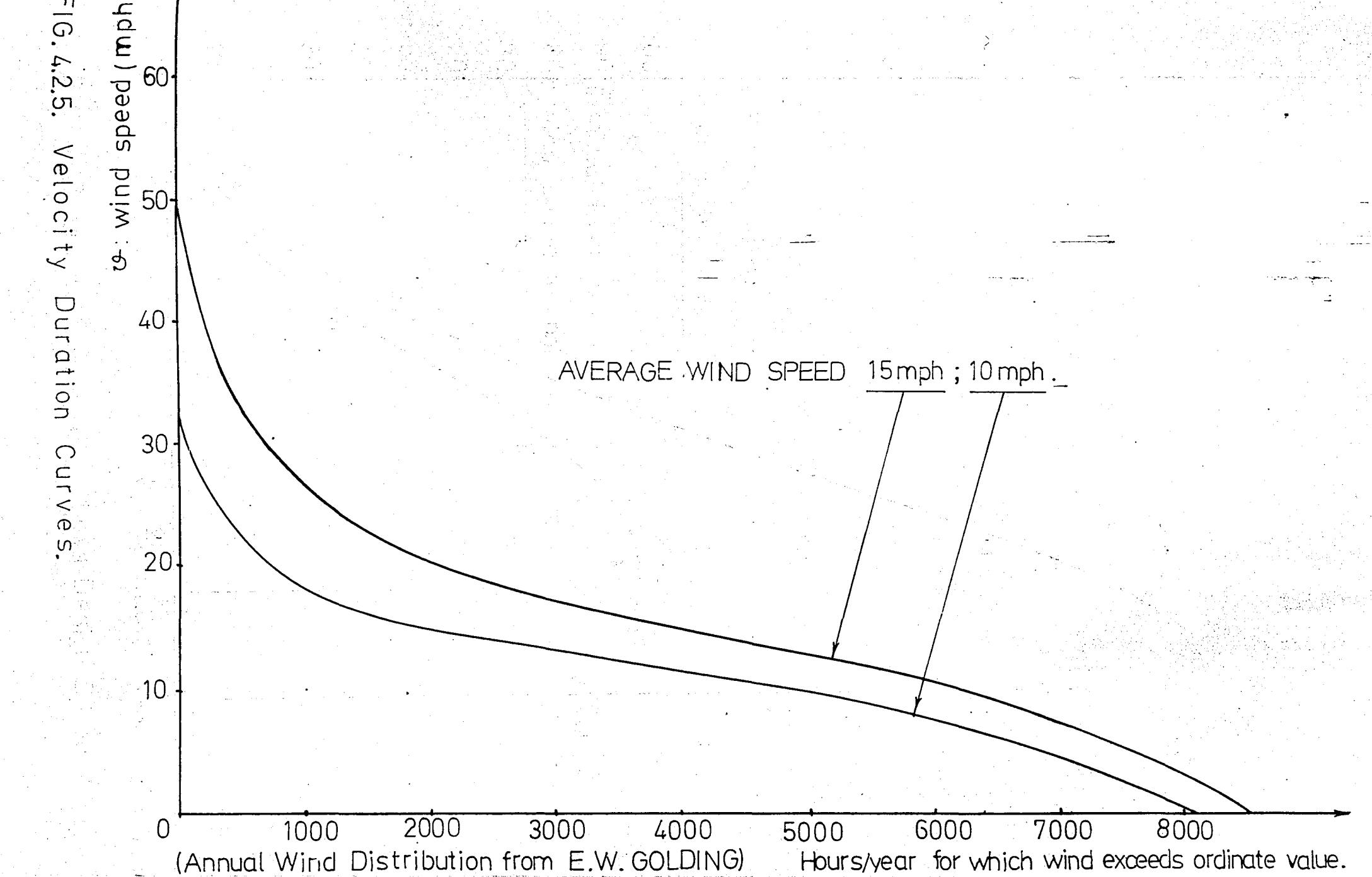
FIG. 4.2.5. Velocity Duration Curves.
v: wind speed (mph)
60
50
40
30
20
10
0
AVERAGE WIND SPEED 15 mph ; 10 mph.
1000
2000
3000
4000
5000
6000
7000
8000
(Annual Wind Distribution from E.W. GOLDING)
Hours/year for which wind exceeds ordinate value.

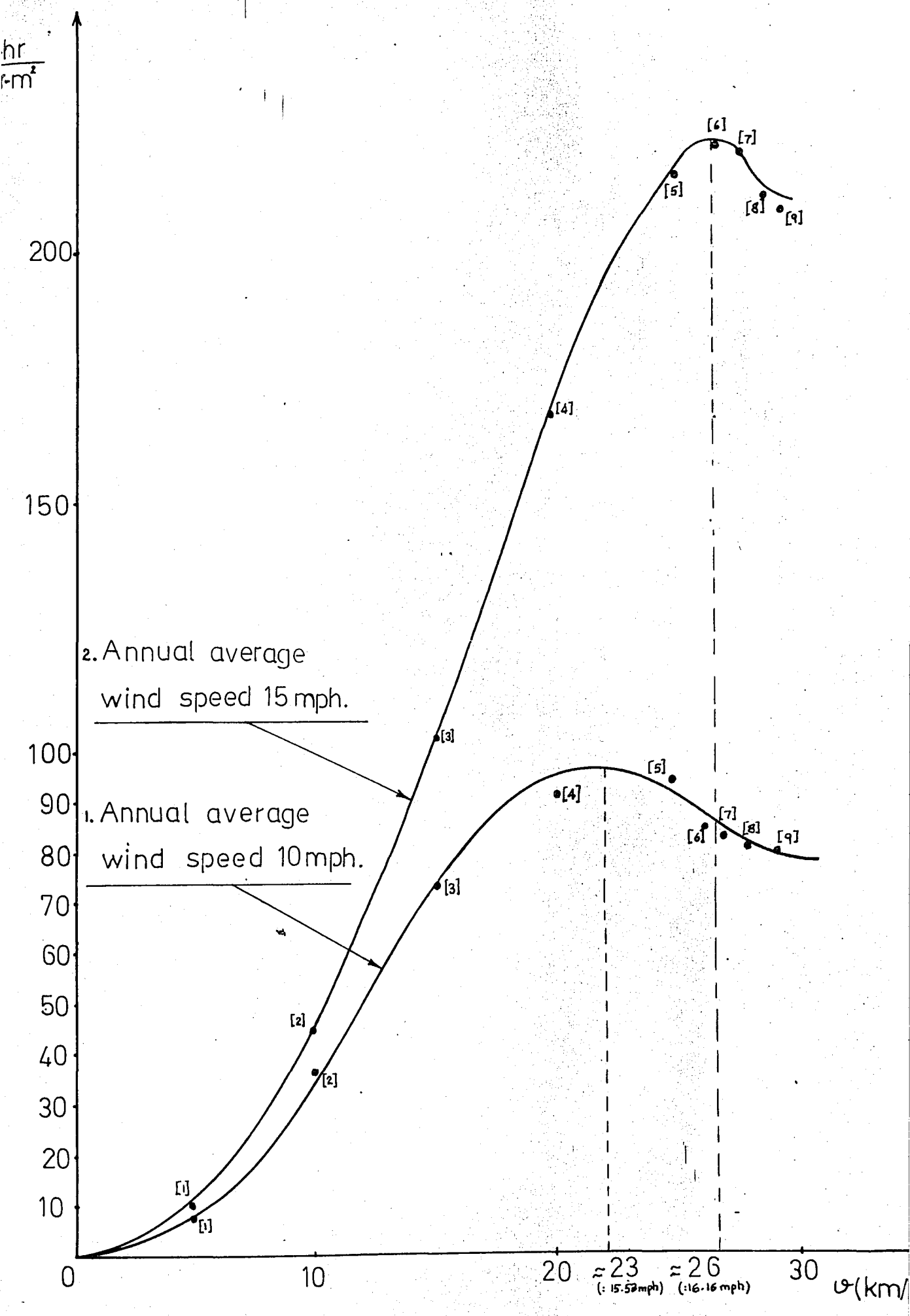

FIG. 4.2.6. Annual Energy Density vs Design Speed Plot.

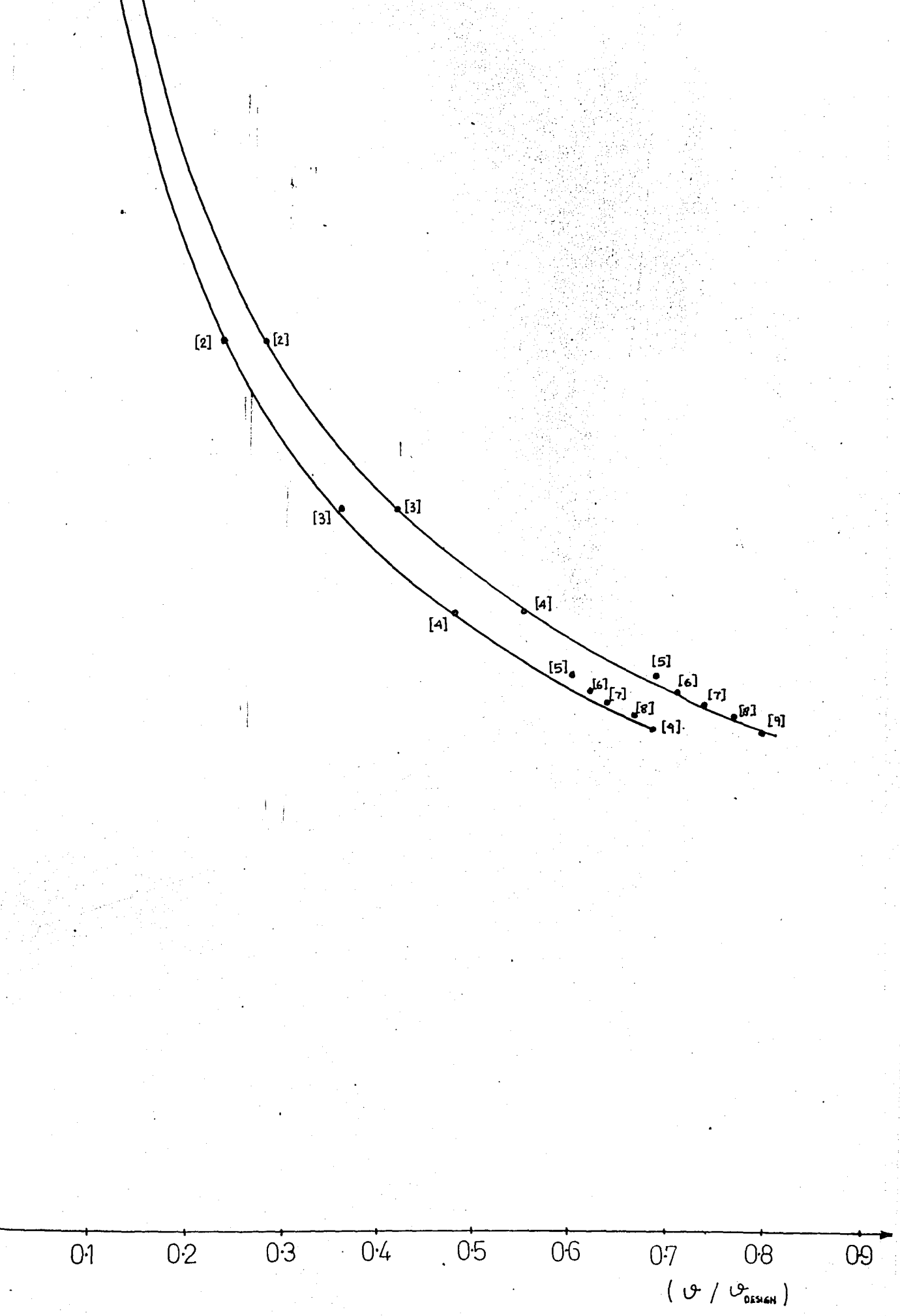

FIG. 4.2.7. Annual Collection Efficiency vs Speed Ratio Plot.

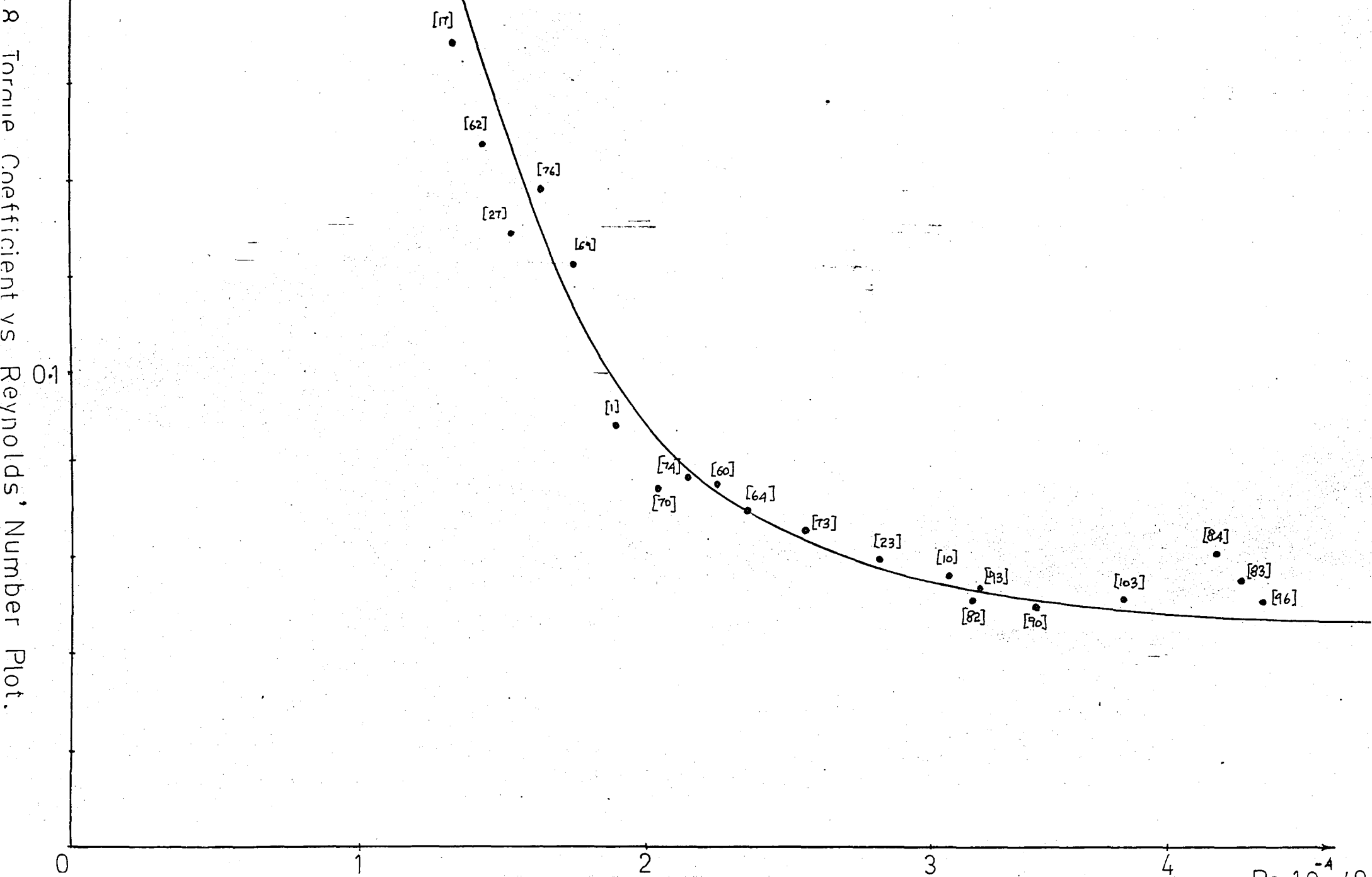
Torque Coefficient vs Reynolds' Number Plot.
0.1
0
1
2
3
4
[17]
[62]
[76]
[27]
[69]
[1]
[74]
[60]
[70]
[64]
[73]
[23]
[10]
[93]
[82]
[90]
[103]
[84]
[83]
[96]

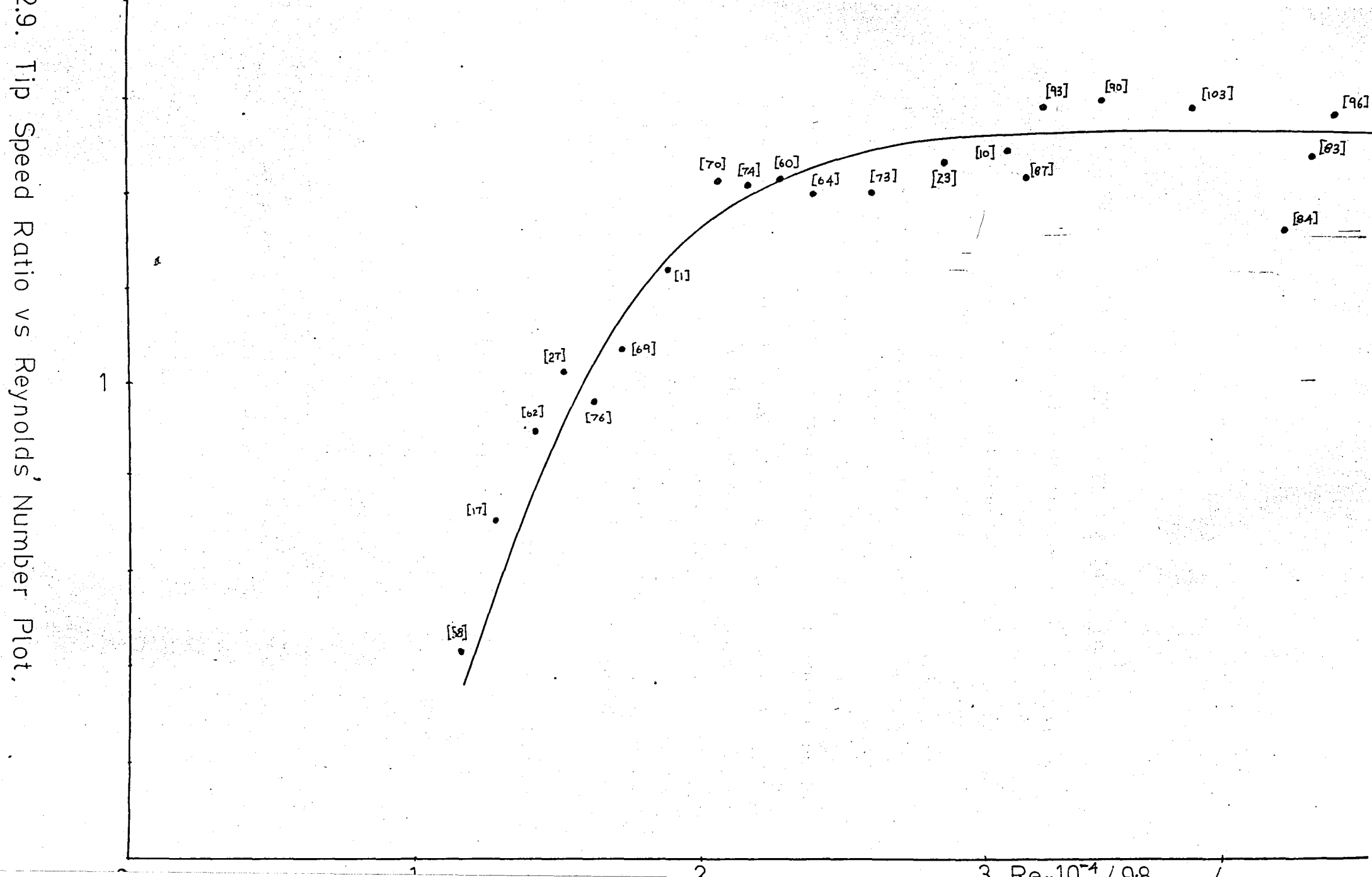

2.9. Tip Speed Ratio vs Reynolds' Number Plot.

4.3. Electric Power Generation With A Car Alternator

The practical serviceability of the rotor was checked by operating a car alternator to generate electric power. Most of the power generated was dissipated in the transmission system. (i = 17.25) It was observed that a continuous operation was impossible in wind speeds below 4.5 m/sec. The rotor stops at the instant when the wind momentarily stops, and does not start until a high value of speed of about 5- 5.5 m/sec is reached to overcome the static resistance of the transmission system, and alternator shaft.

Therefore, a flywheel augmentation to the rotor shaft is recommended together with a control circuit which will cut the load off when the rpm is not sufficient enough for the system to overcome the energy given to the field of the alternator rotor.(*) Under these conditions, a $1m^2$ rotor is sure to charge a battery at wind speeds as low as 2- 2.5 m/sec.

The circuitry and set-up details are given in APPENDIX A

The results are submitted in the below figure.

(*) An important feature of the alternator is that, it will give power at relatively low rates of rotation (as compared to a dynamo) however the field has to be charged.

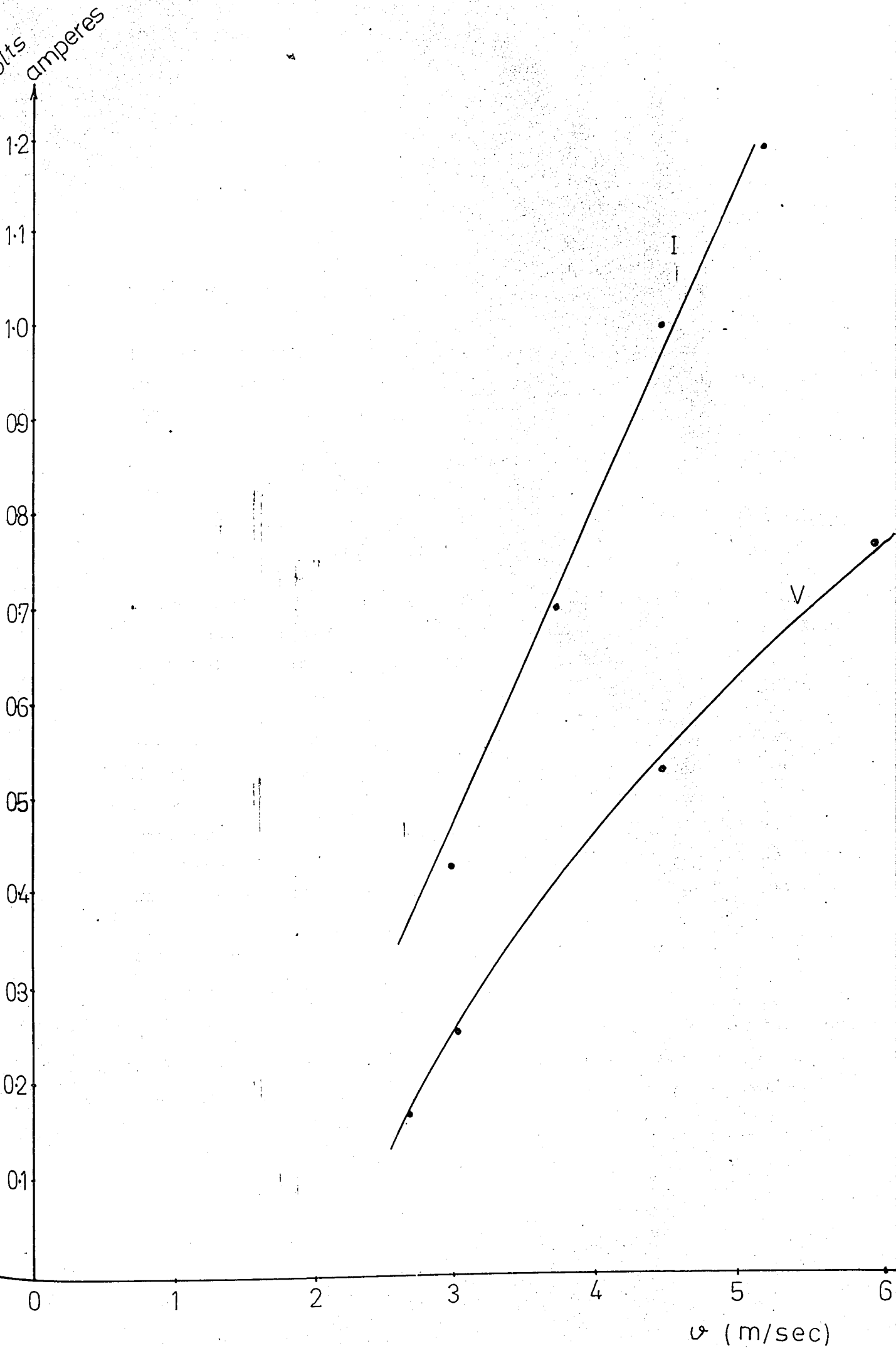

FIG 4.21 Voltage Amperes Output vs Wind Speed Plot

5. CONCLUDING REMARKS

It was mentioned in 1.3.4. that in harvesting the energy in the wind, meaningful results can be achieved by the combination of responses from two sources:

a/ Long term statistical treatment of wind data to find out the power available.
b/ Investigations of the output potential of the wind machine in the full range of wind speeds.

These have also been revealed in chapter 3 that, the aerodynamic design characteristics as well as the dimensions of a particular wind turbine is a strong function of the wind regime in which it is planned to operate.

Therefore, there is absolute necessity to start analyses of the frequency distribution and geographical variation of wind speed all over the country to produce the wind-energy map for Turkey. This information will serve to predict the availability of wind energy between different wind speeds for any location.The relevance of this to the operation of an aerogenerator in determining its mean annual output and operating time is presented in this work using foreign resources.

The experimental set-up and the method of evaluation of results designed and entertained in testing the particular rotor subject to this investigation is repeatable for any other rotor to be tested. This investignation technique has to

be extended to other rotor designs for comparison of their relative merits.

Thus upon the completion of such a programme, one will be able to determine the rotor(s) best suited to various wind regimes, in the aspect of functionalism and efficiency. Cost effectiveness can then be assessed.

Within this perspective, this work providing a reasonably reliable experimental treatment is only an initiative attempt of a chain of investigations.

The reliability of the data points can be improved by avoiding human errors in reading the devices. This can be done by simultaneous instrumental recording of the pertinent parameters namely, wind velocity, rpm of rotor and torque delivered.

A.1. Experimental Details and Rough Data of Model Tests(*) for Determination of Ideal Blade Configuration.

Dimensionless grouping of parameters that determine the relative performance of models were chosen as, C_p and X where,

$$C_p \triangleq \frac{\text{net power output of wind machine}}{\text{power of wind contained in the area of rotor facing the wind.}} , \qquad \text{A.1.1.}$$

and,

$$X \triangleq \frac{wD}{2v_\infty} \qquad \text{A.1.2.}$$

Four models of different gap ratio were tested against a blower. The mechanical power from the impeller was converted to electrical output by means of a small generator. The output of generator was discharged on a resistance load of constant value. (equal to the internal resistance of the generator to maximize the output power). Thus, voltage and revolutions per unit time of the rotor corresponding to each velocity value were recorded respectively by means of a voltmeter and an ascilloscope. A schematic illustration of the set-up is given below:

(*) *Carried out as final year graduation project by S.Gözde and E. Yazgaç (1977).*

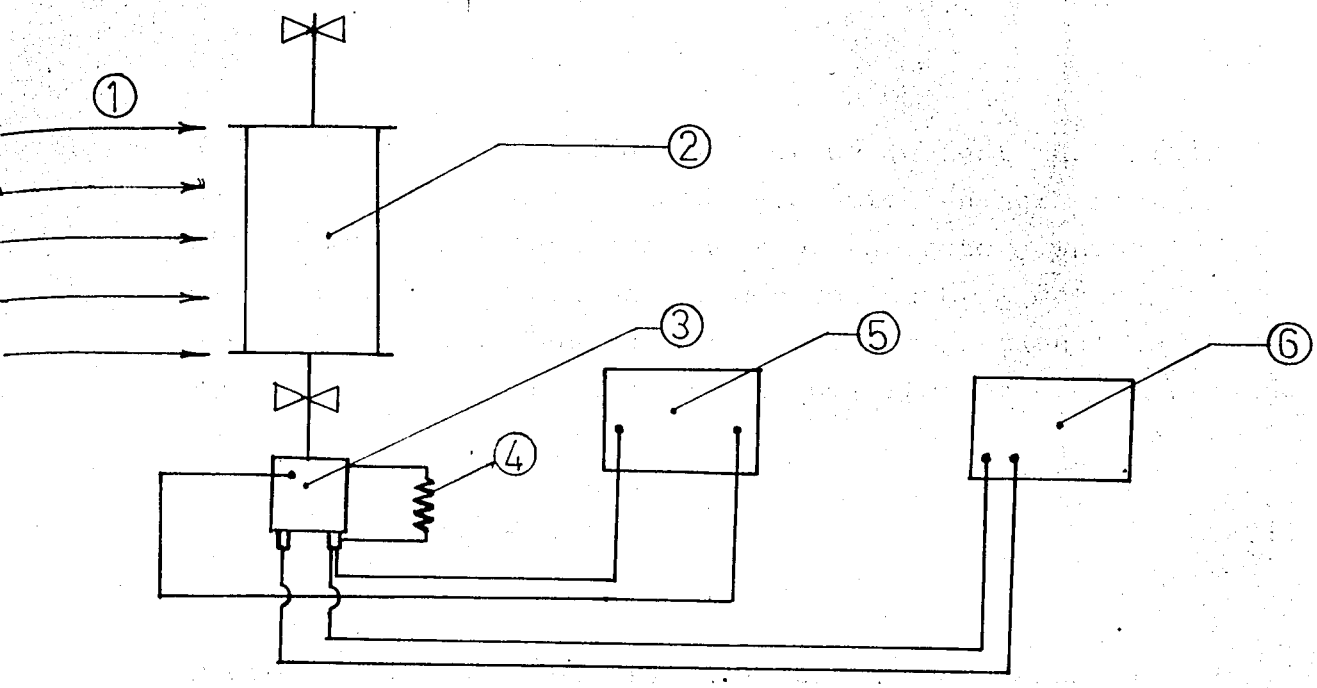

FIG.A.1.1 Experimental Set-up Enternained in Testing Models

1 : Wind obtained from a blower; speed measured by an anemometer and a stopwatch.
2 : rotor.
3 : electric generator
4 : resistance load
5 : voltmeter
6 : oscilloscope.

The analysis was not a constant load - varying Reynolds' number type as might be expected. This is due to the pressence of friction at the bearings supporting the rotor, and within the dynamo. The power dissipated to friction was estimated from,

$$P_f = T_f w. \qquad \text{A.1.3}$$

Where, T_f was computed as the torque (weight multiplied by the shaft radius) balanced by a weight hangi from a string wrapped around the shaft of the rotor, whose constant velocity motion was controlled by a meter stick and a stopwatch. Thus, a power term (proportional to the speed of rotor) was used in the numerator of A.1.1, reading as,

$$C_p = \frac{V^2/R + (T_f\ w)g}{0.62\ A\ v_\infty^3} \quad . \qquad \text{A.1.4.}$$

Where, wind power term is in watts in accordance with 2.3.1-i g is the gravitational acceleration constant to convert $\frac{\text{Kg-m}}{\text{sec}}$ to $\frac{\text{N-m}}{\text{sec}}$ (=watts).

$w = \frac{2\pi}{60} f \frac{\text{rad}}{\text{sec}}$, f being the revolutions of rotor per minute.

The rough data given below, was put into equations A.1.4 and A.1.2. to yield the curves submitted in Chapter 3.

Central position diameter, area (metric units)	Applied wind velocity (m/sec)	Voltage generated (volts)	Resistance Load (ohms)	Revolutions per minute (rpm) f	
X_I=0.06	V_1=6.06	V_1=2.4	R=14.31	1200	
D_I=0.14	V_2=7.41	V_2=3.2		1500	
I	V_3=11.11	V_3=6.8		3000	$\frac{r}{x}$=0.6
A_I=0.0196	V_4=14.26	V_4=8.8		4000	
X_{II}=0.05	V_1=7.14	V_1=2.2		1000	
D_{II}=0.13	V_2=8.33	V_2=4.0		1875	
II	V_3=10.00	V_3=6.2		2857	$\frac{r}{x}$=0.
A_{II}=0.0182	V_4=14.26	V_4=9.6		4286	
X_{III}=0.04	V_1=7.79	V_1=1.0		556	
D_{III}=0.11	V_2=10.00	V_2=2.6		1277	
II A_{III}=0.0154	V_3=11.76	V_3=4.0		1875	$\frac{r}{x}$=1
	V_4=13.33	V_4=4.3		2000	
X_{IV}=0.02	V_1=10.00	V_1=1.3		714	
D_{IV}=0.10	V_2=12.50	V_2=3.2		1500	
IV	V_3=13.70	V_3=3.75		1765	$\frac{r}{x}$= 2
A_{IV}=0.014	V_4= -	V_4= -		-	

L = 0.14 m r = 0.04 m ∀ models.

Frictional weipht ≅ 200 gr radius of rotor shaft ≅ 0.5 cm.

TABLE A.1.1. Rough Data Taken for Determination of optimum gap ratio.

A.2. Determination of Data Points to show the Effect of Aspect Ratio on Rotation Rate of a Savonius Rotor Under Various Reynolds' Numbers

Below is provided the experimental details of the log X vs log Re_D relationship given in Chapter 3.

The layout of the set-up and rough data were given in A.1.

Two rotors were selected having identical geometric parameters except the lengths, and the rough data was prepared to group the information in two dimensionless parameters, the rotation rate X and Reynolds Number Re_D. Computational details are given below:

Rotor 1/ x = 0.05m ; r = 0.04m ; D = 0.13m; H = 0.14m.

test velocity (m/sec)	Reynolds' Number Re_D	
v_1 = 7.14	$Re_1 = \frac{(7.14)(0.13)}{1.46} \times 10^5$	6.36×10^4
v_2 = 8.33	$Re_2 = \frac{(8.33)(0.13)}{1.46} \times 10^5$	7.42×10^4
v_3 = 10.00	$Re_3 = \frac{(10.00)(0.13)}{1.46} \times 10^5$	8.9×10^4
v_4 14.26	Re_4 $\frac{(14.26)(0.13)}{1.46} \times 10^5$	12.7×10^4

Where,

$$Re_D = \frac{\rho V_\infty D}{\mu} = \frac{V_\infty D}{\nu} \qquad \text{A.2.1}$$

and,

$$\nu \triangleq 1.46 \times 10^{-5} \frac{m^2}{sec} .$$

The rotation rate was taken from the oscilloscope as revolutions per unit of time. Denoting ,

$$(f) = \frac{rev}{sec}$$

and.

$(w) = \frac{rad}{sec}$; then,

$$w = 2\pi f \qquad A.2.2$$

f values were computed in $\frac{rev}{min}$ form. Thus,

$$w = \frac{2\pi}{60} f \qquad A.2.3.$$

Where,

$$(W) = \frac{rad}{min} .$$

and,

$$(f) = \frac{rev}{min} .$$

The rotation rates corresponding to the velocities are,

$$w_1 = \frac{2\pi}{60} (1000) = 104.72$$

$$w_2 = \frac{2\pi}{60} (1875) = 196.35$$

$$w_3 = \frac{2\pi}{60} (2857) = 299.18$$

$$w_4 = \frac{2}{60} (4286) = 448.83 \frac{rad}{sec}.$$

The dimensionless tip speed ratio was derived to be,

$$X = \frac{wD}{2v_\infty} \qquad \text{A.2.4.}$$

Using the values of $w_1 - w_4$ in A.2.4,

$$X_1 = \frac{(104.72)(0.13)}{(2)(2.14)} = 0.95$$

$$X_2 = \frac{(196.35)(0.13)}{(2)(8.33)} = 1.53$$

$$X_3 = \frac{(299.18)(0.13)}{(2)(10)} = 1.94$$

$$X_4 = \frac{(448.83)(0.13)}{(2)(14.26)} = 2.04$$

For rotor#2 :

x = 0.05 m
r = 0.04 m
D = 0.13 m
H = 0.28 m.

test velocity (m/sec)	Reynold s Number
$v_1 = 7.31$	$Re_1 = \frac{(7.31)(0.13)}{1.46} \times 10^5 = 6.5 \times 10^4$
$v_2 = 8.33$	$Re_2 = \frac{(8.33)(0.13)}{1.46} \times 10^5 = 7.42 \times 10^4$
$v_3 = 10.00$	$Re_3 = \frac{(10.00)(0.13)}{1.46} \times 10^5 = 8.9 \times 10^4$
$v_4 = 12.00$	$Re_4 = \frac{(12.00)(0.13)}{1.46} \times 10^5 = 10.68 \times 10^4$

The rotor speeds corresponding to the test velocities are,

$$w_1 = \frac{2}{60}\ (1846) = 193.3,$$

$$w_2 = \frac{2}{60}\ (2308) = 241.7,$$

$$w_3 = \frac{2}{60}\ (3000) = 314.16,$$

$$w_4 = \frac{2}{60}\ (3333) = 349.0\ \frac{\text{rad}}{\text{sec}}\ .$$

Using the above values in A.2.4. we find the tip. speed ratios as

$$X_1 = \frac{(193.3)(0.13)}{(2)(7.31)} = 1.71$$

$$X_2 = \frac{(241.7)(0.13)}{(2)(8.33)} = 1.89$$

$$X_3 = \frac{(314.6)(0.13)}{(2)(10.000)} = 2.04$$

$$X_4 = \frac{(349)(0.13)}{(2)(12.00)} = 1.89$$

The velocity ratios (X) were plotted against the Reynold's Numbers (Re_D) for both rotor models. The close correlation among the data points of the two models indicates that, the rotation rate of a Savonius rotor is a strong function of the Reynold's Number based on the diameter of the rotor, not the rotor height H.

Note: The resistance load was held constant for the two models.

A.3. Experimental Prototype Design

The choice of rotor and support structure design was governed by such factors as weight, strength, ease of fabrication and cost. Among the various alternatives considered, (involving fiber - glass materials) 0.30 mm. thick sheet- steel rotor structure, reinforced with steel chasses at the end plates seemed to be the most convenient.

Rotor dimensions had to be large enough to reflect the performance characteristics of the full scale prototype, and small enough to be set up and maintained by an individual. For this purpose, rotor blades were given a circular curvature to take a radius of 270 mm (see fig. A.4.1). The centers were spaced 430 mm. apart to allow a gap ratio $\frac{r}{x} \simeq 0.63$; slightly larger than the ideal proportion to count for the rotor shaft thru the center. Thus, the major diameter came out to be 970 mm (eq. 3.4.1) Height of blades was arbitrarily taken (according to previous research work outlined in A.2) to be 637 mm. Total frontal area facing the wind becoming 1.236 m^2 (= 2x0.637 mx0.97m) (see fig. A.4.2).
Four rotor blades were placed two by two between the end plates such that there was a 90° angle between their frontal planes to avoid the aerodynamic dead point (see fig A.4.7. and A.4.8.i) Blade edges subject to centrifugal loads were reinforced by 10x10 aluminum square profiles as well as double - folding of the sheet. (see fig. A.4.8.ii)

The end plates (see fig. A.4.2) were reinforced against bending due to the own weight of rotor by chasses that also provide housing and fixing extensions for the rotor shaft (see fig A.4.3 and A.4.5.)

The rotor together with shaft and reinforcing elements weighs about 20 Kg, estimated to be lighter than a safe fiber glass design of equal strength.

For supporting structure 50 mm profile was chosen (see fig A.4.9. A.4.10, A.4.11) The connections were made with M-16 bolts. The inverse U shape structure was stiffened by guy wires as depicted in fig. A.4.12. Referring to this figure, the system was fixed to the sides of the penthouse at points B, A. I, H, G and D, from the upper corners J and K of the framework (see fig. A.4.13). There were no direct connections to the roof, in order not to give damage to insulation layers.

The composite shaft of rotor involving a 1"ϕsteel pipe of 1400 mm long, was lengthened by the inserted 20ϕ solid steel shafts from both ends,which provided the necessary elements for the embossing of bearings (sse fig. A.4. 6); deep groove ball bearing above taper roller bearing below. The rotor was fixed to the shaft by means of 4xmx6 screws thru reinforcing elements of the end plates.

Thus, the shaft plus rotor system was inserted thru the slotted carrying elements,fixed to the supporting frame by a couple of M -16 bolts each. (see fig. A.4.16, A.4.19 and A.4.20.) The rotor was locked within the carrying elements by the bolts thru them and the bearing cover plates. (see fig. A.4.17. A.4.18 A.4.19 - and A.4.20).

This design allowed immediate setting - up and removal of the rotor part as a whole from the supporting structure.

The system was planned to be completely portable. It could be detactched or re-constructed within an hour.

The forces affecting design dimensions were:

a/ centrifugal force on blades,
b/ gravitational force on the rotor and base support,
c/ guy-wire tension on the structure,
d/ aerodynamic force developed by blades, and associated cylic loads of vibration.

An exact analytical treatment involving all the forces so as to adjust design dimensions accordingly was impossible, and beyond the purpose of this work.

All forces were considered to be made up of static and dynamic components. Wind force was calculated as a static load assuming the vertical cross - sectional area of the rotor to be a flat plate subject to a flow of magnitude 15 m/sec.

From ref. ((17)), the coefficient of drag was estimated to be 1.12, then from the equation,

$$F = C_D \rho A \frac{v^2}{2} \qquad \text{A.3.1.}$$

$$F = (1.12)\frac{(1.23)}{9.8}\ (1.236)\ \frac{(15)^2}{2}$$

$$\cong 20 \text{ kgf. (= weight of rotor)}$$

Which is a very low value with respect to the strength of elements involved. The load rating of bearings were for example,

	DYNAMIC	STATIC
DEEP GROOVE BALL BEARING	2360 Kgf.	1660 Kgf.
TAPER ROLLER BEARING	2900 Kgf.	2000 Kgf.

Effects of centrifugal and gravitational loads were eliminated by reinforcing-components on rotor blade edges, and end-plates, while for cyclic aerodynamic loads, the rigidity of the system was increased by guy-wires over natural frequency of all modes of vibrations.

A. 4. Working Drawings

A.4.I. Turbine Components

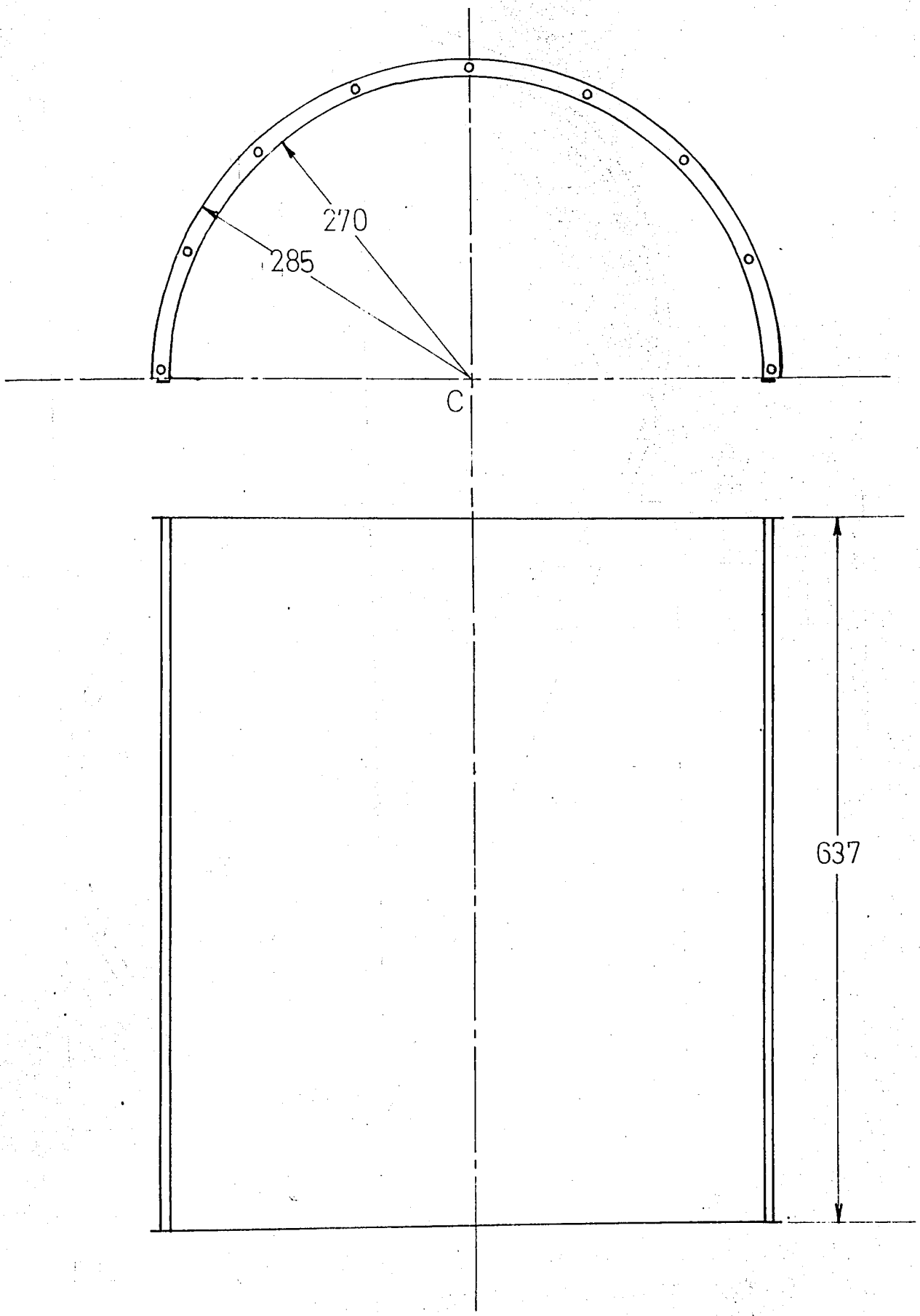

FIG. A.4.1. Semi-Cylindrical Rotor Blade.
(scale 1:5)

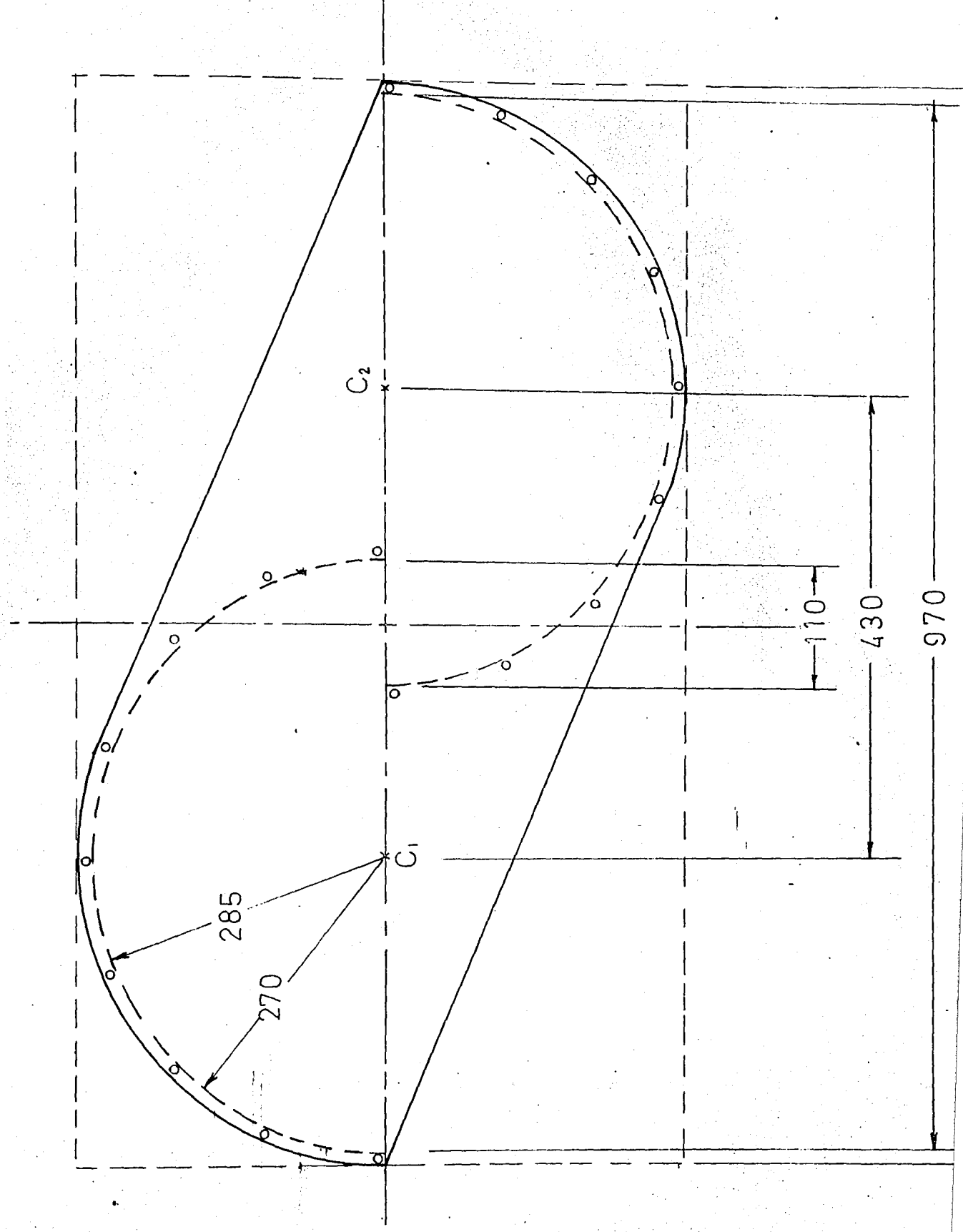

FIG.A.4.2. End Plate(top and bottom) location of blades are denoted at 270 rad. from C_1 and C_2). (scale 1:5).

APPENDICES

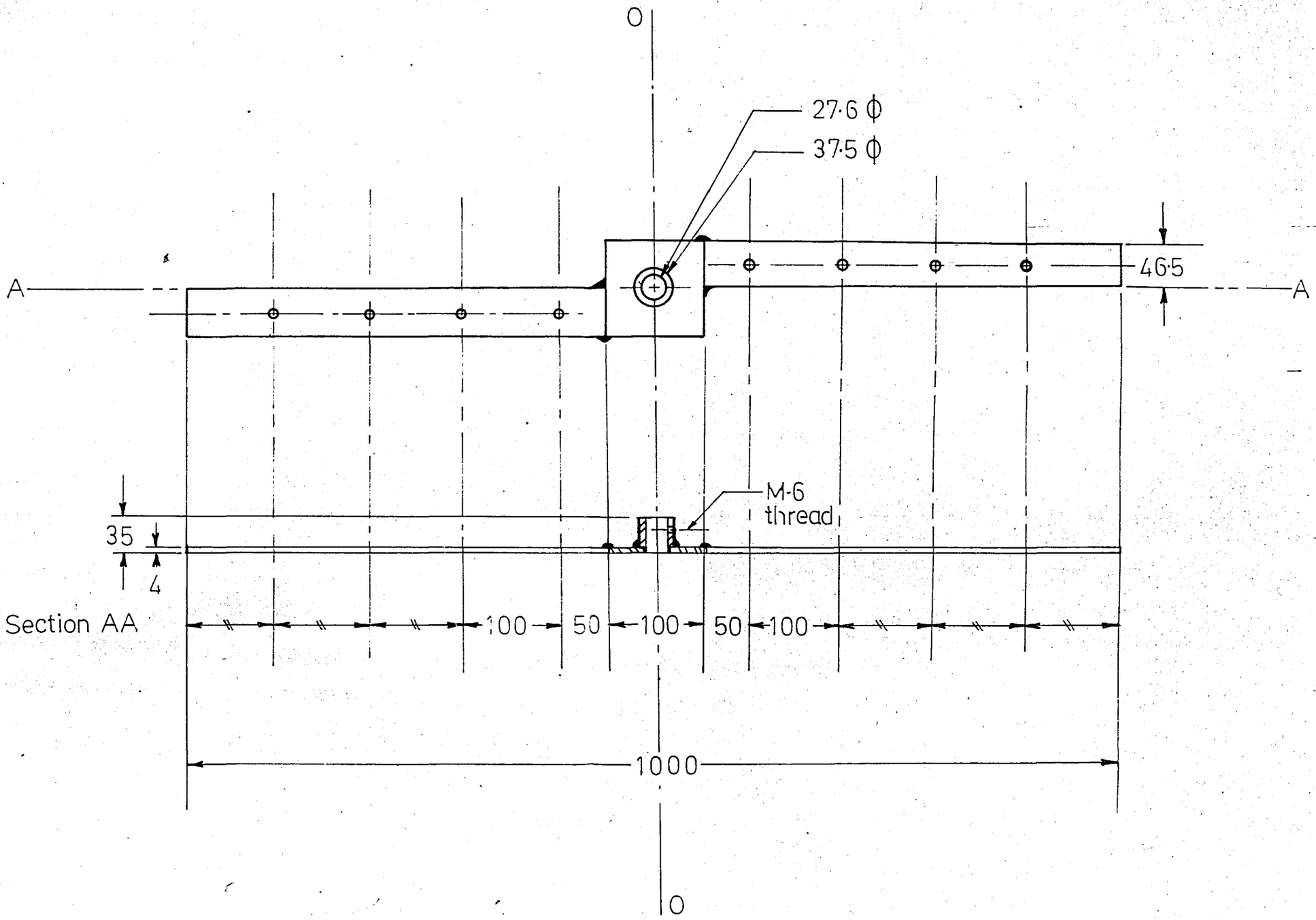

FIG.A.4.3. Connection Elements(×2) of Upper and Lower End Plates. (Scale 1/5).

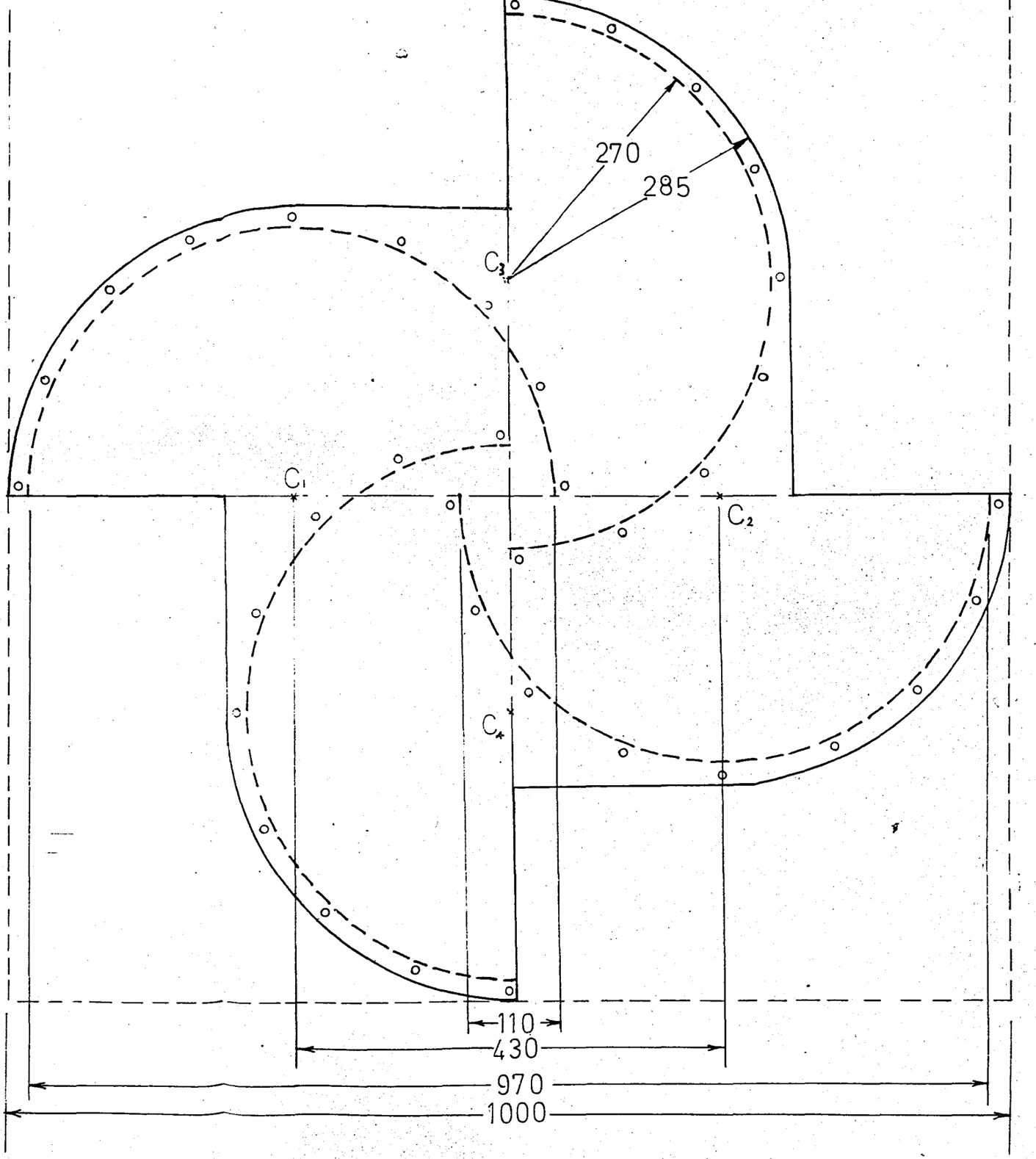

FIG. A.4.4. Mid Plate (location of blades are denoted at 270 rad. from C_1, C_2, C_3, C_4) (scale 1:5).

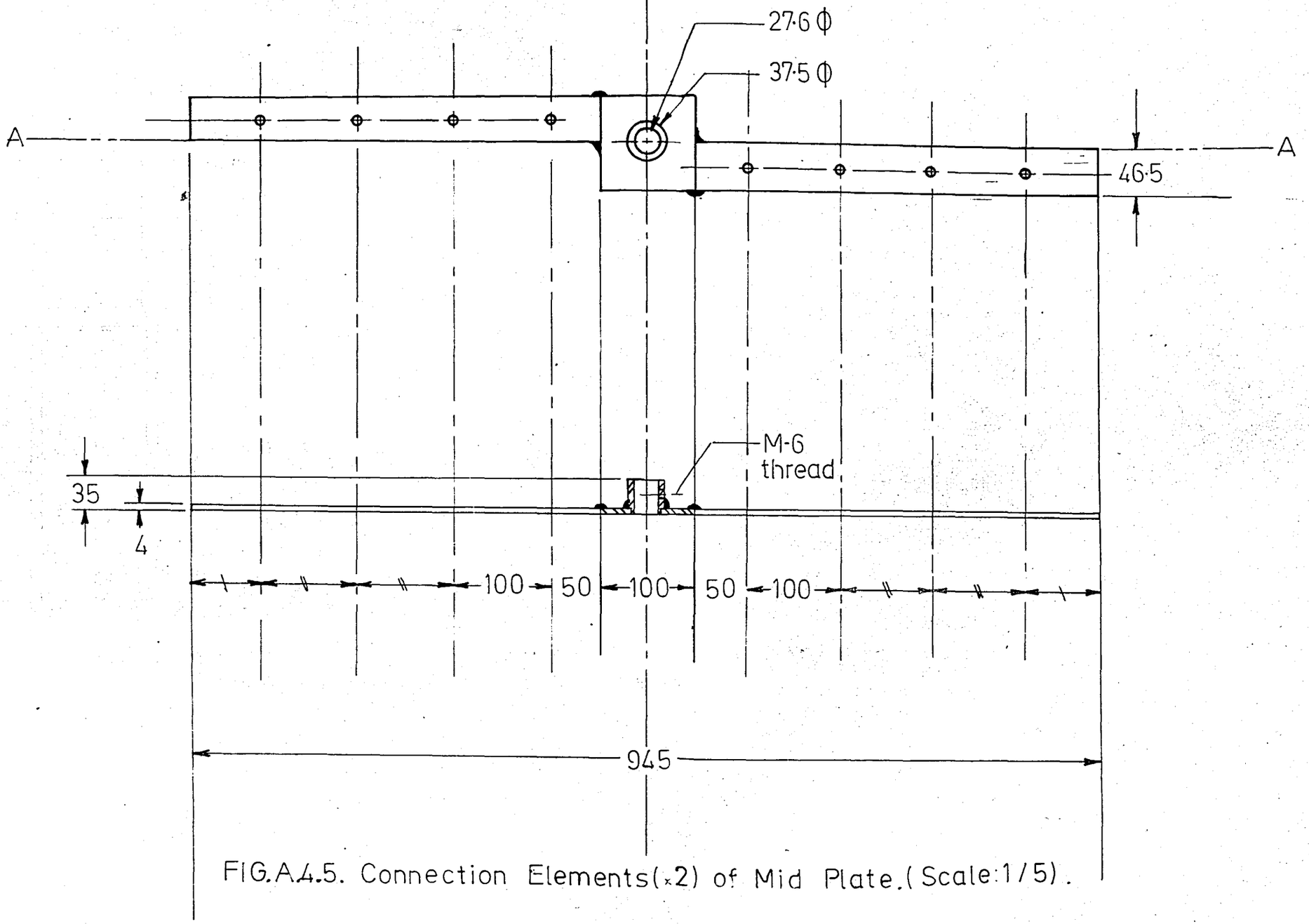

FIG.A4.5. Connection Elements(×2) of Mid Plate.(Scale:1/5).

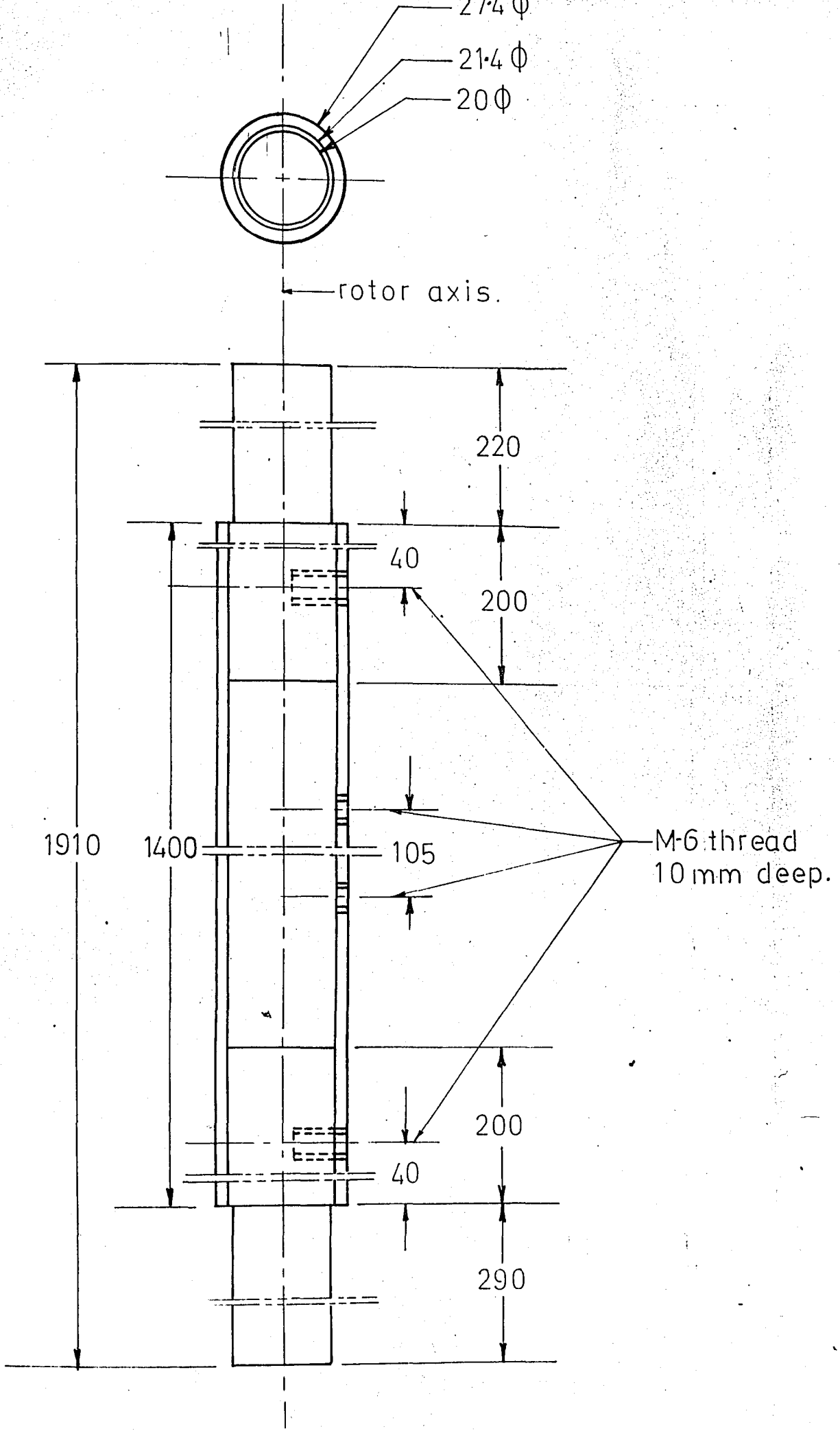

FIG. A.4.6. Rotor Shaft. (scale 1/1)

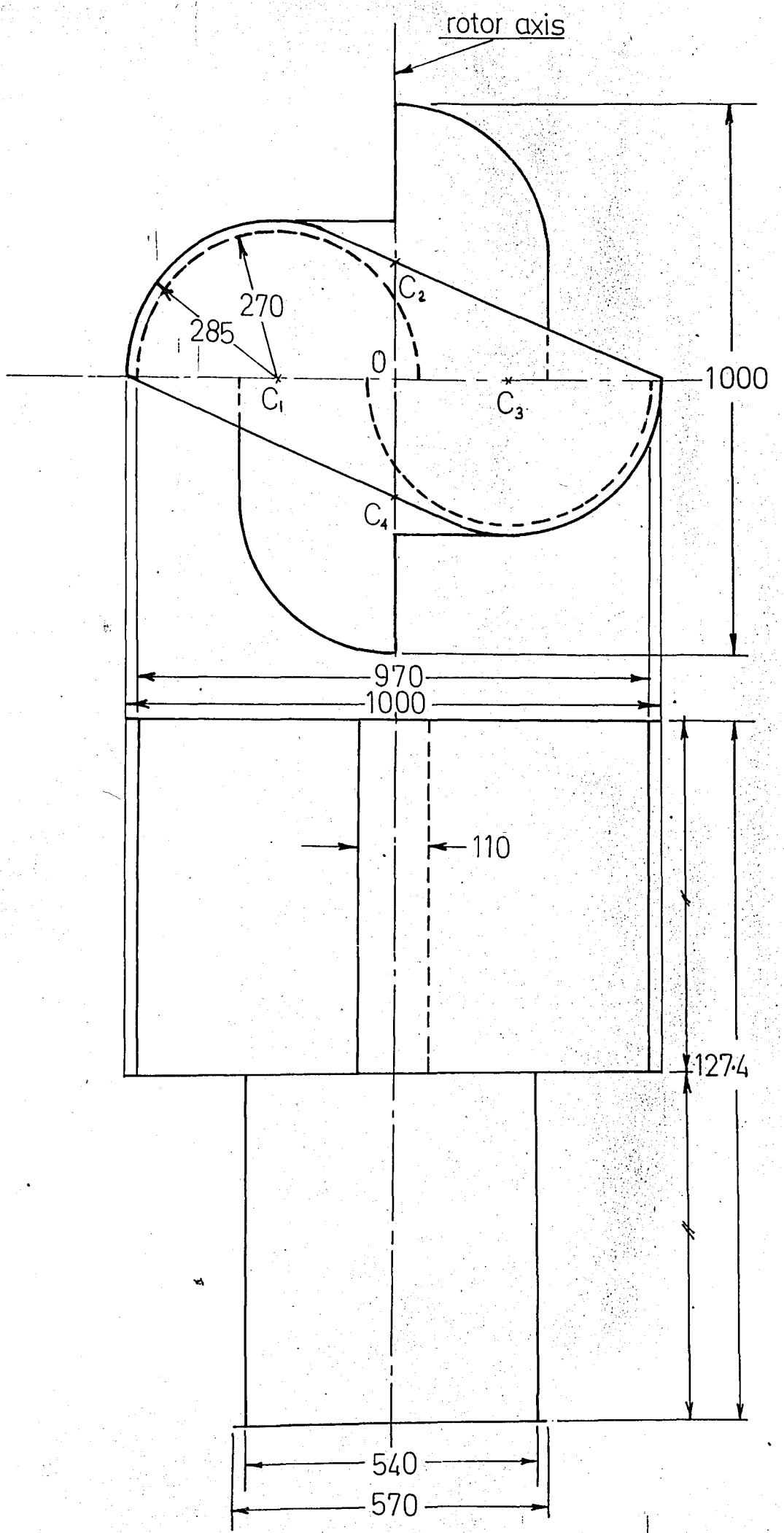

FIG.A.4.7. Mounted Position of the Blades.
(scale 1:10)

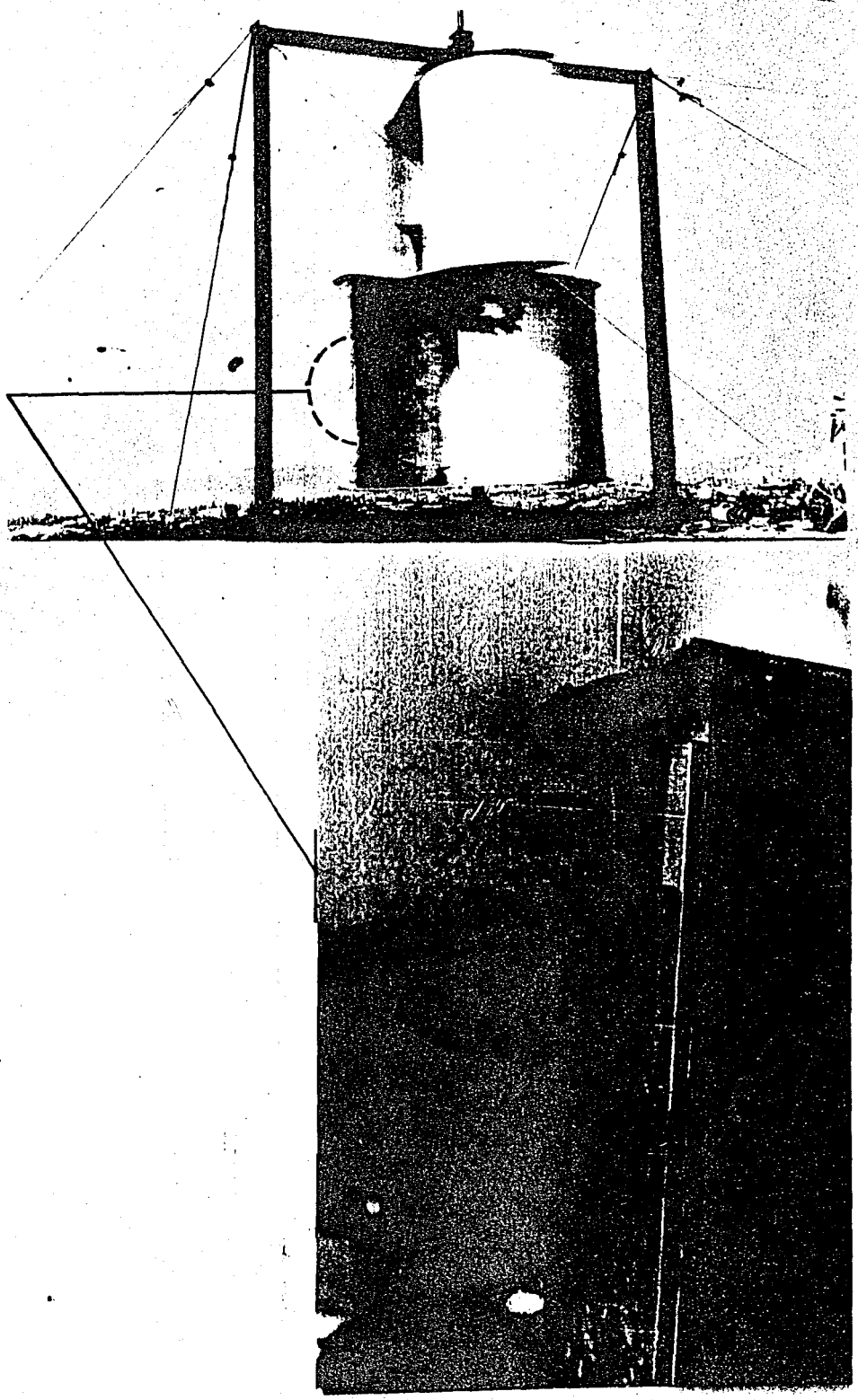

FIG. A.4.8. 10x10 Aluminum Profile Reinforcing Elements Against Cenrifugal Stresses.

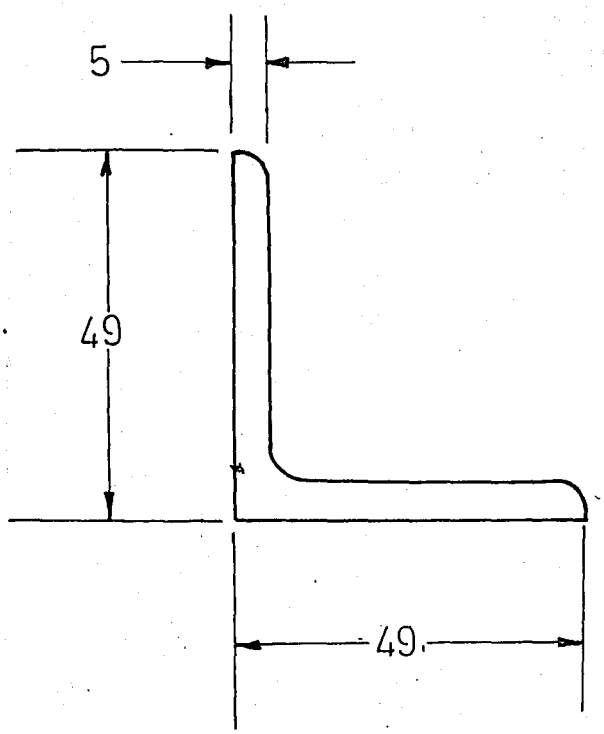

FIG. A.4.09. X-Section of L-Beams Used as Framework Material.

(scale 1:1)

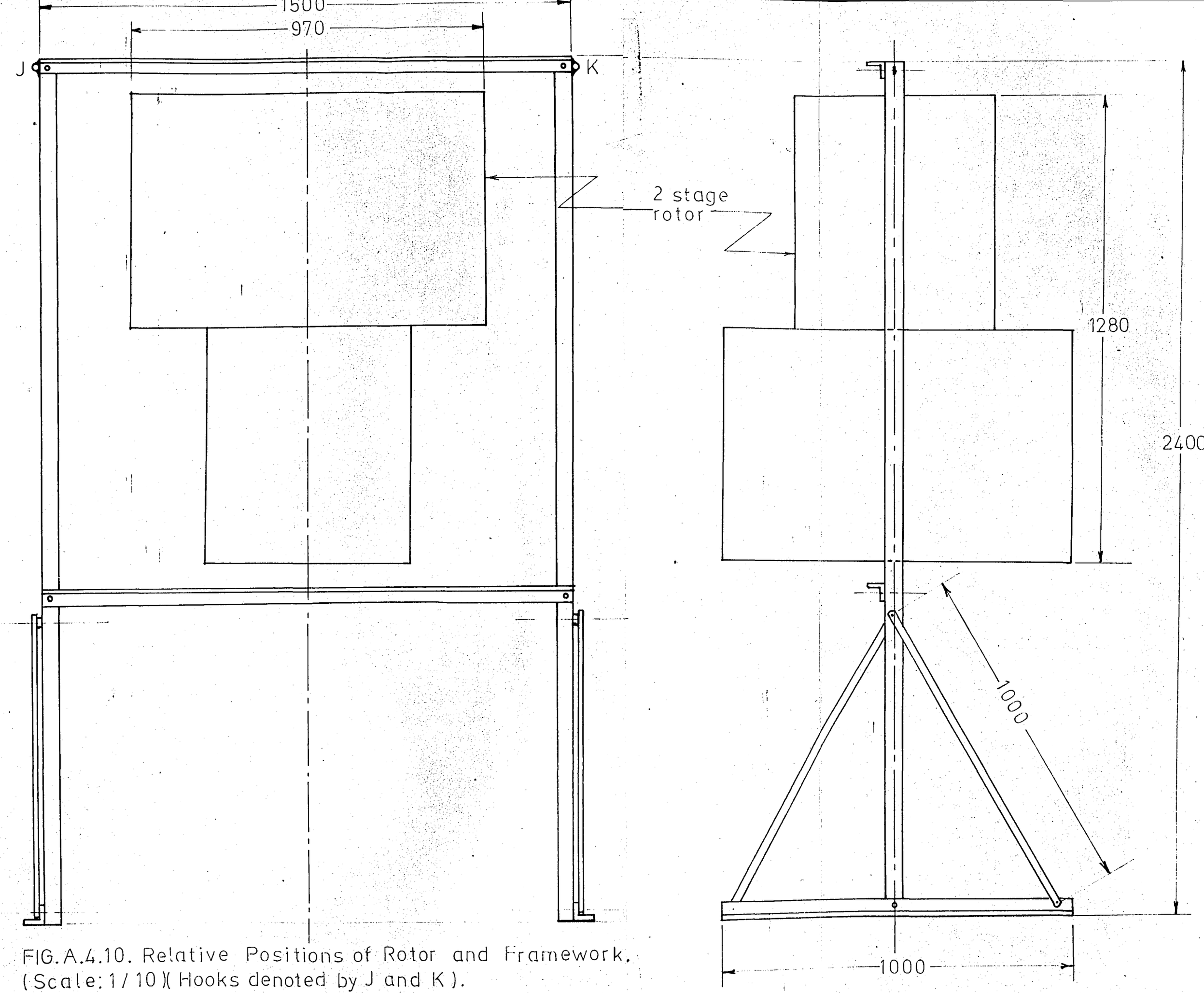

FIG. A.4.10. Relative Positions of Rotor and Framework.
(Scale: 1/10)(Hooks denoted by J and K).

A.4.2. SUPPORTING STRUCTURE

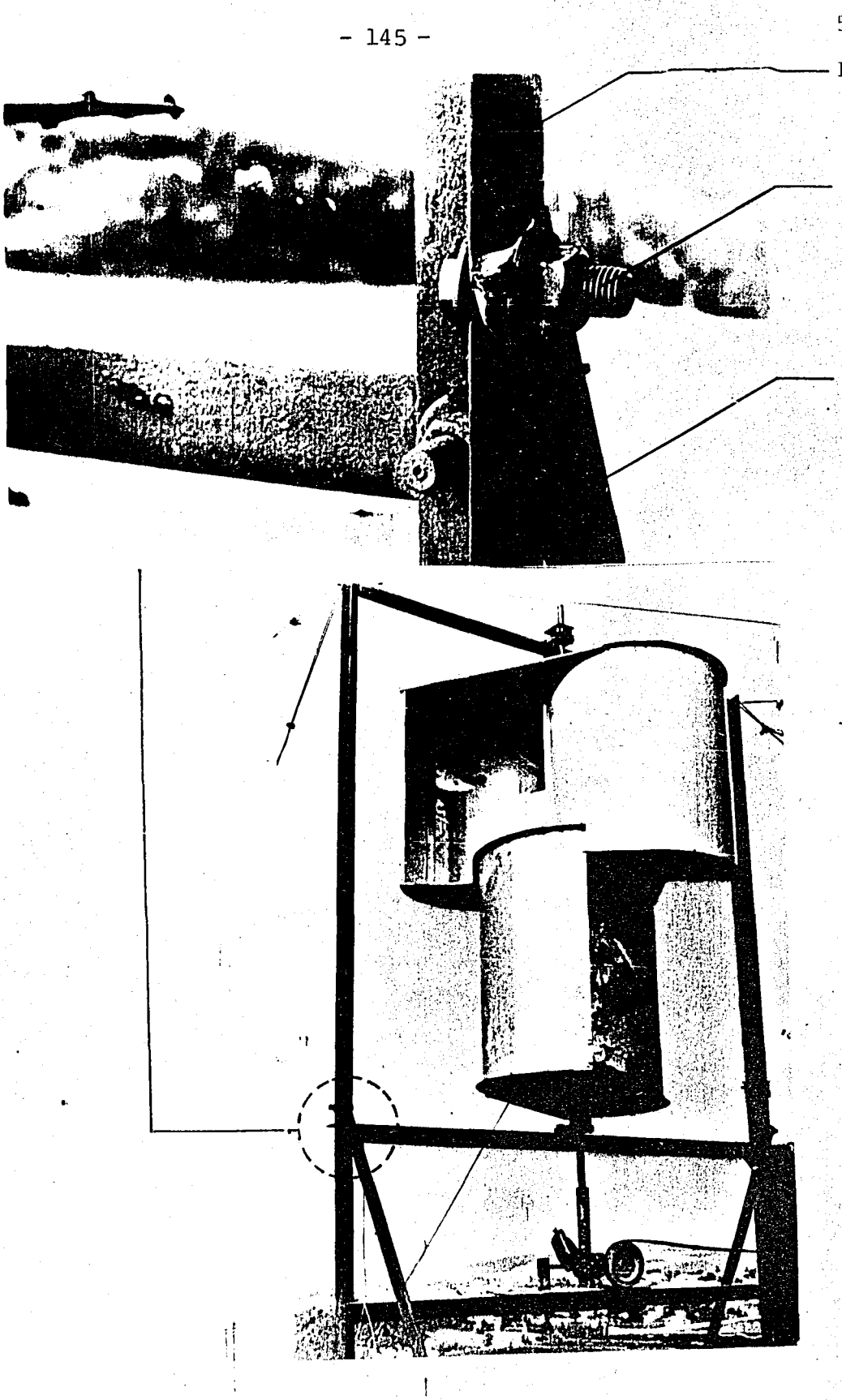

FIG.A.4.11. Supporting Structure

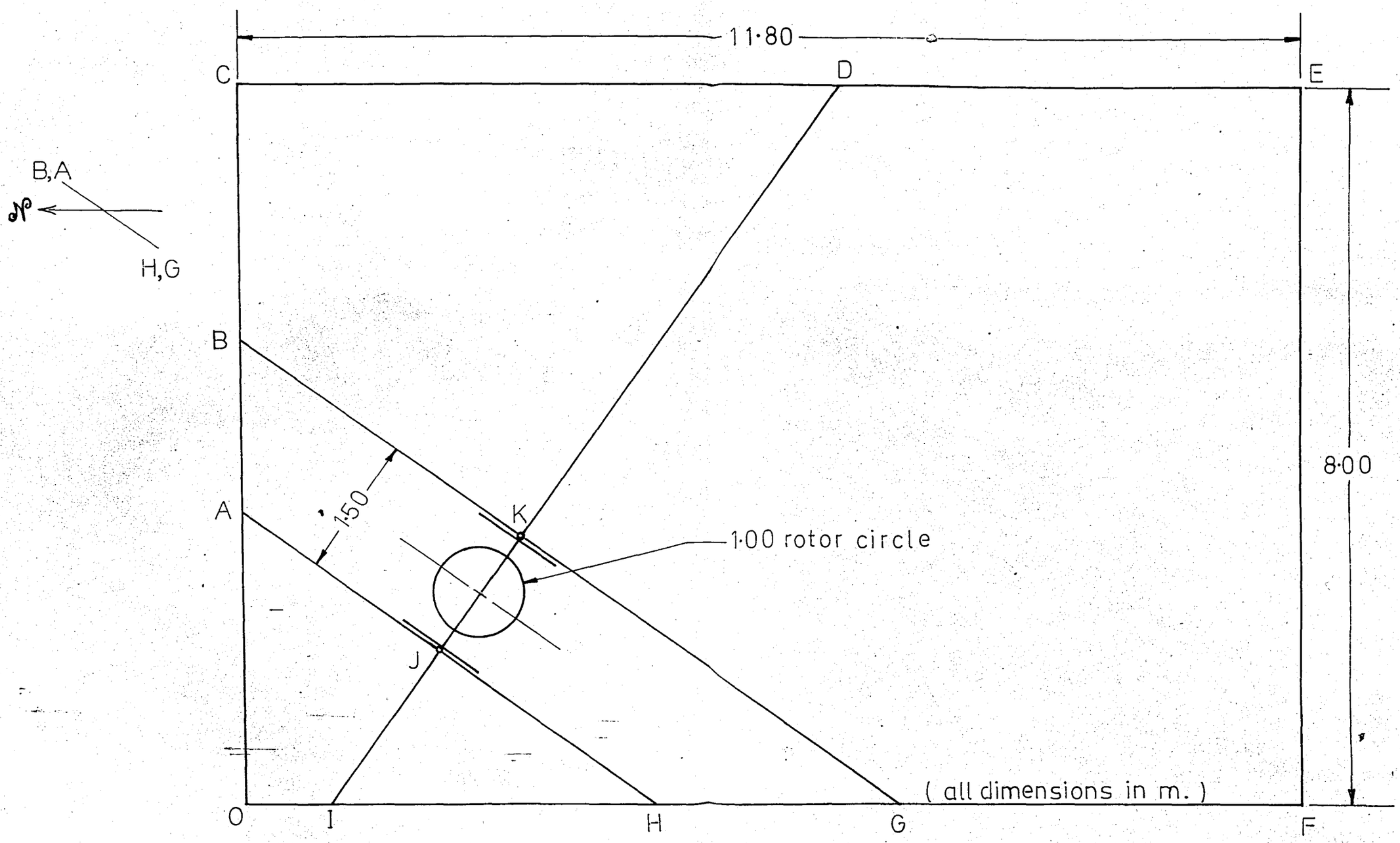

FIG. A.4.12. Top View of the Penthouse Roof Containing the WGS. (Scale: 1/50)
Note: Hooks J and K fixed to rotor frame are 2·40 m. high from the plane of the roof containing the points I, A, H, and B, D, G. Wire lengths are: AJ=3·80, IJ=3·60, HJ=5·40 ; BK=4·60, DK=6·50, GK=7·50.

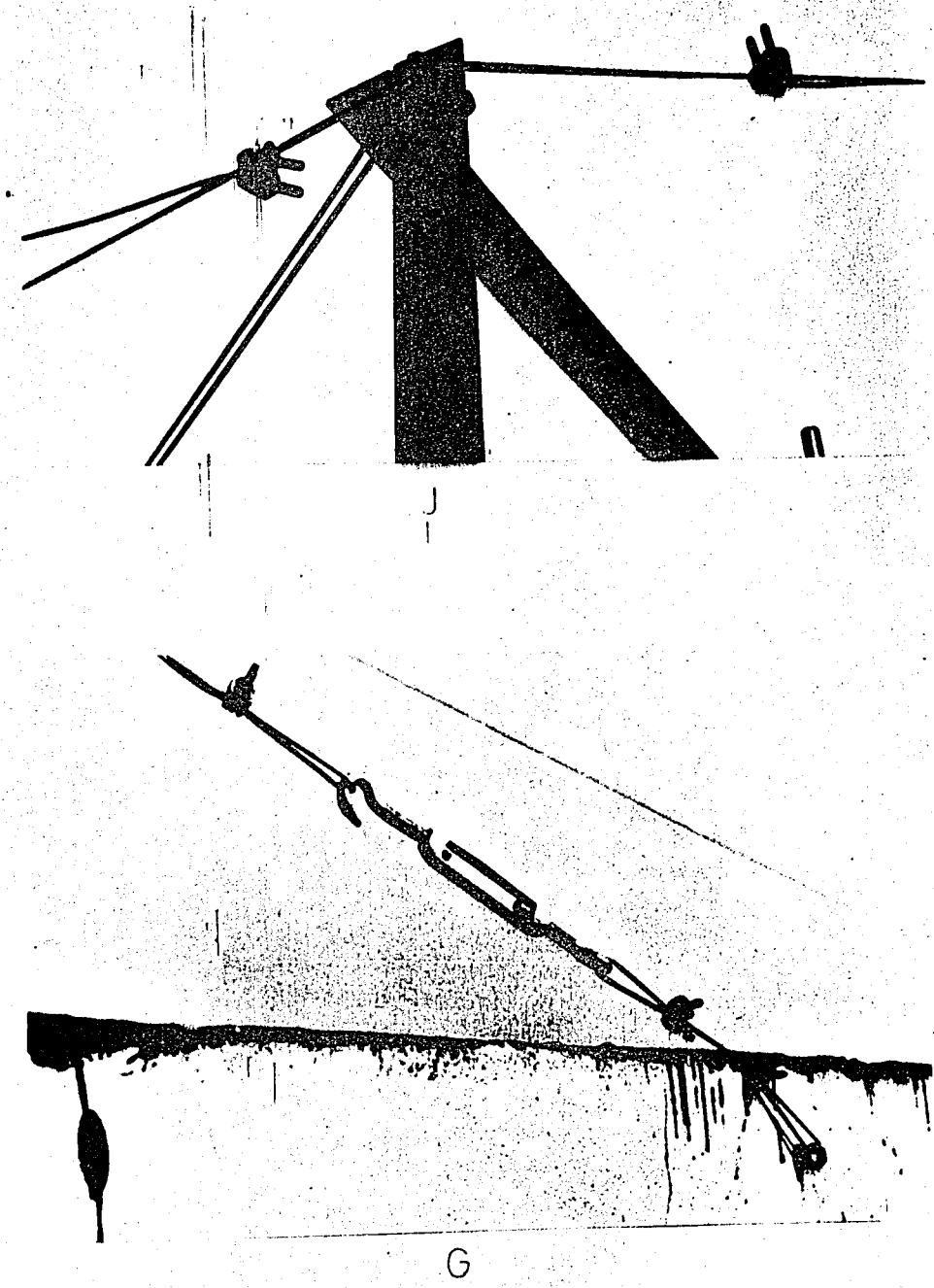

IG, A. 4. 13. Guy Wires.

A. 4. 3. Supporting Elements

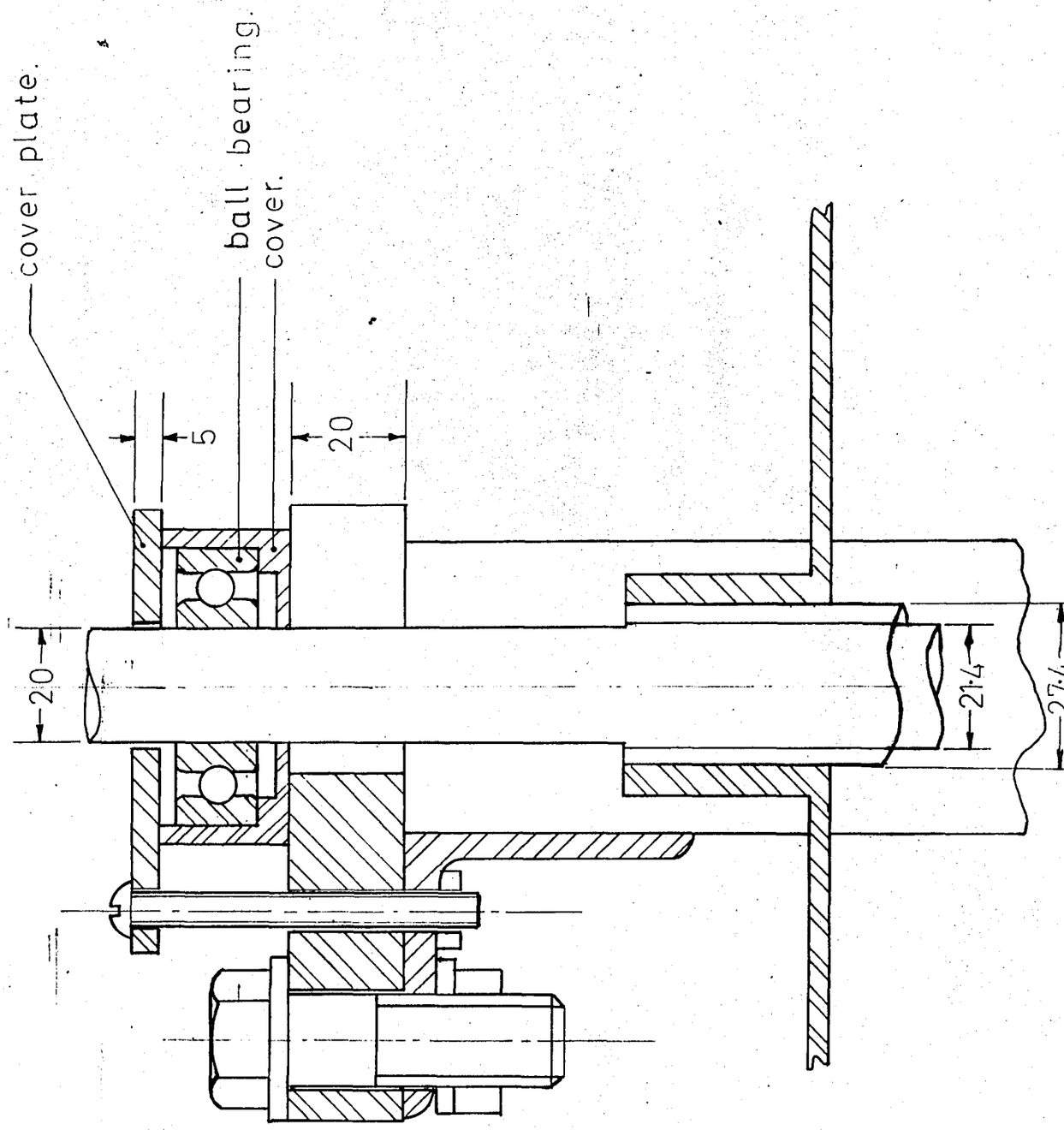

FIG. A.4.14. Upper Bearing System.(scale 1:1)

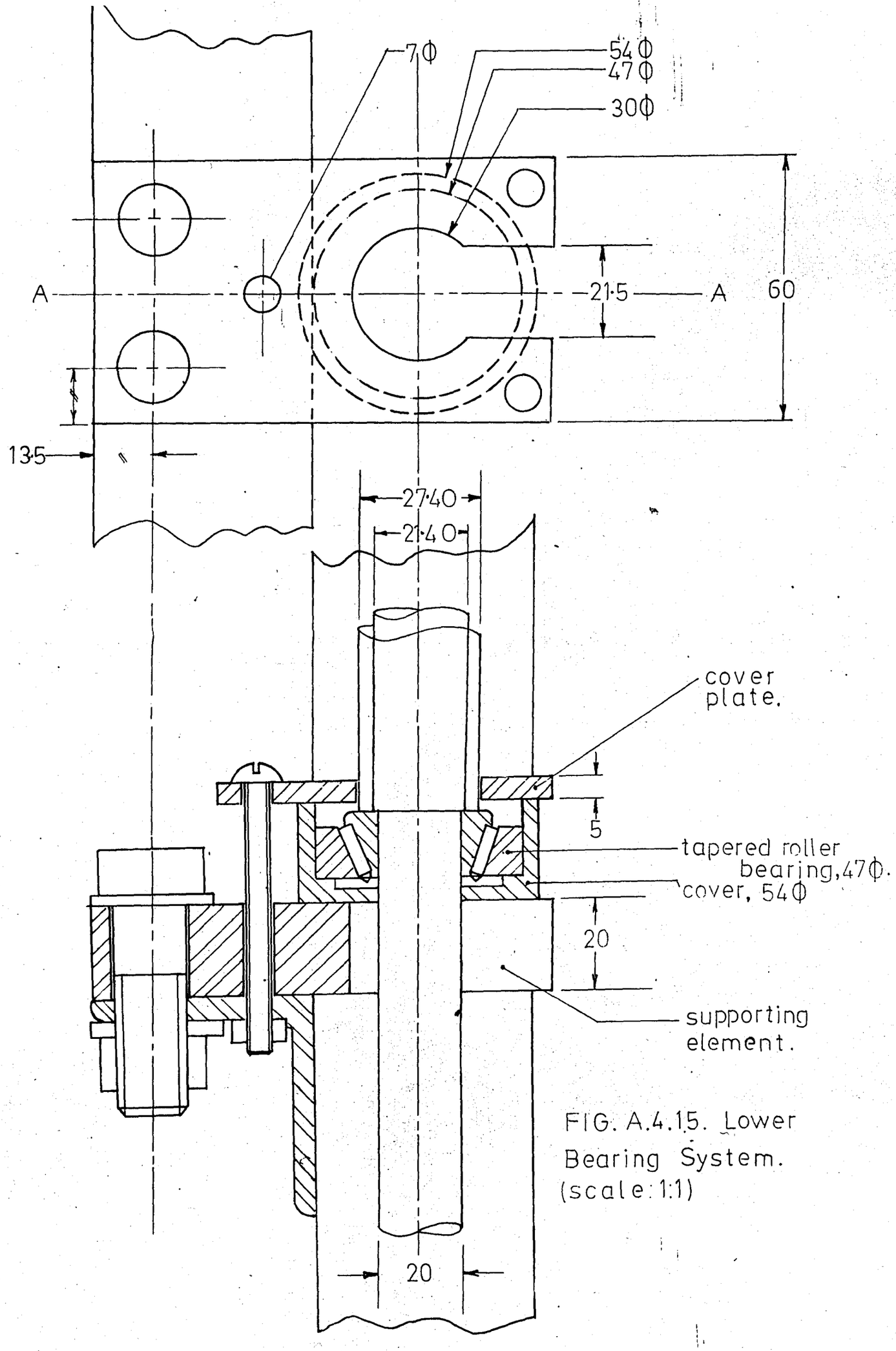

FIG. A.4.15. Lower Bearing System. (scale: 1:1)

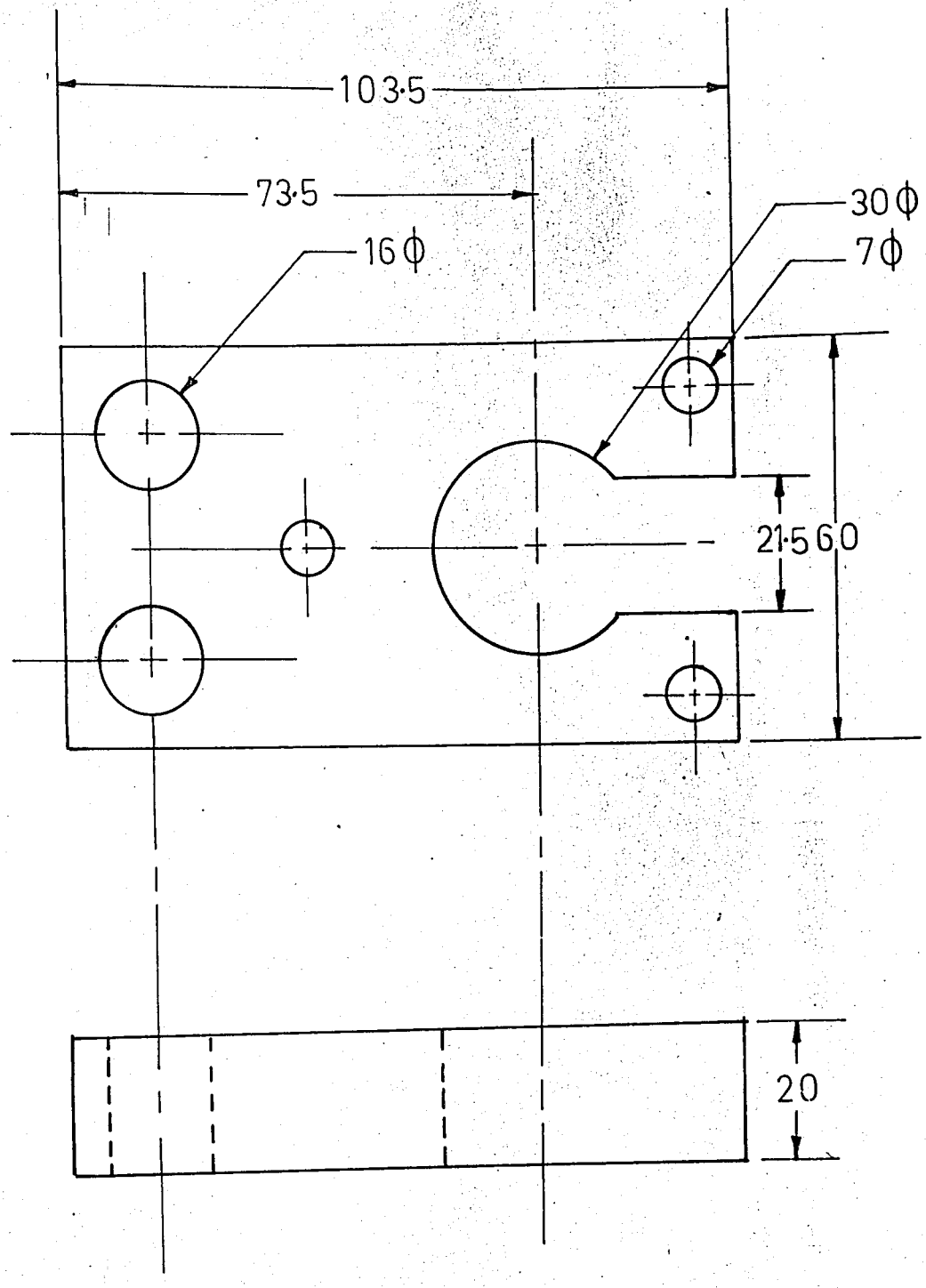

FIG. A.4.16. Rotor Carrying Element (× 2) (scale 1:1).

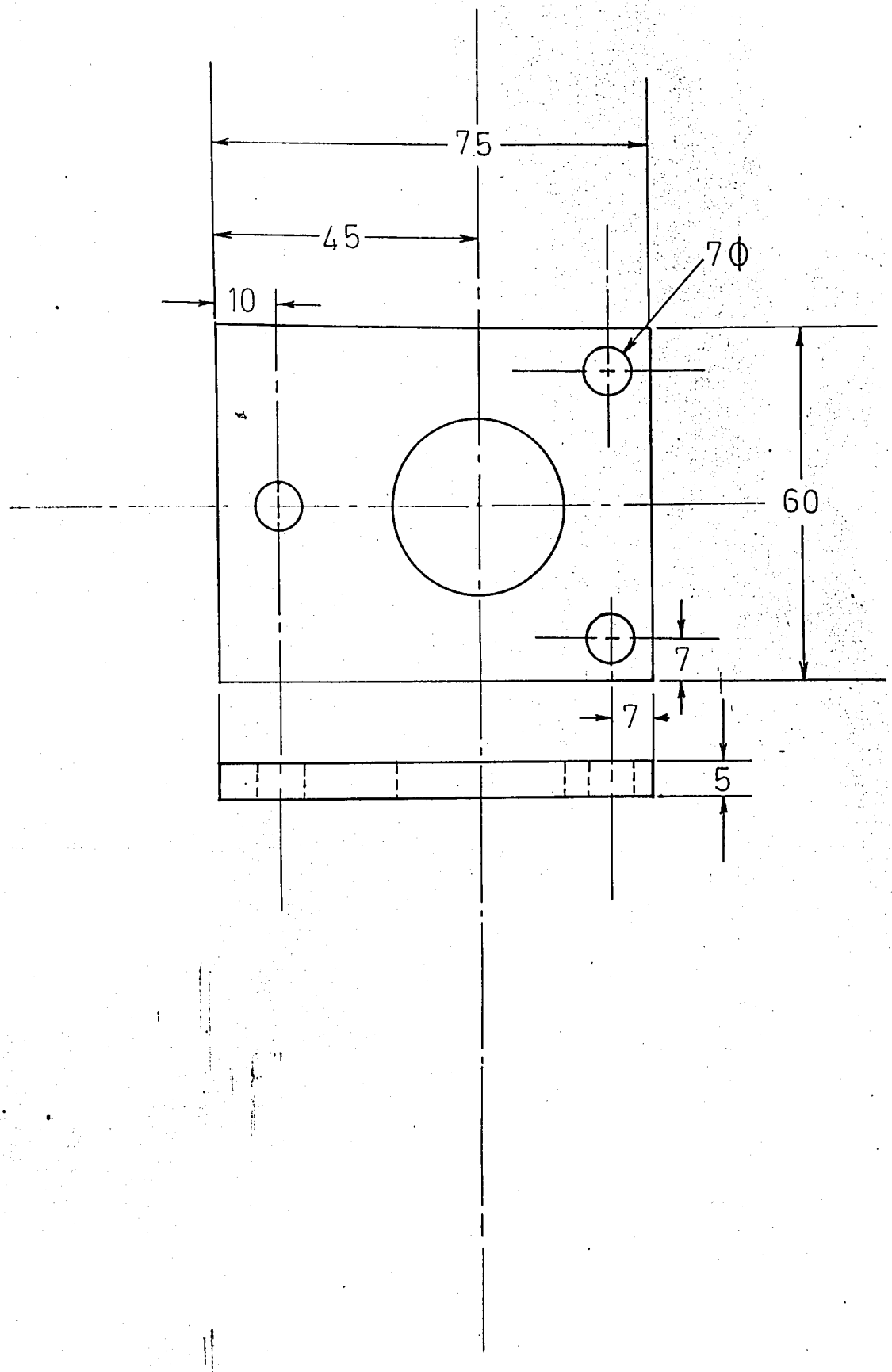

FIG. A.4.17. Bearing Cover Plate, (scale 1:1).

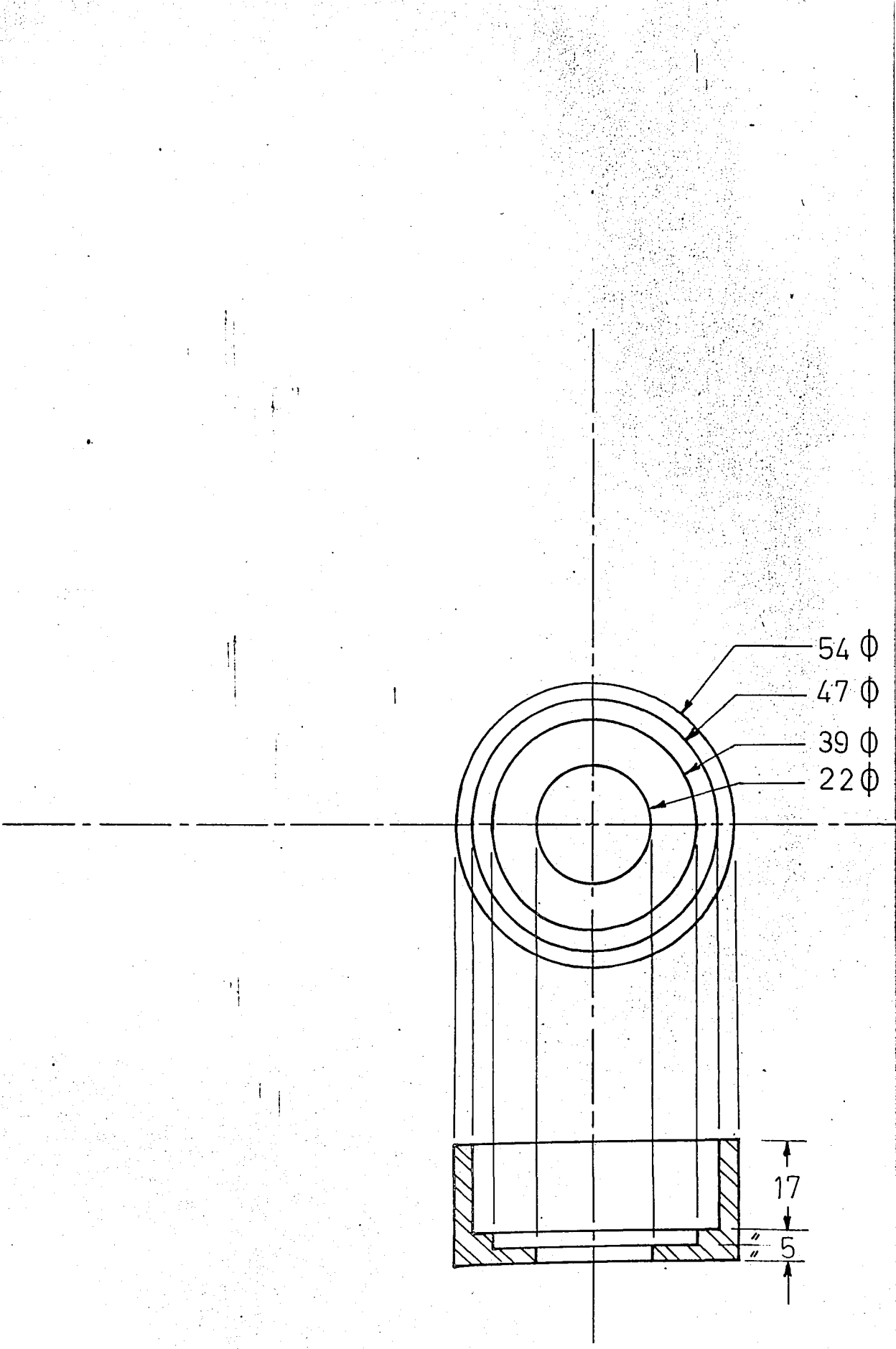

FIG. A.4.18. Bearing Cover (× 2). (scale 1:1)

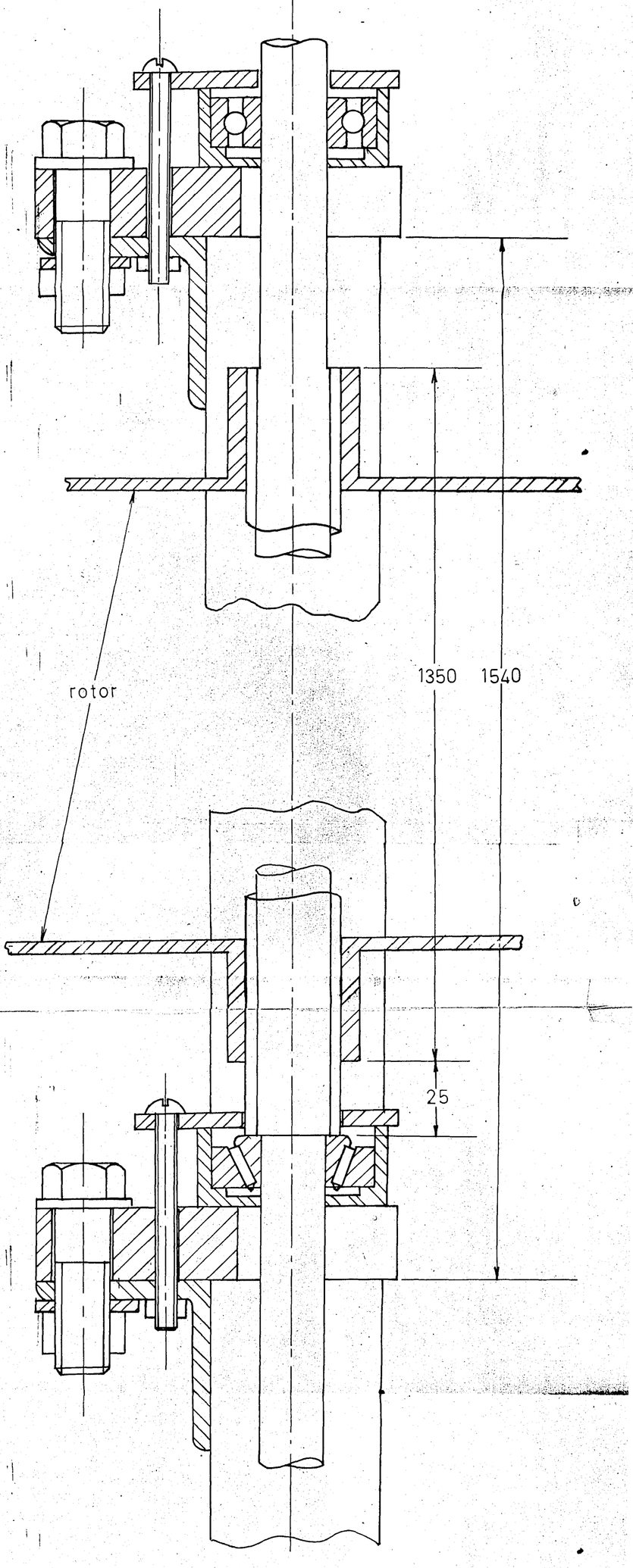

FIG. A.4.19. Upper and Lower Bearing Systems.
(scale 1:1).

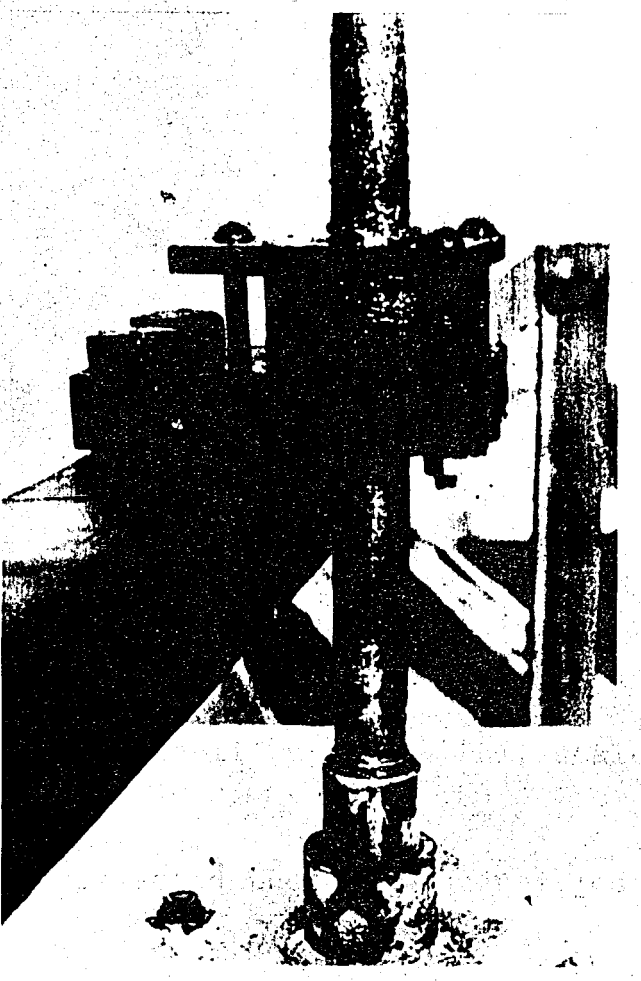

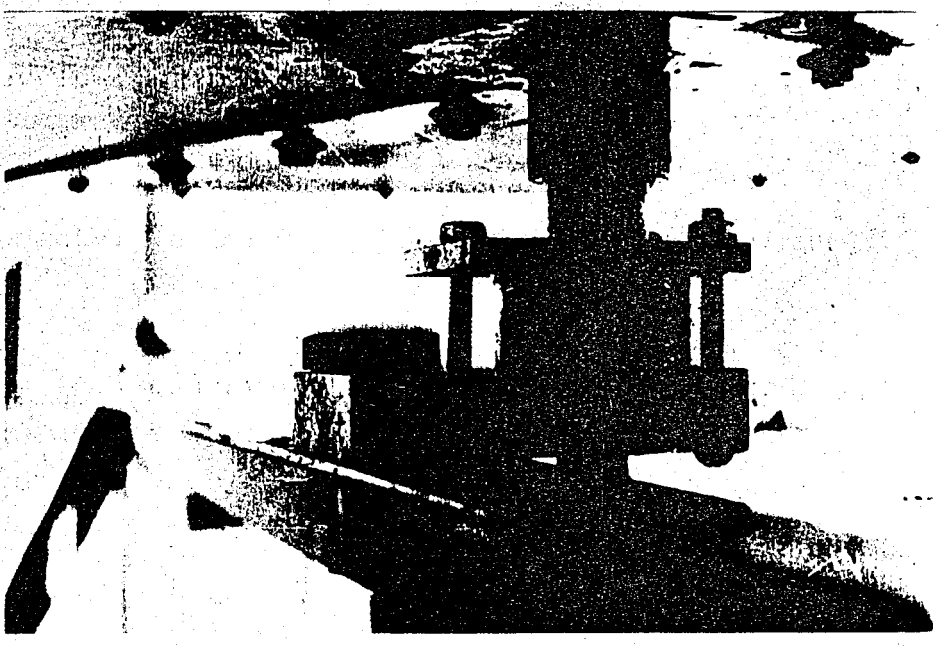

FIG,A.4.20 Upper and Lower Bearing Systems.

A. 5. Instrumentation

Tests were carried out using two sets of apparatus:
I/ Experiments with a torque meter set to determine the torque and power output characteristics of the rotor,
II/ Experimentation with a car alternator set to generate electric power, aiming to :

i/ contribute to the prior investigations (carried out with models in a wind tunnel) by plotting the pertinent dimensionless parameters

ii/ determine the practical serviceability of the full scale device.

I/ The method of analysis necessisated the below quantities to be measured

a/ Wind velocity, to determine the power in the wind thru the effective rotor area;

b/ Number of revolutions per unit time of the impeller;

c) Torque / power delivered by the impeller.

Numerous instrumental features of the set-up are explained below in detail:

a/ Wind velocity was read by means of a self constructed anemometer. This device consisted of a dual range "tacho generator" of very low resistive torque, coupled to a vertical-axis impeller of low inertia.

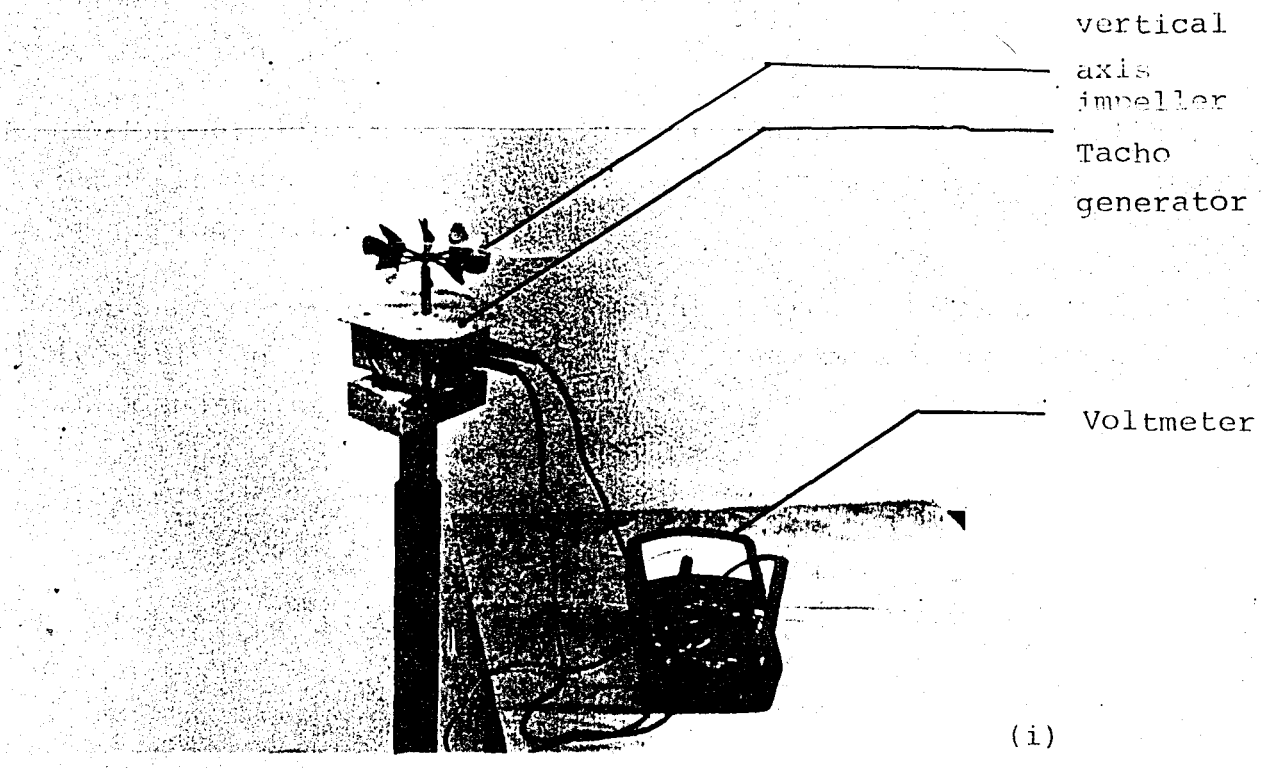

(i)

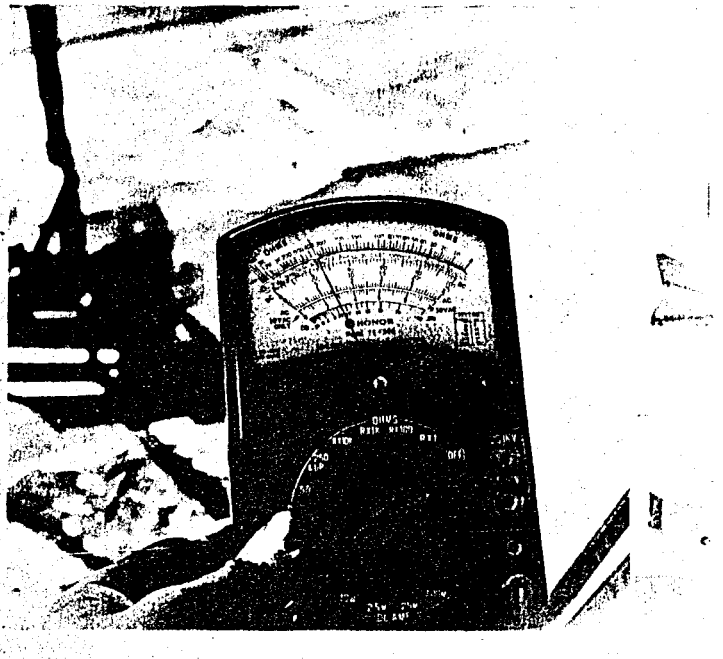

(ii)

FIG. A.5.1. The Anemometer Components

Photographs above illustrate the device prior to calibration and under running conditions.

The output voltage (proportional to the rpm of the impeller, which in turn is proportional to wind velocity) was read from an analog voltmeter.

The anemometer set-up was calibrated with respect to a sensitive photoelectric transducer anemometer, available in the department. Calibration data and curve are given below:

	(x , Anemometer)	y)(*) (voltmeter)
1	0	0
2	0.40	1.20
3	3.00	5.20
4	3.40	6.00
5	6.80	6.80
6	9.00	10.00
7	11.60	14.00
8	12.40	18.00
9	16.00	22.00

TABLE A.5.1 Wind Speed Calibration Data

The least square line

$$y = a_o + a_1 x$$

Approximates the above set of points. Which are observed to group along a straight line from the scatter diagram.

The normal equations giving the constants a_o and a_1 are:

$$\Sigma y = a_o N + a_1 \Sigma x$$
$$\Sigma xy = a_o \Sigma x + a_1 \Sigma x^2$$

(*) *x=2x' ; y = 40 y' where x' y' denote the true readings in m/sec and volts respectively; 2 and 40 being their scale factors entertained in plotting the scatter diagram on the graph paper.*

Where,

$\Sigma x = 62.60$
$\Sigma x^2 = 692.28$
$\Sigma y = 83.2$
$\Sigma y^2 = 1214.72$
$\Sigma xy = 910.32$

Thus, the normal equations read,

$83.2 = 9\ a_o + 62.6\ a_1$
$910.32 = 62.6\ a_o + 692.28\ a_1$

$\Rightarrow a_o = 0.26$; $a_1 = 1.29$
$y = 0.26 + 1.29\ x$,

is the least square line. If x is considered as the dependent variable and y as the independent variable, the equation of the least square line is,

$x = b_o + b_1 y$

The normal equations are,

$\Sigma x = b_o N + b_1 \Sigma y$
$\Sigma xy = b_o \Sigma y + b_1 \Sigma y^2$

Which read as,

$62.6 = 9\ b_o + 83.2\ b_1$
$910.32 = 83.2\ b_o + 1214.72\ b_1$

$\Rightarrow b_o = 0.075$; $b_1 = 0.74$,

$\Rightarrow x = 0.075 + 0.74\ y$

The graphs of the twolines, $y = 0.26+1.29\ x$ ($\triangleq$ regression line of y on x) and $x = 0.075 + 0.74\ y$ ($\triangleq$ regression line of x on y) given below are seen to be practically coincident for this case, which is an indication that the data are very well described by a linear relationship. The line $y = \frac{4}{3} x$ was taken as the calibration curve.
Recalling that $x = 2x'$ and $y = 40y'$, The relationship between wind velocity and voltmeter readings is, $x' = 15y'$.

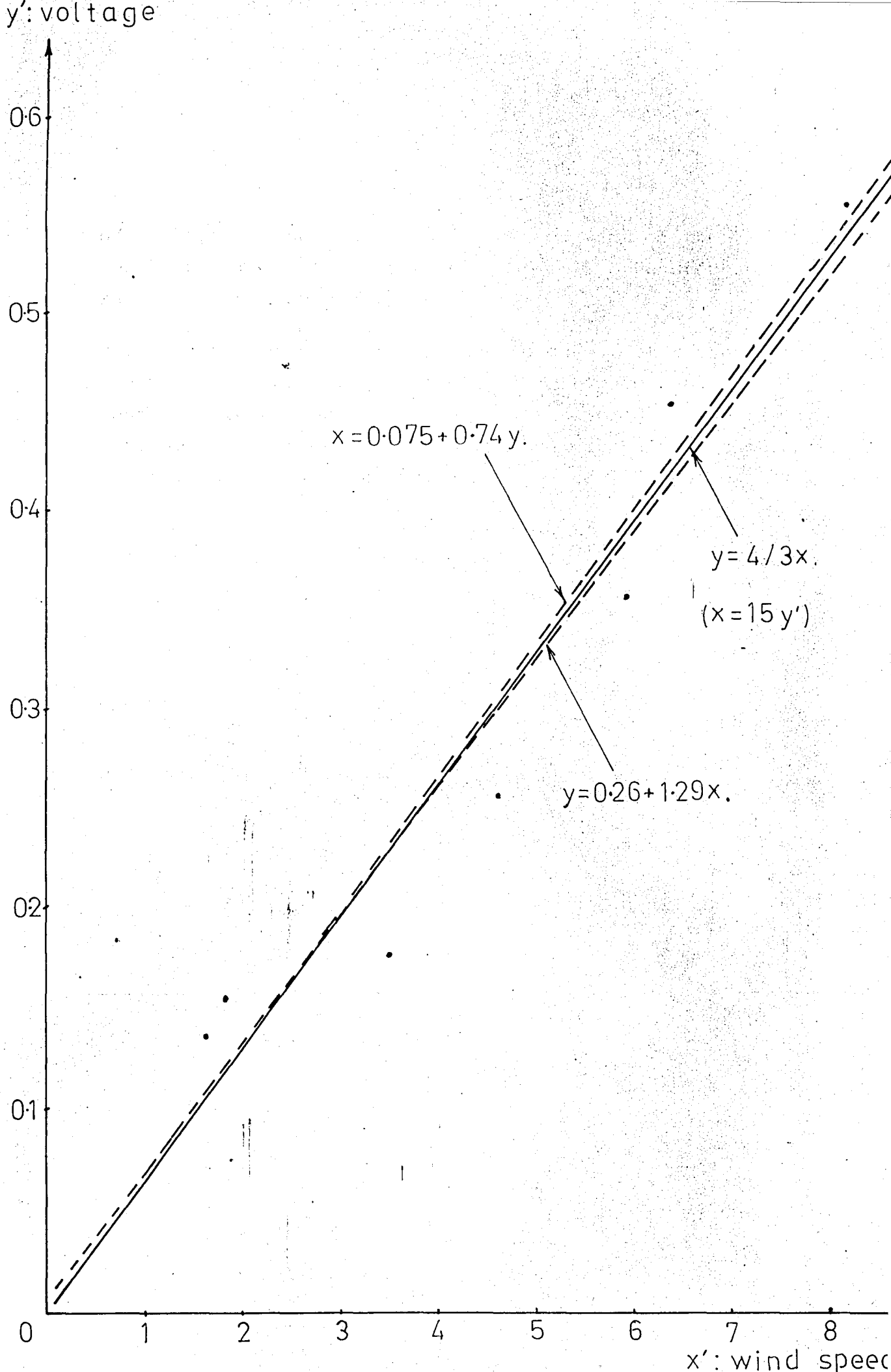

FIG. A.5.2. Wind Speed Calibration Curve.

b/ The rpm or the rotor was found from that of the torque meter shaft upon division of it by the step-up ratio of the transmission system.

Revolutions per unit time of the torque - meter shaft was measured by means of an analog voltmeter which was connected to another tacho generator coupled to the testing set.The calibration was performed by a mechanical tachometer. Related calibration informations are provided below:

$$n_1 = n_2 \, d/D$$

$$n = n_1/i$$

$$= n_2 d/iD$$

Where

d = 31.8 mm

D = 219.9 mm

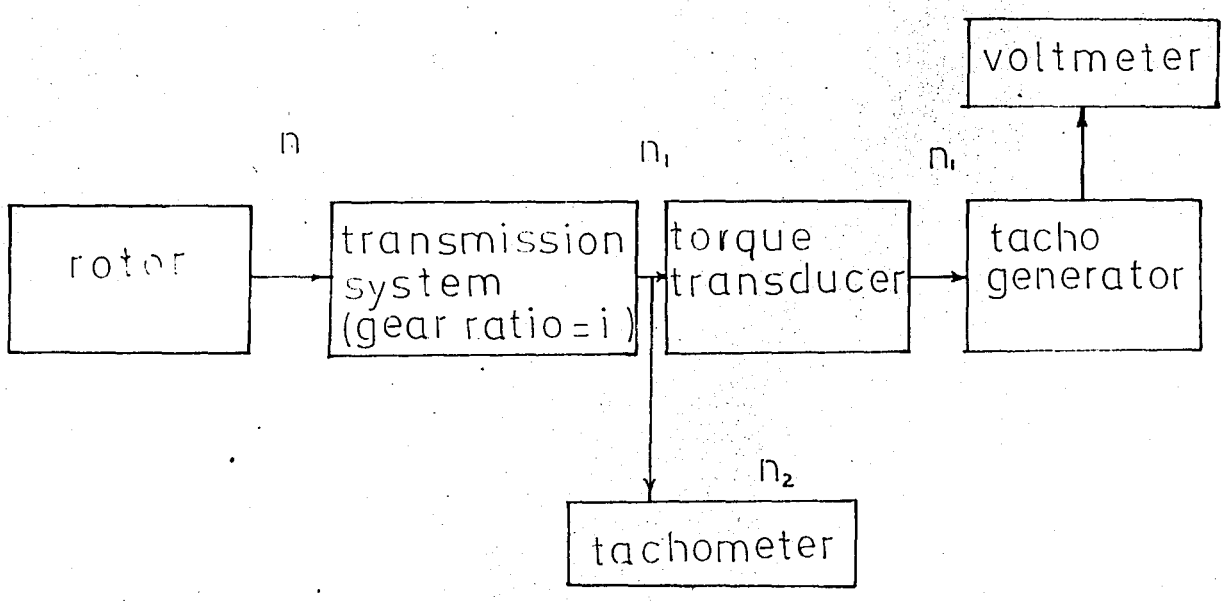

FIG. A.5.3.i Calibration of a Voltmeter for Rotation Rate Measurement of Wind Turbine.

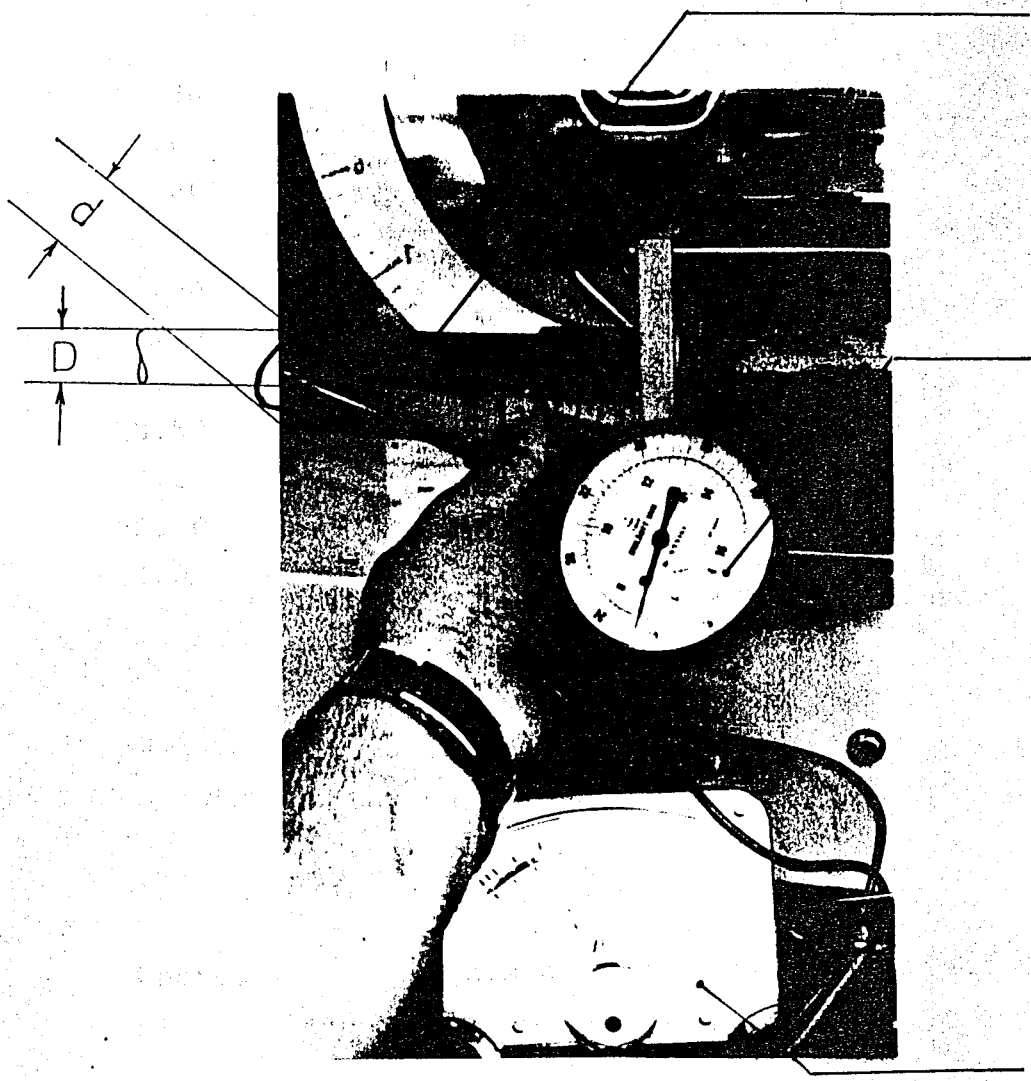

FIG. A.5.3. ii. Calibration of a Voltmeter for Rotation Rate Measurement of Wind Turbine.

(x , tachometer ,	y voltmeter) (*)
0	0
4.20	3.20
6.00	4.00
9.80	6.40
10.40	7.20
12.35	8.00
14.10	9.60
15.00	10.00
18.50	12.00
22.25	12.80
22.50	15.20
24.00	15.60

TABLE A.5.2. Rotation Rate Calibration Data.

The least square line approximating the above set of points has the equation,

$$y = a_o + a_1 x$$

Where, the constants a_o and a_1 are determined by solving simultaneously the normal equations,

$$\Sigma y = a_o N + a_1 \Sigma x$$
$$\Sigma xy = a_o \Sigma x + a_1 \Sigma x^2$$

From the above data,

(*) *$x = 0.05x'$; $y = 40\ y'$ where, x' and y' are the true readings in rgm and volts, while 0.05 and 40 are the scale factors antertained as plotting the scatter diagram of the data.*

$\Sigma x = 159.1$
$\Sigma y = 104$
$\Sigma xy = 1782.4$
$\Sigma x^2 = 2753.74$
$\Sigma y^2 = 1157.44$

The condition of $x = 0 \Rightarrow y = 0$ is imposed by setting $a_o = 0$.

Then,

$104 = 159.1\ a_1$
$\Rightarrow a_1 = 0.65$
and,
$1782.4 = 2753.74\ a_1$
$\Rightarrow a_1 = 0.65$
$\Rightarrow y = 0.65\ x$ is the regression of y on x.

Considering the regression of x on y, namely

$x = b_o + b_1 y$,

$\Sigma x = b_1 \Sigma y$
$\Sigma xy = b_1 \Sigma y^2$

$\Rightarrow 159.1 = (b_1)(104)$
$1782.4 = (b_1)(1157.44)$

$\Rightarrow b_1 = 1.53$; $b_1 = 1.54$
$\Rightarrow x = 1.53\ y$ is the regression of x on y.

$y = 0.65\ x$ and $x = 1.53\ y$ exactly coinciding implies that the linear relationship is perfect to express the data.

Hence y = 0.65x is taken as the calibration line.

Recalling x = 0.05 x' and y = 40 y' , the relationship between tachometer and voltmeter readings is,

$$x' = 1231\ y'$$

Recalling A.5.1,

$$n = \frac{n_2 d}{iD} \quad ; \quad x' = n_2$$

$$n = \frac{(1231\ y)(31.8)}{i\ (21.9)}$$

$$\Rightarrow n = \frac{1787\ y'}{i}$$

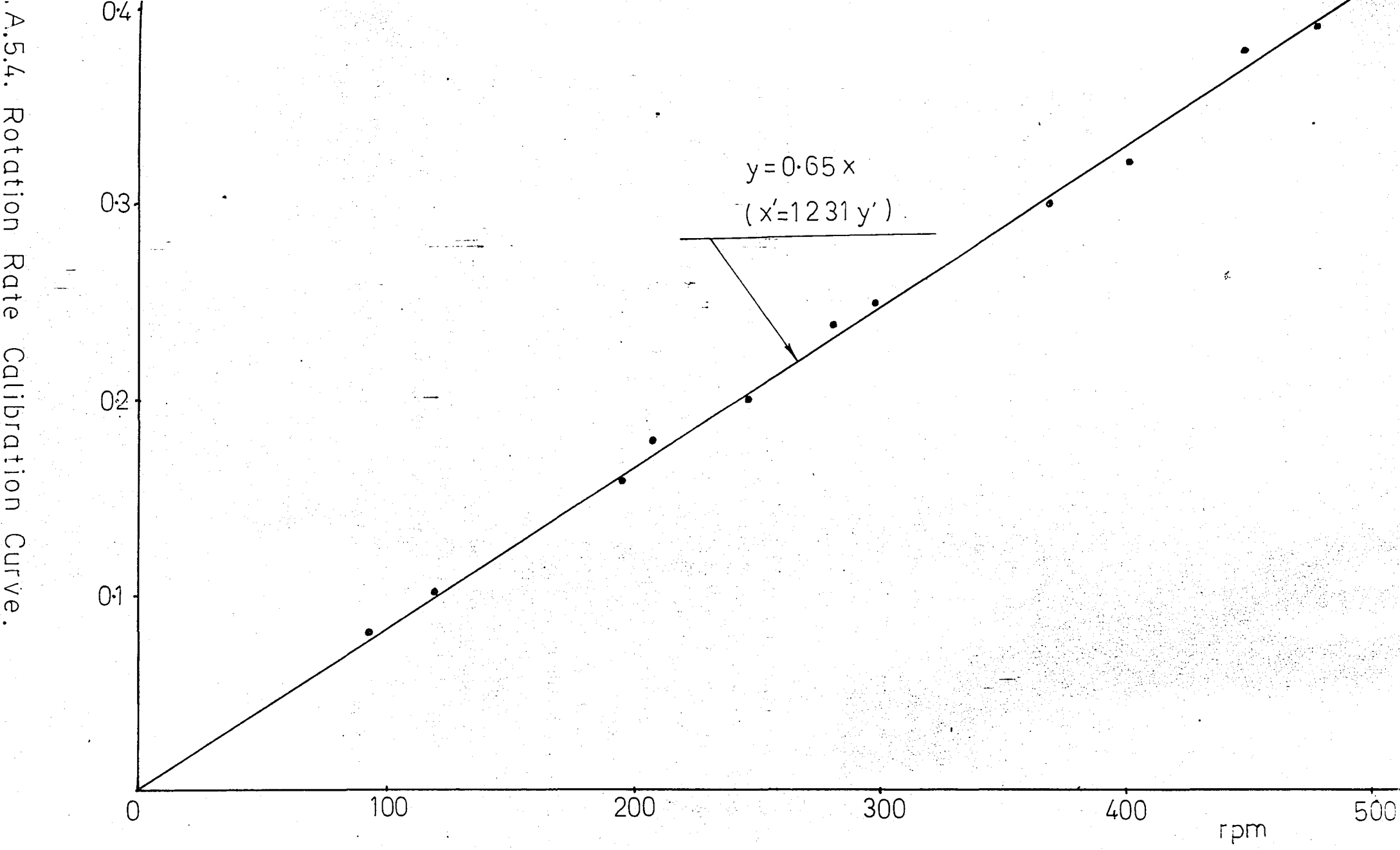

A.5.4. Rotation Rate Calibration Curve.

c/ The most important problem was to measure the output power estimadet to be in the range 0-400 watts.

The simplest mechanism would be a prony brake, as used by some of the wind-power investigators. However inaccuracy inherent in its oversimple construction was the major drawback, since very typical characteristics of the impeller were expected under low and intermediate loadings, which called sensitivity and accuracy in the resistive torque applying element. Friction brake techniques fail greatly on this score. Severe snatch accurs as stalling point is approached, and it is difficult to maintain a steady small load over a period without overheating ((21)).

Another practical idea was to couple the rotor shaft to a car alternator. This was found worth to realize. However, another problem induced, related with the efficiency of the alternator. It had to be determined as a function of the input power and rpm, so that the net efficiency of the impeller could be determined.Instrumental facilities of the mechanical and electrical departments were found to be insufficient to realize this. Even personal contacts with the manufacturers in Bursa were resultless to solve the problem.

Finally, a component of a generalized set for motor testing involving an eddy current brake and a calibrated dynamometer was adapted for coupling to the impeller.

The photographs and circuitry (*) of the instrument are given below :

(*) *Full information can be obtained from the catologs ((13)) and ((14)).*

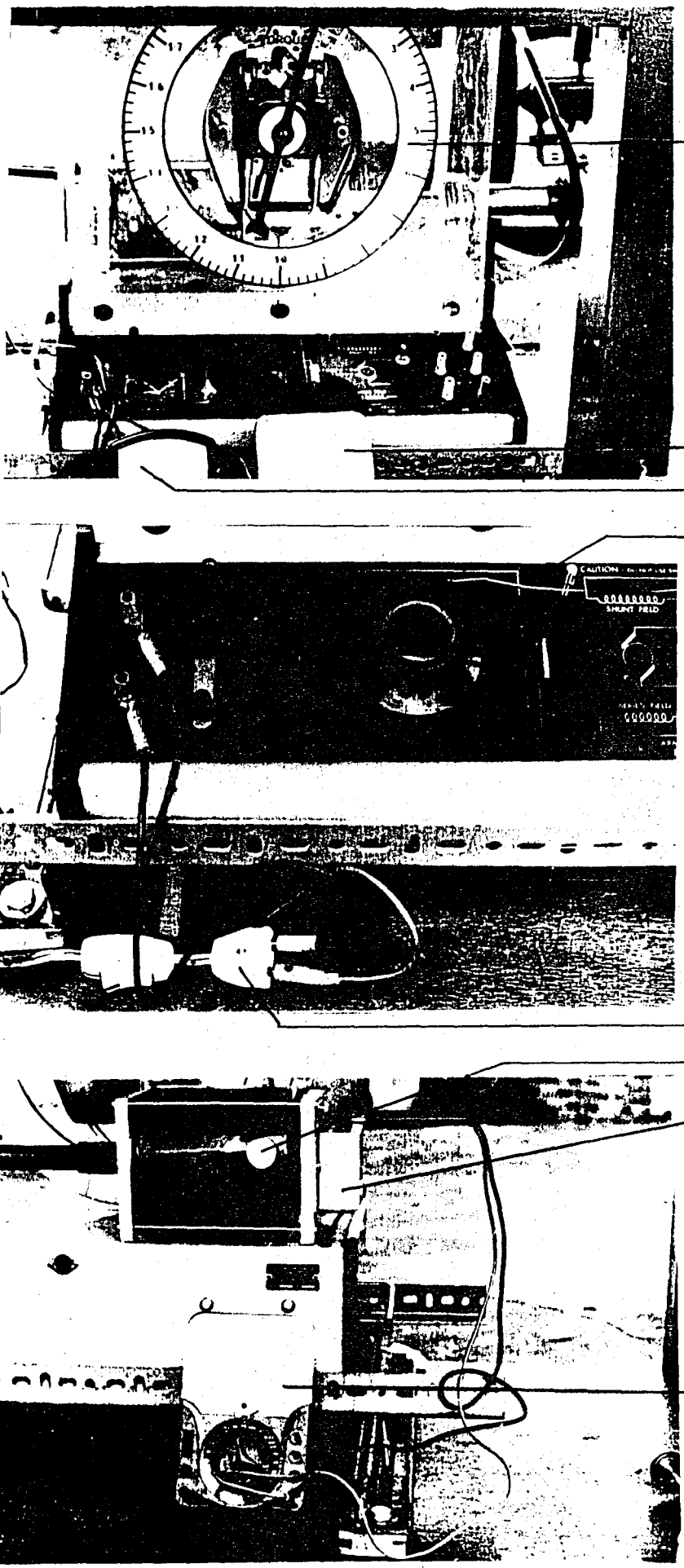

FIG.A.5.5.i The torque-meter Set

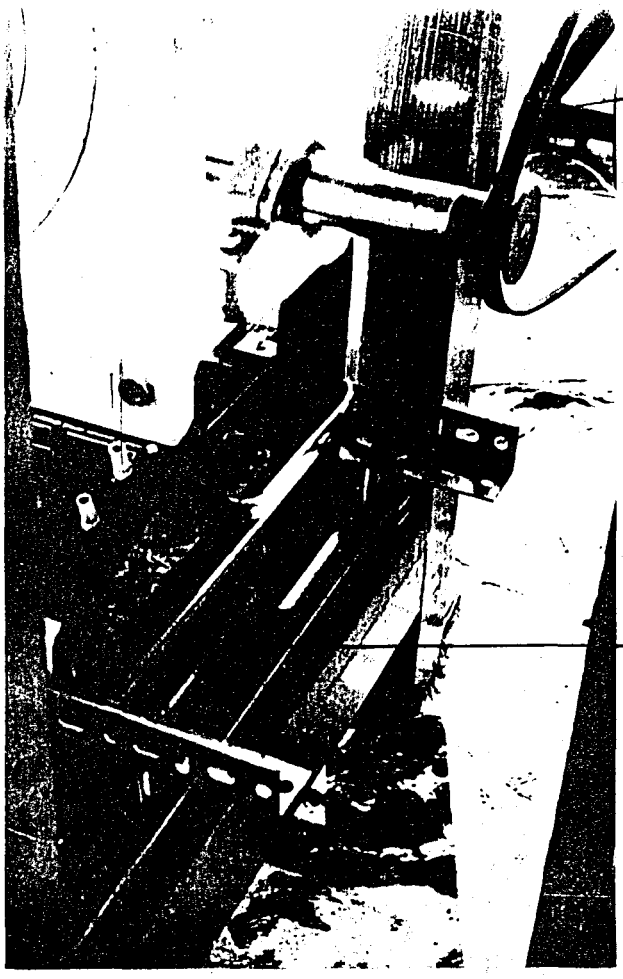

FIG. A.55. ii Connections.

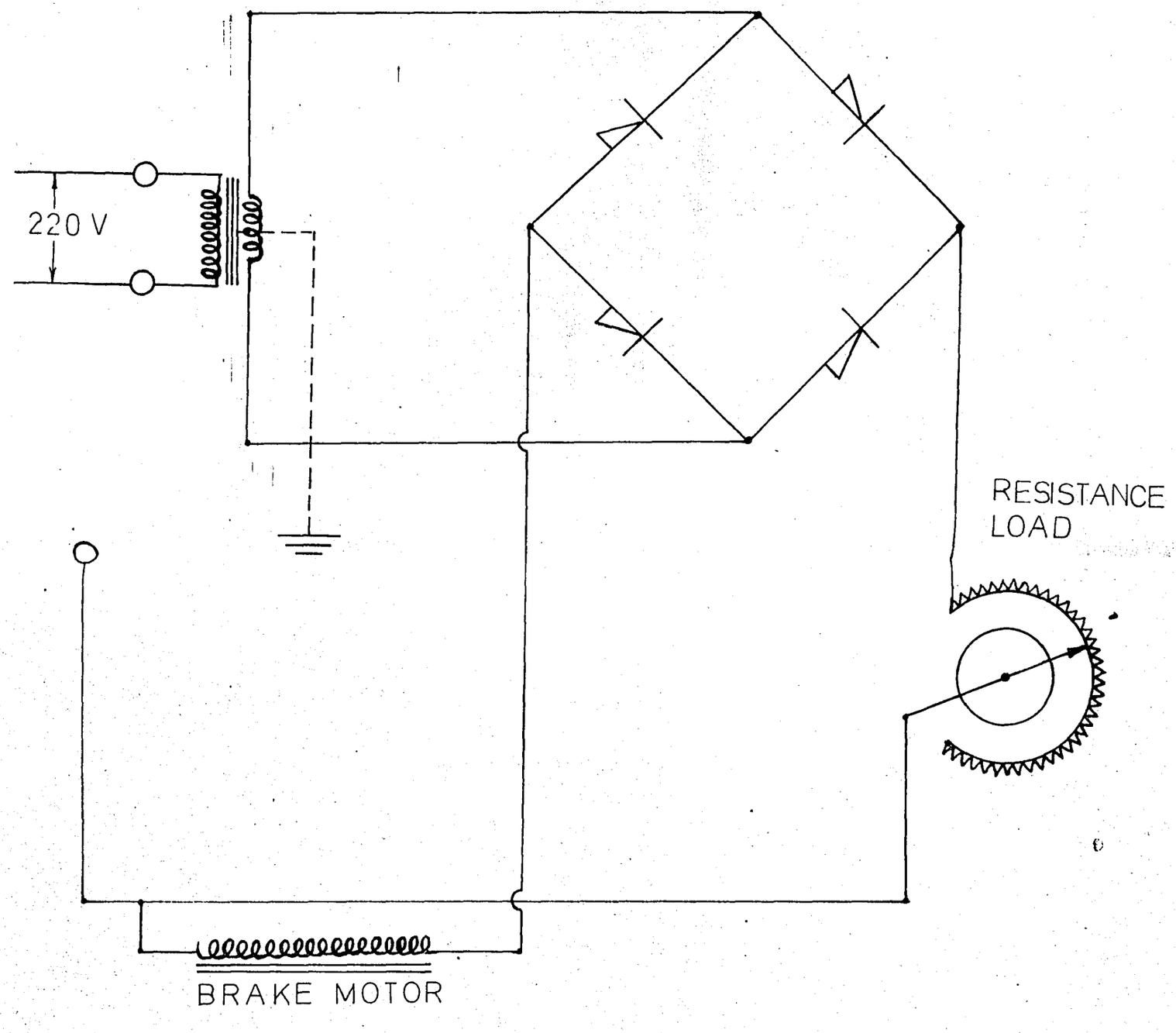

FIG.A.5.6. Circuitry of the Brake Motor System.

The eddy current brake of the instrument has the great advantage that it has got no slip rings or commutator to introduce frictional losses. A further advantage of using an eddy current brake is that, unlike a d.c. dynamometer which must be designed for a specific speed, tho torque developed for a given excitation is almost independent of speed. The same dynamometer may be used for testing a high speed rotor, or for toading a relatively low speed one. The eddy current dynamometer also aperates a little more than a crawl, and may therefore be used for studying "run-up" torque. It can also load a rotor to its stalling point((13)).

The only problem was that, the torque scale of the device had a narrow range between 0- 2.4. Newton - meters.

Assuming 100 rpm of the rotor under full deflection of the torque scale, the power absorbtion capacity of the device can be estimated as,

$$(100.\ \frac{2\pi}{60}\ \frac{\text{rad}}{\text{sec}})\ \ 2.4.\ \text{N-m}) = 25.\ 13\ \frac{\text{N-m}}{\text{sec}}\ (= \text{watts}).$$

On the other hand, from the power density curves of §2.3 , it was estimated that the impeller could generate power up to in the order of 400 watts in wind velocitics of about 30 mph.

The gap had to be closed to analyse the behavior of the impeller at the stalling point. This was accomplished by a high step -up ratio transmission system(*) so that,

---

(*) *Design details of the transmission system is given in the next section.*

assuming constant power thru the system,

$$P_1 = P_2$$
$$\Rightarrow T_1 W_1 = T_2 W_2$$
$$\Rightarrow \frac{T_1}{T_2} = \frac{W_2}{W_1} .$$

Where,

P = power
T = Torque
w = revolutions per unit time $(\frac{rad}{sec})$;

the subscripts 1 and 2 referring to the wind turbine and torque transducer shafts respectively .

Thus, increasing the rpm of the torque transducer shaft with a step-up transmission system would lower the brake torque safely within the torque scale of the device.

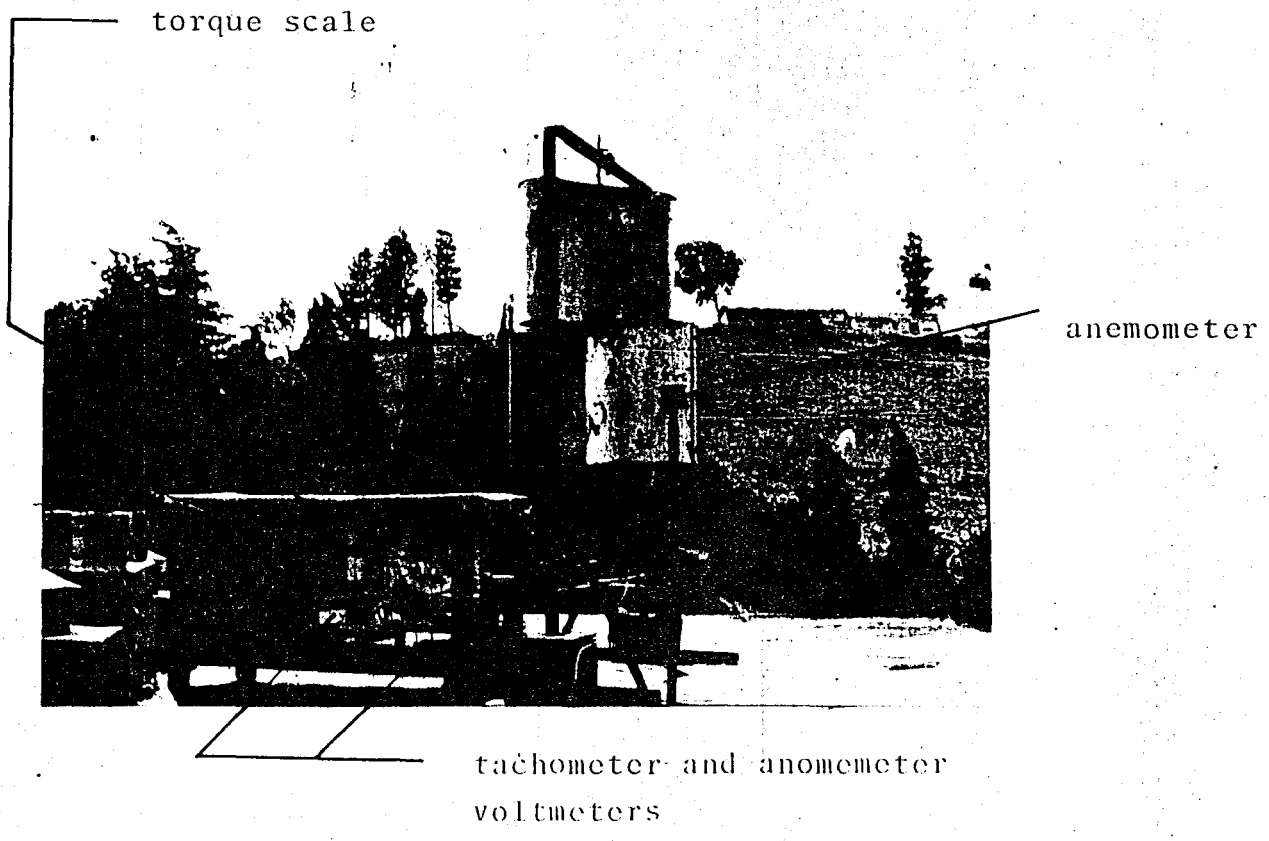

FIG. A. 5. 7. General View of set-up(I)

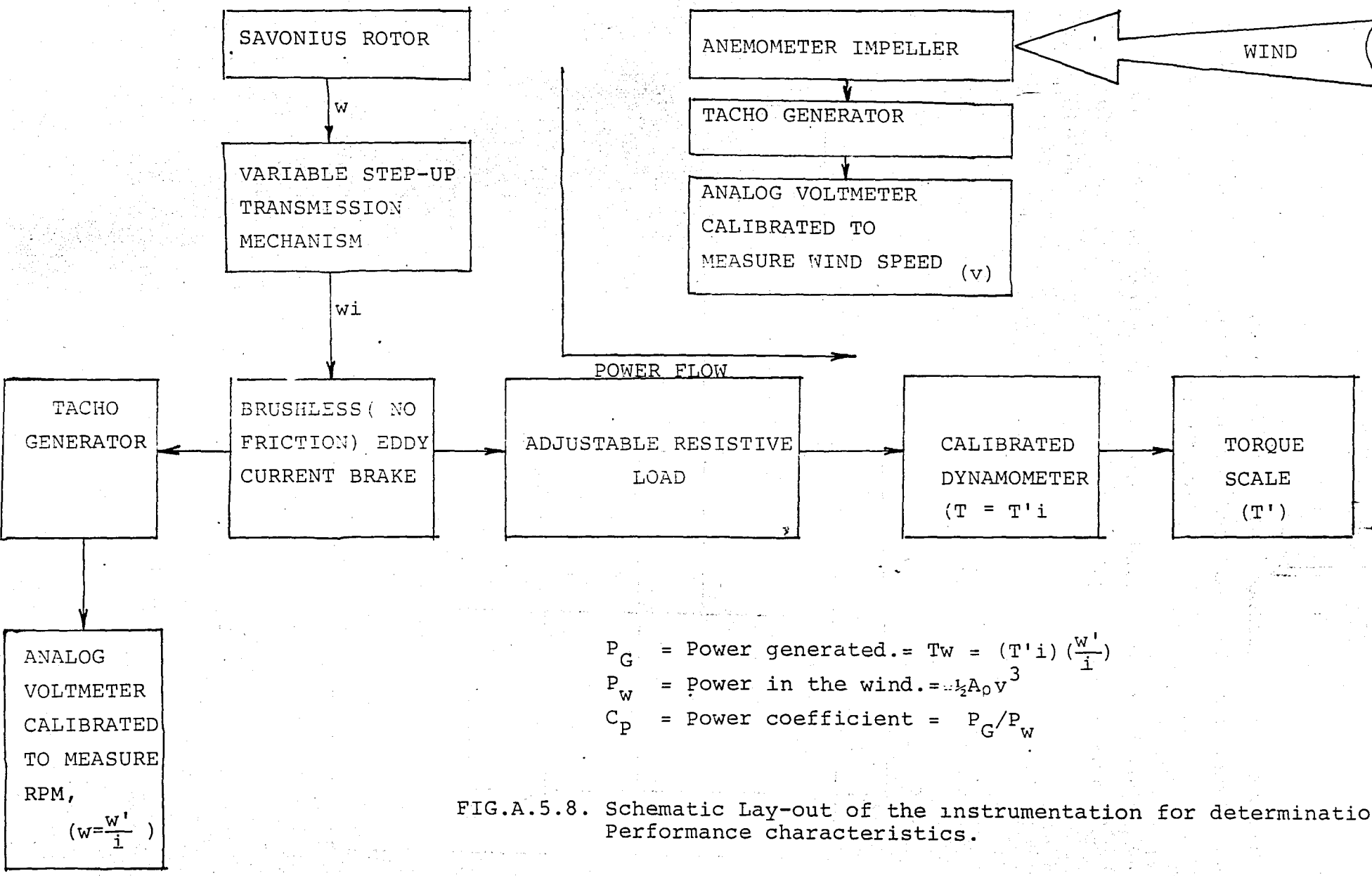

P_G = Power generated. = Tw = (T'i) $(\frac{w'}{i})$

P_w = Power in the wind. = $\frac{1}{2}A_0 v^3$

C_P = Power coefficient = P_G/P_w

FIG.A.5.8. Schematic Lay-out of the instrumentation for determination of Performance characteristics.

II/ In this part, means of charging a battery was searched by coupling a car alternator to the rotor thru a transmission system of step-up ratio of 17.25

Related voltage and current output characteristics are given in Chapter 4. Photographs and circuitry of the set-up are below.

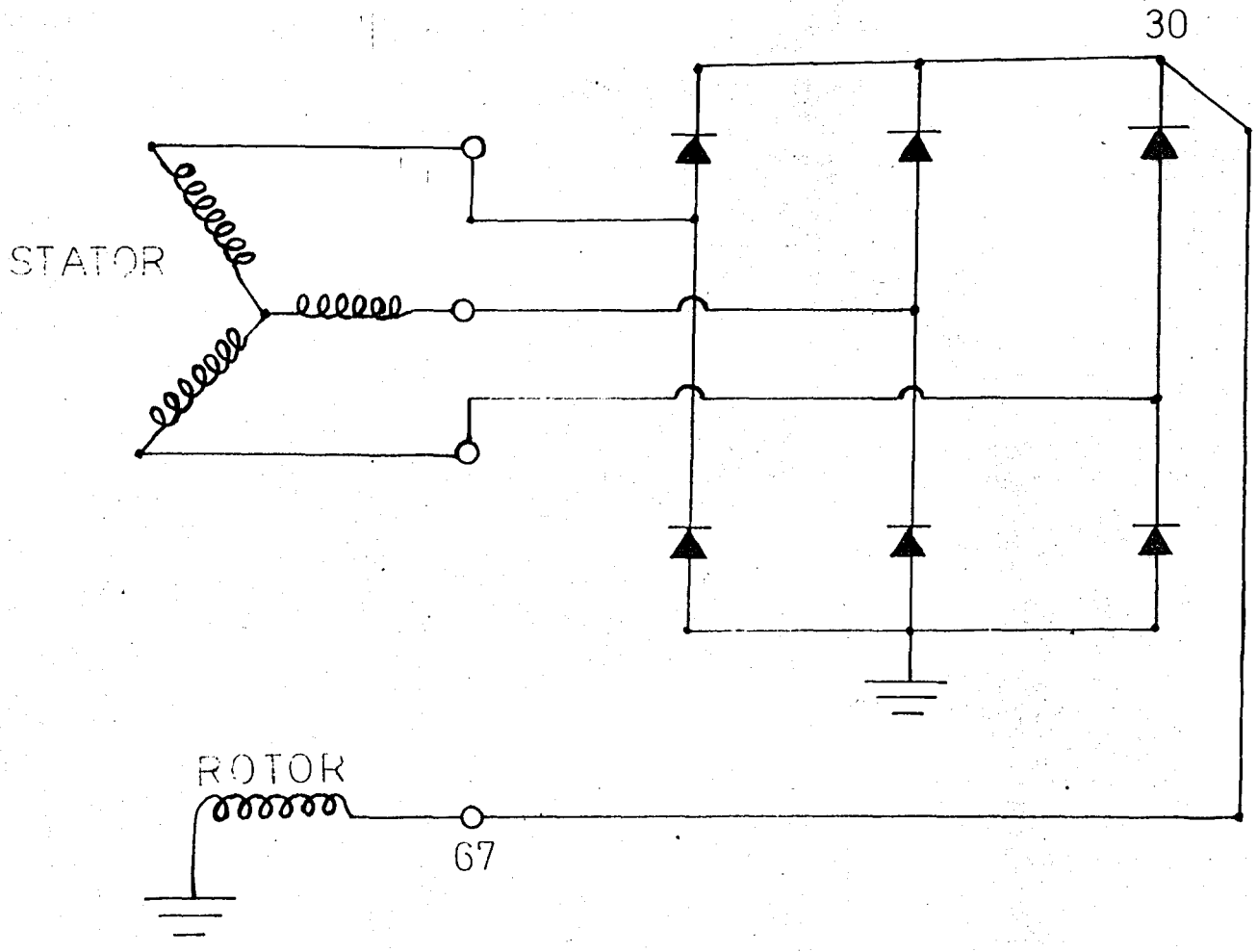

FIG, A.5.9. Alternator Circuitry.

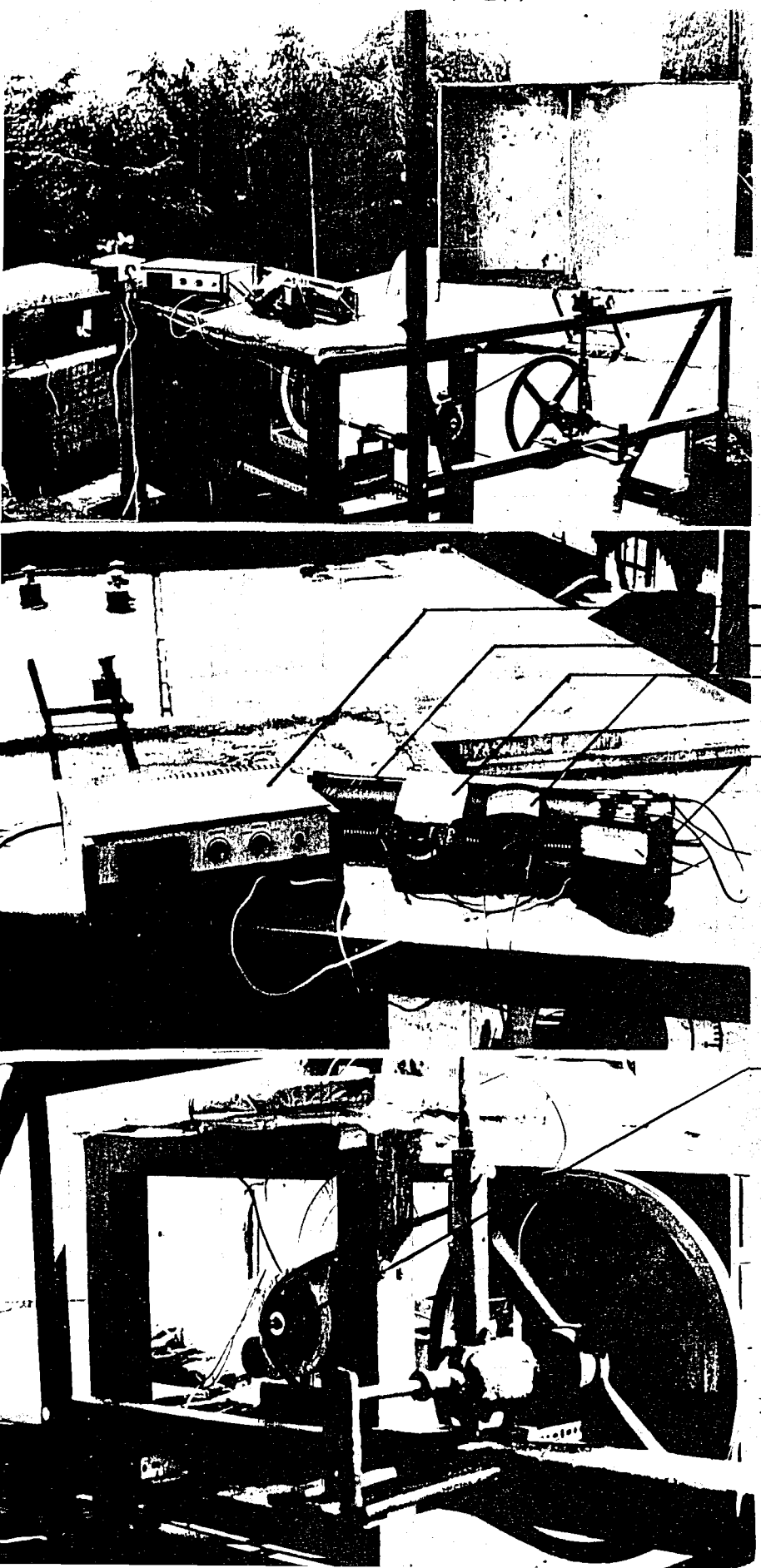

FIG.A.5.10. General View o
Set - up II.

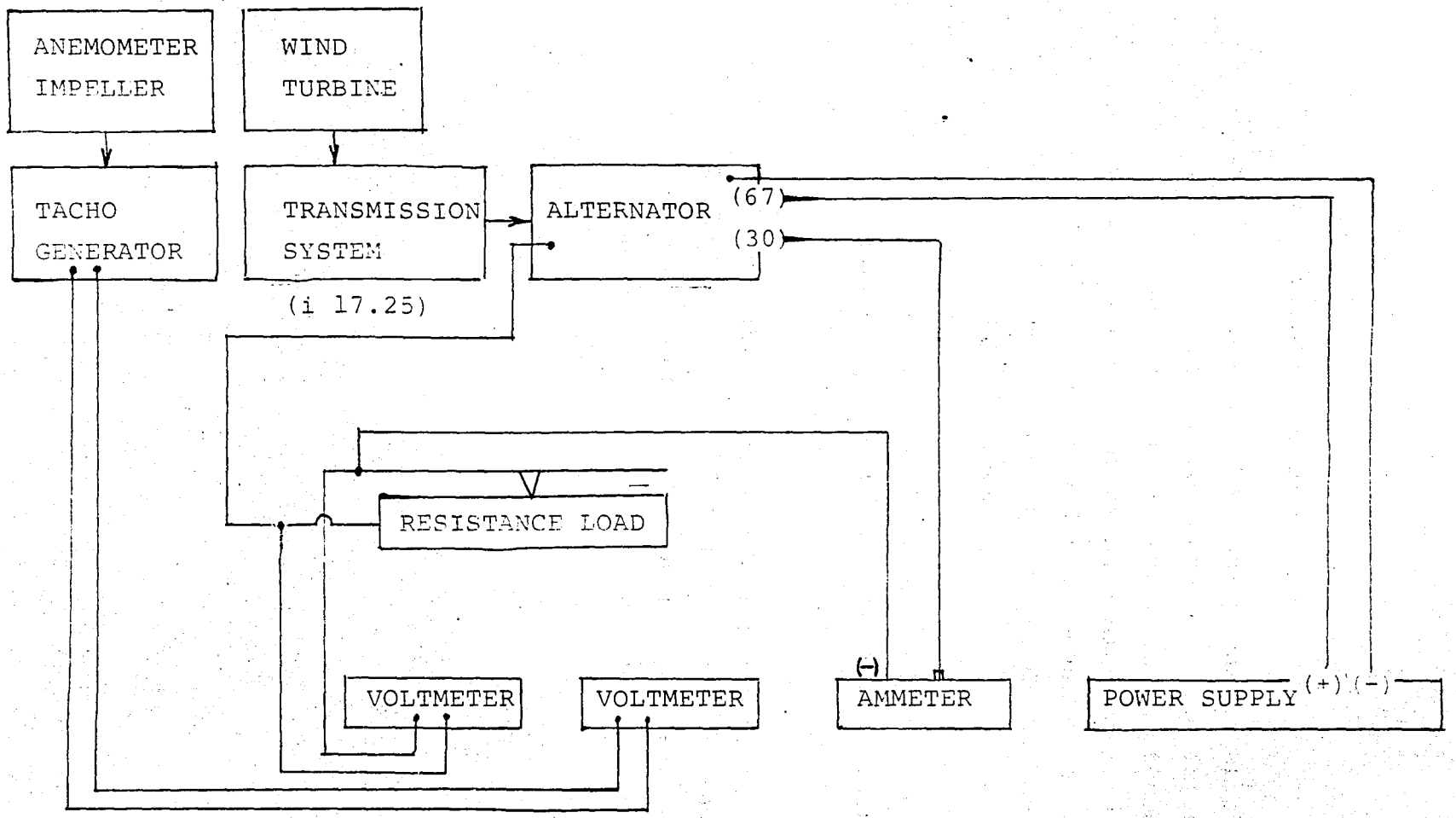

FIG.A.5.11. Schematic Lay-out of the experimental set-up for electric power generation with a car alternator.

A.6. Transmission System :

The no-load rpm vs wind velocity characteristic of the prototype rotor (in accordance with the estimates carried out using the wind-tunnel test results of model rotors) proved the necessity of using a high ratio step-up transmission system in order to measure the output torque with the transducer set-up, or to generate electric power with a car alternator.

A practical system was designed and realized involving a two speed gear box (of a hand braze) in combination with a variable pulley single belt system.

The step-up ratio of the gear box was either 1:1.75, or, 1 : 3.00. Two pulleys of diameters 391 mm and 117 mm were prepared to be fixed to the output shaft of the box to deliver the rotor power either to the dynamic torque transducer, or car alternator,

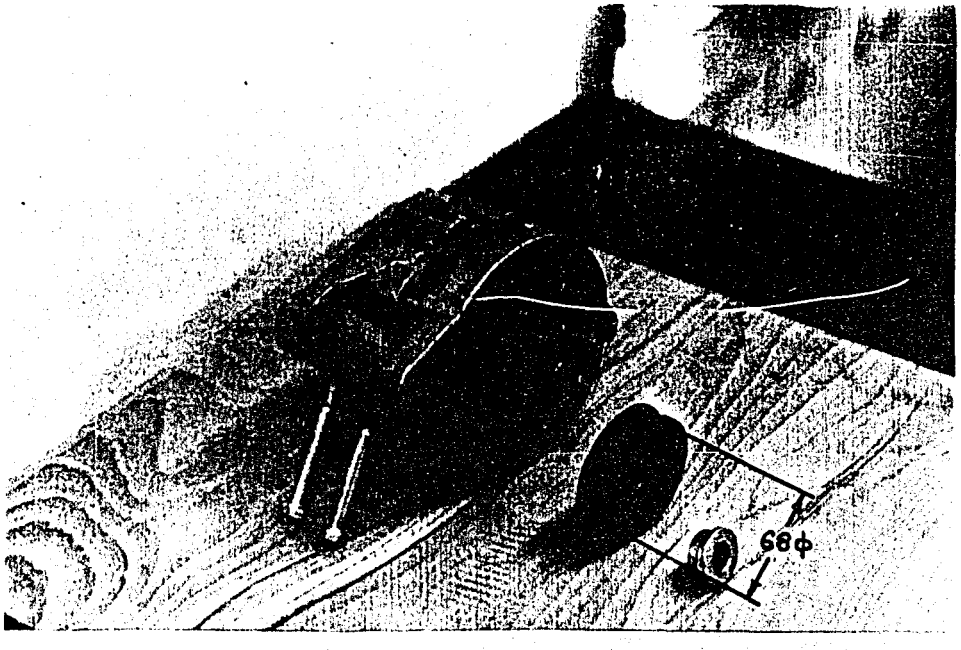

FIG.A.6.1 Car Alternator and its Pulley.

at several step-up ratios, which had pulleys of dimaters 52 mm and 68 mm respectively.

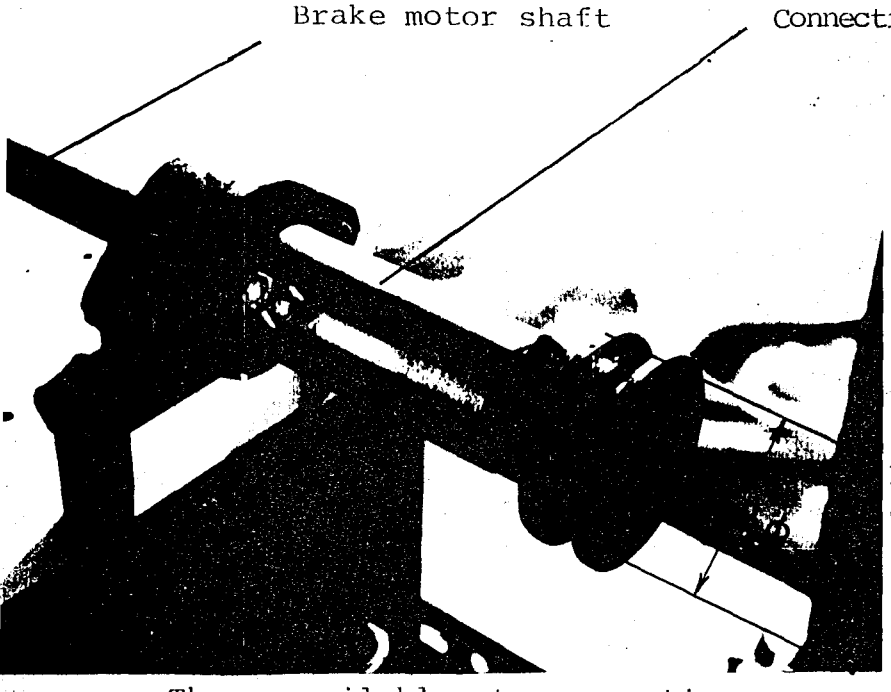

FIG.A.6.2. Brake Motor Shaft and its Pulley

Thus, available step-up ratios are :

1/ for dynamic torque transducer :

$$(\frac{1.75}{1})(\frac{117}{52}) = 3.94 \quad ; \quad (\frac{1.75}{1})(\frac{391}{52}) = 13.16$$

$$(\frac{3.0}{1})(\frac{117}{52}) = 6.75 \quad ; \quad (\frac{3.0}{1})(\frac{391}{52}) = 22.56.$$

2/ for the car alternator :

$$(\frac{1.75}{1})(\frac{117}{68}) = 3.01 \quad ; \quad (\frac{1.75}{1})(\frac{391}{68}) = 10.06$$

$$(\frac{3.0}{1})(\frac{117}{68}) = 5.16 \quad ; \quad (\frac{3.0}{1})(\frac{391}{68}) = 17.25$$

Below are related photographs of the transmission system at various step-up ratios.

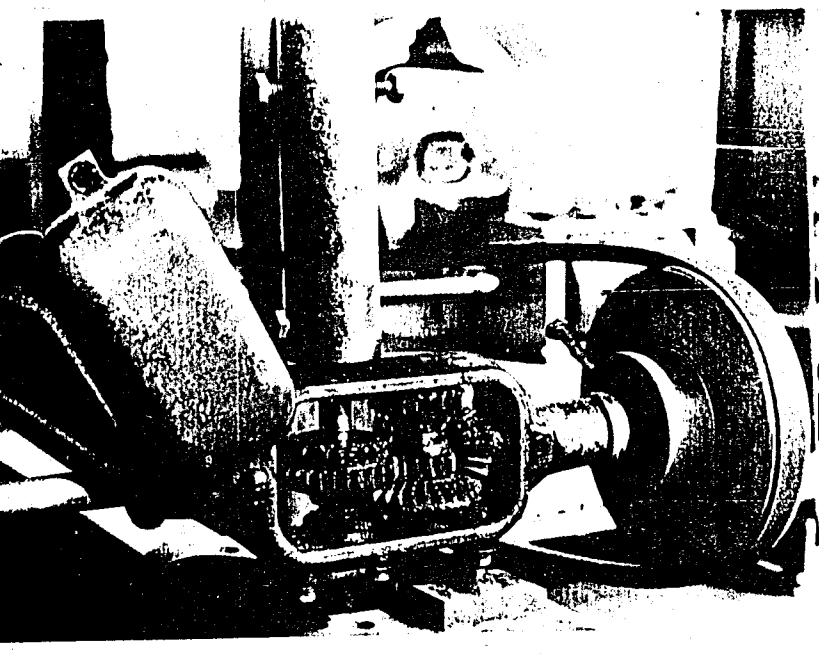

$i = 351/\phi$

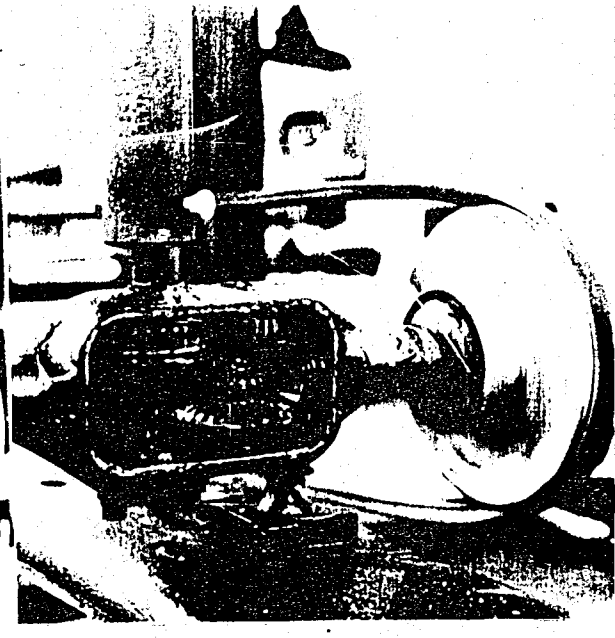

$i = 205/\phi$

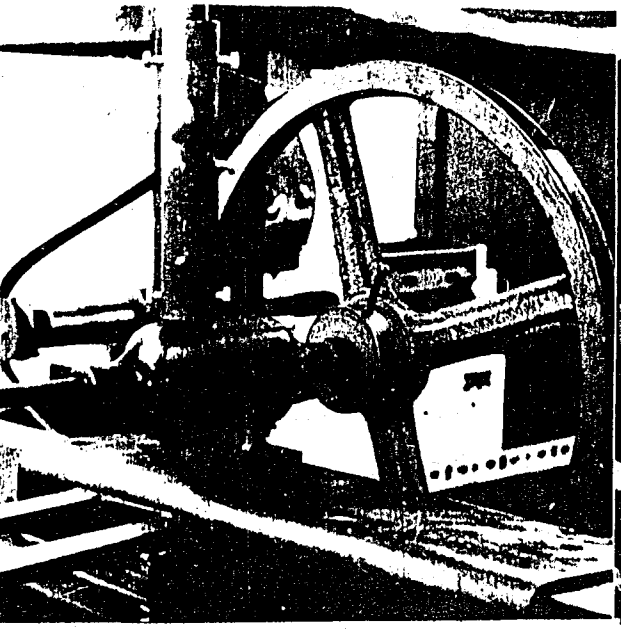

$i = 1173/\phi$

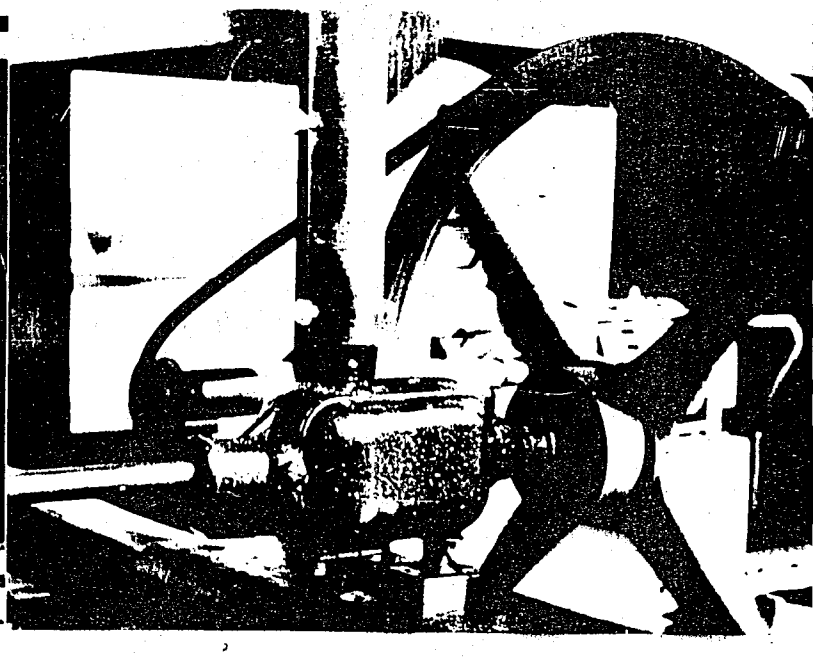

$i = 684/\phi$

FIG. A.6.3. Transmission system With Available step-up Ratios.

1/ In case of coupling of the rotor to the torque transducer, high transmission ratios were used at high wind velocity values so as to lower the rotor torque by means of increasing to rpm, such that 2.4. N-m maximum resistance capacity of the device was sufficient to stop the rotor. The readings of torque were later multiplied by the transmission ratios used.

2/ The car alternator was operated at maximum transmission ratio.

Computational details of belt and pulley designs, based on reference ((15)) are submitted below:

Assume we use "o" type of belt with a= 10 mm; h = 6 mm $F = 0.47\ cm^2$. Where the quantities respectively denote the width height and cross - sectional area. Other parameters are :

$i \triangleq$ velocity ratio.
$D_1 \triangleq$ diameter of small pulley.
$D_2 \triangleq$ diameter of larger pulley.
$A_o \triangleq$ center to center distance of pulleys.
$u \triangleq$ number of runs of the belt per second.
$L \triangleq$ design length of belt.
$L_o \triangleq$ standard length of belt.
$v \triangleq$ belt velocity.
$N \triangleq$ transmitted power.
$P \triangleq$ peripheral belt force.
$\epsilon \triangleq$ coefficient accounting for the creep of the belt.
$k_u \triangleq$ allowable useful belt stress.

ku_o ≜ limit useful stress.
C_1 ≜ correction factor accounting for the effect of the angle of contact.
C_2 ≜ Velocity "conrrection factor
C_3 ≜ coefficient of operating conditions
Z ≜ number of belts to be used.

The problem was to design a drive means selecting a belt of standard profile and length, and to determine the number of belts (Z) necessary to transmit the assigned power N.

i= 7 was desired.

D_1=63 mm. (diameter of the pulley fixed to torque transducer shaft).

$$D_2 = d_1(1-\varepsilon)i$$
$$= 63\ (1-0.02)\ 7$$
$$= 432 \text{ mm.}$$

Where, $0.01 \leq \varepsilon \leq 0.03$.

$$A_{min} = 0.5\ (D_1 + D_2) + 3h$$
$$= 0.5\ (63 + 432) + 18$$
$$= 265.5. \text{ mm.}$$

⇒ A can be estimated as 300 mm.

$$L = 2A + \frac{\pi}{2}(D_1+D_2) + \frac{(D_2-D_1)^2}{4A}$$

$$L = (2)(300) + \frac{\pi}{2}(63 + 432) + \frac{(432 - 63)^2}{(4)(300)}$$

$$= 1491 \text{ mm.}$$

$\Rightarrow L_o$ = 1600 mm. is the nearest greater standard length.

Assume 300 rpm (maximum rotation rate) of driver pulley.

$= 5 \frac{rev}{sec}$

$= 10 \frac{rad}{sec}$.

$\Rightarrow v = wr$

$= (10) \left(\frac{432}{2}\right)$

$= 6786 \frac{mm}{sec}$

$= 6.78 \frac{m}{sec}$

Circumferential velocity of the driven pulley is :

i (6.78)

$= 47.46 \frac{m}{sec}$

Satisfying the condition 5m/sec < v < 50 m/sec.

Also number of runs per second at the driver pulley $\left(= \frac{v}{L_o}\right)$

$= \frac{6.78}{1.6}$

$= 4.24$

Satisfying the condition that $\frac{V}{L_o} \leq 10 \frac{1}{sec}$.

Implying no need to increase A ; thus L.

$$A_o = A_1 + (A_1^2 - A_2)^{1/2}$$

Where,

$$A_1 = \frac{1}{4}\{L_o - \frac{\pi}{2}(D_1+D_2)\}$$

$$= \frac{1}{4}\{1600 - \frac{\pi}{2}(63+432)\}$$

$$\cong 206 \text{ mm.}$$

$$A_2 = \frac{(D_2-D_1)^2}{8}$$

$$= \frac{(432-63)^2}{8}$$

$$= 17020 \text{ mm.}$$

$$\Rightarrow A_o = 206 + (206^2 - 17020)^{1/2}$$

$$= 365 \text{ mm.}$$

Assuming a power 0.5 Kw to be transmitted, the peripheral force is,

$$P = \frac{(1000)(0.5)}{6.78}$$

$$\cong 75 \text{ N.}$$

For the diameter of smaller pulley D_1 = 63 mm, and "o" type of belt, $ku_o = 1.35 \text{ N/mm}^2$

$C_1 = C_2 = C_3 = 1.$

Thus,

$$ku = C_1 C_2 C_3 ku_o$$
$$= 1.35 \text{ N/mm}^2$$

$$\Rightarrow Z \geq \frac{P}{Ku\ F}$$

$$Z \geq \frac{75}{(1.35)(47)}$$

$\Rightarrow Z \geq 1.18$, indicating that it is not convenient to use a single "o" type of belt.

Going thru the same manupulations for an "A" type of belt, a = 13. mm; h = 8mm ; $F = 0.81 \text{ cm}^2$,

$i = 7$; $D_1 = 63$ mm.

$$\Rightarrow D_2 = D_1 (1-\epsilon)\ i$$

$$= 63\ (1-0.02)\ 7$$

$$= 432 \text{ mm.}$$

$$A_{min} = 0.5\ (D_1+D_2) + 3h$$

$$= 0.5\ (63+432) + 24$$

$$= 272 \text{ mm.}$$

$$=_{J} A = 300 \text{ mm.}$$

$$L = (2)(300) + \frac{\pi}{2}\ (63+432) + \frac{(432-63)^2}{(4)(300)}$$

$$= 1491. \text{ mm.}$$

$$\Rightarrow L_o = 1600 \text{ mm.}$$

$$v = 6.78 \text{ m/sec}$$

$$\Rightarrow u\ \left(= \frac{v}{L_o}\right) < 10\ \frac{1}{\text{sec}}$$

$$A_o = A_1 + (A_1^2 - A_2)^{\frac{1}{2}}$$

Where,

$$A_1 = \frac{1}{4}\ \{1600 - \frac{\pi}{2}\ (63+432)\}$$

$$= 206. \text{ mm.}$$

$$A_2 = \frac{(432-63)^2}{8}$$

$$= 17020 \text{ mm.}$$

$$\Rightarrow A_o = 206 + (206^2 - 17020)^{\frac{1}{2}}$$

$$= 365 \text{ mm.}$$

$$p \simeq \frac{(1000)(0.5)}{6.78}$$

$$\simeq 74 \text{ N.}$$

$$Z \geq \frac{74}{(1.35)(81)} = 0.67 \Rightarrow \text{use "A" type of belt, and take } Z = 1.$$

A.7. Test Procedure and Method of Analysis

The voltage values proportional to the rotation rate of rotor (=w) and wind speed (=v) were recorded for each value of the torque delivered (= T'). Relations to obtain pertinent values of the basic variables recorded are :

$$v = 15 \text{ V} \qquad \text{A.7.1}$$

$$n = \frac{1787 \text{ V}}{1} \qquad \text{A.7.2}$$

$$w = \frac{2\pi n}{60} \qquad \text{A.7.3.}$$

$$T = T' \text{ i} \qquad \text{A.7.4.}$$

Where,

v = wind speed in m/sec.
n = rpm.
i = step-up transmission ratio.
w = rotation rate (rad/sec).
T = torque delivered by rotor.
T' = torque from dynamometer.
V = voltage from anemometer or tachometer voltmeter.

Respective values of the quantities obtained from A.7.1, A.7.2 and A.7.3. were used in the equations below to form the table submitted in §APPENDIX A8, from where the plots given in §3.4 and 3.5 are realized.

$$P' = Tw = (T' i)\left(\frac{2\pi}{60} \cdot \frac{1787V}{i}\right) \qquad \text{A.7.5.}$$

$$P_G = \frac{P'}{A} \cong 0.47\ v^{2.48} \text{ for } v > 2.5 \text{ m/sec} \quad (\text{see §APPENDIX A8}) \qquad \text{A.7.6}$$

$$P'w = \frac{1}{2}\rho A\ v^3 = 0.766\ v^3 \quad \left(A = 1.236 m^2; \rho = 123\ \frac{kgf}{m^3}\right) \qquad \text{A.7.7.}$$

$$Pw = 0.620\ v^3 \qquad \text{A.7.8.}$$

$$C_p = \frac{P'}{P'w} \qquad \text{A.7.9}$$

$$X = \frac{wD}{2v} = 0.485\ \frac{w}{v} \qquad \text{A.7.10}$$

$$Re_D = \frac{\rho v D}{\mu} \simeq 6.8 \times 10^3 \times 9.8\ v \qquad \text{A.7.11}$$

$$C_T = \frac{T}{\rho v^2 \frac{}{HD^2}} \simeq 0.678\ \frac{T}{v^2} \qquad \text{A.7.12}$$

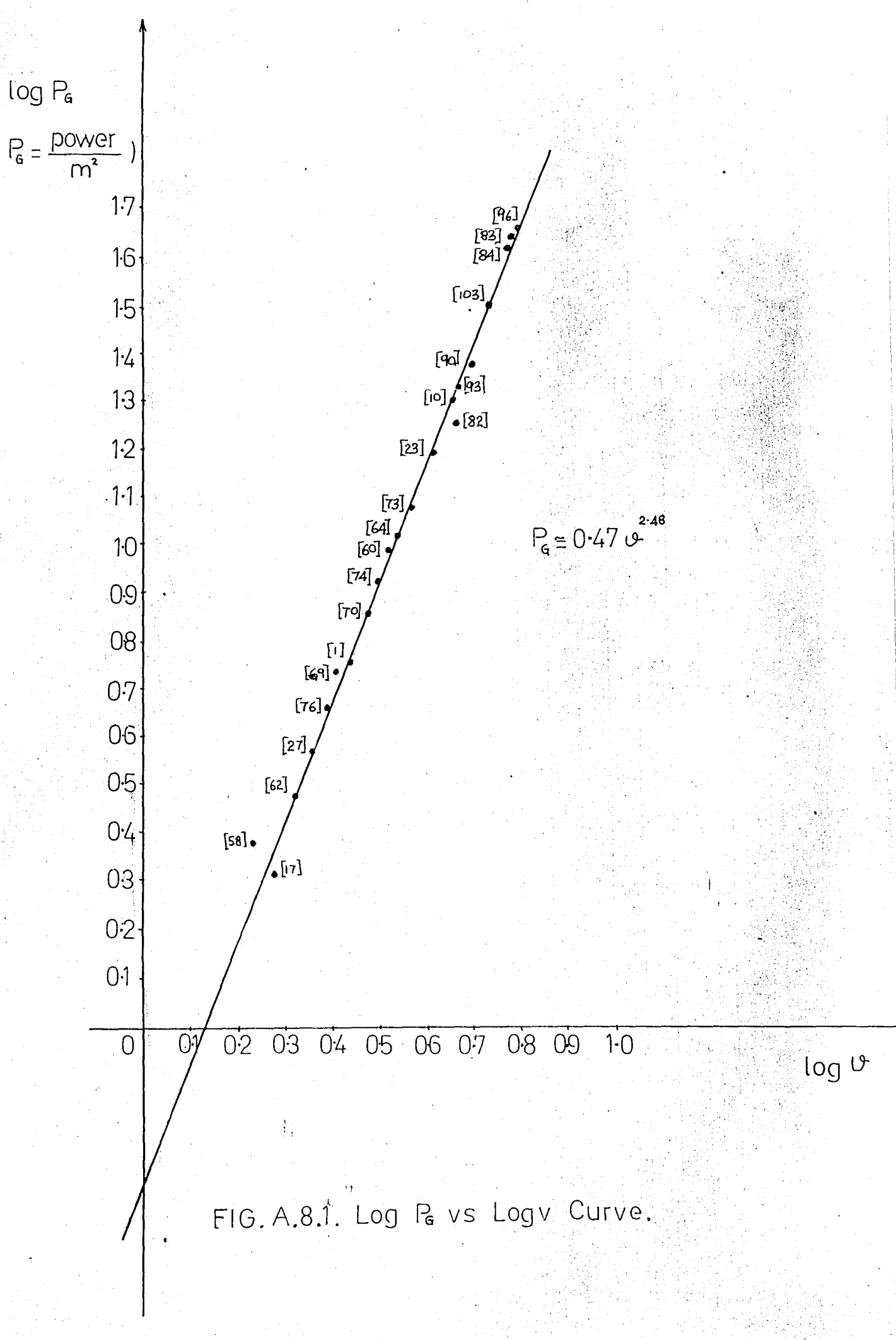

FIG. A.8.1. Log P_G vs Logv Curve.

	WIND SPEED v=15 V		TORQUE	ROTATION RATE rpm=1787/i v			POWER GENERATED POWER DENSITY P_G=1w/P_G/m^2	POWER IN THE WIND P_w=0.766v^3	OVERALL EFFICIENCY C_p=P_G/P_w	TIP SPEED RATIO X=wD/2v	REYNOLDS NUMBER Re=cvD/ν =6.8x10^{3}v	TORQUE CONFICIENT C_T=T/$\rho v^2 HD^2$ =0.678T/v^2	LogP_G	Log v	Log(C_P/C_T)	4X
	V	v	i=3.94	v	rpm	w										
(70)	0.200	5.00	1.000	0.187	84.99	8.90	8.90/1.20	20.68	0.450	1.44	2.04x10^4	0.075	0.86	0.477	5.73	7.20
(74)	0.210	5.15	1.120	0.196	89	9.32	10.44/8-44	23.94	0.436	1.43	2.14x10^4	0.077	0.93	0.498	5.66	7.15
(60)	0.220	5.30	1.220	0.206	93.49	9.79	11.94/9-66	27.53	0.454	1.44	2.24x10^4	0.076	0.99	0.519	5.71	7.20
(10)	0.300	4.50	1.700	0.295	133.69	12.0	24.92/20.16	69.80	0.350	1.51	3.06x10^4	0.057	1.31	0.655	6.14	7.55
(62)	0.140	2.10	0.960	0.082	37.24	5.90	5.74/ 5.08	7.08	0.550	0.90	1.43x10^4	0.148	0.48	0.322	5.58	4.50
(58)	0.115	1.70	1.360	0.052	14.52	1.50	1.35/1.09	3.76	0.360	0.45	1.16x10^4	0.211	0.038	0.250	1.71	2.15
(73)	0.250	5.75	0.960	0.232	105.04	11.00	14.96/12-11	40.40	0.370	1.42	2.55x10^4	0.066	1.08	0.574	5.61	5.68
(27)	0.150	2.25	1.280	0.101	45.84	4.80	4.61/3-73	8.73	0.550	1.03	1.53x10^4	0.129	0.57	0.352	4.11	5.15
(64)	0.230	3.45	0.900	0.211	95.49	10.00	12.80/10.35	31.45	0.410	1.41.	2.35x10^4	0.070	1.02	0.538	5.86	7.05
(17)	0.125	1.90	1.510	0.054	26.74	2.80	2.52/2.04	5.25	0.480	0.71	1.53x10^4	0.169	0.31	0.279	2.84	5.55
(25)	0.277	4.15	1.800	0.267	121.28	12.7	19.18/15-52	54.75	0.350	1.48	2.35x10^4	0.060	1.19	0.618	5.83	7.40
(90)	0.330	4.95	2.960	0.347	157.56	16.50	29.70/2403	92.91	0.320	1.62	1.29x10^4	0.050	1.58	0.695	6.40	8.10
(85)	0.400	6.00	1.730	0.392	177.62	18.60	55.00/44.51	165.49	0.330	1.50	2.82x10^4	0.056	1.65	0.778	5.89	7.50
(95)	0.510	4.55	2.250	0.322	146.10	15.30	26.47/21.42	77.02	0.340	1.60	3.37x10^4	0.054	1.55	0.667	5.30	8.00
(103)	0.360	5.90	2.800	0.375	169.98	17.80	40.05/32.41	120.65	0.330	1.60	4.08x10^4	0.052	1.51	0.732	5.35	8.00
(96)	0.407	6.10	1.182	0.42	190.99	20.00	56.00/45/32	173.87	0.320	1.59	3.16x10^4	0.051	1.66	0.785	6.27	7.95
(76)	0.160	2.40	1.187	0.10	45.56	4.75	5.61/4.54	10.58	0.530	0.96	3.67x10^4	0.039	0.66	0.380	5.81	4.80
(69)	0.170	2.55	0.905	0.12	54.36	5.70	6.74/5.45	12.69	0.530	1.08	4.15x10^4	0.123	0.74	0.407	4.31	5.40
(1)	0.183	2.75	1.576	0.15	67.32	7.05	6.94/5.62	15.93	0.436	1.24	1.63x10^4	0.088	0.75	0.439	4.95	6.20
(82)	0.307	4.60	3.152	0.29	131.53	13.77	21.71/17.57	74.58	0.382	1.45	1.73x10^4	0.051	1.25	0.663	7.49	7.25
(84)	0.390	5.85		0.34	154.21	16.15	50.90/41.9	153.35	0.332	1.34	1.87x1x^4	0.062	1.62	0.767	5.35	6-70

TABLE A.8 . 1 SELECTED DATA AND RELATED RESULTS.

WIND VELOCITY	P_G $(\frac{watt}{m^2})$ $(\frac{POWER\ GENERATED}{AREA})$ $P_G = 0.47\ v^{2.48}$	P_w $(\frac{Watt}{m^2})$ $(\frac{POWER\ IN\ WIND}{AREA})$	$(\frac{HOURS}{YEAR})_1$	$(\frac{HOURS}{YEAR})_2$	$(\frac{Kw\text{-}hr}{YEAR\text{-}m^2})_{G1}$	$(\frac{kw\text{-}hr}{YEAR\text{-}m^2})_{G2}$	$(\frac{kw\text{-}hr}{YEAR\text{-}m^2})_{w1}$	$(\frac{kw\text{-}hr}{YEAR\text{-}m^2})_{w2}$	$(\frac{v}{v_{DESIGN}})_1$ v_D=23mph	$(\frac{v}{v_{DESIGN}})_2$ v_D=26.5mph	Yearly conversion efficiency based on constant torque operation n_1	
5 km/hr (=1.39m/sec) (=3.1 mph)	1 1.064	1.66	7400	8150	7.87	8.67	12.32	13.53	0.135	0.117	0.640	0.6
10 km/hr (=2.78m/sec) (=6.21 mph)	2 5.93	13.32	6050	7300	35.89	43.29	80.88	97.23	0.270	0.230	0.445	0.4
15 km/hr (=4.17m/sec) (=9.32 mph)	3. 16.22	44.94	4520	6320	73.31	102.51	203.13	284.02	0.410	0.350	0.361	0.36
20 km/hr (=5.56m/sec) (=12.34 mph)	4. 33.10	106.52	2750	5100	91.04	168.83	292.93	534.24	0.540	0.470	0.310	0.31
25 km/hr (=6.94m/sec) (=15.53 mph)	5. 57.37	207.15	1650	3750	94.66	215.14	341.80	776.81	0.680	0.590	0.280	0.28
26 km/hr (=7.22m/sec) (=16.16 mph)	6. 63.28	233.25	1320	3500	85.53	221.48	307.80	816.38	0.700	0.610	0.270	0.27
27 km/hr (=7.5 m/sec) (=16.78 mph)	7. 69.54	261.45	1220	3150	84.84	219.03	318.97	823.57	0.730	0.630	0.265	0.26
28 km/hr (=7.77m/sec) (=17.40mph)	8 75.92	290.72	1080	2780	81.99	211.00	313.98	808.20	0.760	0.660	0.260	0.26
29 km/hr (=8.08m/sec) (=18.02mph)	9 83.11	326.92	970	2500	60.65	207.85	317.11	817.30	0.790	0.680	0.250	0.25

TABLE A.8.2. Design Speed-Efficiency Valines

REFERENCES(*)

(*) *Books and papers are numbered separately, which are respectively enclosed by double and single square brackets.*

((1)) Floyd Hickok,
Handbook of Solar and Wind Energy
Cohner's Publisting Co, Inc., 1975.

((2)) Michael Kenward.,
Potential Energy, An Analysis of World Energy Technology.

((3)) Erol Inelmen.,
Thesis (TE 1965), Boğaziçi University.

((4)) A.H. Shapiro.,
The Dynamics and Thermodynamics of Compressible Fluid Flows vol. 1. p.39
Ronald Press Co., N.Y. 1953.

((5)) W.F. Hughes and, J.A. Brighton.,
Fluid Dynamics
Mc Graw Hill Book Co., 1967, pp 62-74

((6)) Baumeister, Theodore and Marks, Lionel S.,
Standard Handbook for Mechanical Engineers.
Mc. Grow - Hill Book Co., 7th ed., 1967, pp.98 to 9-13

((7)) Ronald V. Giles.,
Fluid Mechanics and Hydraulics.
Mc. Grow - Hill Book Co., 1977 , pp 50-69

((8)) P.C. Putnam.,
Power From the Wind.
Van Nostrand, N.Y. 1948.

((9)) E.W. Golding.,
The Generation of Electricity by Wind Power.
Philosophical Library, NY, 1956.

((10)) Glouert. H.,
Aerodynamic Theory.
Vol. IV chap. XI , Windmills and Fans
Edited by W.F. Durand, Reprinted by Peter Smith, Inc,
Gloucester, Mass., 1976, pp.324-340.

((11)) Daniel M. Simmons.,
Wind Power.
Noyes Data Corporation 1975.

((12)) Edward M.Noll,
Wind/Solar Energy for Radiocommunications and Low Power Electronic / Electric Applications.
Howard W. Sams and Co., Inc.
The Bobbs - Merrill Co., Inc. 1975.

((13)) J.J. Instruments, Laboratory Machine System(Catolog)

((14)) J.J. Instruments Electrical Machines and Contrals
Laboratory System (Catolog).

((15)) M. Movnin, D. Goltziker.,
Machine Design,
Mir Poblishers, Moscow.

(1) Tresher, Robert W., Wilson

Design Considerations for the Darrieus Rotor.
Intersoc Energy Convers Eng. Conf. II th proc. State Line, Nev, Sep 12-17 1976. Publ by AI ch E, New York NY, 1976 V2 SAE Pap 769307 p 1787 - 1794.

(2) Stickney, G.H.

Windmill Optimization.
Los Angeles Counc. of Eng. and Sci., Proc. Ser. V2:Energy LA; Tackling the Crisis, Greater Los Angeless Area Energy symp, Calif, May 19 1976 Publ by West Period Co, North Hollywood, Calif, 1976 p 197-202.

(3) Lapin,

Thearetical Performance of Vertical-Axis Wind Turbines.
ASME Pap n 75 - WA/ Ener-1 for Meet Nov 30 Dec 4 1975 11p.

(4) Royment R.

Wind Energy in the U.K.,
(Build Res Establ) Build. Serv. Eng. v 44 n3 Jun 1976 p 63 - 69

(5) Yen, J.T.,

Tornado Type Wind Energy,
Tenth Intersociety Energy Conversion Engincering Conference Record, Aug. 18-22, 1975, pp 978-994. Publ by IEEE (Cot n 75 CHO 983-7 TAB)New York, NY 1975.

(6) Mc Connel, R.D., Von Sant, J.H. Fortin, M.Piche, B.

Experimental 200 Kw Vertical Axis Wind Turbine For the Mogdolen Islands.,

Intersoc Energy Convers. Eng. Conf. II th Proc., State Line, Nev, Sep 12-17 1976 Publ by AI ch E, New York, NY , 1976 , Vol. 2 SAE Pap 769311 p 1798-1802.

(7) Ramaqumar, R.

Harnessing Wind Power in Developing Countries., Stillwater Intersoc Energy Convers. Eng. Conf. 10th Ree, Univ. of Del, Newark, Aug. 18-22 1975 Pap 759145 p 966-973. Publ by IEEE (Catn 75 CHo 983-7-TAB) New York, NY, 1975.

(8) R.S. Rangi, P. South and R.J. Templin.,

Wind Power and the Vertical-Axis Wind Turbine Developed at the National Research Council.,

Nat. Res. Coun. Canada, Div. Mech. Eng. Q Bull., 1974 n 2 p 1-14.

(9) Richard Stepler,

Eggbeater Windmill.,
Popular Science , May 1975.

(10) Vertical - Axis Windmill to Produce one House Power.

(11) Samuel Walters.,

Seven Story-High 'Eggbeater' Delivers 65 k2w.,
Mechanical Engineering, Aug., 1977

(12) W.F. Baker.,

A Design Idea For a Small Vertical-Axis Turbine,
Electronics and Power, March 1975.

(13) W.F. Baker.,

Wind Energy.,
Electronics and Power, March 1978.

(14) N.L. Kochhara.,

Utilization of Wind Power in Arid Areas of Rojasthan.,
Indian Journal of Power and River Valley Development
Aug. 1957 v 17, part n. 18.

(15) E.W. Golding.,

Electrical Energy From the Wind.,
Engineering Journal, June 1957 vol 40 pard 6.

(16) Wind Generated Electricity.,

Engineering, Mar 25 1955 vol. 179, part n-4652

(17) F.O. Ringleb.,

.....
Journal of Basic Engineering., p 617 (1962)

(18) S.J. Ying, and C.C. Chang.,

Explotory Model Study of Tornado-Like Vortex
Dynamics,

(19) South Peter.,
NRC's Vertical Wind Turbine.,
Notl. Res. Counc. Ottawa, ont; Rangi, Raj Agrig Eng
v 55 n2 Feb 1974 p 14-16.

(20) Todd, C.J., Eddy, R.L. , James, R.C., Howell, W.E..

Cost Effective Electric Power Generation From the Wind : A system linking Wind Power with Hydroelectric Storage and Long Distance Transmission.
Wind Eng. Vw nl 1978 p 10-24

(21) Sheldahl, Robert E., Blockwell, Bennie F., Feltz, Louis V

Wind Tunnel Performance Data for Two and Three Bucket Savonius Rotors.
J. Energy v2 n3 Jun 1978 p 160-164

(22) Hoffern, Martin I., Matloff, Gregory L., Rugg, Barry A..

Lebost Wind Turbine : Laboratory Tests and Data Analysis.

(23) J.A.C. Kentfield.,

A Modified Savonius Wind Turbine With Good Low Velocity Ratio Torque Characteristics.
Publication of the Univ. of Calgary p 168-187

(24) B.G. Newman,

Measurements on a Savonius Rotor with Variable Gap.
Publication of Mc Gill University.

(25) S. Sivasegaram.,

Resistance-Type Vertical-Axis Wind Turbines: Optimizatio of the Rotor Geometry.,
University of Paradenia.

(26) Wiley, R.A.

Vortexing as a Mathemathical Catastrophe.,
Utilization of Vortexing to Increase the Efficiency of an Ideal Wind Energy System Above the Betz Limit, Bulletion of the American Physical Society, Vol. 22, 1977 p. 1277

(27) Loth, J.L.,

Betz Type Limitation of Vortex Wind Machines.,

Bulletion of the Amerikan Physical Society, vol 22. p. 1277

(28) Oman R.A., and Foreman, K.M.,

Advantages of the Diffuser Augmented Wind Turbine.,

Wind Energy Conversion Conference Piaceedings, Washington D.C., June 11-13, 1973, edited by J.M. Savino, NASA Lewis Research Center, Cleveland, Ohio, Rept. No. NSF / RA / W -73-006, Dec 1973

(29) Sforza, P.M.,

Vortex Augmentor Concepts for Wind Energy Conversion, Proceedings of the Second Workshop on Wind Energy Conversion Systems, Vashington, D.C., June 9-11 1975, Mitre Corporation, Mc Lean, Va., pp 433-442

(30) Oman, R.A., and Foreman, K.M.

Cost Effective Diffuser Augmentation of Wind Turbine Power Generators.,

(31) Vance, W_Y

Vertical - Axis Rotors: Status and Potential.,
Wind Energy Conversion Conference Proceedings, Washington, D.C., June 11-13,1973, edited by J.M. Savino, NASA Lewis Research Center, cleveland, ohio, Rept. No. NSF/RA/W-73-006, Dec 1973. pp 96-102

(32) Blockwell, B.F., Sheldahl, R.E., and Feltz, L.V.,

Wind Tunnel Performance Data for the Darrieus Wind Turbine with NACA 0012 Blades.
Sandia Laboratories, Albuquerque, N.Mex., Rept. No. SAND 76-0130, May 1976.

(33) Broasch, R.H.,

Power Generation with a Vertical-Axis Wind Turbine.,
Proceedings of the Second Workshop on Wind Energy Conversion Systems, Vashington, D.C., June 9-11 1975, Mitre Corporation, Mc Lean, Va., NSF-RA--N-75-050 pp 417-425

(34) R.P. Gupta and S.K. Chandra.,

Development of 1 Kw Vertical-Axis Wind Generator.,(*)
Proceeding of the Int'l Solar En. Cong. New Delhi, India-Jan' 78.

(35) K.L. Kumar and O.P. Grover and R.C. Sachdeva.,

Windmills for Rural Indial.,
Proc. of the Int'l Solar En. Cong. New Delhi, India-Jan'78

(36) G.E. Bronvold.,

Vertical-Axis Wind Turbine Status., (*)
Proc. of the Int'l Solar En. Cong. New Delhi, India-Jan478

(37) D. Pol and C.E. Parker.,

A Technique For Longitudinal Correlation of Wind Data Theory and Its Applications to Siting of Wind Power Plants., (*)
Proc. of the Int'l Solar Eng. Cong. New Delhi; India-Jan'78

(38) V. Mukhopadhyay.,

A Vertical-Axis Tilting Blade Windmill Suitable for use In Rural Areas In Indial, (*)
Proc. of the Int'l Solar En. Cong. New Delhi; India-Jan'78

(39) Birol Kılkış.,

The Use of Wind Energy for Irrigation Energy Supply Purposses in a Turkish Village (**)
Iut'l Solar Forum 1978.

(40) H. Ashley.,

Some Contributions to Aerodynamic Theory for Vertical Axis Wind Turbiness (***)
Proc. of the 12 th En. Conv. Eng. Conf.

(*) *SUN, Mankind's Future Source of Energy ; v3 Pergamon (BU Library).*
(**) *Vol.3. of the Collected Papers*
(***) *Vol. 2. of 2 volumes.*

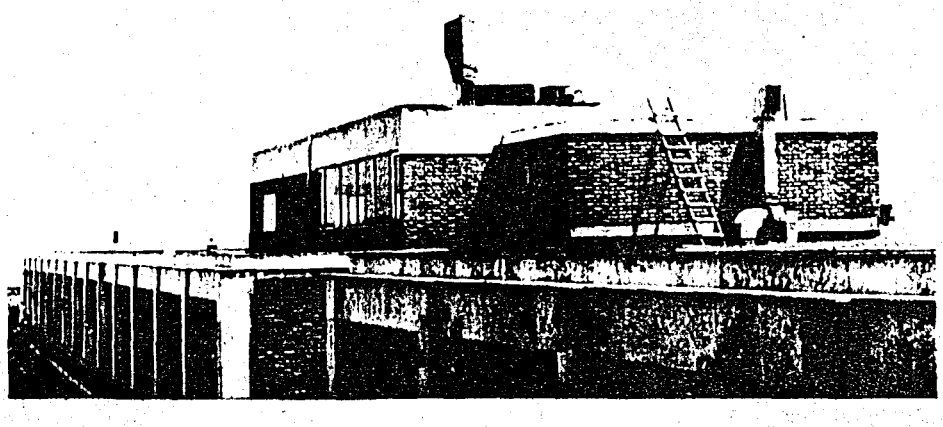

~ The End ~